Determining the spatial and temporal trends of mesophotic fish biodiversity and reef-scale calcification using novel approaches

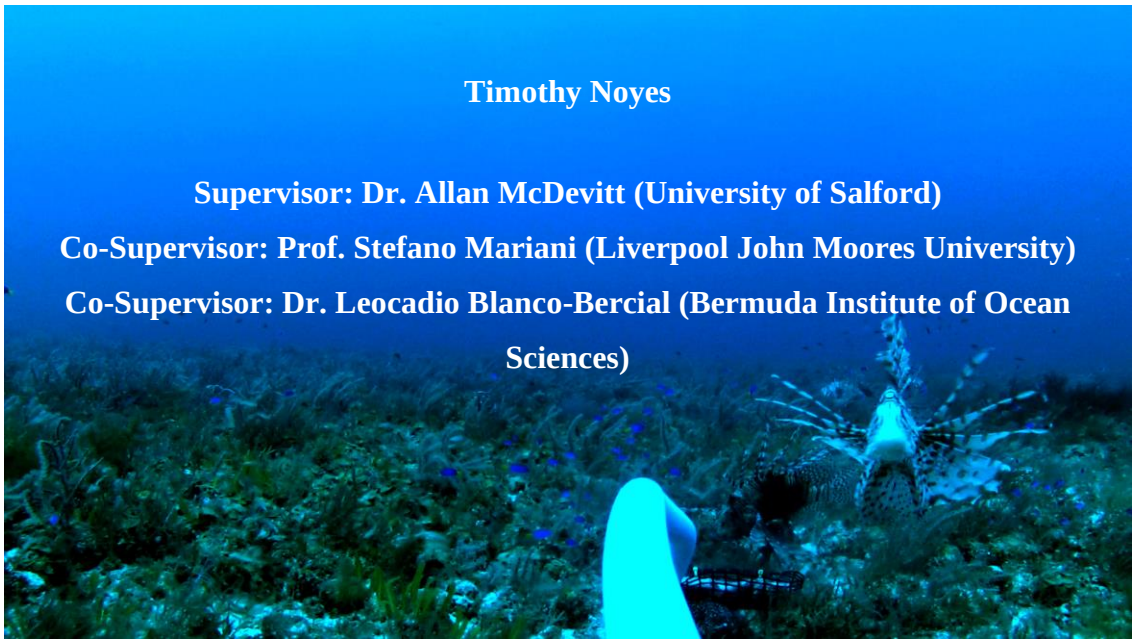

Timothy Noyes

Supervisor: Dr. Allan McDevitt (University of Salford)

Co-Supervisor: Prof. Stefano Mariani (Liverpool John Moores University)

Co-Supervisor: Dr. Leocadio Blanco-Bercial (Bermuda Institute of Ocean Sciences)

University of Salford MANCHESTER

BIOS Bermuda Institute of Ocean Sciences

BEST VOLUNTARY SCHEME FOR BIODIVERSITY AND ECOSYSTEM SERVICES IN TERRITORIES OF EUROPEAN OVERSEAS

This thesis is submitted to the University of Salford, School of Science, Engineering and Environment, in fulfilment of the requirements for the degree of Doctor of Philosophy (PhD).

February 2023

List of Tables

Chapter 2.

Chapter 3.

Chapter 4.

List of Figures

Chapter 1.

Chapter 2.

normalized to values of 36.6 g kg-1. The black dot - dash line depicts $\Omega_{aragonite}$ = 1, thermodynamically, dissolution is anticipated if Ω < 1; grey dashed line depicts $\Omega_{aragonite}$ = 3.4, transition from coral reef to non-reef coral community; pink shaded area $\Omega_{aragonite}$ 3.0 – 3.5 defined as the global limit for reef development.

Figure 2.3. Mean seasonal climatology of net ecosystem calcification (NEC; g $CaCO_3$ m^{-2} d^{-1}) and net ecosystem production (NEP; g C m^{-2} d^{-1}) for 30 m, 40m, 60 m reefs. Grey symbols represent actual samples (**a**) NEC, dark green circles denote monthly mean values for 2017, light green circles denote monthly mean values for 2018; (**b**) NEP, dark green diamonds denote monthly mean values for 2017, light green diamonds circles denote monthly mean values for 2018; (**c**) NEC, orange circles denote monthly mean values for 2017, dark orange circles denote monthly mean values for 2018; (**d**) NEP, orange diamonds denote monthly mean values for 2017, dark orange diamonds denote monthly mean values for 2018; (**e**) NEC, dark blue circles denote monthly mean values for 2017, light blue circles denote monthly mean values for 2018; (**f**) NEP, dark blue diamonds denote monthly mean values for 2017, light blue diamond's denote monthly mean values for 2018. Dashed lines equal calcification and trophic status are in balance (e.g., NEC = 0, NEP = 0).

Chapter 3.

Figure 3.1. Map of Bermuda and study site locations (**a**) Bathymetric map of Bermuda illustrating the main study locations (red circles) and proximity to land and open ocean, 10 m contour line in orange, 30 m contour dashed red lines, 150 m contour solid red line, 1000 m contour solid black line. (**b**) location BT2 showing typical spatial orientation of 30 m (black circles), 60 m (red circles) and 130 m sites (yellow triangle) per location (sites ~ 350 m apart). Note, the location for reference biogeochemical measurements taken at the site of the Bermuda Atlantic Time- series Study site ~ 80 km SE of Bermuda.

Figure 3.2. Mean temperature (°C) of surface water (1 m) and mesophotic reefs data at 30 m, 40 m, 60 m and 130 m depths. (**a – e**; 2017 mean red symbols, 2018 mean dark

red symbols, in situ measurements light grey circles). Note, no 130 m samples were collected 2017.

Figure 3.3 Summaries of α- and β-diversity between locations BT1 (dark gray symbols and lines), BT2 (peril symbols and lines), BT3 (blue symbols and lines): (**a**) boxplot of taxon richness, boxes indicating 25th, 50th and 75th percentiles and whiskers sow 5th and 95th percentiles. (**b**) sample size-based rarefication and extrapolation curves, (**ci-iii**) non-metric multidimensional scaling plots of β-diversity components.

Figure 3.4 Summaries of α- and β-diversity pooled across sample depths. 1 m (purple circles/lines/ellipses), 20 m (orange circles/lines/ellipses), 30 m (grey circles/lines/ellipses), 40 m (blue circles/lines/ellipses), 60m (black circles/lines/ellipses), 130 m (red circles/lines/ellipses): (**a**) boxplot of taxon richness, boxes indicating 25th, 50th and 75th percentiles and whiskers sow 5th and 95th percentiles. (**b**) sample size-based rarefication and extrapolation curves, (**ci-iii**) non-metric multidimensional scaling plots of β-diversity components.

Figure 3.5 Summaries of α-diversity seasonal comparison across the three study locations, Summer 2017 (orange squares), Autumn 2017 (purple squares), Winter 2017 (green squares), Spring 2018 (red inverted triangles). Summer 2018 (blue circles). Autumn 2018 (dark red diamonds), Autumn 2020 (grey square). Note, sampling was not possible in Winter 2017 at BT2 and Autumn 2020 at BT3 due to inclement weather.

Figure 3.6 Bubble plot showing proportional read counts for taxa classified by trophic position (Deep seas species are categorised by origin) pooled by sampling depth across the three locations for the duration of the study. Taxa are identified in accordance with local management status (yellow = Protected, Orange dots = Regulated) and International Commission for the Conservation of Atlantic Tunas status (ICCAT, Blue dots), Additionally, endemic (Black dots) and invasive species (Red dots) have been highlighted. The trophic classifications are represented as Sharks (SH), Macro Carnivores (MC), Mobile Invertebrate Feeders (MIF), Omnivores (OM), Planktivore (PL), Roving

Herbivores (RH), Sessile Invertebrate Feeders (SIF), Territorial Herbivores (TH) and Deep-sea species (DS).

Figure 3.7 Bubble plot showing proportional read counts for taxa classified by trophic position (Deep seas species are categorised by origin) pooled by season across the three locations for the duration of the study. Taxa are identified in accordance with local management status (yellow = Protected, Orange dots = Regulated) and International Commission for the Conservation of Atlantic Tunas status (ICCAT, Blue dots), Additionally, endemic (Black dots) and invasive species (Red dots) have been highlighted. The trophic classifications are represented as Sharks (SH), Macro Carnivores (MC), Mobile Invertebrate Feeders (MIF), Omnivores (OM), Planktivore (PL), Roving Herbivores (RH), Sessile Invertebrate Feeders (SIF), Territorial Herbivores (TH) and Deep-sea species (DS).

Figure 3.8 Bubble plot showing proportional read counts for taxa pooled across depth ranges classified by trophic position. The trophic classifications are represented as Sharks (SH), Macro Carnivores (MC), Mobile Invertebrate Feeders (MIF), Omnivores (OM), Planktivore (PL), Roving Herbivores (RH), Sessile Invertebrate Feeders (SIF), Territorial Herbivores (TH) and Deep-sea species (DS).

Figure 3.9 RDA Triplot of Hellinger-transformed species data constrained by abiotic factors (Table 1), scaling 2 correlation plot with site fitted scores. Red arrows indicate species, the blue arrows represent explanatory variables. Shapes represent physical site depth (m), colours represent seasons. Note, the full suite of species has not been visualized to limit the plotting space from becoming overwhelmed with data points.

Chapter 4.

Figure 4.1. (**a – d**), 30 m depth contour dashed red line, 150 m depth solid red line, (**a**). Map of Bermuda and study locations (red circles), 10 m contour orange dotted line, 1000 m contour solid black line. (**b**) Bathymetric map of Location BT3, red circles = 60 m sites,

(**c**) Bathymetric map of Location BT2, red circles = 60 m sites, (**d**) Bathymetric map of Location BT1, red circles = 60 m sites.

Figure 4.2. Seabed complexity observed at site BT1 on survey 1 (**a**) and survey 4 (**b**) differences are caused by changes in BRUVs orientation upon contact with the seabed (depth ~ 60 m). Image (**a**) depicts rhodolith beds foreground with ~ 5 m reef structure in the background and a shoal of Gwelly jacks (*Pseudocaranx dentex*, Bloch & Schneider 1801) in the field of view. Image (**b**) depicts rhodolith beds and brown algae (*Sporochnus bolleanus*, Montagne 1856), two Sand tilefish (*Malacanthus plumieri*, Bloch 1786) and one terminal phase Yellowhead wrasse (*Halichoeres garnoti*, Valenciennes 1839).

Figure 4.3. Venn diagrams of the number of corresponding and unique (**a**) species (**b**) genera detected by the two assessment methodologies, Baited Under Water Video systems (BRUVs; dark grey squares and semi circles) and environmental DNA (eDNA; orange squares and semi circles). The blue intersect indicates the number of species (a) and genera (b) detected by both methodologies.

Figure 4.4. Sample size-based rarefaction/extrapolation (R/E) curves for each location BT1 (dark gray symbols and lines), BT2 (peril symbols and lines), BT3 (blue symbols and lines): (**a**) environmental DNA (eDNA) metabarcoding methodology, (**b**) Baited Remote Underwater Video systems (BRUVs) methodology.

Figure 4.5. Summaries of α- and β-diversity between locations partitioned by sampling methodology: (**a**) boxplot of species richness, boxes indicating 25th, 50th and 75th percentiles and whiskers show 5th and 95th percentiles, eDNA (orange triangles) and BRUVs (dark grey circles). (**b**) boxplot of genus richness, boxes indicating 25th, 50th and 75th percentiles and whiskers show 5th and 95th percentiles, eDNA (orange triangles) and BRUVs (dark grey circles) (**c**) non-metric multidimensional scaling plots of β-diversity components, eDNA (triangles) and BRUVs (circles), locations: BT1 (dark grey symbols and ellipses), BT2 (peril symbols and ellipses), BT3 (blue symbols and ellipses).

Figure 4.6. Redundancy analysis ordination diagram (triplots): location BT1 (dark grey square), BT2 (peril circles), BT3 (blue triangles). (a) environmental DNA (eDNA) metabarcoding community detection, (b) Baited Remote Underwater Video systems (BRUVs) community detection, explanatory variables (benthic composition and standardised physicochemical variables) blue arrows. First axis is horizontal, second axis is vertical. The angles among arrows denote the degree of correlation between the individual variables, and the smaller the angle, the greater the positive correlation. Negatively correlated variables are pointing in opposite directions.

Acknowledgements

First and foremost, I would like to thank my wife for having the belief in me and encouraging me (us) to pursue this adventure. It has been a roller coaster of a ride for many reasons, but you have always been there to provide support and more recently, make sure I was fed and watered. No longer will you have to refer to yourself as a “PhD widow”!

I would like to express my sincerest thanks to Stefano for deciding to take me on as a PhD student after only 30 mins of us meeting. It has been a whirl wind ever since. I will admit, I did not know of the University of Salford until I started to do background research on eDNA groups in the UK. Stefano’s name came up time and time again. After our initial meeting, I knew that was who I wanted to pursue the PhD with. Whilst I am immensely proud of this achievement, it does come with some regret, mainly that I was not able to spend more time with the Mariani lab group in person. A group that I will happily recommend to any aspiring students.

Thank you to Allan for taking up the “Salford” reins and becoming my primary university supervisor after Stefano moved down the M62 to Liverpool John Moores. You have continued to make sure I am on track and provided guidance as and when needed.

Thank you to Leo for agreeing to be my on-site supervisor and persevering with my endless questions at all times of day and night. It has been eventful, and I am fully appreciative of the support you have given me over this journey and continue to give.

I would like to thank all the students who participated with field trips enduring the long days bobbing around on a 26ft boat 10 km from land, Rosie Dowell, Jonas Schroder, Emma O’Donnell, Ellie Corbet, Alex Lundberg, your assistance was very much appreciated!

Thank you to the unconditional support from both sides of the family, my forever supportive parents and brother despite the insurmountable challenges they have had to face in the last few years. Chris, I truly wish you were here to “FINALLY” witness the handing in and completion of this degree. To the “Baird 5” for continuing to champion my cause from the US and allowing me to commandeer the basement for weeks on end.

Finally, to my son Oliver who was born into the thick of PhD world, while you are too young to realise your impact and how you helped, your presence was an important reality check from the all-consuming final write up months/days! The sound of the squeaky walker will forever bring a smile to my face.

Funding acknowledgement

This study was based partially on work supported by the European Union, BEST 2.0 Programme Project No.1634 and 2274. Additional financial support was provided by BIOS Ocean Academy and Groundswell Bermuda.

Abstract

Mesophotic Coral Ecosystems (MCEs) occur in the middle to lower photic zone (~30–150 m) of tropical and subtropical regions and are often extensions of shallow reef communities. Mesophotic reefs have been traditionally understudied primarily due to inaccessibility via traditional monitoring and assessment methodologies. As a result, there are significant knowledge gaps in the understanding of ecosystem functioning within MCEs such as biogeochemical cycling and diversity of organisms at these depths. This study applied environmental DNA (eDNA) metabarcoding and Baited Underwater Video stations (BRUVs) coupled with biogeochemical measurements to investigate the trophic status and biodiversity of Bermuda mesophotic reef fish communities over an ~ 18-month period. These reef systems were determined to be chemical conducive for calcification to occur, in a net state of calcification (i.e., accretion of calcium carbonate, $CaCO_3$) and net autotrophic. Fish community trophic structures were deemed to be comparable across the upper mesophotic depth gradient. In addition, this study supports species overlap between mesophotic and shallow reef fish communities and does detect distinct faunal breaks i.e., a holistic system. However, spatial, and temporal influences were detected in both α- and β diversity of fish communities with taxon replacement (turnover) the primary driver β diversity. Environmental DNA detected fish communities exhibiting stronger associations with abiotic variables, whereas the BRUVs detected communities associated more with the biotic variables. This study provides the first data of their kind for understanding mesophotic biogeochemical processes in addition to providing a more "complete" biodiversity assessment through the combined use of eDNA and BRUVs. Overall, this study derived biodiversity patterns which will enable more effective marine spatial planning policy through an ecosystem-based approach.

Chapter 1. Introduction

1.1 Project Introduction

Tropical and subtropical coral reefs have a global distribution and are some of the most biologically diverse ecosystems on the planet with an estimated 830,000 associated species (Fisher et al., 2015) of which approximately 4,000 are species of fish (Souter et al., 2021). These ecosystems provide a range of ecosystem services ranging from the provision of biogeochemical cycling, coastal protection, fisheries, habitat, and tourism (Woodhead et al., 2019).

Zooxanthellate hermatypic scleractinian coral species can persist to depths of ~ 150 m in clear water environments that allow sufficient light penetration for photosynthesis. The reef ecosystems that persist in the intermediate and lower extend (~30 – 150 m) of these photic zones are known as Mesophotic Coral Ecosystems (MCEs; Puglise et al., 2008; Hinderstein et al., 2010) and the focal ecosystems of this thesis.

Mesophotic reefs are often extensions of shallow reef communities, harbour high geographic endemism and are important refugia for vital taxonomic groups including fish, corals and sponges (Baker et al., 2016a; Loya et al., 2016; Kosaki et al., 2017). MCEs have been traditionally understudied and undervalued and a key research focus has been prioritizing the establishment of standardised and practical methodologies for monitoring regimes to ensure effective management practices and maintenance of ecosystem health (Hoegh-Guldberg et al., 2017; Turner et al., 2017). There are significant knowledge gaps in understanding ecosystem functions within MCEs such as biogeochemical cycling, calcification and the physiology and diversity of organisms at these depths (Slattery et al., 2011; Turner et al., 2019).

Although these ecosystems have long been discussed as being environmentally “stable”, there is limited research to date to demonstrate their environmental stability over geographical and longer temporal scales (months to years). One of the longest time-series of mesophotic abiotic data in the form of temperature records (2000-2016) from the outer reef slopes of Palau (Colin, 2009; Colin and Lindfield, 2019) demonstrates the extreme level of variability these ecosystems can experience. Whilst environmental

stability does not infer increased biodiversity within an ecosystem (i.e., intermediate-disturbance hypothesis; Connell, 1978), it does provide the foundation to allow for greater levels of biodiversity. Therefore, one would expect greater population resiliency to invasion and anticipate rapid recovery from such disturbances. Although it has been demonstrated that mesophotic hermatypic corals accrete calcium carbonate at a much lower rate (Weinstein et al., 2019), they remain vitally important for fisheries (Hoegh-Guldberg et al., 2017).

However, inaccessibility via traditional self-contained underwater breathing apparatus (SCUBA) diving techniques has been a limiting factor to understanding the biodiversity of these ecosystems. Advances in research technology (e.g., environmental DNA metabarcoding and baited cameras) have allowed researchers greater access to MCEs to investigate a variety of research areas including the ecology and biology of mesophotic species, connectivity, biodiversity and conservation and management. Central to these research areas is the 'deep-reef refugia hypothesis' (DRRH; Glynn, 1996; Bongaerts et al., 2010)[1] that proposes MCEs are less vulnerable to natural and anthropogenic disturbances that typically occur on shallow-water coral reefs (SWRs) through greater environmental stability and can provide a viable reproductive source. Various studies have demonstrated the species overlap between MCE and SWR fish populations. The emerging consensus is that MCEs have significant ecological importance for reef fishes through providing refuge from fishing pressure and as spawning aggregations for shallow reef fish species. This study will quantify biodiversity within a spatial and temporal gradient across Bermudan MCEs using the non-invasive methodologies of eDNA and Baited Underwater Video stations (BRUVs; Figure 1.2).

The valuable ecological services (Holmlund and Hammer, 1999) that MCEs provide in Bermuda are under threat due to the presence of two invasive lionfish species, Red lionfish (*Pterois volitans* Linnaeus, 1758) and Devil firefish (*P. miles* Bennett, 1829). Studies have reported increases in lionfish sp. abundance correlate with significant

[1] This has recently been redefined as the 'deep reef refuge hypothesis' (Bongaerts et al. 2017) following the classification of "refugia" by Keppel et al. (2012) as "large geographic areas offering an escape over evolutionary time scales".

declines in prey fishes (Albins and Hixon, 2008; Morris and Green, 2012). Lionfish are known to occupy the depth ranges of the proposed study sites (~30 - 70 m) and have been observed as deep as 304 m on recent submersible dives (Gress et al., 2017). However, little is known about their potential effect on fish biodiversity or the population structure of their prey species on Bermudan mesophotic reefs. Andradi-Brown et al. (2017b) reported larger lionfish being recorded in both western Atlantic and Pacific MCEs when compared to adjacent shallow reefs. This raises critical questions with respect to conservation and management approaches since lionfish will also be afforded the benefits of the hypothesised greater ecological stability provided by MCEs.

1.2 Mesophotic coral ecosystems

Mesophotic coral ecosystems (MCEs; Glynn, 1996; Riegl and Piller, 2003) are reef systems found in the mesophotic zone, ‘meso’ for middle and ‘photic’ for light. These ecosystems are “characterized by the presence of light-dependent corals and associated communities that are typically found at depths ranging from 30 to 40 m and extending to over 150 m in tropical and subtropical regions. The dominant benthic communities providing structural habitat in the mesophotic zone can be comprised of coral, sponge, and algal species (Hinderstein et al., 2010). MCEs are often extensions of shallow-water reef communities (SWRs; Hinderstein et al., 2010) with many common species shared across the two communities. Demonstrated commonality of species, along with the suggestion that MCEs could be buffered from anthropogenic (e.g., ocean warming and acidification) and natural disturbances (Bongaerts et al., 2010; Hinderstein et al., 2010) has driven an increase in MCE themed workshops and publications over the last decade (Turner et al., 2017). Advances in research technology (e.g., rebreather diving, ROVs, baited cameras) have allowed researchers greater access to MCEs to investigate a variety of research areas including the connectivity, biodiversity, conservation and management and the ecology and biology of mesophotic species (Bridge et al., 2012; Slattery and Lesser, 2012; Kahng et al., 2014). The assumed reduction of anthropogenic and natural threats across MCEs coupled with the potential to act as a refuge for SWR

species and provide source larvae (re-seeding potential), led to the ‘deep reef refugia hypothesis’ (DRRH; Glynn, 1996; Bongaerts et al., 2010). This hypothesis formalized the concept proposed by Hughes and Tanner (2000) and further developed by Riegl and Piller (2003). Studies have demonstrated that mesophotic reefs are able to mitigate localised disturbances to some extent (Sinniger et al., 2013; Smith et al., 2016). Work by Cinner et al. (2016) concluded that proximity to deep-water refuges correlated with areas of increased reef health based on environmental and socioeconomic metrics. Genetic connectivity between shallow-mesophotic coral communities has exhibited ambiguous patterns to date (Serrano et al., 2014), thus inhibiting a general consensus on the function of MCEs in shallow reef benthic community recovery (Baker et al., 2016a; Bongaerts et al., 2017). To further inhibit the refuge concept, various studies have identified faunal breaks leading to MCEs often being divided into “upper” and “lower” depth zones (Bongaerts et al., 2010, 2015; Kahng et al., 2010; Slattery and Lesser, 2012; Bejarano et al., 2014; Baker et al., 2016a; Loya et al., 2016; Pinheiro et al., 2016; Rosa et al., 2016; Baldwin et al., 2018; Rocha et al., 2018). However, various studies have demonstrated species overlap between MCE and SWR fish populations (Loya et al., 2016). It can be assumed the faunal breaks are not ubiquitous and vary geographically. See Pyle et al. (2019) for an in-depth discussion on the current status of mesophotic depth categorisation. Despite the identification of faunal breaks there remains a consensus within the scientific community that MCEs have significant ecological importance for reef fishes through providing refuge (Loya et al., 2016) from fishing pressure (Bejarano et al., 2014; Lindfield et al., 2014) and as spawning aggregations for shallow reef fish species (Nemeth, 2005; Kadison et al., 2006; Luckhurst, 2010).

1.3 Invasive lionfish: threats to Bermudan mesophotic biodiversity

The colonization of the tropical and subtropical western Atlantic, Caribbean Sea and Gulf of Mexico by the Indo-Pacific lionfishes (*Pterois volitans* (Linnaeus 1758) and *P. miles* (Bennett 1828)), represents one of the fastest reported invasions for a marine

species to date (Schofield, 2010). Lionfish[2] were introduced off the east coast of Florida U.S.A in early 1980s and first observed in Bermuda in 2000 (Whitfield et al., 2002). Schofield, (2009, 2010) and Hixon et al. (2016) provide in-depth descriptions of the lionfish invasion throughout this region.

Lionfish are opportunistic generalist predators that consume a wide range of native fishes and invertebrates (Morris and Akins, 2009; Côté et al., 2013). A recent study of stomach content analysis demonstrated the same generalist-feeding pattern for lionfish in Bermuda (Eddy et al., 2016). This feeding strategy combined with prey naivety, a lack of predators and extensive thermal tolerance (Morris and Akins, 2009) has led to numerous accounts of negative impacts on native fish populations, primarily significant declines in prey fishes (Albins and Hixon, 2008; Green et al., 2012; Côté et al., 2013; Ballew et al., 2016). Like many reef fish species, lionfish exhibit ontogenetic migrations with juveniles found in shallow habitats (seagrasses, mangroves and shallow reefs) before migrating to deeper reef habitats (Claydon et al., 2012). Lionfish have been recorded on Bermudan MCEs (Eddy et al., 2016; Pinheiro et al., 2016; Andradi-Brown et al., 2017b; Goodbody-Gringley et al., 2019b) and recently observed at 304 m (Gress et al., 2017) during submersible dives during the 2016 Mission I: XL Catlin Deep Ocean Survey — Nekton mission to the Northwest Atlantic and Bermuda (www.nektonmission.org). Baker et al., (2016a) suggested these populations could be a potential range extension due to ontogenetic migration. Andradi-Brown et al., (2017b) highlighted the potential threats the presence of lionfish can have on mesophotic communities and the ecological services they provide. Whilst the detrimental effects lionfish can have on shallow reef fish communities has been demonstrated (Albins and Hixon, 2008; Green et al., 2012; Côté et al., 2013; Ballew et al., 2016), little is known about the effects on mesophotic fish populations. Andradi-Brown et al., (2017b) reported larger lionfish being recorded in both western Atlantic and Pacific MCEs when compared to adjacent shallow reefs. More specifically the same study found lionfish had higher densities on Bermudan mesophotic reefs (~ 250 fish/ha, ranging from 0-1100 fish/ha;

[2] Lionfish refers to the 2 allopatric sibling species *Pterois volitans* and *P. miles*.

(Eddy et al., 2016) than adjacent shallow water reefs. However, these densities were not ubiquitous across these mesophotic ecosystems with dense aggregations of lionfish being found at a few select 60 m depth locations (Goodbody-Gringley et al., 2018) during a Darwin Plus grant entitled the Bermuda Invasive Lionfish Control Initiative (DPLUS001) funded by the UK's Department of Environment, Food and Rural Affairs (DEFRA). These dense aggregations of lionfish later termed "hotspots", raise critical questions with respect to conservation and management approaches since lionfish will also be afforded any "refuge" benefits (Lindfield et al., 2014) provided by MCEs especially from culling programs (i.e., a reduction in fishing pressure; Andradi-Brown et al., 2017b, 2017a).

Following the findings of project DPLUS001, a subset of the identified 60 m mesophotic lionfish "hotspots" at the eastern side of the Bermuda reef system were utilised by two consecutive EU BEST 2.0 Projects which assessed the effectiveness of lionfish management through targeted removal by technical SCUBA divers (Project 1634) and nonselective non-containment clam-shell traps (Project 2274). Whilst these projects focused on invasive species management, this thesis focuses on the biodiversity and community structure of mesophotic ichthyofauna and the overall trophic balance and calcification status of these ecosystems.

1.4 Study Locations

The mesophotic locations studied in this thesis correspond to those utilised by BEST 2.0 Projects 1634 & 2274 which in turn were defined a posteriori following the findings of a Darwin Plus (DPLUS001) Lionfish control initiative project. Locations refer to the general area of interest whilst sites refer to discrete sampling points within each location. Three locations (Figure 1.1; BT1, BT2, BT3) ~10 km apart was established to investigate both spatial and temporal variability of mesophotic ichthyofauna and allow for increased spatial determination of oceanographic conditions of MCEs, specifically the biogeochemical processes occurring at these depths. Within each location there are six discrete sites ~ 350 m apart (Dorman et al. 2012), three "deep" outer sites at ~ 60 m depth and three inner "shallow" sites at ~ 30 - 40 m depth.

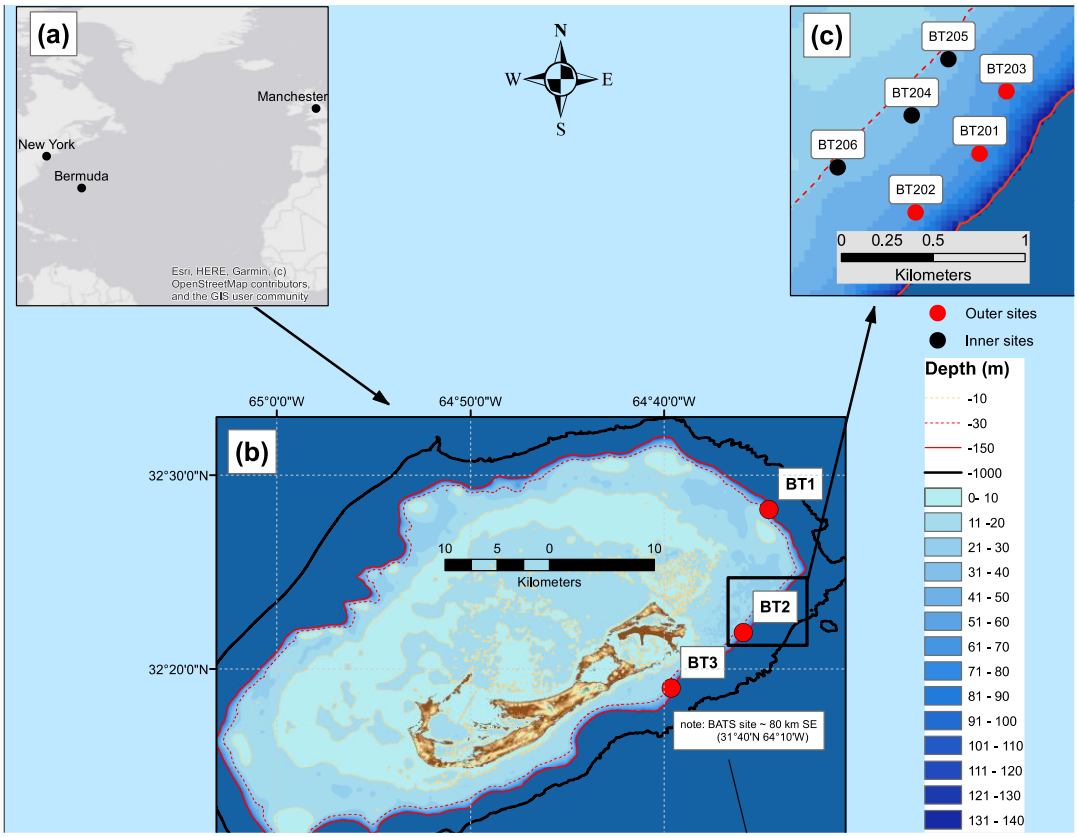

Figure 1.1. (**a**) Map showing geographical location of Bermuda. (**b**) Bathymetric map of Bermuda illustrating the study locations (red circles) and proximity to land and open ocean, 10 m contour line in orange, 30 m depth contour dashed red line, 150 m depth solid red line, 1000 m contour solid black line. (**c**) typical spatial orientation of 30 – 40 m (black circles) and 60 m sites (red circles) studied per location, 30 m depth contour dashed red line, 150 m depth solid red line.

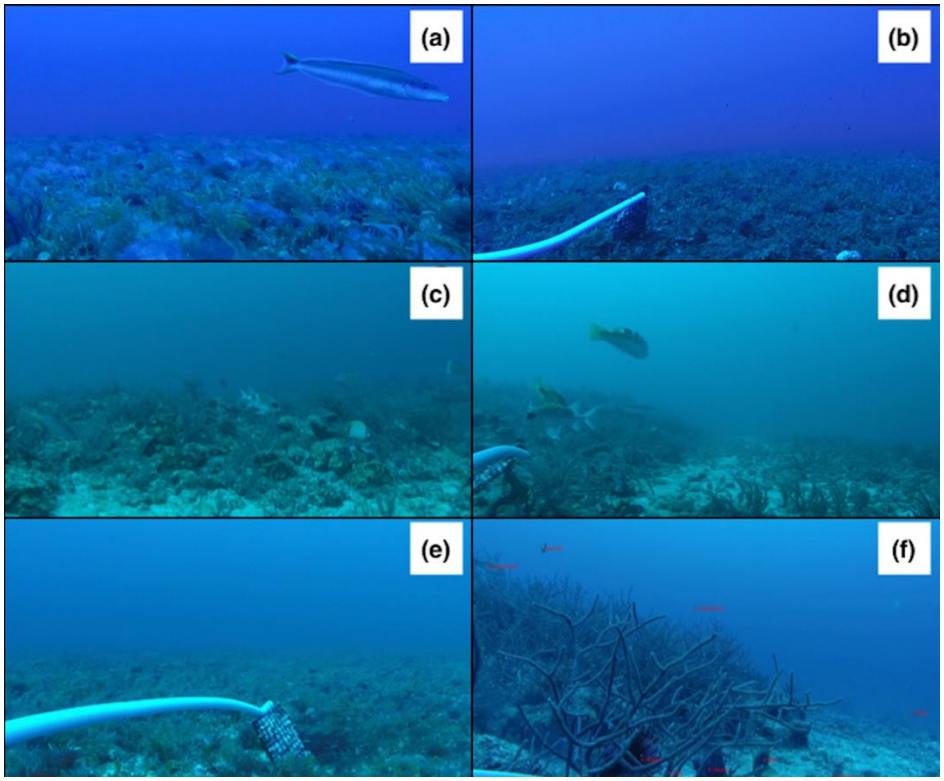

Figure 1.2. Example images of benthos recorded by BRUVs from 60 m study sites, (**a**) site BT101; (**b**) site BT102; (**c**) site BT201; (**d**) site BT202; (**e**) site BT302; (**f**) site BT302.

1.5 Mesophotic fish biodiversity

Ichthyologists recognise mesophotic reef fish fauna as those tropical and sub-tropical demersal and cryptic species (moray eels, blennies, gobies) that inhabit and utilise mesophotic benthic communities (Baldwin et al., 2018). These fish communities represent a combination of shallow water species with a wide depth distribution, those confined to mesophotic depths and deeper species that migrate into mesophotic ecosystems (Bejarano et al., 2014; Papastamatiou et al., 2015a; Baker et al., 2016a; Pinheiro et al., 2016; Rosa et al., 2016; Baldwin et al., 2018; Rocha et al., 2018). The mobility and potential overlaps in depth distribution of reef ichthyofauna communities (Actinopterygii and Chondrichthyes) combined with the ecosystem services (Holmlund and Hammer, 1999) generated by fish populations, allow for a rigorous investigation of

(1) mesophotic fish biodiversity, (2) levels of connectivity between MCEs and adjacent ecosystems (e.g., shallow reef and deep-sea).

To date, all families of fish recorded using traditional survey methods on Atlantic mesophotic reefs are common to SWRs (García-Sais et al., 2010; Baker et al., 2016a; Goodbody-Gringley et al., 2019b). Differences in fish community structure (increases in planktivores and macro carnivore densities with increased depth) are now providing biological evidence for the division between shallow and mesophotic reefs (Muñoz et al., 2017). Traditionally the upper boundary of MCEs has been determined by the limitation of conventional SCUBA diving (maximum depth 39 m). Additionally, there are distinct differences in species composition and abundance that result in a faunal break between ~60 and 90 m (Garcia-Sais, 2010; Bryan et al., 2013; Bejarano et al., 2014; Andradi-Brown et al., 2016b; Pinheiro et al., 2016; Rosa et al., 2016; Baldwin et al., 2018; Rocha et al., 2018; Goodbody-Gringley et al., 2019b) that are used to define the “upper” and “lower” mesophotic zones for certain fish species. Literature suggests these breaks occur at ~ 60 m in Atlantic MCEs (Pinheiro et al., 2016; Semmler et al., 2017) and ~ 90 m for Pacific MCEs (Pyle et al., 2016). However, Baldwin et al. (2018) determined a distinct faunal break at ~ 80 m for Curaçao during an investigation of what has been termed the “rariphotic” zone: the demersal zone between the mesophotic and aphotic regions. Whilst the research community agrees there are distinct faunal breaks for both benthic and fish communities, it cannot agree on the refugia potential (Bongaerts et al., 2017) of mesophotic reefs. Below is a selection of recent studies to illustrate the conflicting findings on this topic. Rocha et al. (2018) determined that MCEs are ecologically distinct from shallow reefs with a limited refuge capacity. Studies by Muñoz et al. (2017) and Semmler et al. (2017) determined Gulf of Mexico (USA) mesophotic reefs have the capacity to serve as refuges for SWR species. However, the study by Muñoz et al., (2017) was confined to the upper mesophotic region of the reef system (< 45 m). The study by Semmler et al. (2017) concluded mid and lower mesophotic habitats (60 -150 m) of the same reef system to have the capacity to act as a refuge due to having a 15-25% taxonomic overlap (based on co-presence of species). Bongaerts et al. (2017) redefined the deep reef refuge hypothesis (DRRH; Bongaerts et al., 2010) to one that was deemed relevant for individual species but should not be considered a ubiquitous function for

mesophotic communities. The increasing examples of geographic endemism being discovered within mesophotic fish species (Brokovich et al., 2008; Kane et al., 2014; Anderson et al., 2016; Pyle et al., 2016; Anderson and David Johnson, 2017; Kosaki et al., 2017) would support this redefined concept. A significant proportion of these endemic species have been identified in the Hawaiian Archipelago (Pyle et al., 2016). Pinheiro et al. (2016) and Goodbody-Gringley et al. (2019) recorded the endemic species Bermuda chromis (*Chromis bermudae* Nichols 1920) and Bermuda porgy (*Diplodus bermudensis* Caldwell 1965) on Bermudan mesophotic reefs. To date, there have been fewer records of Atlantic MCE endemic fish species in comparison to the Pacific region (Baker et al., 2016a).

1.6 Community assessments

1.6.1 Environmental DNA

The decreasing cost and increasing reliability of targeting environmental DNA (eDNA) through next-generation sequencing (NGS) is rapidly making eDNA-based studies a tool of choice for ecologists and natural resource managers. Taberlet et al. (2018) defined eDNA as a complex mixture of genomic DNA from many different organisms found in an environmental sample. These environmental samples are generally defined as the medium the DNA is being extracted from for example, water, soil or marine sediments. The principles of what is now known as DNA metabarcoding (Riaz et al., 2011) originate from the study of microbes in sediments (Ogram et al., 1987). The first known publication on metabarcoding was a study on the diversity of bacterioplankton in the Sargasso Sea published by Giovannoni et al.1990). Environmental DNA studies can generally be divided into two approaches, those that target single-species detection through a quantitative PCR approach (qPCR) and those that are designed to detect multiple taxa. Thanks to the development of next-generation sequencing (NG; Shendure and Ji, 2008), eDNA assessments do not have to be limited to a single-species approach and can target multiple-species (multiple-taxon) using generic primers for the target group species. The method is non-invasive and likely to have a higher detection rate of rare and

cryptic species unlike trawling methodologies that are traditionally used for fisheries population studies. The development of eDNA protocols for aquatic environments begin in the mid 2000's (Ficetola et al., 2008; Thomsen et al., 2012). The aquatic medium provides ample opportunity for the detection of a species or community due to the release of genetic material such as faeces, mucus, skin cells and gametes (Thomsen et al., 2012; Kelly et al., 2014) by all organisms present in the water. Due to the limited persistence of genetic material in aquatic systems (2 - 48 hours for marine environments, high salinity; Murakami et al., 2019; Ely et al., 2021), it offers the potential to collect ecological community data of high local fidelity (Collins et al., 2018).

Environmental DNA is proving to be a robust multi species detection approach for biodiversity monitoring in a wide range of environments (Bohmann et al., 2014; Kelly et al., 2014, 2016; Port et al., 2016a; Deiner et al., 2017) including marine systems (Thomsen et al., 2012; Miya et al., 2015). The collection of eDNA sequences have proven successful for determining organismal biodiversity and community structure across differing time scales (Thomsen and Willerslev, 2015), environmental gradients (Kelly et al., 2016), assessing the effectiveness of protective areas and detecting elusive megafauna (Bakker et al., 2017; Gargan et al., 2017; Baker et al., 2018; Boussarie et al., 2018). Whilst metrics such as species richness are not dissimilar to more traditional assessment methods, the speed and "completeness" of eDNA metabarcoding has the potential to be far greater. This was demonstrated by Drummond et al. (2015) in a near complete study of flora and fauna from topsoil. Given the rates at which biodiversity is changing globally (Butchart et al., 2010), the emergence of eDNA monitoring could provide cost effective rapid assessments of biodiversity departures from established baselines (Deiner et al., 2017). This in turn could deliver an early warning for changes in ecosystem function(s) and ultimately provide data to allow effective management at the ecosystem scale (Bohan et al., 2017). Another important application for eDNA monitoring is the detection of invasive species. Ficetola et al. (2008) demonstrated the method's uses through the detection of the invasive North American Bullfrog (*Rana catesbeiana* Shaw 1802) in France. Environmental DNA monitoring can provide an early warning detection to changes in biodiversity such as the detection of invasive species (Deiner et al., 2017) and human-ecosystem interactions (Kelly et al., 2016). Environmental DNA

monitoring provides an extensive taxonomic coverage that is applicable to both basic and applied sciences (Kelly et al., 2016).

As outlined in Section 1.5, Actinopterygii and Chondrichthyes were the target taxa for this thesis. The MiFish universal primers (Miya et al., 2015, 2020; ca. 171 bp fragments) which target the hypervariable region of the 12S ribosomal RNA gene marker were selected to maximise detection of multiple fish taxa from low template concentration extra-organismal DNA obtained from seawater samples. The 12S ribosomal gene provides the benefit of conserved priming sites (Deagle et al., 2014) and allows for comprehensive amplification of an extensive array of fish taxa. A study by of eDNA fragment size (Bylemans et al., 2018) demonstrated that shorter mitochondrial eDNA fragments were more abundant than longer fragments in water when fish are present, with no discernible differences in decay rates between the fragment lengths. These findings indicate shorter mitochondrial fragments are likely to be the better alternative for eDNA metabarcoding applications. The overall performance of the MiFish primer assay in terms of universality, specificity, and reproducibility (Collins et al., 2019; Zhang et al., 2020) has led them to become one of the most universally adopted assays for fish biodiversity studies having been used for eDNA metabarcoding applications in multiple aqueous environments (Jeunen et al., 2019; Miya et al., 2020).

Whilst the performance of the MiFish assay has been demonstrated in recent comparative primer studies (Collins et al., 2019; Zhang et al., 2020), it is known to not be truly universal for all fishes as indicated by the development of separate assays for elasmobranchs (MiFish-E, Miya et al., 2015). The application of multiple primer sets and/or markers can be used to overcome primer amplification bias and improve total biodiversity detection (Stat et al., 2017; Zhang et al., 2020) however, Collins et al., (2019) suggested a single assay for a specific taxon (i.e., fishes) should prove sufficient for analysing taxon specific community diversity, e.g., fishes. To determine the performance of the MiFish U/E assays for Bermudan reef fish communities, preliminary paired MiFish-U/MiFish-E trials (data not presented in this thesis) were conducted at the local aquarium by sampling tanks of known communities consisting of common local marine fishes including elasmobranchs. The MiFish-U primers successfully detected the presence of elasmobranchs housed in the aquaria, whilst the MiFish-E primers did not. These

preliminary findings in addition to the increased economic costs associated with a multiple assay study, were the justification for proceeding with a single universal assay approach.

Despite the ability of eDNA metabarcoding studies to significantly advance our knowledge of marine fish biodiversity, the current limitations of this approach (Thomsen and Willerslev, 2015; Yao et al., 2022) need to be acknowledged to allow for responsible reporting of these types of data. Whilst several studies have demonstrated the effectiveness of eDNA based studies for determining the functional and phylogenetic diversity of fish communities (Aglieri et al., 2020; Marques et al., 2021), alternative approaches (e.g., capture-based, behaviour and life-stage studies) are required to generate essential information on fish characteristics. Environmental DNA samples often contain degraded DNA (Collins et al., 2018) of target taxa as well as significant quantities of non-target DNA that may co-amplify (Stat et al., 2017) despite the use of universal primers. The introduction of false positives through contamination is one of the primary risks to low template concentration DNA analysis (Champlot et al., 2010). However, the adoption of strict clean-lab protocols for example, the use of separate labs for pre- and post- polymerase chain reaction (PCR) steps (Miya et al., 2020) and inclusion of blanks at all steps of the laboratory analytical process (Thomsen and Willerslev, 2015; Yao et al., 2022) can significantly constrain these risks. The inhibition of DNA amplification by organic material during PCR-based assays can lead to reduced eDNA yield (Hunter et al., 2019) and potentially false negatives. It has become common practice to chemically remove inhibitors prior to PCR during the DNA isolation/extraction phase using cationic detergents, for example Cetyltrimethylammonium Bromide (Hunter et al., 2019). Whilst universal primers such as the MiFish assay used by this study have been designed to equally co-amplify target taxa, they do exhibit amplification bias which can lead to certain species (in particular rare taxa) amplifying less efficiently than others (Jørgensen et al., 2012; Deagle et al., 2014; Miya et al., 2020). A reduction in PCR cycles numbers (30 cycles used in Chapters 3 and 4 PCR conditions) can mitigate against amplification bias (Krehenwinkel et al., 2017) since template DNA is exponentially amplified with each cycle, therefore the bias would be a function of cycle numbers (Suzuki and Giovannoni, 1996). It has been recommended that in vitro tests (Zhang et al., 2020) of eDNA samples from the study area be performed to evaluate primer performance (Yao et al., 2022).

Preliminary results from such tests can be compared to those of direct observations (Miya et al., 2020) of species found within the study area (e.g., a known community housed within an aquarium setting) to ascertain any potential primer affinity bias. Errors associated with PCR amplification (Doi et al., 2019; Miya et al., 2020), NGS (e.g. index tag jumps; Schnell et al., 2015) and bioinformatic processing (Rossberg et al., 2014; Doi et al., 2019) can lead to the creation of technical artifacts (Coissac et al., 2012; Deiner et al., 2017) and have repercussions for the translation of NGS data to taxonomic assignment and/or to determining the sample origin of amplicons. Such errors could lead to the incorrect ecological conclusion through the misinterpretation of a false positive of the associated taxon (Taberlet et al., 2018). The interpretation of eDNA sequences to taxonomic assignment ultimately relies on the completeness of available reference database which are often developed on an ad hoc basis (Collins et al., 2019). For ribosomal markers such as the MiFish assay, there can still be a lack of interspecific variation within some taxa (Thomsen et al., 2016; Andruszkiewicz et al., 2017; Collins et al., 2019; Miya et al., 2020) that limit the assignment of assembled Operational Taxonomic Units (OTUs) to species level. For certain taxa (e.g., Thunnus, South 1845 and Anguilla, Schrank 1798), this has led to the development of genus-specific primers (Miya et al., 2015; Takeuchi et al., 2019) to enable the correct species assignment. With the rapid uptake and adoption of eDNA metabarcoding for environmental science applications (Hering et al., 2018; Tsuji et al., 2019), it is inevitable that there will be a corresponding increase in taxonomic coverage of regional (Shen et al., 2019) and global reference databases.

Environmental DNA metabarcoding is highly effective at providing qualitative (binary presence-absence) fish diversity data (Yao et al., 2022). However, the quantitative ability of the methodology is currently unclear due to the taxa specific biases incurred by commonly used PCR approaches that can lead to inaccurate abundance estimates (Polz and Cavanaugh, 1998; Krehenwinkel et al., 2017; Kelly et al., 2019; Lamb et al., 2019). Additionally, these biases can be compounded by biotic factors directly related to eDNA production (Rourke et al., 2022) such as variations in taxa's DNA shredding rates, for example due to differences in age (Thomsen et al., 2016), physiological (Klymus et al., 2015) and behaviour patterns (Sassoubre et al., 2016). In addition, interactive effects

between biotic and abiotic variables are often identified that significantly influence eDNA concentration. Some of the most crucial abiotic factors that have direct effects on eDNA concentrations are hydrology (Harrison et al., 2019), water temperature (Takahara et al., 2012a; Lacoursière-Roussel et al., 2016), spatio-temporal variability (Takahara et al., 2012a; Shelton et al., 2019), eDNA decay rates (Sassoubre et al., 2016; Collins et al., 2018; Lamb et al., 2022) and eDNA sample methodology (Eichmiller et al., 2016; Lacoursière-Roussel et al., 2016). Despite these uncertainties, relative species abundances are often inferred in the literature based on proportional composition of sequence reads.

Various empirical studies have sought to demonstrate quantitative correlations between eDNA metabarcoding signals and multispecies abundances (Kelly et al., 2014; Evans et al., 2016; Hänfling et al., 2016; Port et al., 2016a; Saitoh et al., 2016; Shaw et al., 2016; Thomsen et al., 2016; Pont et al., 2018; Ushio et al., 2018; Sard et al., 2019; Blabolil et al., 2021). A recent review of the quantitative functionality of eDNA metabarcoding (Rourke et al., 2022), determined positive correlations between eDNA sequence read counts and fish abundance in 11 of the 12 studies assessed. However, results were not always consistent within the same study. For example, Shaw et al. (2016) determined a linear correlation between eDNA sequence abundance, and the physical numbers of fish caught by netting in one of two rivers sampled. The study by Hänfling et al. (2016) of three lentic fish communities, demonstrated a correlation with rank abundance estimates from gill-net surveys with eDNA read count data (proxy for relative abundance). However, the strength of these correlations varied across the three lakes sampled. Thomsen et al. (2016) reported variability in the strength of correlations between relative eDNA sequence abundance of marine fishes and bottom-trawl surveys.

To overcome such variations in results, one recent approach adopted by eDNA metabarcoding studies has been to incorporate an internal standard (ISD) into the eDNA processing procedure (Ushio et al., 2018; Harrison et al., 2021; Sato et al., 2021). This technique typically utilises foreign biological or synthetic DNA molecules added to all samples in equal absolute amounts (measured in moles) prior to sequencing. Harrison et al. (2021) advocate for the use of synthetic ISDs since the sequence will not occur naturally and therefore will be distinguishable from other sequences. By calculating the

ratio of the relative abundance of non-synthetic sequences within each sample to the relative abundance of the ISD, the non-synthetic sequences become proportional to the ISD and assume the same units. These values can be scaled to alternative units since the quantity of the ISD added to each sample is known (correction factor). Whilst the ISD technique is highly encouraging, the practice still has challenges, namely, the ISD must be indistinguishable from all naturally occurring template DNA within the study region. The point of introduction during the sample processing procedure and volume of ISD to be added is crucial as they can have adverse effects on performance (Harrison et al., 2021). Finally, the chosen ISD must behave in the same way as template DNA during the processing procedures (Hardwick et al., 2017). Internal standards can be prone to the same bias (e.g., primer affinity, PCR inhibition) that persist throughout eDNA processing. Whilst the use of ISDs has been a positive technical advancement that has enabled quantitative eDNA metabarcoding, it is still only possible for among-sample variation of specific taxon. The method does not currently allow for the comparison of abundance variation of different taxa either within or between samples (Harrison et al., 2021).

An alternative approach to generating quantitative sequence data applies stochastic labelling of the target gene with a random tag during a single primer extension prior to PCR amplification, otherwise known as quantitative sequencing (qSeq; Hoshino and Inagaki, 2017; Hoshino et al., 2021). After high throughput sequencing (HTS), the number of template sequences are estimated by Poisson distribution by counting the variation of random-sequence tags. In theory the qSeq technique has limited quantitative bias due to the introduction of the random tag prior to a two-step PCR process (Hoshino and Inagaki, 2017). However, the potential introduce of erroneous sequences could lead to overestimation of target sequences (Hoshino and Inagaki, 2017). To reduce the influence of such errors, it is recommended that number of sequence cycles be kept to a minimum for the quantification portion of the methodology. Hoshino et al. (2021) applied qSeq to eDNA sampled from aquaria housing five species of fish. During the four-day study, the eDNA quantification by qSeg was consistent with levels determined by digital PCR (dPCR), a precise methodology for single species quantification. The qSeq approach allows parallel taxonomic sequencing and quantification of multiple target taxa to occur at the same time (Hoshino and Inagaki, 2017). This technique highlights the

potential for future quantitative eDNA metabarcoding to be possible within a natural marine environment.

1.6.2 Baited underwater video systems

Baited Remote Underwater Video systems (BRUVs) are cost effective sampling units (Langlois et al., 2010) that produce robust spatially explicit quantitative data on reef ichthyofauna abundance and diversity. Whilst BRUVs have primarily been used for the assessment of demersal communities (Whitmarsh et al., 2017), they have been successfully used for pelagic species assessments (Santana-Garcon et al., 2014). The method has been used for various methodology comparative studies for example between Underwater Visual Census (UVC; Lowry et al., 2012) and Diver Operated Videos (DOVs; Langlois et al., 2010; Andradi-Brown et al., 2016b). The use of bait with a video camera deployment increases the number of species and individuals recorded (Harvey et al., 2007; Dorman et al., 2012). The presence of bait aggregates fish through olfactory, auditory (noises made by attracted fishes) and behavioural cues (Cappo et al., 2007) allowing researchers to count and measure target species. Video footage creates a permanent survey record that can be data mined at a later date. Observational data including metrics on behaviour (activities such as feeding and chasing conspecifics) can be recorded using EventMeasure (www.seagis.com.au); software specifically designed for logging and reporting events that occur in digital imagery. Videos can be analysed to provide a relative abundance metric defined as the maximum number of individuals per species seen at once during a 60-minute video or “MaxN”.

Despite the robust nature of BRUVs methodology for assessing fish assemblages, there can be inherent bias. The application of bait can be bias towards carnivorous fishes (Stobart et al., 2007; Lowry et al., 2012) which in turn may lead to small individuals exhibiting predator prey avoidance behaviour (Lowry et al., 2012). The distance fish are attracted to the BRUVs will be directly related to the dispersal of the bait plume (Lowry et al., 2012). Due to the hydrographically dynamic nature of marine environments, it is often beyond the scope of a project to attempt to quantify the dispersal of the bait plume prior to sampling efforts (Hardinge et al., 2013). To minimise the over estimation of a

population, the MaxN metric is a conservative estimate of relative abundance since it is not possible to differentiate between individuals until there are multiples within the field of view. In incidents where there are high abundances of fish around the bait, the MaxN metric may not correlate to true abundance due to screen saturation (Schobernd et al., 2014; Stobart et al., 2015). This occurs when additional fish are unable to physically fit in the field of view therefore leading to an underestimation of the population. Whilst BRUVs routinely provide imagery that allows for fish identification to family and genus level, it is not always possible to visually differentiate between closely related congeners within certain species, for example the two lionfish species *Pterois volitans* and *P. miles*. The orientation of BRUVs is stochastic in nature when landing on the benthos which can lead to the variability in the field of view and ultimately species of fish (e.g., cryptic species) and habitat type observed when attempting temporal studies of discrete survey sites.

1.7 Physicochemical environment of mesophotic reefs

Shallow coral reef systems support highly diverse and productive communities in tropical and sub-tropic nutrient limited environments (Morais and Bellwood, 2019). Determining the levels of oceanographic connectivity between mesophotic and adjacent shallow-water reefs is a key research priority for multiple research disciplines (e.g., biogeochemistry, coral reef ecology, fisheries management).

Fundamental information on thermal regimes and flow dynamics (interactions and feedbacks) that drive species distribution patterns and biogeochemical processes, will be required to understand the level of resilience coral reef ecosystems have to anthropogenic and natural stressors. The hypothesised reduction of anthropogenic (e.g., elevated sea surface temperatures and ocean acidification) and natural threats to MCEs has generated a significant level of research interest in mesophotic coral reefs. Broadly speaking, studies have concentrated on quantifying the “deep reef refuge hypothesis” through determining species distribution patterns and levels of genetic connectivity. Recent studies identify “ocean connectivity” as a key knowledge gap (Van Oppen et al., 2011; Serrano et al., 2014; Baker et al., 2016a) for coral reef science. The study by

Soares and Lucas (2018) on southern Atlantic MCEs concluded that baseline chemical and physical oceanography measurements are essential to examine the role of MCEs as refuges and should be a focus of future investigations. Understanding the level of connectivity (flow dynamics) of MCEs with shallow reefs has been classified as "High Priority" in the recent United Nations publication "Mesophotic Coral Ecosystems A lifeboat for coral reefs?" (Baker et al., 2016a). Mesophotic reefs are not resistant to thermal stress or coral bleaching[3] (Neal et al., 2014; Reed et al., 2014; Smith et al., 2016). The study by Smith et al. (2016) demonstrated Caribbean mesophotic corals have a reduced bleaching threshold that declines by 0.26 ^{o}C every +10 m. However, the same study suggested that strong internal waves might mitigate thermal stress effects under the correct conditions. Bleaching events have been recorded on mesophotic reefs that are subject to the influx of cold water and elevated surface waters through internal waves and vertical mixing (Bak et al., 2005; Smith et al., 2016). The mesophotic reefs of Palau experience daily temperature fluctuations (~ 10 ^{o}C, maximum ~ 20 ^{o}C; Wolanski et al., 2004; Colin, 2009; Colin and Lindfield, 2019) that can occur in semi-diurnal cycles (Wolanski et al., 2004). The several degrees Celsius changes over the course of 60 minutes is hypothesised to be the cause of the reduced biodiversity found on the reef slopes between 60 – 120 m. Whilst not as extreme as the Pacific region, rapid temperature fluctuations (drops of 1-3 ^{o}C over ~30 minutes) on Caribbean mesophotic reefs have been recorded in Curaçao (Bongaerts et al., 2015). The assumption is that upwelled cooler waters inject nutrients in the form of dissolved nutrients and suspended particles (Leichter et al., 1998, 2003; Wolanski et al., 2004) to both mesophotic and shallow water reefs. In a study of the population structure of the *Montastraea cavernosa* (Linnaeus 1767), Goodbody-Gringley et al. (2015) posited reductions in colony sizes at depth were a likely result of reduced light-dependent productivity due to nutrient limitation (nitrate and nitrite). However, enhanced growth rates of *Madracis aurentenra* (Locke et al., 2007) have been correlated with environmental variability associate with internal waves (Leichter et al., 1998). Lesser

[3] A physiological sublethal stress response of corals whereby the coral-algal symbiosis 'dissociates' leaving the corals white or 'bleached.'

et al. (2010) revealed evidence of a trophic switch in *M. cavernosa* from autotrophy to heterotrophy based on $\delta^{13}C$ signatures in both the animal tissue and skeleton. Trophic shifts between summertime net autotrophy and wintertime net heterotrophy have been between established for the shallow Bermuda reef system (Yeakel et al., 2015; Bates, 2017). Bates (2017) estimated the rate of net calcification and net heterotrophy increased by ~ 30% over a 20-year period (1996 – 2016). Both studies posited these shifts were due to nutrient inputs to the reef system due to increased offshore productivity with the caveat that no biogeochemical measurements were made extending directly off the shallow reef platform. The inference was made through direct comparisons of surface seawater samples (1 m depth) above shallow reefs and samples taken from the offshore Bermuda Atlantic Time-series Study site (BATS) ~80 km south of Bermuda (Figure 1.1).

The advection of biomass (e.g., plankton and particulate matter) and dissolved inorganic matter from oceanic sources on to mesophotic reefs would be expected due to the proximity of both ecosystems. Increases in both phytoplankton and zooplankton biomass have been documented at the BATS site (Steinberg et al., 2012). These allochthonous inputs enable coral heterotrophy and are a critical component of coral reef fish productivity which can be sustained through multiple heterotrophy trophic pathways (Chassot et al., 2010; Morais and Bellwood, 2019). Morais and Bell (2019) determined the primary energetic pathways for coral reef fish productivity to be derived via water column photosynthesis (41%; conversion of light energy into chemical energy) and from the epibenthic reef surface (29%; autotrophy and/or heterotrophy). Both pathways indicate the critical links between fish populations and biogeochemical processes that influence reef metabolism (Kavanagh and Galbraith, 2018a). However, it has been recognised that biogeochemical measurements for mesophotic reefs are a significant knowledge gap (Baker et al., 2016a; Hoegh-Guldberg et al., 2017; Turner et al., 2017).

1.8 Overarching Aims of the Thesis

This study aims to quantify biodiversity within a geographic range in Bermuda using rapid non-invasive methodologies. The use of complementary detection

methodologies coupled with biogeochemical measurements will potentially garner a more comprehensive inventory of the fish biodiversity and overall mesophotic ecosystem status than if only a single methodology was adopted. The investigation assessed the spatial and temporal variability of Bermudan mesophotic fish communities during an 18-month period by applying eDNA metabarcoding and BRUVs methodologies. These assessments were coupled with *in situ* environmental measurements to characterise biogeochemical processes that influence mesophotic reef metabolism (e.g., net ecosystem calcification and net ecosystem production). Shallow water reef metabolism has been extensively studies both *in situ* and under controlled laboratory conditions with the assumption that the findings are equally applicable to mesophotic reefs. To date, there have been no empirical studies of these processes. This study aims to explicitly address this knowledge gap through monthly measurements of in situ physicochemical measurements at three MCE locations ~10 km apart. These data will quantify the level of environmental fluctuation on both a spatial and temporal scale and determine the metabolic status of these reefs and establish the first biogeochemical dataset for mesophotic reefs.

1.8.1 Chapters

Chapter 2.

Understanding the threat of climate change on mesophotic coral ecosystems requires a fundamental understanding of the biogeochemical status of the environment. A suite of *in situ* biogeochemical measurements were made both spatially and temporally at three locations across a depth range to determine the calcification status (calcium carbonate accretion vs. dissolution) and trophic balance (primary production – autotrophic vs. heterotrophic respiration) of these reef systems.

Chapter 3.

Environmental DNA metabarcoding of the 12S region was used to characterise spatial and temporal variation in α- and β-diversity of mesophotic fish communities across a

depth range at the sampling locations established in Chapter 2. Taxa were subset based trophic position and in accordance with current management status. The abiotic variables characterised in Chapter 2 were used to determine if there was a relationship between eDNA signals (i.e., detected fish communities) and the environmental conditions of the sampled habitats.

Chapter 4.

The complementary methodologies of eDNA metabarcoding and baited remote underwater video systems (BRUVs) were utilised to investigate fish biodiversity at the 60 m depth zone, that has been determined to be the upper / lower mesophotic interface (faunal break) in other mesophotic regions. A subset of the eDNA metabarcoding survey data from Chapter 3 were compared to fish observations detected by BRUVs. The approach aimed to minimise the biases of each methodology and maximise community detection. To determine if habitat and/or abiotic metrics associations differed between the two methodologies, the relationships between both datasets were assessed independently.

1.9 References

Aglieri, G., Baillie, C., Mariani, S., Cattano, C., Calò, A., Turco, G., et al. (2020). Environmental DNA effectively captures functional diversity of coastal fish communities. *Mol Ecol*, 1–13. doi: 10.1111/mec.15661.

Albins, M. A., and Hixon, M. A. (2008). Invasive Indo-Pacific lionfish Pterois volitans reduce recruitment of Atlantic coral-reef fishes. *Mar Ecol Prog Ser* 367, 233–238. doi: 10.3354/meps07620.

Anderson, W. D., and David Johnson, G. (2017). Two new species of callanthiid fishes of the genus *Grammatonotus* (Percoidei: Callanthiidae) from Pohnpei, western Pacific. *Zootaxa* 4243, 187–194. doi: 10.11646/zootaxa.4243.1.10.

Anderson, W. D., Greene, B. D., and Rocha, L. A. (2016). *Grammatonotus brianne*, a new callanthiid fish from Philippine waters, with short accounts of two other *Grammatonotus* from the Coral Triangle. *Zootaxa* 4173, 289–295. doi: 10.11646/zootaxa.4173.3.7.

Andradi-Brown, D. A., Grey, R., Hendrix, A., Hitchner, D., Hunt, C. L., Gress, E., et al. (2017a). Depth-dependent effects of culling—do mesophotic lionfish populations undermine current management? *R Soc Open Sci* 4. doi: 10.1098/rsos.170027.

Andradi-Brown, D. A., Vermeij, M. J. A., Slattery, M., Lesser, M., Bejarano, I., Appeldoorn, R., et al. (2017b). Large-scale invasion of western Atlantic mesophotic reefs by lionfish potentially undermines culling-based management. *Biol Invasions* 19, 939–954. doi: 10.1007/s10530-016-1358-0.

Andradi-Brown, D., Macaya-Solis, C., Exton, D., Gress, E., Wright, G., and Rogers, A. (2016). Assessing caribbean shallow and mesophotic reef fish communities using Baited-Remote Underwater Video (BRUV) and diver-operated video (DOV) survey techniques. *PLoS One* 11. doi: 10.1371/journal.pone.0168235.

Andruszkiewicz, E. A., Starks, H. A., Chavez, F. P., Sassoubre, L. M., Block, B. A., and Boehm, A. B. (2017). Biomonitoring of marine vertebrates in Monterey Bay using eDNA metabarcoding. *PLoS One* 12. doi: 10.1371/journal.pone.0176343.

Bak, R. P. M., Nieuwland, G., and Meesters, E. H. (2005). Coral reef crisis in deep and shallow reefs: 30 years of constancy and change in reefs of Curacao and Bonaire. *Coral Reefs* 24, 475–479. doi: 10.1007/s00338-005-0009-1.

Baker, C. S., Steel, D., Nieukirk, S., and Klinck, H. (2018). Environmental DNA (eDNA) from the wake of the whales: Droplet digital PCR for detection and species identification. *Front Mar Sci* 5. doi: 10.3389/fmars.2018.00133.

Baker, E. K., Puglise, K. A., and Harris, P. T. (2016). Mesophotic coral ecosystems - a lifeboat for coral reefs?

Bakker, J., Wangensteen, O. S., Chapman, D. D., Boussarie, G., Buddo, D., Guttridge, T. L., et al. (2017). Environmental DNA reveals tropical shark diversity in contrasting levels of anthropogenic impact. *Sci Rep* 7. doi: 10.1038/s41598-017-17150-2.

Baldwin, C. C., Tornabene, L., and Robertson, D. R. (2018). Below the Mesophotic. *Sci Rep* 8. doi: 10.1038/s41598-018-23067-1.

Ballew, N. G., Bacheler, N. M., Kellison, G. T., and Schueller, A. M. (2016). Invasive lionfish reduce native fish abundance on a regional scale. *Sci Rep* 6, 1–7. doi: 10.1038/srep32169.

Bates, N. R. (2017). Twenty years of marine carbon cycle observations at Devils Hole Bermuda provide insights into seasonal hypoxia, coral reef calcification, and ocean acidification. *Front Mar Sci* 4, 1–23. doi: 10.3389/fmars.2017.00036.

Bejarano, I., Appeldoorn, R. S., and Nemeth, M. (2014). Fishes associated with mesophotic coral ecosystems in La Parguera, Puerto Rico. *Coral Reefs* 33, 313–328. doi: 10.1007/s00338-014-1125-6.

Blabolil, P., Harper, L. R., Říčanová, Š., Sellers, G., di Muri, C., Jůza, T., et al. (2021). Environmental DNA metabarcoding uncovers environmental correlates of fish communities in spatially heterogeneous freshwater habitats. *Ecol Indic* 126. doi: 10.1016/j.ecolind.2021.107698.

Bohan, D. A., Vacher, C., Tamaddoni-Nezhad, A., Raybould, A., Dumbrell, A. J., and Woodward, G. (2017). Next-Generation Global Biomonitoring: Large-scale, Automated Reconstruction of Ecological Networks. *Trends Ecol Evol* 32, 477–487. doi: 10.1016/j.tree.2017.03.001.

Bohmann, K., Evans, A., Gilbert, M. T. P., Carvalho, G. R., Creer, S., Knapp, M., et al. (2014). Environmental DNA for wildlife biology and biodiversity monitoring. *Trends Ecol Evol* 29, 358–367. doi: 10.1016/j.tree.2014.04.003.

Bongaerts, P., Frade, P. R., Hay, K. B., Englebert, N., Latijnhouwers, K. R. W., Bak, R. P. M., et al. (2015). Deep down on a Caribbean reef: Lower mesophotic depths harbor a specialized coral-endosymbiont community. *Sci Rep* 5. doi: 10.1038/srep07652.

Bongaerts, P., Ridgway, T., Sampayo, E. M., and Hoegh-Guldberg, O. (2010). Assessing the “deep reef refugia” hypothesis: Focus on Caribbean reefs. *Coral Reefs* 29, 1–19. doi: 10.1007/s00338-009-0581-x.

Bongaerts, P., Riginos, C., Brunner, R., Englebert, N., Smith, S. R., and Hoegh-Guldberg, O. (2017). Deep reefs are not universal refuges: Reseeding potential varies among coral species. *Sci Adv* 3. doi: 10.1126/sciadv.1602373.

Boussarie, G., Bakker, J., Wangensteen, O. S., Mariani, S., Bonnin, L., Juhel, J. B., et al. (2018). Environmental DNA illuminates the dark diversity of sharks. *Sci Adv* 4. doi: 10.1126/sciadv.aap9661.

Bridge, T. C. L., Fabricius, K. E., Bongaerts, P., Wallace, C. C., Muir, P. R., Done, T. J., et al. (2012). Diversity of Scleractinia and Octocorallia in the mesophotic zone of the Great Barrier Reef, Australia. *Coral Reefs* 31, 179–189. doi: 10.1007/s00338-011-0828-1.

Brokovich, E., Einbinder, S., Shashar, N., Kiflawi, M., and Kark, S. (2008). Descending to the twilight-zone: Changes in coral reef fish assemblages along a depth gradient down to 65 m. *Mar Ecol Prog Ser* 371, 253–262. doi: 10.3354/meps07591.

Bryan, D. R., Kilfoyle, K., Gilmore, R. G., and Spieler, R. E. (2013). Characterization of the mesophotic reef fish community in south Florida, USA. *Journal of Applied Ichthyology* 29, 108–117. doi: 10.1111/j.1439-0426.2012.02055.x.

Butchart, S. H. M., Walpole, M., Collen, B., Van Strien, A., Scharlemann, J. P. W., Almond, R. E. A., et al. (2010). Global biodiversity: Indicators of recent declines. *Science (1979)* 328, 1164–1168. doi: 10.1126/science.1187512.

Bylemans, J., Furlan, E. M., Gleeson, D. M., Hardy, C. M., and Duncan, R. P. (2018). Does Size Matter? An Experimental Evaluation of the Relative Abundance and

Decay Rates of Aquatic Environmental DNA. *Environ Sci Technol* 52, 6408–6416. doi: 10.1021/acs.est.8b01071.

Cappo, M., Harvey, E., and Shortis, M. (2007). Counting and measuring fish with baited video techniques - an overview. *Cutting-Edge Technologies in Fish and Fisheries Science*, 101–114. doi: 10.1007/978-1-62703-724-2_1.

Champlot, S., Berthelot, C., Pruvost, M., Andrew Bennett, E., Grange, T., and Geigl, E. M. (2010). An efficient multistrategy DNA decontamination procedure of PCR reagents for hypersensitive PCR applications. *PLoS One* 5. doi: 10.1371/journal.pone.0013042.

Chassot, E., Bonhommeau, S., Dulvy, N. K., Mélin, F., Watson, R., Gascuel, D., et al. (2010). Global marine primary production constrains fisheries catches. *Ecol Lett* 13, 495–505. doi: 10.1111/j.1461-0248.2010.01443.x.

Cinner, J. E., Huchery, C., MacNeil, M. A., Graham, N. A. J., McClanahan, T. R., Maina, J., et al. (2016). Bright spots among the world's coral reefs. *Nature* 535, 416–419. doi: 10.1038/nature18607.

Claydon, J. A. B. B., Calosso, M. C., and Traiger, S. B. (2012). Progression of invasive lionfish in seagrass, mangrove and reef habitats. *Mar Ecol Prog Ser* 448, 119–129. doi: 10.3354/meps09534.

Coissac, E., Riaz, T., and Puillandre, N. (2012). Bioinformatic challenges for DNA metabarcoding of plants and animals. *Mol Ecol* 21, 1834–1847. doi: 10.1111/j.1365-294X.2012.05550.x.

Colin, P. L. (2009). *Marine environments of Palau*. San Diego: Indo-Pacific Press.

Colin, P. L., and Lindfield, S. J. (2019). "Palau," in *Mesophotic Coral Ecosystems Coral Reefs of the World 12*, eds. Y. Loya, K. Puglise, and T. C. L. Bridge (Springer International Publishing), 285–320. doi: 10.1007/978-3-319-9275-0_16.

Collins, R. A., Bakker, J., Wangensteen, O. S., Soto, A. Z., Corrigan, L., Sims, D. W., et al. (2019). Non-specific amplification compromises environmental DNA metabarcoding with COI. *Methods Ecol Evol* 10, 1985–2001. doi: 10.1111/2041-210X.13276.

Collins, R. A., Wangensteen, O. S., O'Gorman, E. J., Mariani, S., Sims, D. W., and Genner, M. J. (2018). Persistence of environmental DNA in marine systems. *Commun Biol* 1, 185. doi: 10.1038/s42003-018-0192-6.

Connell, J. H. (1978). Diversity in tropical rain forests and coral reefs. *Science (1979)* 199, 1302–1310. doi: 10.1126/science.199.4335.1302.

Côté, I. M., Green, S. J., and Hixon, M. A. (2013). Predatory fish invaders: Insights from Indo-Pacific lionfish in the western Atlantic and Caribbean. *Biol Conserv* 164, 50–61. doi: 10.1016/j.biocon.2013.04.014.

Deagle, B. E., Jarman, S. N., Coissac, E., Pompanon, F., and Taberlet, P. (2014). DNA metabarcoding and the cytochrome c oxidase subunit I marker: Not a perfect match. *Biol Lett* 10, 2–5. doi: 10.1098/rsbl.2014.0562.

Deiner, K., Bik, H. M., Mächler, E., Seymour, M., Lacoursière-Roussel, A., Altermatt, F., et al. (2017). Environmental DNA metabarcoding: Transforming how we survey animal and plant communities. *Mol Ecol* 26, 5872–5895. doi: 10.1111/mec.14350.

Doi, H., Fukaya, K., Oka, S. ichiro, Sato, K., Kondoh, M., and Miya, M. (2019). Evaluation of detection probabilities at the water-filtering and initial PCR steps in environmental

DNA metabarcoding using a multispecies site occupancy model. *Sci Rep* 9, 1–8. doi: 10.1038/s41598-019-40233-1.

Dorman, S. R., Harvey, E. S., and Newman, S. J. (2012). Bait effects in sampling coral reef fish assemblages with stereo-BRUVs. *PLoS One* 7, 1–12. doi: 10.1371/journal.pone.0041538.

Drummond, A. J., Newcomb, R. D., Buckley, T. R., Xie, D., Dopheide, A., Potter, B. C. M., et al. (2015). Evaluating a multigene environmental DNA approach for biodiversity assessment. *Gigascience* 4. doi: 10.1186/s13742-015-0086-1.

Eddy, C., Pitt, J., Morris, J. A., Smith, S., Goodbody-Gringley, G., and Bernal, D. (2016). Diet of invasive lionfish (Pterois volitans and P. miles) in Bermuda. *Mar Ecol Prog Ser* 558, 193–206. doi: 10.3354/meps11838.

Eichmiller, J. J., Miller, L. M., and Sorensen, P. W. (2016). Optimizing techniques to capture and extract environmental DNA for detection and quantification of fish. *Mol Ecol Resour* 16, 56–68. doi: 10.1111/1755-0998.12421.

Ely, T., Barber, P. H., Man, L., and Gold, Z. (2021). Short-lived detection of an introduced vertebrate eDNA signal in a nearshore rocky reef environment. *PLoS One* 16. doi: 10.1371/journal.pone.0245314.

Evans, N. T., Olds, B. P., Renshaw, M. A., Turner, C. R., Li, Y., Jerde, C. L., et al. (2016). Quantification of mesocosm fish and amphibian species diversity via environmental DNA metabarcoding. *Mol Ecol Resour* 16, 29–41. doi: 10.1111/1755-0998.12433.

Ficetola, G. F., Miaud, C., Pompanon, F., and Taberlet, P. (2008). Species detection using environmental DNA from water samples. *Biol Lett* 4, 423–425. doi: 10.1098/rsbl.2008.0118.

Fisher, R., O'Leary, R. A., Low-Choy, S., Mengersen, K., Knowlton, N., Brainard, R. E., et al. (2015). Species richness on coral reefs and the pursuit of convergent global estimates. *Current Biology* 25, 500–505. doi: 10.1016/j.cub.2014.12.022.

Garcia-Sais, J. R. (2010). Reef habitats and associated sessile-benthic and fish assemblages across a euphotic-mesophotic depth gradient in Isla Desecheo, Puerto Rico. *Coral Reefs* 29, 277–288. doi: 10.1007/s00338-009-0582-9.

García-Sais, J. R., Castro-Gomez, R. L., Sabater-Clavell, J., Esteves, R., Williams, S., and Carlo, M. (2010). Mesophotic benthic habitats and associated marine communities at Abrir La Sierra, Puerto Rico. *Differences*, 122.

Gargan, L. M., Morato, T., Pham, C. K., Finarelli, J. A., Carlsson, J. E. L., and Carlsson, J. (2017). Development of a sensitive detection method to survey pelagic biodiversity using eDNA and quantitative PCR: a case study of devil ray at seamounts. *Mar Biol* 164. doi: 10.1007/s00227-017-3141-x.

Giovannoni, S. J. ;, Britschgi, T. B. ;, Moyer, C. L. ;, and Field, K. G. K. G. (1990). Genetic diversity in Sargasso Sea bacterioplankton. *Nature* 345, 60–63. doi: 10.1038/345060a0.

Glynn, P. W. (1996). Coral reef bleaching: Facts, hypotheses and implications. *Glob Chang Biol* 2, 495–509. doi: 10.1111/j.1365-2486.1996.tb00063.x.

Goodbody-Gringley, G., Marchini, C., Chequer, A. D., and Goffredo, S. (2015). Population structure of Montastraea cavernosa on shallow versus mesophotic reefs in Bermuda. *PLoS One* 10. doi: 10.1371/journal.pone.0142427.

Goodbody-Gringley, G., Noyes, T., and Smith, S. R. (2019). "Bermuda," in *Mesophotic Coral Ecosystems, Coral Reefs of the World 12*, eds. L. Yossi, K. A. Puglise, and T.

Bridge (Springer International Publishing), 31–45. doi: 10.1007/978-3-319-92735-0_2.
Goodbody-Gringley, G., Pitt, J. M., Eddy, W. C., Chequer, A., Noyes, T., Blanco-bercial, L., et al. (2018). Assessment and Management of Invasive Lionfish Populations in Bermuda. in (San Andres, Columbia: Proceedings of the 71st Gulf and Carribean Fisheries Institute), 0–3.
Green, S. J., Akins, J. L., Maljković, A., and Côté, I. M. (2012). Invasive lionfish drive Atlantic coral reef fish declines. *PLoS One* 7. doi: 10.1371/journal.pone.0032596.
Gress, E., Andradi-Brown, D. A., Woodall, L., Schofield, P. J., Stanley, K., and Rogers, A. D. (2017). Lionfish (Pterois spp.) invade the upper- bathyal zone in the western Atlantic. *PeerJ* 2017. doi: 10.7717/peerj.3683.
Hänfling, B., Handley, L. L., Read, D. S., Hahn, C., Li, J., Nichols, P., et al. (2016). Environmental DNA metabarcoding of lake fish communities reflects long-term data from established survey methods. *Mol Ecol* 25, 3101–3119. doi: 10.1111/mec.13660.
Hardinge, J., Harvey, E. S., Saunders, B. J., and Newman, S. J. (2013). A little bait goes a long way: The influence of bait quantity on a temperate fish assemblage sampled using stereo-BRUVs. *J Exp Mar Biol Ecol* 449, 250–260. doi: 10.1016/j.jembe.2013.09.018.
Hardwick, S. A., Deveson, I. W., and Mercer, T. R. (2017). Reference standards for next-generation sequencing. *Nat Rev Genet* 18, 473–484. doi: 10.1038/nrg.2017.44.
Harrison, J. B., Sunday, J. M., and Rogers, S. M. (2019). Predicting the fate of eDNA in the environment and implications for studying biodiversity. *Proceedings of the Royal Society B: Biological Sciences* 286. doi: 10.1098/rspb.2019.1409.
Harrison, J. G., John Calder, W., Shuman, B., and Alex Buerkle, C. (2021). The quest for absolute abundance: The use of internal standards for DNA-based community ecology. *Mol Ecol Resour* 21, 30–43. doi: 10.1111/1755-0998.13247.
Harvey, E. S., Cappo, M., Butler, J. J., Hall, N., and Kendrick, G. A. (2007). Bait attraction affects the performance of remote underwater video stations in assessment of demersal fish community structure. *Mar Ecol Prog Ser* 350, 245–254. doi: 10.3354/meps07192.
Hering, D., Borja, A., Jones, J. I., Pont, D., Boets, P., Bouchez, A., et al. (2018). Implementation options for DNA-based identification into ecological status assessment under the European Water Framework Directive. *Water Res* 138, 192–205. doi: 10.1016/j.watres.2018.03.003.
Hinderstein, L. M., Marr, J. C. A., Martinez, F. A., Dowgiallo, M. J., Puglise, K. A., Pyle, R. L., et al. (2010). Theme section on “Mesophotic Coral Ecosystems: Characterization, Ecology, and Management.” *Coral Reefs* 29, 247–251. doi: 10.1007/s00338-010-0614-5.
Hixon, M. A., Green, S. J., Albins, M. A., Akins, J. L., and Morris, J. A. (2016). Lionfish: A major marine invasion. *Mar Ecol Prog Ser* 558, 161–165. doi: 10.3354/meps11909.
Hoegh-Guldberg, O., Poloczanska, E. S., Skirving, W., and Dove, S. (2017). Coral reef ecosystems under climate change and ocean acidification. *Front Mar Sci* 4. doi: 10.3389/fmars.2017.00158.
Holmlund, C. M., and Hammer, M. (1999). Ecological Economics Ecosystem services generated by fish populations. *Ecological Economics* 29, 253–268.

Hoshino, T., and Inagaki, F. (2017). Application of stochastic labeling with random-sequence barcodes for simultaneous quantification and sequencing of environmental 16S rRNA genes. *PLoS One* 12. doi: 10.1371/journal.pone.0169431.
Hoshino, T., Nakao, R., Doi, H., and Minamoto, T. (2021). Simultaneous absolute quantification and sequencing of fish environmental DNA in a mesocosm by quantitative sequencing technique. *Sci Rep* 11, 1–9. doi: 10.1038/s41598-021-83318-6.
Hughes, T. P., and Tanner, J. E. (2000). Recruitment failure, life histories, and long-term decline of Caribbean corals. *Ecology* 81, 2250–2263. doi: 10.1890/0012-9658.
Hunter, M. E., Ferrante, J. A., Meigs-Friend, G., and Ulmer, A. (2019). Improving eDNA yield and inhibitor reduction through increased water volumes and multi-filter isolation techniques. *Sci Rep* 9, 1–9. doi: 10.1038/s41598-019-40977-w.
Jeunen, G. J., Knapp, M., Spencer, H. G., Lamare, M. D., Taylor, H. R., Stat, M., et al. (2019). Environmental DNA (eDNA) metabarcoding reveals strong discrimination among diverse marine habitats connected by water movement. *Mol Ecol Resour* 19, 426–438. doi: 10.1111/1755-0998.12982.
Jørgensen, T., Kjær, K. H., Haile, J., Rasmussen, M., Boessenkool, S., Andersen, K., et al. (2012). Islands in the ice: Detecting past vegetation on Greenlandic nunataks using historical records and sedimentary ancient DNA Meta-barcoding. *Mol Ecol* 21, 1980–1988. doi: 10.1111/j.1365-294X.2011.05278.x.
Kadison, E., Nemeth, R. S., Herzlieb, S., and Blondeau, J. (2006). Temporal and spatial dynamics of Lutjanus cyanopterus (Pisces: Lutjanidae) and L. jocu spawning aggregations in the United States Virgin Islands.
Kahng, S. E., Copus, J. M., and Wagner, D. (2014). Recent advances in the ecology of mesophotic coral ecosystems (MCEs). *Curr Opin Environ Sustain* 7, 72–81. doi: 10.1016/j.cosust.2013.11.019.
Kahng, S. E., Garcia-Sais, J. R., Spalding, H. L., Brokovich, E., Wagner, D., Weil, E., et al. (2010). Community ecology of mesophotic coral reef ecosystems. *Coral Reefs* 29, 1–21. doi: 10.1007/s00338-010-0593-6.
Kane, C., Kosaki, R. K., and Wagner, D. (2014). High levels of mesophotic reef fish endemism in the Northwestern Hawaiian Islands. *Bull Mar Sci* 90, 693–703. doi: 10.5343/bms.2013.1053.
Kavanagh, L., and Galbraith, E. (2018). Links between fish abundance and ocean biogeochemistry as recorded in marine sediments. *PLoS One* 13. doi: 10.1371/journal.pone.0199420.
Kelly, R. P., O'Donnell, J. L., Lowell, N. C., Shelton, A. O., Samhouri, J. F., Hennessey, S. M., et al. (2016). Genetic signatures of ecological diversity along an urbanization gradient. *PeerJ* 2016. doi: 10.7717/peerj.2444.
Kelly, R. P., Port, J. A., Yamahara, K. M., and Crowder, L. B. (2014). Using environmental DNA to census marine fishes in a large mesocosm. *PLoS One* 9. doi: 10.1371/journal.pone.0086175.
Kelly, R. P., Shelton, A. O., and Gallego, R. (2019). Understanding PCR Processes to Draw Meaningful Conclusions from Environmental DNA Studies. *Sci Rep* 9, 1–14. doi: 10.1038/s41598-019-48546-x.
Klymus, K. E., Richter, C. A., Chapman, D. C., and Paukert, C. (2015). Quantification of eDNA shedding rates from invasive bighead carp Hypophthalmichthys nobilis and

silver carp Hypophthalmichthys molitrix. *Biol Conserv* 183, 77–84. doi: 10.1016/j.biocon.2014.11.020.
Kosaki, R. K., Pyle, R. L., Leonard, J. C., Hauk, B. B., Whitton, R. K., and Wagner, D. (2017). 100% endemism in mesophotic reef fish assemblages at Kure Atoll, Hawaiian Islands. *Marine Biodiversity* 47, 783–784. doi: 10.1007/s12526-016-0510-5.
Krehenwinkel, H., Wolf, M., Lim, J. Y., Rominger, A. J., Simison, W. B., and Gillespie, R. G. (2017). Estimating and mitigating amplification bias in qualitative and quantitative arthropod metabarcoding. *Sci Rep* 7, 1–12. doi: 10.1038/s41598-017-17333-x.
Lacoursière-Roussel, A., Rosabal, M., and Bernatchez, L. (2016). Estimating fish abundance and biomass from eDNA concentrations: variability among capture methods and environmental conditions. *Mol Ecol Resour* 16, 1401–1414. doi: 10.1111/1755-0998.12522.
Lamb, P. D., Fonseca, V. G., Maxwell, D. L., and Nnanatu, C. C. (2022). Systematic review and meta-analysis: Water type and temperature affect environmental DNA decay. *Mol Ecol Resour* 22, 2494–2505. doi: 10.1111/1755-0998.13627.
Lamb, P. D., Hunter, E., Pinnegar, J. K., Creer, S., Davies, R. G., and Taylor, M. I. (2019). How quantitative is metabarcoding: A meta-analytical approach. *Mol Ecol* 28, 420–430. doi: 10.1111/mec.14920.
Langlois, T. J., Harvey, E. S., Fitzpatrick, B., Meeuwig, J. J., Shedrawi, G., and Watson, D. L. (2010). Cost-efficient sampling of fish assemblages: Comparison of baited video stations and diver video transects. *Aquat Biol* 9, 155–168. doi: 10.3354/ab00235.
Leichter, J., G, S., Genovese, S., and SR, W. (1998). Breaking internal waves on a Florida (USA) coral reef: a plankton pump at work? *International Geoscience and Remote Sensing Symposium (IGARSS)* 166, 83–97. doi: 10.1109/IGARSS.2018.8517318.
Leichter, J. J., Stewart, H. L., and Miller, S. L. (2003). Episodic nutrient transport to Florida coral reefs. *Limnol Oceanogr* 48, 1394–1407. doi: 10.4319/lo.2003.48.4.1394.
Lesser, M. P., Slattery, M., Stat, M., Ojimi, M., Gates, R. D., and Grottoli, A. (2010). Photoacclimatization by the coral Montastraea cavernosa in the mesophotic zone: light, food, and genetics.
Lindfield, S. J., Mcilwain, J. L., and Harvey, E. S. (2014). Depth refuge and the impacts of SCUBA spearfishing on coral reef fishes. *PLoS One* 9, 1–12. doi: 10.1371/journal.pone.0092628.
Locke, J. M., Weil, E., and Coates, K. A. (2007). A newly documented species of Madracis (Scleractinia: Pocilloporidae) from the Caribbean. *Proceedings of the Biological Society of Washington* 120, 214–226. doi: 10.2988/0006-324.
Lowry, M., Folpp, H., Gregson, M., and Suthers, I. (2012). Comparison of baited remote underwater video (BRUV) and underwater visual census (UVC) for assessment of artificial reefs in estuaries. *J Exp Mar Biol Ecol* 416–417, 243–253. doi: 10.1016/j.jembe.2012.01.013.
Loya, Y., Eyal, G., Treibitz, T., Lesser, M. P., and Appeldoorn, R. (2016). Theme section on mesophotic coral ecosystems: advances in knowledge and future perspectives. *Coral Reefs* 35, 1–9. doi: 10.1007/s00338-016-1410-7.
Luckhurst, B. E. (2010). Observations of a Black Grouper (Mycteroperca bonaci) Spawning Aggregation in Bermuda. *Gulf Caribb Res* 22. doi: 10.18785/gcr.2201.05.

Marques, V., Castagné, P., Polanco, A., Borrero-Pérez, G. H., Hocdé, R., Guérin, P. É., et al. (2021). Use of environmental DNA in assessment of fish functional and phylogenetic diversity. *Conservation Biology* 35, 1944–1956. doi: 10.1111/cobi.13802.

Miya, M., Gotoh, R. O., and Sado, T. (2020). *MiFish metabarcoding: a high-throughput approach for simultaneous detection of multiple fish species from environmental DNA and other samples*. Springer Japan doi: 10.1007/s12562-020-01461-x.

Miya, M., Sato, Y., Fukunaga, T., Sado, T., Poulsen, J. Y., Sato, K., et al. (2015). MiFish, a set of universal PCR primers for metabarcoding environmental DNA from fishes: detection of more than 230 subtropical marine species. *R Soc Open Sci* 2, 150088. doi: 10.1098/rsos.150088.

Morais, R. A., and Bellwood, D. R. (2019). Pelagic Subsidies Underpin Fish Productivity on a Degraded Coral Reef. *Current Biology* 29, 1521-1527.e6. doi: 10.1016/j.cub.2019.03.044.

Morris, J. A., and Akins, J. L. (2009). Feeding ecology of invasive lionfish (Pterois volitans) in the Bahamian archipelago. *Environ Biol Fishes* 86, 389–398. doi: 10.1007/s10641-009-9538-8.

Morris, J. a, and Green, S. J. (2012). *Lionfish Research: Current Findings an Remaining Questions*.

Muñoz, R. C., Buckel, C. A., Whitfield, P. E., Viehman, S., Clark, R., Taylor, J. C., et al. (2017). Conventional and technical diving surveys reveal elevated biomass and differing fish community composition from shallow and upper mesophotic zones of a remote United States coral reef. *PLoS One* 12. doi: 10.1371/journal.pone.0188598.

Murakami, H., Yoon, S., Kasai, A., Minamoto, T., Yamamoto, S., Sakata, M. K., et al. (2019). Dispersion and degradation of environmental DNA from caged fish in a marine environment. *Fisheries Science* 85, 327–337. doi: 10.1007/s12562-018-1282-6.

Neal, B. P., Condit, C., Liu, G., dos Santos, S., Kahru, M., Mitchell, B. G., et al. (2014). When depth is no refuge: Cumulative thermal stress increases with depth in Bocas del Toro, Panama. *Coral Reefs* 33, 193–205. doi: 10.1007/s00338-013-1081-6.

Nemeth, R. S. (2005). Population characteristics of a recovering US Virgin Islands red hind spawning aggregation following protection. *Mar Ecol Prog Ser* 286, 81–97. doi: 10.3354/meps286081.

Ogram, A., Sayler, G. S., and Barkay, T. (1987). The extraction and purification of microbial DNA from sediments. *J Microbiol Methods* 7, 57–66. doi: 10.1016/0167-7012(87)90025-X.

Papastamatiou, Y. P., Meyer, C. G., Kosaki, R. K., Wallsgrove, N. J., and Popp, B. N. (2015). Movements and foraging of predators associated with mesophotic coral reefs and their potential for linking ecological habitats. *Mar Ecol Prog Ser* 521, 155–170. doi: 10.3354/meps11110.

Pinheiro, H. T., Goodbody-Gringley, G., Jessup, M. E., Shepherd, B., Chequer, A. D., and Rocha, L. A. (2016). Upper and lower mesophotic coral reef fish communities evaluated by underwater visual censuses in two Caribbean locations. *Coral Reefs* 35, 139–151. doi: 10.1007/s00338-015-1381-0.

Polz, M. F., and Cavanaugh, C. M. (1998). Bias in template-to-product ratios in multitemplate PCR. *Appl Environ Microbiol* 64, 3724–3730. doi: 10.1128/aem.64.10.3724-3730.1998.

Pont, D., Rocle, M., Valentini, A., Civade, R., Jean, P., Maire, A., et al. (2018). Environmental DNA reveals quantitative patterns of fish biodiversity in large rivers despite its downstream transportation. *Sci Rep* 8. doi: 10.1038/s41598-018-28424-8.

Port, J. A., O'Donnell, J. L., Romero-Maraccini, O. C., Leary, P. R., Litvin, S. Y., Nickols, K. J., et al. (2016). Assessing vertebrate biodiversity in a kelp forest ecosystem using environmental DNA. *Mol Ecol* 25, 527–541. doi: 10.1111/mec.13481.

Puglise, K., Hinderstein, L., Marr, J., Dowgiallo, M., and Martinez, F. (2008). Mesophotic Coral Ecosystems Research Strategy. Silver Spring.

Pyle, R. L., Boland, R., Bolick, H., Bowen, B. W., Bradley, C. J., Kane, C., et al. (2016). A comprehensive investigation of mesophotic coral ecosystems in the Hawaiian Archipelago. *PeerJ* 4, e2475. doi: 10.7717/peerj.2475.

Pyle, R. L., Copus, J. M., Pyles, R. L., and Copus, J. M. (2019). "Mesophotic Coral Ecosystems: Introduction and Overview," in *Mesophotic Coral Ecosystems, Coral Reefs of the World 12*, eds. Y. Loya, K. A. Puglise, and T. Bridge (Springer International Publishing), 3–27. doi: 10.1007/978-3-319-92735-0.

Reed, J. K., Farrington, S., Moe, H., Harter, S., Hanisak, D., and David, A. (2014). Characterization of the mesophotic benthic habitat and fish assembledges from ROV dives on Pulley Ridge and Tortugas during 2012 and 2013 R/V Walton Smith cruises. *NOAA Cooperatice Institute for Ocean Exploration, Research and Technology.* Report to, 51.

Riaz, T., Shehzad, W., Viari, A., Pompanon, F., Taberlet, P., and Coissac, E. (2011). EcoPrimers: Inference of new DNA barcode markers from whole genome sequence analysis. *Nucleic Acids Res* 39, 1–11. doi: 10.1093/nar/gkr732.

Riegl, B., and Piller, W. E. (2003). Possible refugia for reefs in times of environmental stress. *International Journal of Earth Sciences* 92, 520–531. doi: 10.1007/s00531-003-0328-9.

Rocha, L. A., Pinheiro, H. T., Shepherd, B., Papastamatiou, Y. P., Luiz, O. J., Pyle, R. L., et al. (2018). Mesophotic coral ecosystems are threatened and ecologically distinct from shallow water reefs. *Science (1979)* 361, 281–284. doi: 10.1126/science.aaq1614.

Rosa, M. R., Alves, A. C., Medeiros, D. V., Coni, E. O. C., Ferreira, C. M., Ferreira, B. P., et al. (2016). Mesophotic reef fish assemblages of the remote St. Peter and St. Paul's Archipelago, Mid-Atlantic Ridge, Brazil. *Coral Reefs* 35, 113–123. doi: 10.1007/s00338-015-1368-x.

Rossberg, A. G., Rogers, T., and McKane, A. J. (2014). Current noise-removal methods can create false signals in ecogenomic data. *Proceedings of the Royal Society B: Biological Sciences* 281. doi: 10.1098/rspb.2014.0191.

Rourke, M. L., Fowler, A. M., Hughes, J. M., Broadhurst, M. K., DiBattista, J. D., Fielder, S., et al. (2022). Environmental DNA (eDNA) as a tool for assessing fish biomass: A review of approaches and future considerations for resource surveys. *Environmental DNA* 4, 9–33. doi: 10.1002/edn3.185.

Saitoh, S., Aoyama, H., Fujii, S., Sunagawa, H., Nagahama, H., Akutsu, M., et al. (2016). A quantitative protocol for DNA metabarcoding of springtails (Collembola). in *Genome* (Canadian Science Publishing), 705–723. doi: 10.1139/gen-2015-0228.

Santana-Garcon, J., Newman, S. J., and Harvey, E. S. (2014). Development and validation of a mid-water baited stereo-video technique for investigating pelagic fish assemblages. *J Exp Mar Biol Ecol* 452, 82–90. doi: 10.1016/j.jembe.2013.12.009.

Sard, N. M., Herbst, S. J., Nathan, L., Uhrig, G., Kanefsky, J., Robinson, J. D., et al. (2019). Comparison of fish detections, community diversity, and relative abundance using environmental DNA metabarcoding and traditional gears. *Environmental DNA* 1, 368–384. doi: 10.1002/edn3.38.

Sassoubre, L. M., Yamahara, K. M., Gardner, L. D., Block, B. A., and Boehm, A. B. (2016). Quantification of Environmental DNA (eDNA) Shedding and Decay Rates for Three Marine Fish. *Environ Sci Technol* 50, 10456–10464. doi: 10.1021/acs.est.6b03114.

Sato, M., Inoue, N., Nambu, R., Furuichi, N., Imaizumi, T., and Ushio, M. (2021). Quantitative assessment of multiple fish species around artificial reefs combining environmental DNA metabarcoding and acoustic survey. *Sci Rep* 11, 1–14. doi: 10.1038/s41598-021-98926-5.

Schnell, I. B., Bohmann, K., and Gilbert, M. T. P. (2015). Tag jumps illuminated - reducing sequence-to-sample misidentifications in metabarcoding studies. *Mol Ecol Resour* 15, 1289–1303. doi: 10.1111/1755-0998.12402.

Schobernd, Z. H., Bacheler, N. M., and Conn, P. B. (2014). Examining the utility of alternative video monitoring metrics for indexing reef fish abundance. *Canadian Journal of Fisheries and Aquatic Sciences* 71, 464–471. doi: 10.1139/cjfas-2013-0086.

Schofield, P. J. (2009). Geographic extent and chronology of the invasion of non-native lionfish (Pterois volitans [Linnaeus 1758] and P. miles [Bennett 1828]) in the Western North Atlantic and Caribbean Sea. *Aquat Invasions* 4, 473–479. doi: 10.3391/ai.2009.4.3.5.

Schofield, P. J. (2010). Update on geographic spread of invasive lionfishes (Pterois volitans [Linnaeus, 1758] and P. miles [Bennett, 1828]) in the Western North Atlantic Ocean, Caribbean Sea and Gulf of Mexico. *Aquat Invasions* 5, 117–122. doi: 10.3391/ai.2010.5.S1.024.

Semmler, R. F., Hoot, W. C., and Reaka, M. L. (2017). Are mesophotic coral ecosystems distinct communities and can they serve as refugia for shallow reefs? *Coral Reefs* 36, 433–444. doi: 10.1007/s00338-016-1530-0.

Serrano, X. M., Baums, I. B., O'Reilly, K., Smith, T. B., Jones, R. J., Shearer, T. L., et al. (2014). Geographic differences in vertical connectivity in the Caribbean coral Montastraea cavernosa despite high levels of horizontal connectivity at shallow depths. *Mol Ecol* 23, 4226–4240. doi: 10.1111/mec.12861.

Shaw, J. L. A., Clarke, L. J., Wedderburn, S. D., Barnes, T. C., Weyrich, L. S., and Cooper, A. (2016). Comparison of environmental DNA metabarcoding and conventional fi sh survey methods in a river system. *Bioc* 197, 131–138. doi: 10.1016/j.biocon.2016.03.010.

Shelton, A. O., Kelly, R. P., O'Donnell, J. L., Park, L., Schwenke, P., Greene, C., et al. (2019). Environmental DNA provides quantitative estimates of a threatened salmon species. *Biol Conserv* 237, 383–391. doi: 10.1016/j.biocon.2019.07.003.

Shen, Y., Hubert, N., Huang, Y., Wang, X., Gan, X., Peng, Z., et al. (2019). DNA barcoding the ichthyofauna of the Yangtze River: Insights from the molecular inventory of a mega-diverse temperate fauna. *Mol Ecol Resour* 19, 1278–1291. doi: 10.1111/1755-0998.12961.

Shendure, J., and Ji, H. (2008). Next Generation DNA Sequencing. *Nat Biotechnol* 26, 1135–1145. doi: 10.1002/9780471650126.dob1009.

Sinniger, F., Morita, M., and Harii, S. (2013). “Locally extinct” coral species Seriatopora hystrix found at upper mesophotic depths in Okinawa. *Coral Reefs* 32, 153. doi: 10.1007/s00338-012-0973-1.

Slattery, M., and Lesser, M. P. (2012). Mesophotic coral reefs: a global model of community structure and function. *Proceedings of the 12th International Coral Reef Symposium*, 9–13.

Slattery, M., Lesser, M. P., Brazeau, D., Stokes, M. D., and Leichter, J. J. (2011). Connectivity and stability of mesophotic coral reefs. *J Exp Mar Biol Ecol* 408, 32–41. doi: 10.1016/j.jembe.2011.07.024.

Smith, T. B., Gyory, J., Brandt, M. E., Miller, W. J., Jossart, J., and Nemeth, R. S. (2016). Caribbean mesophotic coral ecosystems are unlikely climate change refugia. *Glob Chang Biol* 22, 2756–2765. doi: 10.1111/gcb.13175.

Soares, M. de O., and Lucas, C. C. (2018). Towards large and remote protected areas in the South Atlantic Ocean: St. Peter and St. Paul´s Archipelago and the Vitória-Trindade Seamount Chain. *Mar Policy* 93, 101–103. doi: 10.1016/j.marpol.2018.04.004.

Souter, D., Planes, S., Wicquart, J., Logan, M., Obura, D., and Staub, F. (2021). Status of Coral Reefs of the World.

Stat, M., Huggett, M. J., Bernasconi, R., Dibattista, J. D., Berry, T. E., Newman, S. J., et al. (2017). Ecosystem biomonitoring with eDNA: Metabarcoding across the tree of life in a tropical marine environment. *Sci Rep* 7, 1–11. doi: 10.1038/s41598-017-12501-5.

Steinberg, D. K., Lomas, M. W., and Cope, J. S. (2012). Long-term increase in mesozooplankton biomass in the Sargasso Sea: Linkage to climate and implications for food web dynamics and biogeochemical cycling. *Global Biogeochem Cycles* 26. doi: 10.1029/2010GB004026.

Stobart, B., Díaz, D., Álvarez, F., Alonso, C., Mallol, S., and Goñi, R. (2015). Performance of baited underwater video: Does it underestimate abundance at high population densities? *PLoS One* 10. doi: 10.1371/journal.pone.0127559.

Stobart, B., García-Charton, J. A., Espejo, C., Rochel, E., Goñi, R., Reñones, O., et al. (2007). A baited underwater video technique to assess shallow-water Mediterranean fish assemblages: Methodological evaluation. *J Exp Mar Biol Ecol* 345, 158–174. doi: 10.1016/j.jembe.2007.02.009.

Suzuki, M. T., and Giovannoni, S. J. (1996). Bias caused by template annealing in the amplification of mixtures of 16S rRNA genes by PCR. *Appl Environ Microbiol* 62, 625–630. doi: 10.1128/aem.62.2.625-630.1996.

Taberlet, P., Bonin, A., Zinger, L., and Coissac, E. (2018). *Environmental DNA: For Biodiversity Research and Monitoring*. Oxford University Press doi: 10.1093/oso/9780198767220.001.0001.

Takahara, T., Minamoto, T., Yamanaka, H., Doi, H., and Kawabata, Z. (2012). Estimation of fish biomass using environmental DNA. *PLoS One* 7, 3–10. doi: 10.1371/journal.pone.0035868.

Takeuchi, A., Sado, T., Gotoh, R. O., Watanabe, S., Tsukamoto, K., and Miya, M. (2019). New PCR primers for metabarcoding environmental DNA from freshwater eels, genus Anguilla. *Sci Rep* 9, 7977. doi: 10.1038/s41598-019-44402-0.

Thomsen, P. F., Møller, P. R., Sigsgaard, E. E., Knudsen, S. W., Jørgensen, O. A., and Willerslev, E. (2016). Environmental DNA from seawater samples correlate with trawl catches of subarctic, deepwater fishes. *PLoS One* 11, 1–22. doi: 10.1371/journal.pone.0165252.

Thomsen, P. F., and Willerslev, E. (2015). Environmental DNA - An emerging tool in conservation for monitoring past and present biodiversity. *Biol Conserv* 183, 4–18. doi: 10.1016/j.biocon.2014.11.019.

Thomsen, P., Kielgast, J., Iversen, L., Møller, P., Rasmussen, M., and Willerslev, E. (2012). Detection of a Diverse Marine Fish Fauna Using Environmental DNA from Seawater Samples. *PLoS One* 7, 1–9. doi: 10.1371/journal.pone.0041732.

Tsuji, S., Takahara, T., Doi, H., Shibata, N., and Yamanaka, H. (2019). The detection of aquatic macroorganisms using environmental DNA analysis—A review of methods for collection, extraction, and detection. *Environmental DNA* 1, 99–108. doi: 10.1002/edn3.21.

Turner, J. A., Babcock, R. C., Hovey, R., and Kendrick, G. A. (2017). Deep thinking: A systematic review of mesophotic coral ecosystems. *ICES Journal of Marine Science* 74, 2309–2320. doi: 10.1093/icesjms/fsx085.

Turner, J., Andradi-Brown, D., Gori, A., Bongaerts, P., Burdett, H., Ferrier-Pagès, C., et al. (2019). “Key Questions for Research and Conservation of Mesophotic Coral Ecosystems and Temperate Mesophotic Ecosystems,” in *Mesophotic Coral Ecosystems Coral Reefs of the World 12* (Loya, Yossi Puglise, Kimberly A Bridge, Tom C L), 989–1003. doi: 10.1007/978-3-319-92735-0.

Ushio, M., Murakami, H., Masuda, R., Sado, T., Miya, M., Sakurai, S., et al. (2018). Quantitative monitoring of multispecies fish environmental DNA using high-throughput sequencing. *Metabarcoding Metagenom* 2, 1–15. doi: 10.3897/mbmg.2.23297.

Van Oppen, M. J. H., Bongaerts, P., Underwood, J. N., Peplow, L. M., and Cooper, T. F. (2011). The role of deep reefs in shallow reef recovery: An assessment of vertical connectivity in a brooding coral from west and east Australia. *Mol Ecol* 20, 1647–1660. doi: 10.1111/j.1365-294X.2011.05050.x.

Weinstein, D. K., Sharifi, A., Klaus, J. S., Smith, T. B., Giri, S. J., and Helmle, K. P. (2019). Erratum: Coral growth, bioerosion, and secondary accretion of living orbicellid corals from mesophotic reefs in the US Virgin Islands (Mar Ecol Prog Ser (2016) 559(45-63)). *Mar Ecol Prog Ser* 619, 215–217. doi: 10.3354/meps11883.

Whitfield, P. E., Gardner, T., Vives, S. P., Gilligan, M. R., Courtenay, W. R., Ray, G. C., et al. (2002). Biological invasion of the Indo-Pacific lionfish Pterois volitans along the Atlantic coast of North America. *Mar Ecol Prog Ser* 235, 289–297. doi: 10.3354/meps235289.

Whitmarsh, S. K., Fairweather, P. G., and Huveneers, C. (2017). What is Big BRUVver up to? Methods and uses of baited underwater video. *Rev Fish Biol Fish* 27, 53–73. doi: 10.1007/s11160-016-9450-1.

Wolanski, E., Colin, P., Naithani, J., Deleersnijder, E., and Golbuu, Y. (2004). Large amplitude, leaky, island-generated, internal waves around Palau, Micronesia. *Estuar Coast Shelf Sci* 60, 705–716. doi: 10.1016/j.ecss.2004.03.009.

Woodhead, A. J., Hicks, C. C., Norström, A. V., Williams, G. J., and Graham, N. A. J. (2019). Coral reef ecosystem services in the Anthropocene. *Funct Ecol* 33, 1023–1034. doi: 10.1111/1365-2435.13331.

Yao, M., Zhang, S., Lu, Q., Chen, X., Zhang, S. Y., Kong, Y., et al. (2022). Fishing for fish environmental DNA: Ecological applications, methodological considerations, surveying designs, and ways forward. *Mol Ecol*, 5132–5164. doi: 10.1111/mec.16659.

Yeakel, K. L., Andersson, A. J., Bates, N. R., Noyes, T. J., Collins, A., and Garley, R. (2015). Shifts in coral reef biogeochemistry and resulting acidification linked to offshore productivity. *Proc Natl Acad Sci U S A* 112, 14512–14517. doi: 10.1073/pnas.1507021112.

Zhang, S., Zhao, J., and Yao, M. (2020). A comprehensive and comparative evaluation of primers for metabarcoding eDNA from fish. *Methods Ecol Evol* 11, 1609–1625. doi: 10.1111/2041-210X.13485.

Chapter 2. Calcification and trophic responses of Mesophotic reefs to carbonate chemistry variability

2.1 Abstract

Mesophotic coral reefs (MCEs) are direct extensions of adjacent shallow water coral reefs. Accessibility to these ecosystems is challenging due to the upper depth limit (~ 30 m) being at the lower end of conventional SCUBA diving limits. As a result, the traditional knowledge of coral reef science generally equates to this depth limit. It has been posited that the depth limits of MCEs diminish anthropogenic effects. A lack of empirical measurements makes it impossible to determine if this is true for mesophotic reef metabolism. Using chemistry-based assessments of Mesophotic Coral Ecosystem (MCE) net ecosystem calcification (NEC), the seawater chemistry on Bermudan mesophotic reefs was determined to be chemical conducive for calcification (average aragonite saturation $\Omega_{aragonite}$ of 3.58, average calcite saturation $\Omega_{calcite}$ of 5.44). Mesophotic reefs are in a net state of calcification (i.e. accretion of calcium carbonate, $CaCO_3$) with estimates of monthly mean NEC (± SE) calculated the for the upper mesophotic, 30 m, 40 m and 60 m deep reefs as 4.96 ± 0.74 g $CaCO_3$ m^{-2} d^{-1}, 10.02 ± 2.32 g $CaCO_3$ m^{-2} d^{-1}, 5.38 ± 1.42 g $CaCO_3$ m^{-2} d^{-1} and 2.81 ± 0.70 g $CaCO_3$ m^{-2} d^{-1} which fall within the range of average global coral reef NEC values 2.00 – 25.00 g $CaCO_3$ m^{-2} d^{-1}. There are seasonal changes of NEC with the strongest periods of calcification in the late summer coupled with strong autotrophic signals. These periods are followed by suppressed calcification and autotrophy and in the case of the 60 m reefs, a switch to heterotrophy. Switches from wintertime net heterotrophy to summertime net autotrophy suggest the occurrence of the “Carbonate Chemistry Coral Reef Ecosystem Feedback” (CREF hypothesis), a process previously described as regulating reef metabolism of Bermuda’s shallow reef system. Whilst there was variability between the three reefs depths, the overall status of the mesophotic system was net autotrophic and not in a state of balance. This determination was the opposite of the estimated trophic status for Bermudan shallow reefs. Whilst there were periods of net dissolution, the mesophotic reef system was net accretive (i.e., gross calcification > gross $CaCO_3$ dissolution). The

measured inorganic carbon chemistry and estimates of NEC and NEP represent the first such biogeochemical measurements for MCEs. The values established by this study demonstrate just how close these understudied ecosystems are in terms of the known boundary thresholds for low saturation state reefs. Making predictions on how these ecosystems will respond to further climate change, will be difficult and require more sampling effort over long times scales to decouple the environmental controls exerted on such ecosystems.

2.2 Introduction

Coral reefs are highly diverse marine ecosystems forming complex three-dimensional frameworks, generated through biogenically precipitated calcium carbonate (CaCO3) primarily produced by hermatypic corals, calcareous algae and foraminifera. Such calcification is responsible for ~50% of net annual $CaCO_3$ oceanic precipitation (Dubinsky and Stambler, 2011). Globally, coral reef ecosystems provide numerous socio-economic and ecological functions (Moberg and Folke, 1999; Sarkis et al., 2013). Their global decline through disturbance events, climate change and a myriad of anthropogenic activities have been well documented in the literature (e.g., (Wilkinson, 1999, 2008; Jackson et al., 2001, 2014; Pandolfi et al., 2003; Hughes et al., 2007; Hoegh-Guldberg, 2011; Tanzil et al., 2013). These declines have led to increased scientific interest in deeper reef ecosystems (e.g., mesophotic, generally deeper than 30 m) that may exhibit reduced susceptibilities and greater resistance to such environmental change (Glynn, 1996; Puglise et al., 2008; Bongaerts et al., 2010, 2017; Baker et al., 2016b; Cinner et al., 2016; Loya et al., 2016; Semmler et al., 2017; Turner et al., 2017).

Deeper reef systems (generally deeper than 30 m with depths up to ~ 150 m) termed “mesophotic coral ecosystems” (MCEs; Hinderstein et al., 2010) have a near-ubiquitous presence below shallow coral reefs (Bridge et al., 2013). The consensus within the research community is that MCEs are often extensions of shallow coral reef systems (Hinderstein et al., 2010; Pyle et al., 2019 and references therein) with common species shared between the two communities. Subdivisions of the MCE habitat based on

biodiversity changes across depth have been proposed (Pyle et al., 2019 references therein). It is this commonality of species combined with the suggestion that MCEs could be buffered from anthropogenic influence (e.g., ocean warming and acidification) and natural disturbances (Bongaerts et al., 2013; Loya et al., 2016) that makes these ecosystems of particular scientific interest. Determining the levels of oceanographic connectivity between mesophotic and adjacent shallow-water reefs has become a key research priority across disciplines (e.g., biogeochemistry, marine spatial planning). Given that biological carbonates are the largest carbon reservoirs in the biosphere (i.e., aragonite, calcite, and magnesian calcite; Cohen, 2003), to truly comprehend the level of resilience coral reef systems have to anthropogenic and natural stressors, understanding the interactions and feedbacks that drive these biogeochemical processes (e.g., calcification rates, thermal regimes, flow dynamics) are fundamental requirements. Oceanic uptake of anthropogenic CO_2 has led to significant changes in seawater chemistry (Orr et al., 2005) which in turn has raised concerns about the consequences to marine calcifiers (e.g., hermatypic corals, calcareous algae and foraminifera; Kleypas et al., 1999; Hoegh-Guldberg et al., 2007) to generate and maintain $CaCO_3$ structures through a reduction in seawater pH and aragonite saturation state ($\Omega_{aragonite}$; Cyronak et al., 2018; Eyre et al., 2018). Of equal importance is the potential for rates of bioerosion and dissolution of $CaCO_3$ structures (Andersson et al., 2009; Tribollet et al., 2009; Dove et al., 2013) to increase under the same conditions. The persistence of coral reefs is dependent on their ability to calcify and produce $CaCO_3$ and maintain net positive accretion. At reef scale, net accretion of $CaCO_3$ and external sediment supply (e.g., broken down framework, shells) must be greater than any loss by dissolution, transport, or erosion (Kleypas et al., 2001; Andersson and Gledhill, 2013; Eyre et al., 2018).

$$CaCO_{3accretion} = CaCO_{3production} - CaCO_{3dissolution} - \text{physical loss of } CaCO_3 \quad (1)$$

Both models and mesocosm studies on individual and community calcifiers have measured decreased rates in calcification (net accretion) and increases in $CaCO_3$ dissolution ultimately transitioning to a state of net dissolution under projected atmospheric and seawater CO_2 conditions (Pandolfi et al., 2011; Andersson and Gledhill,

2013; Lantz et al., 2014). However, there is considerable uncertainty as to when this inferred threshold may be crossed (Andersson and Gledhill, 2013). Rates of net coral $CaCO_3$ production can be determined through chemistry-based methods (i.e., net ecosystem calcification [NEC] = gross calcification – gross $CaCO_3$ dissolution) and can provide a top-down integrated measurement of the entire reef NEC (Courtney et al., 2016). Modification of CO_2-carbonate chemistry of Bermudan mesophotic reefs will reflect the main biogeochemical processes occurring on the reef system (Bates, 2002, 2017; Bates et al., 2010; Andersson et al., 2014; Yeakel et al., 2015; Courtney et al., 2016). It is accepted that inorganic $CaCO_3$ accretion occurs at seawater saturation state (Ω) >1 whereas the dissolution of $CaCO_3$ occurs when Ω <1. However, biogenic reef carbonate dissolution has been determined to occur well above this expected thermodynamic transition value (Langdon et al., 2000; Bates et al., 2010; Andersson et al., 2014). Differences in open ocean source water CO_2-carbonate chemistry are compared to water collected from mesophotic reefs thus allowing the determination of NEC (accretion or dissolution) and NEP (autotrophy or heterotrophy) consequently resolving if Bermudan MCEs will remain net calcifying and in which trophic state, under predicted future environmental change.

2.3 Methodology

2.3.1 Study Locations

Bermuda is located approximately 1000 km east south-east of the United States (Jones et al., 2012) in the northwest of the Sargasso Sea (Coates et al., 2013) and considered the northernmost reefs of the Atlantic (Spalding et al., 2001; Logan and Murdoch, 2011). Bermuda's coral reef system transitions through a series of shallow patch reefs, shallow rim reefs, and terraced reefs (Logan, 1988; Logan and Murdoch, 2011) dropping quickly to deeper mesophotic reefs that surround the main reef platform (Goodbody-Gringley et al., 2019b). Using the 30 – 150m contours in a Bermuda 1 arc-second sea level digital elevation model (Sutherland et al., 2014) as a proxy for the extent of the mesophotic zone surrounding Bermuda, the system covers 76 km^2 which equates

to 8% of habitats < 30 m (908 km^2). All physiographic reef zones are influenced by the offshore waters from the Sargasso Sea (Steinberg et al., 2001; Bates, 2017). The study was performed on three mesophotic reef locations between August 2017 and October 2018 (Figure 2.1). The choice of locations was defined a posteriori following the findings of a Darwin Plus (DPLUS001) lionfish control initiative project completed in 2015. At each location, a grid of six sites approximately ~ 350 m apart were arranged in a pattern of three shallow (30 ~ 40 m) and three deep sites (60 m; Figure 2.1). The benthic community composition followed the pattern reported by Fricke and Meischner (1985) and expanded upon in the review of Bermuda's mesophotic reefs by Goodbody-Gringley et al. (2019). Moving in a seaward direction, shallow mesophotic sites (~30 m depth) were dominated by hermatypic scleractinian corals whilst the deeper sites exhibited greater benthic heterogeneity as macroalgae (Stefanoudis et al., 2019b) and rhodolith beds became more dominant.

2.3.2 Seawater Carbonate Chemistry Determination

Carbon chemistry samples were collected on an ad hoc basis between August 2017 and October 2018 using a 12-liter Niskin bottle at ~2 m above the benthos (Bates et al., 1996; Dickson et al., 2007). Comparative offshore samples were collected monthly as part of the Bermuda Atlantic Time-series Study (BATS; Bates et al., 2012). Samples for dissolved inorganic carbon (DIC) and total alkalinity (TA) were drawn into clean 200-ml Kimax glass sample bottles and fixed with 100 µl of saturated mercuric chloride ($HgCl_2$) solution to prevent biological alteration. DIC was analysed using coulometric technique on an Automated InfraRed Inorganic Carbon Analyzer (AIRICA, Marianda Inc) or on a VINDTA system (Versatile INstrument for the Determination of Total inorganic carbon and titration Alkalinity, VINDTA 3C, Marianda Inc). DIC is defined as (Dickson, Sabine and Christian, 2007; equation 2):

$$DIC = [CO_2]^* + [HCO_3^-] + [CO_3^{2-}] \quad (2)$$

All reef TA samples were analysed via closed-cell potentiometric titration with HCl of approximate normality of ~0.1 and ionic strength of ~0.7 using the VINDTA3S system (Marianda Inc). The offshore BATS TA samples were analysed on a VINDTA2S system (Marianda Inc) with similar solutions. The VINDTA2S system is the previous model of VINDTA3C system and although it performs the same analytical function, BATS samples are preferentially run on this machine to maintain continuity, but with no demonstrable difference between analytical systems. TA is typically defined as (equation 3):

$$TA = [HCO_3^-] + 2[CO_3^{2-}] + [B(OH)_4^-] + [OH^-] + [HPO_4^{2-}] + 2[PO_4^{3-}] + [SiO(OH)_3^-] + [HS^-] + [NH_3] + \text{minor constituents} - [H^+] + [HSO_4^-] + [HF^-] - [H_3PO_4] - \text{minor constituents} \quad (3)$$

Seawater certified reference materials (CRMs; prepared by A.G. Dickson, Scripps Institution of Oceanography; http//www.dickson.ucsd.edu) were used to ensure the precision and accuracy of both DIC and TA values (typically ±1 to 2 μmoles kg^{-1}). For both reef and BATS measurements, seawater pH, pCO2 and Ω were calculated using CO2SYS (Lewis and Wallace, 1998) from measured DIC and TA at in situ salinity and temperature conditions using the K1 and K2 dissociation constants from Mehrbach et al. (1973) refitted by Dickson and Millero (1987).

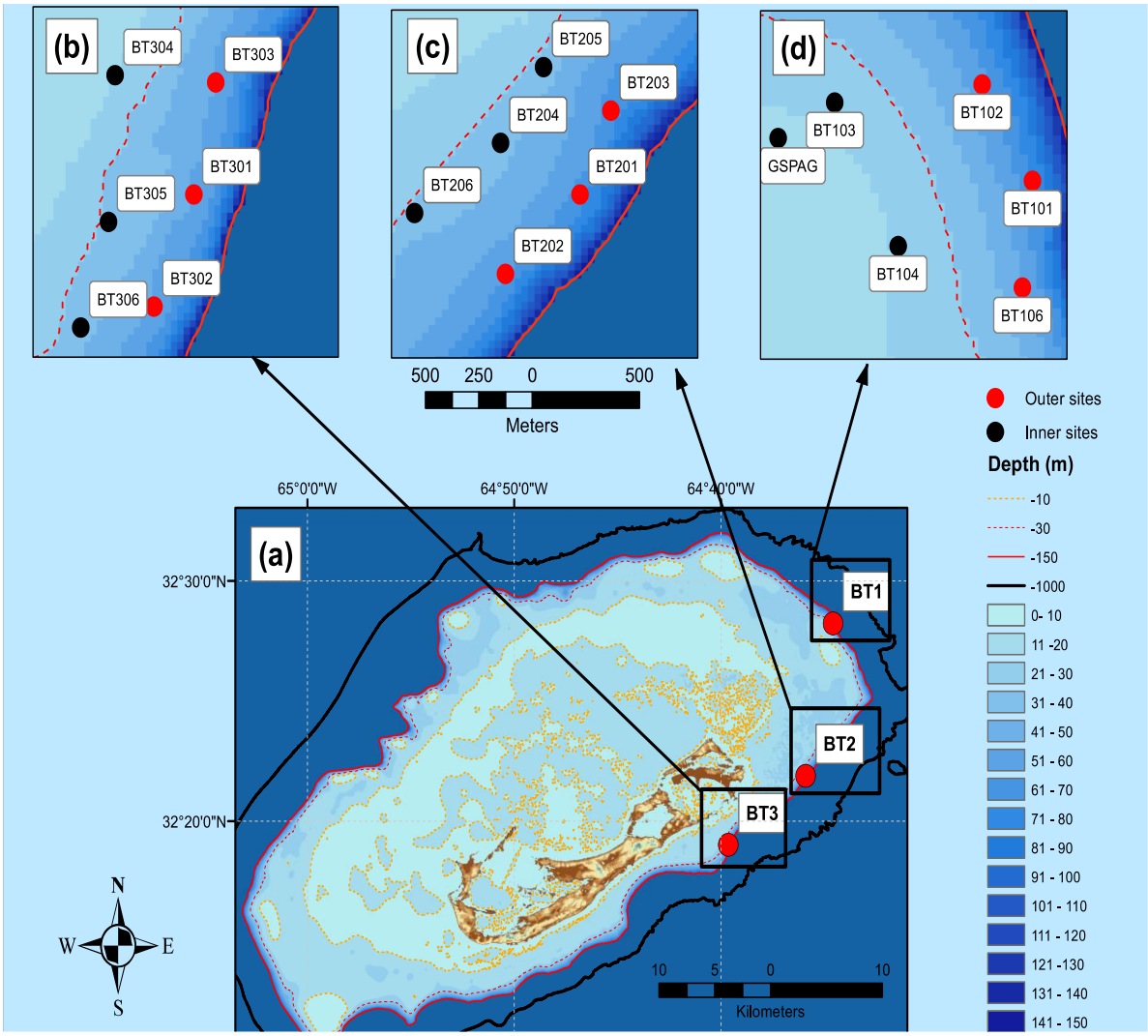

Figure 2.1. (**a**) Bathymetric map of Bermuda illustrating the main study locations (red circles) and proximity to land and open ocean, 10 m contour line in orange, 30 m contour dashed red line, 150 m contour solid red line, 1000 m contour solid black line. (**b**) location BT3 showing spatial orientation of ~ 30 - 40 m (black circles), 60 m (red circles). (**c**) location BT2 showing spatial orientation of ~ 30 - 40 m (black circles), 60 m (red circles). (**d**) location BT1 showing spatial orientation of ~ 30 - 40 m (black circles), 60 m (red circles). Note, the red dashed line represents the ~ 45 m contour for this location only.

2.3.3 Physical and biogeochemical parameters

Salinity samples were paired with all reef and BATS DIC and TA samples and collected in accordance with best practices (Knap et al., 1997). Samples were drawn into 250 ml clear borosilicate glass bottles with plastic screw caps. A plastic insert was used to form an airtight seal and stop sample evaporation. All samples were analysed on a

Guildline AutoSal 8400A laboratory salinometer (± 0.002) following the manufacturers recommendations for standard practices. Salinity measurements were calibrated against IAPSO standard seawater (Ocean Scientific, UK) to give a precision of ± 0.001-0.002 Practical Salinity Units (PSU). *In situ* temperatures were measured with an ONSET HOBO Water Temp Pro v2 (accuracy ±0.2°C between -40°C and 70°C). Inorganic nutrient samples were collected on an ad hoc basis at central shallow and deep sites per location only (Figure 2.1b). Samples were collected following best practices (Knap et al., 1997), filtered through a 0.8 µm NucleporeTM filter (Whatman®) into prewashed 60 ml amber bottles (Nalgene® HDPE) stored on ice and immediately frozen on return to BIOS, prior to shipping to the Woods Hole Oceanographic Institution Nutrient Analytical Facility. All samples were analysed on a SEAL Analytical AA3 HR Auto Analyzer using U.S. Environmental Protection Agency methods for ammonium (method G-171-96, detection limit 0.015 µmoles L^{-1}), nitrate + nitrate (method G-172-96, detection limit 0.040 µmoles L^{-1}), silicate (method G-177-96, detection limit 0.030 µmoles L^{-1}), and phosphate (G-297-03, detection limit 0.009 µmoles L^{-1}).

Table 2.1. Summary of the number of physico-chemical parameters measured at three reef zones.

Reef zone	Temperature	Salinity	DIC	TA	NH_4^+	$NO_2^- \pm NO_3^-$
30 m	38	38	38	38	17	17
40 m	41	41	41	41	17	17
60 m	98	98	98	98	33	33
Total	177	177	177	177	67	67

Reef zone	PO_4^{3-}	Silicate
30 m	17	17
40 m	17	17
60 m	33	33
Total	67	67

2.3.4 Determination of Net Ecosystem Calcification (NEC) and Net Ecosystem Production (NEP)

The relative changes in DIC and TA reflect biogeochemical partitioning of carbon between the inorganic and organic cycles (Suzuki and Kawahata, 2003). The changes in DIC and TA relative to NEC change in a ratio 1:2 DIC:TA. Net NEC (NEC > 0) will reduce both DIC and TA which causes a lowering of pH and $\Omega_{aragonite}$. To account for local evaporation and precipitation changes, all (i.e., MCE and BATS) TA (i.e., nTA) and DIC (i.e., nDIC) were salinity normalised to a mean measured salinity of MCE reefs of 36.67 (Courtney et al., 2021).

The determination of net ecosystem calcification (NEC) is based on the widely accepted alkalinity anomaly-water residence time technique (Smith and Key, 1975; Bates et al., 2010; Langdon et al., 2010; Andersson and Gledhill, 2013; Courtney et al., 2016; Bates, 2017). The offshore BATS samples are assumed to be representative of waters flowing onto Bermudan mesophotic reefs. The sampling regimes between the MCE sites and BATS were typically conducted within 1-2 weeks of each other (Bates, 2017). To minimise the influence of isopycnal lifting as water transitions onto Bermuda MCEs, comparative offshore data were selected based on salinity and temperature. The method assumes any differences in total alkalinity (TA) between offshore and mesophotic reef seawater (i.e., $nTA_{offshore} - nTA_{MCE}$) are a relative expression of MCE calcification and calculated as per the method of Langdon et al. (2010):

$$NEC_{MCE} = -0.5(nTA_{offshore} - nT_{MCE}) \bullet ((\sigma/Z)/t) \quad (4)$$

Where σ is the density of seawater, Z is the depth of water and t is the water residence time for the mesophotic reef. Water depths for MCE sites were measured using a vessel mounted depth sounder (Garmin GPSmap 441s/Aimar P79 50/200 kHz transducer). Sample depths for offshore (BATS) samples were recorded by a Sea-Bird SBE 911 CTD instrument package (SBE 9 underwater unit, SBE 11 Deck unit). Sites were categorized as 30 m, 40 m and 60 m as determined by average depth measurements recorded over the duration of the study. Seawater residence times for mesophotic sites were deemed to be 0.5 days based on hydrological modelling (R. Johnson unpublished data). All discrete reef level samples were collected from ~ 2 m above the benthos, as

such, any calcification and or dissolution signals (i.e., $CaCO_3$ precipitation/dissolution) are estimated to be detected within a 5 m^3 volume above the benthos. Rates of NEC_{MCE} are calculated in units of mmoles $CaCO_3$ m^{-2} d^{-1} (or expressed as g $CaCO_3$ m^{-2} d^{-1} using the molecular weight 100.09).

$$Ca^{2+} + 2\ HCO_3^- = CaCO_3 + H_2O + CO_2 \quad (5)$$

Net calcification (NEC > 0) draws down both DIC and TA causing a reduction in seawater pH and $\Omega_{aragonite}$. NEP alters DIC content of the water however, neither photosynthesis or respiration alter TA, therefore NEP_{MCE} is calculated as the difference between offshore BATS and onshore MCE samples as follows (Romanó de Orte et al., 2021):

$$NEP_{MCE} = nDIC_{offshore} - nDIC_{MCE} - \Delta nDIC_{NEC} \quad (6)$$

Air–sea CO_2 gas exchange were deemed minor relative to the calculations of NEC and NEP (Bates, 2017). Rates of NEP_{MCE} are calculated in units of mmoles C m^{-2} d^{-1} (or expressed as g C m^{-2} d^{-1} using a molecular weight of 12).

2.3.5 Propagation of Uncertainty

Uncertainty for bottle NEC and NEP calculations were estimated using procedures outlines by Ku (1966). The uncertainty of measured DIC and TA (±1 µmoles kg^{-1}) was obtained from routine measurement of CRMs (prepared by A.G. Dickson, Scripps Institution of Oceanography; http//www.dickson.ucsd.edu) with the DIC and TA samples.

2.4 Results

2.4.1 Physical and biogeochemical variability

In total 177 paired comparisons were made between mesophotic reefs and reference samples taken at the BATS site which when delineated to depth categories, equated to 30 m = 38, 40 m = 41, 60 m = 98 samples respectively. Monthly benthic seawater temperatures exhibited seasonal variability across all study sites ranging from 19.6 – 27.5 ± 2.2 °C between winter and summer (Figure 2.2a–c). The summer monthly climatology of 60 m reefs tended to be ~ 3.5 to 4°C and ~ 2.5 to 3°C cooler than the 30 m and 40 m reefs respectively. Short term deployments (~ 12 days) of temperature loggers at 60 m sites recorded ~4 °C daily variability. High degrees of thermal oscillation at mesophotic depths are known to occur (Wolanski et al., 2004; Colin, 2009; Colin and Lindfield, 2019) and have been attributed to internal waves. In the Pacific region of Micronesia, extreme daily thermal isolations at a 90 m depth (~ 20 °C) where linked to a possible coupling of internal waves with a Rossby wave causing a deepening of the thermocline (Colin and Lindfield, 2019). Salinity across all mesophotic sites had a similar seasonal range to offshore values recorded at BATS 36.67 ± 0.09 g kg^{-1}, however, samples from 2017 were slightly fresher than 2018 but still within the limits reported for the Bermuda environment (36.3 – 36.7; Coates et al., 2013; Yeakel et al., 2015). Inorganic nutrients concentrations were typically below 0.1 µmoles L^{-1} (oligotrophic water column) and consistent with values previously published for Bermuda mesophotic reefs (Goodbody-Gringley et al., 2015). Approximately 50% of all inorganic nutrient measurements were below detection limits suggesting rapid uptake of dissolved inorganic nutrients and/or limited nutrient availability. Nutrient measurements were collected at a subset of sites (n = 67) over the duration of the study with a focus on the central 60 m site per location.

Table 2.2. Summary of physico-chemical parameter averages ± SE over the duration of the study for the mesophotic coral reef and three reef zones. Note, nutrients were collected over the duration of the study at a subset of study locations.

Reef zone	Temperature	NEC	NEP	Ω Aragonite	Ω Calcite	Salinity
	°C	g $CaCO_3$ m^{-2} d^{-1}	g C m^{-2} d^{-1}			g kg^{-1}
Mesophotic	23.09 ± 0.16	4.96 ± 0.74	-0.34 ± 0.07	3.58 ± 0.01	5.44 ± 0.02	36.65 ± 0.01
30 m	24.28 ± 0.25	10.02 ± 2.32	-0.64 ± 0.14	3.59 ± 0.02	5.44 ± 0.03	36.65 ± 0.02
40 m	23.8 ± 0.32	5.38 ± 1.42	-0.35 ± 0.10	3.61 ± 0.02	5.48 ± 0.03	36.67 ± 0.01
60 m	22.33 ± 0.20	2.81 ± 0.70	-0.22 ± 0.10	3.56 ± 0.02	5.42 ± 0.02	36.68 ± 0.01

Reef zone	DIC	TA	NH_4^+	$NO_2^- \pm NO_3^-$	PO_4^{3-}	Silicate
	µmoles kg^{-1}	µmoles kg^{-1}	µmoles L^{-1}	µmoles L^{-1}	µmoles L^{-1}	µmoles L^{-1}
Mesophotic	2073.09 ± 1.25	2398.93 ± 0.81	0.13 ± 0.05	0.17 ± 0.05	0.01 ± 0.01	0.97 ± 0.04
30 m	2068.41 ± 2.36	2392.39 ± 2.18	0.08 ± 0.03	0.27 ± 0.14	0.01 ± 0.01	1.05 ± 0.08
40 m	2070.57 ± 2.31	2398.09 ± 1.56	0.05 ± 0.04	0.12 ± 0.05	0.01 ± 0.01	1.01 ± 0.07
60 m	2075.97 ± 1.79	2401.81 ± 0.87	0.19 ± 0.09	0.14 ± 0.05	0.01 ± 0.01	0.91 ± 0.05

NEC calcuated using the molecular weight of 100.09 NEP calcuated using the molecular weight of 12

2.4.2 Temporal changes in seawater carbonate chemistry and trophic status

The 2017 monthly observations of nDIC (Figure 2.2g-i) at the shallow mesophotic sites (30 m, 40 m) were generally higher than values calculated from BATS (~3 - 4 µmoles kg^{-1}). However, in 2018, the shallow reef observation fluctuated ± ~ 1 µmoles kg^{-1}around those observed at BATS. Observations from the 2017 60 m reefs fluctuated ± ~ 8 µmoles kg^{-1} the BATS value whilst they were ~ 8 µmoles kg^{-1} higher than values observed at BATS in 2018. The mean nDIC values (± standard deviation) for BATS, the 30 m, 40 m and 60 m MCEs over this study period were 2068.67 ± 10.90 µmoles kg^{-1}, 2065.31 ± 10.37 µmoles kg^{-1}, 2066.68 ± 11.20 µmoles kg^{-1} and 2071.46 ± 14.21 µmoles kg^{-1} respectively. Generally, the mesophotic reefs had lower nTA values than BATS for the duration of the study, with concentrations ranging between ~ 2 – 45 µmoles kg^{-1} lower. The mean nTA values (Figure 2.2j-l) for the 30 m, 40 m, 60 m MCEs and BATS over this study period were 2388.83 ± 12.94 µmoles kg^{-1}, 2393.60 ± 7.53 µmoles kg^{-1}, 2396.62 ± 5.63 µmoles kg^{-1}, 2399.20 ± 10.90 µmoles kg^{-1} respectively. The values recorded from mesophotic reefs followed the seasonal pattern recorded at BATS for both nDIC and nTA

(Figure 2.2g-l). The saturation states for aragonite ($\Omega_{aragonite}$) and calcite ($\Omega_{calcite}$) remained stable for the duration of the study (Figure 2.2m-o).

With the exception of the 60 m reefs, the monthly mean NEP of MCEs exhibited similar albeit it, inverted (i.e., decreases of NEP coincided with increases in NEC) seasonal patterns to those observed for NEC (Figure 2.3). There were seasonal differences in NEP signals recorded from the three reef zones (H = 17.144, p = <0.0001; Table 2.3) that reflected the trophic switch over the course of the year (Figure 2.3). Net ecosystem production did not differ across the three reef zones (H = 3.728, p = 0.155) despite the observed differences in the monthly mean patterns. Between May and December, the 30 – 40 m NEP values were generally negative and symptomatic of autotrophy (photosynthesis > respiration; minimum value -3.14 g C m^{-2} d^{-1}). Positive increases in NEP indicative with heterotrophy (i.e., photosynthesis < respiration) occurred later in the year and for longer time periods with increasing depth. Generally, periods of heterotrophy occurred in the winter for 30 m reefs, early summer in the 40 m reefs and throughout the summer and fall in the 60 m reefs (Figure 2.3b,d,f). Calcification (positive NEC; Figure 2.3a,c,e) generally occurred between May and December with the greatest rates measured at the 30 m depths and steadily decreased with increased depth (Z = 2.803, p = 0.015; Table 2.3). The peak monthly average (± standard deviation) calcification periods for all three depth ranges occurred in September (30 m = 36.62 ± 4.23 g $CaCO_3$ m^{-2} d^{-1} in 2017, 40 m = 30.90 ± 0.01 g $CaCO_3$ m^{-2} d^{-1} in 2017) and October (60 m = 16.44 ± 11.74 g $CaCO_3$ m^{-2} d^{-1} in 2018).

Table 2.3. Summary of analyses statistically comparing Net Ecosystem Calcification (NEC) and Net Ecosystem Production (NEP) between sampling depth (m) and time of year (Kruskal-Wallis H test). Variation in community NEC and NEP between sampling depth (m) and time of year (Dunn's test).

NEC	**Kruskal-Wallis H**			**NEC**	**Dunn's test (Kruskal-Wallis multiple comparison)**	
	df	***H***	***P***		***Z***	***P.adj***
Depth	2	9.013	**0.011**	**Depth**		
				30 m - 40 m	0.862	0.388
				30 m - 60 m	2.803	**0.015**
				40 m - 60 m	1.835	0.100
Season	3	35.686	**<0.001**	**Season**		
				Autumn - Spring	5.320	**<0.001**
				Autumn - Summer	4.892	**<0.001**
				Spring - Summer	-1.213	0.270
				Autumn - Winter	2.096	0.072
				Spring - Winter	-1.691	0.136
				Summer - Winter	-0.949	0.342
NEP	**Kruskal-Wallis H**			**NEP**	**Dunn's test (Kruskal-Wallis multiple comparison)**	
	df	***H***	***P***		***Z***	***P.adj***
Depth	2	3.728	0.155	**Depth**		
				30 m - 40 m	-0.945	0.517
				30 m - 60 m	-1.910	0.168
				40 m - 60 m	-0.818	0.413
Season	3	17.144	**<0.001**	**Season**		
				Autumn - Spring	0.338	0.735
				Autumn - Summer	-2.931	**0.010**
				Spring - Summer	-2.939	**0.020**
				Autumn - Winter	-2.750	**0.009**
				Spring - Winter	-2.846	**0.009**
				Summer - Winter	-0.956	0.407

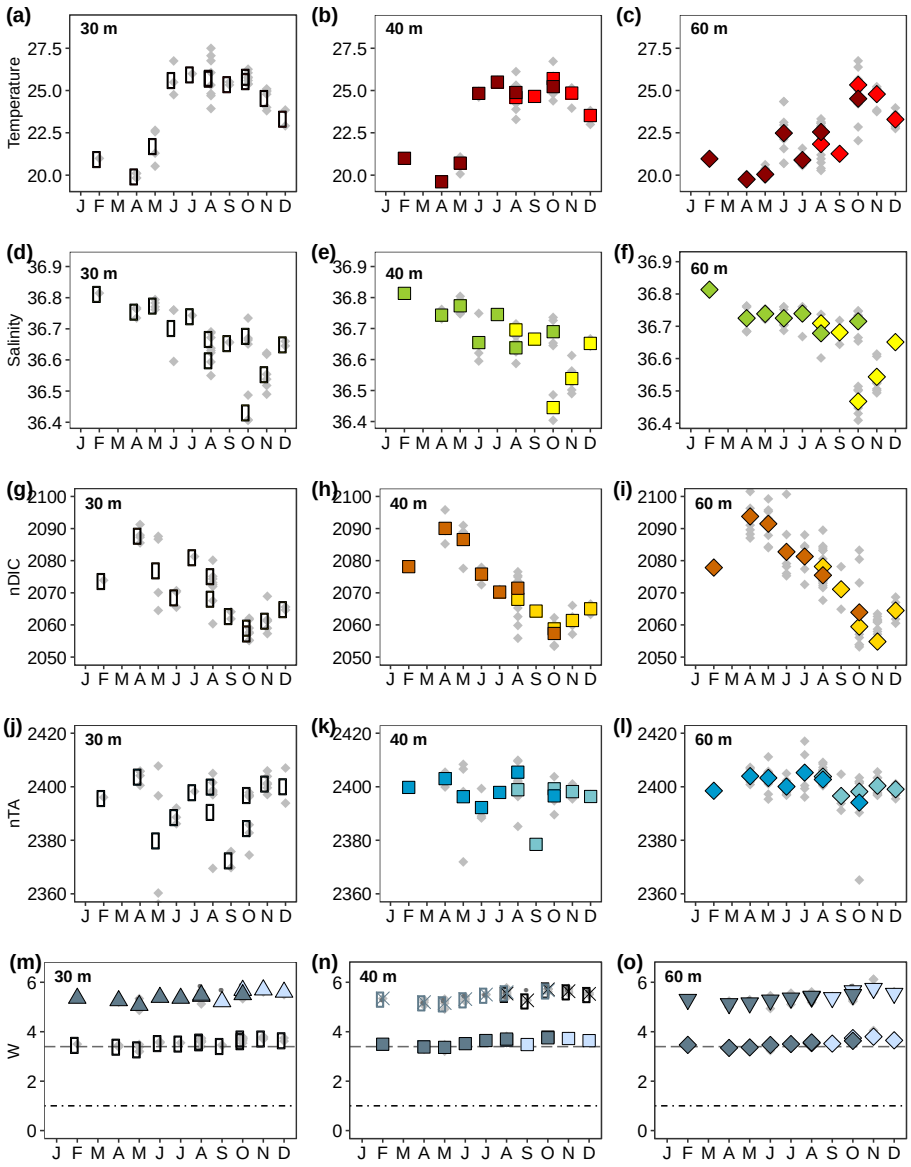

Figure 2.2. Mesophotic carbonate chemistry data at 30 m, 40 m and 60 m depths. (**a – o**), BATS data (dark grey circles), MCE 2017 data (light grey circles), 2018 (grey diamonds). (**a - c**) Temperature °C (2017 red symbols, 2018 dark red symbols); (**d - f**) salinity PSU (2017 yellow symbols, 2018 green symbols); (**g - i**) nDIC (µmoles kg^{-1}, 2017 orange symbols, 2018 dark orange symbols); (**j - l**) nTA (µmoles kg^{-1} , 2017 blue symbols, 2018 dark blue symbols; (**m**) $\Omega_{aragonite}$ (2017 light blue circles, 2018 grey circles), $\Omega_{calcite}$ (2017 light blue triangles, 2018 grey triangles); (**n**) $\Omega_{aragonite}$ (2017 light blue squares, 2018 grey squares), $\Omega_{calcite}$ (2017 black hatched circles, 2018 light grey hatched circles); (**o**) $\Omega_{aragonite}$ (2017 light blue diamonds, 2018 grey diamonds), $\Omega_{calcite}$ (2017 light blue inverted triangles, 2018 grey inverted triangles). DIC, TA, $\Omega_{aragonite}$ and $\Omega_{calcite}$ have been salinity normalized to values of 36.6 g kg-1. The black dot - dash line depicts $\Omega_{aragonite}$ = 1, thermodynamically, dissolution is anticipated if Ω < 1; grey dashed line depicts $\Omega_{aragonite}$ = 3.4, transition from coral reef to non-reef coral community; pink shaded area $\Omega_{aragonite}$ 3.0 – 3.5 defined as the global limit for reef development.

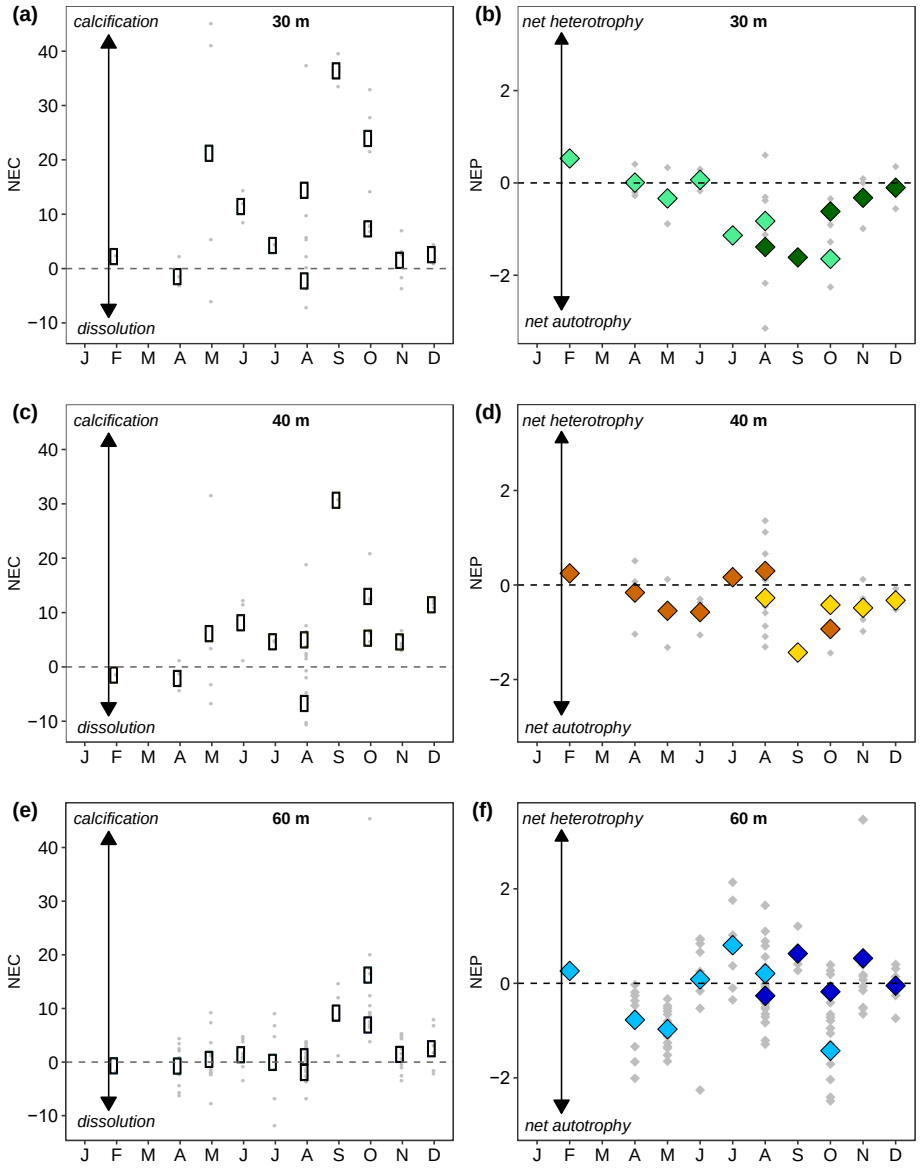

Figure 2.3. Mean seasonal climatology of net ecosystem calcification (NEC; g $CaCO_3$ m^{-2} d^{-1}) and net ecosystem production (NEP; g C m^{-2} d^{-1}) for 30 m, 40m, 60 m reefs. Grey symbols represent actual samples (**a**) NEC, dark green circles denote monthly mean values for 2017, light green circles denote monthly mean values for 2018; (**b**) NEP, dark green diamonds denote monthly mean values for 2017, light green diamonds circles denote monthly mean values for 2018; (**c**) NEC, orange circles denote monthly mean values for 2017, dark orange circles denote monthly mean values for 2018; (**d**) NEP, orange diamonds denote monthly mean values for 2017, dark orange diamonds denote monthly mean values for 2018; (**e**) NEC, dark blue circles denote monthly mean values for 2017, light blue circles denote monthly mean values for 2018; (**f**) NEP, dark blue diamond's denote monthly mean values for 2017, light blue diamond's denote monthly mean values for 2018. Dashed lines equal calcification and trophic status are in balance (e.g., NEC = 0, NEP = 0).

2.5 Discussion

2.5.1 Calcification status

Bermudan mesophotic reefs exhibit both spatial and temporal variability in biogeochemical processes (i.e., the balance of photosynthesis, respiration, calcification, and $CaCO_3$ dissolution). The mean NEC for the collective mesophotic reef system and individual reef depths investigated were positive thus indicative of net calcification (Figure 2.3a,c,e). The greatest rates of NEC were measured at the 30 m depths and steadily decreased with increased depth to the point that the 60 m reefs were in a state of equilibrium (calcification = dissolution) for ~ 6 months of the year. The peak calcification period for all three depth ranges occurred in September and October followed by a period of equilibrium and or dissolution in the winter months. This switch between net accretion and net dissolution has been documented on a seasonal basis for Bermuda shallow reefs (Yeakel et al., 2015; Muehllehner et al., 2016; Bates, 2017; Cyronak et al., 2018). The peak calcification periods are comparable to a recent study on shallow reef calcification (Bates, 2017). The same study also recorded a reduction of accretion rates to near zero during an annual cycle over the duration of the 20-year time-series study. The monthly mean NEC (± standard deviation) for the 30 m, 40 m and 60 m reefs was 10.02 ± 14.32 g $CaCO_3$ m^{-2} d^{-1}, 5.38 ± 9.09 g $CaCO_3$ m^{-2} d^{-1} and 2.81 ± 6.94 g $CaCO_3$ m^{-2} d^{-1}. These calcification rates are comparable to scaled *in situ* skeletal growth rates of the Grooved brain coral (*Diploria labryinthiformis* Linnaeus 1758; ~1.30 - 3.20 g $CaCO_3$ m^{-2} d^{-1}; Bates et al., 2010) located on the north coral platform of Bermuda at ~10 m depth. However, these skeletal rates should not be taken as a direct comparison since the reef types and environmental conditions are not cognate (Andersson and Gledhill, 2013). Literature on mesophotic biogeochemistry and influences thereof are lacking (Hoegh-Guldberg et al., 2017), therefore it makes it impossible for direct NEC comparisons to other mesophotic locations but to give these values context, they fall within the range of average global coral reef NEC values 2.00 – 25.00 g $CaCO_3$ m^{-2} d^{-1} (Atkinson, 2011). Interestingly, the 60 m locations show variability of calcification estimates (NEC). The three locations (Figure 2.1) spend differing accumulative time in a state of net calcification (BT1= 69%, BT2 =76%, BT3 66%) over duration of the study period (monthly; August 2017 – October

2018). The mean calcification rates for BT1, BT2 and BT3 were 2.63 ± 6.03g $CaCO_3$ m^{-2} d^{-1}, 7.38 ± 11.67 g $CaCO_3$ m^{-2} d^{-1}, and 4.40 ± 10.11 g $CaCO_3$ m^{-2} d^{-1} respectfully. The reason for this variability is currently unknown but may be influenced by local hydrology. Bates (2017) determined that Bermuda shallow coral reef NEC have increased at approximately 3% per year (~0.7 ± 0.3 g $CaCO_3$ m^{-2} d^{-1}) over a 20-year period (1996 – 2016). Since such mesophotic rate measurements constitute the first study, it is impossible to say if this trend will extend into mesophotic depths. However, both the study by Bates (2017) and a separate study by Yeakel et al. (2015) suggested episodic events of elevated NEC indicative of high calcification could be enhanced through alternative carbon sources (i.e., acquisition of organic nutrients through advection of biomass, e.g., zooplankton) as indicated by increased heterotrophy (> NEP; Figure 2.3e,f). This potential response appears to be evident in elevated measurements of NEP from the 60 m reefs in September and November 2017. Whilst autotrophy (photosynthesis by symbiont) is the primary source for most scleractinian corals, it has been demonstrated that up to ~ 60% of the metabolic requirements a of a coral (Houlbrèque and Ferrier-Pagès, 2009) can be supplied through heterotrophy (i.e., incorporation of particulate and dissolved organic matter, respiration). Mesocosm based feeding experiments have shown this input of organic carbon can maintain calcification rates under ocean acidification conditions (Drenkard et al., 2013; Towle et al., 2015) as well as enhance photosynthesis (Houlbrèque and Ferrier-Pagès, 2009). Yeakel et al. (2015) postulate these changes in metabolite source led to elevated summertime calcification rates (NEC), draw down of nTA and a reduction in pH and $\Omega_{aragonite}$. These high calcification / acidification events are correlated with a negative winter North Atlantic Oscillation (NAO). One could hypothesize that through geographical location, mesophotic reefs, at least for Bermuda, are the "boundary layer" between the open ocean and shallow reefs. One would surmise that any benefits episodic events such as the winter NAO afford shallow corals through advection of biomass onto the reef, could be happening on a more frequent basis for mesophotic reefs. A study of coral trophic zonation on Palmyra Atoll determined that internal waves (example of a transport mechanism of oceanic plankton) were depth restricted with only 4 – 8 % of events extending up reef slopes shallower than 30 m (Williams et al., 2018). Increases in both phytoplankton and zooplankton biomass have been documented at the

Bermuda Atlantic Time-series Study site (~ 80 km southeast of Bermuda), with resultant increases in active carbon flux due to diel vertical migration (zooplankton) and passive carbon flux by faecal pellets export (i.e., particulate organic matter; Steinberg et al., 2012).

The three locations were all accumulatively in a state of net heterotrophy for ~ 30 % of the study period, however BT3 had the greatest accumulative time at 38%. Whilst elevated calcification levels and corresponding draw down of nTA were observed on the 60 m reefs in latter part of 2017 (September and November), there appeared to be no reduction in $\Omega_{aragonite}$ or pH. Whilst there were increases in the heterotrophy signal on the 60 m reef during this period, the same responses were not observed on the 30 m or 40 m reefs. In fact, there were stronger periods of mean autotrophy during September relative to the previous month. This trend also occurred in November on the 40 m reefs. It would be expected that there would be an increased reliance on heterotrophy with increased depth by scleractinian corals (Williams et al., 2018) due to increased light attenuation and increased particulate resource availability (Fox et al., 2018) driven by hydrodynamic processes such as upwelling and internal waves.

The reason(s) for the apparent variations in trophic status between the three reef zones is currently unknown however, it is suspected that fine-scale hydrodynamic and hydrographic regimes are likely drivers of these spatial disparities (Williams et al., 2018). Longer term measurements of mesophotic biogeochemistry and a better understanding of hydrology will (1) validate the theory of augmented calcification through increased nutrition (i.e., heterotrophy); (2) help delineate the environmental controls on these deeper reef systems.

In addition to the advection of biomass (e.g., plankton and POM) from oceanic sources, deep-water upwelling and internal waves are known to influence nutrient availability through influxes of inorganic nutrients onto reef systems (Stuhldreier et al., 2015). These allochthonous inputs are often rapidly converted to particulate resources therefore leading to increased primary productivity. The increase in POM resource availability enables coral heterotrophy and is a critical component of fish productivity which can be sustained through multiple heterotrophy trophic pathways (Chassot et al., 2010; Morais and Bellwood, 2019).

Primary productivity within coral reef systems has traditionally been viewed as the regulator of higher trophic levels (bottom-up control). However, it has been postulated that top-down control (biomass altered by predation) enables fish communities to influence biogeochemical cycling rates (Kavanagh and Galbraith, 2018a), for example through consumer-mediated nutrient dynamics (Allgeier et al., 2017). Primary production would potentially be enhanced through the excretion and egestion of essential nutrients.

2.5.2 Trophic status

The three reef systems exhibited differences in estimated trophic status over the course of the study. The monthly mean NEP estimates for the 30 m reefs between February and June were generally negative and symptomatic of autotrophy (photosynthesis > respiration). During this same timeframe, the 40 m reef systems switched to a state of net autotrophy during May and June. The 60 m reefs were generally in a state of equilibrium or net autotrophy during this period followed by positive NEP indicative with heterotrophy (i.e., photosynthesis < respiration) or equilibrium between June – February. This pattern of net autotrophy in the early summer with a shift to strong heterotrophy in late summer was described by Bates et al. (2010) as the “Carbonate Chemistry Coral Reef Ecosystem Feedback” (CREF hypothesis). During the summer months, elevated autotrophy (e.g., scleractinian coral calcifying) heighten the $\Omega_{aragonite}$, and [CO_3^{2-}] conditions (e.g., CO_2 uptake and photosynthesis). In the late summer, there is a switch in metabolic source, CO_2 released through respiration leads to a suppression of photosynthetic activity. Evidence for this can be seen in Figure 2.3b,d,f albeit the estimated NEP values to not become positive (i.e., heterotrophic) for either the 30 m or 40 m reefs. Instead, the feedback causes a strong reduction in autotrophy closer to a state of equilibrium. Whilst there was variability between the three reefs depths, the overall status of the mesophotic system was net autotrophic (-0.34 ± 0.92 g C m^{-2} d^{-1}) and not in a state of balance. This determination is the opposite of the trophic evaluation for Bermuda shallow reefs (net heterotrophic; + 0.20 ± 0.9 g C m^{-2} d^{-1}). These findings present an interesting conundrum. Zooxanthellate corals are generally restricted to depths where light levels typically exceed the 0.5% of the subsurface intensity (Dubinsky and Stambler, 2011). Therefore, light availability is a primary factor that drives the vertical

zonation of communities. The classical viewpoint would be to expect that the shallow water reefs would be more likely to derive carbon by way of the inorganic carbon cycle (i.e., photosynthesis) due to greater levels of surface irradiance. However, as discussed in the calcification section, there are energetic benefits when zooxanthellate corals utilize both inorganic and organic carbon sources (photosynthesis + respiration). It does raise the question about the exact composition of the primary calcifiers at mesophotic depths and how representative are these rate measurements and if we truly are "taking the metabolic pulse" of these communities (Cyronak et al., 2018). To further complicate our understanding of these complex biogeochemical processes, there are alternative inputs of $CaCO_3$ and alkalinity fluxes that have not been considered. Scleractinian corals are considered dominant calcifiers on reef systems, however all marine teleosts produce and excrete $CaCO_3$ as an osmoregulatory product due to the constant swallowing of seawater (Wilson et al., 2009). Calcium carbonate precipitates into the digestive tract and is excreted either as pellets or with faecal matter which is estimated to contribute ~ 3 – 15% of total new $CaCO_3$ production to the upper oceanic environment (Wilson et al., 2009). Dissolution of the excreted $CaCO_3$ would lead to increases in total alkalinity. It should be noted that the calculated NEC rates are a relative expression of the balance of calcification and dissolution based on observed differences between offshore and *in situ* normalised TA measurements (Equation 4). Increases in offshore TA values would result in a stronger positive NEC signal. Alternatively, increases in mesophotic TA values would correspond to a stronger negative NEC signal. Hypothetically, fluctuations in fish abundances at either survey or reference sites (e.g., diel vertical migration of deep-sea fish) could lead to direct changes in biogeochemical processes and alternative interpretation of calcification/dissolution results.

2.5.3 Other considerations

Knowledge on benthic community composition for mesophotic reefs is lacking on a global scale (Loya et al., 2019). Goodbody-Gringley et al. (2019) summarise known information for Bermuda and a recent field guide to Bermuda's MCEs has been produced (Stefanoudis et al., 2018). Based on a limited number of quantitative surveys (n = 5) algae

and a sand/rubble complex account for 69% and ~25% of the broad functional groupings of the benthic community at 60 m depths. For context, Scleractinia represent 0.02% of these data. It could be postulated that these measurements of calcification/dissolution and autotrophic/heterotrophic may not be directly coupled to coral calcification and may in fact be an alternative signal such as a seasonal reduction in $CaCO_3$ dissolution/bioerosion or fish movement patterns. Within the algal grouping, encrusting crustose coralline algae (CCA) and rhodoliths are the main calcifying taxa. Rhodoliths and CCA perform a valuable ecosystem services of substrate provision through calcification. Which carbonate mineral phase (i.e., aragonite, calcite, and magnesian calcite - Mg-calcite) these red algae utilize for calcification is taxa specific (Nash et al., 2019) but in the case of *Corallinales*, the carbonate mineral phase is Mg-calcite (Nash et al., 2011). Gorgonians are known to calcify using Mg-calcite and are one of the most diverse coral groups on Caribbean MCES below 60 m depths. A recent study on the effects of ocean acidification on *Corallium rubrum* (Linnaeus, 1758) demonstrated lower pH (7.81 pH) significantly reduced skeletal growth (Bramanti et al., 2013), therefore till disproven, one could assume a similar response by mesophotic *Corallinales*. The effect of ocean acidification (OA) and the reduction of seawater saturation state on marine organisms' ability to accrete $CaCO_3$ has been well documented in the literature. However, studies do not tend to delineate between different carbonate mineral phases (i.e., aragonite, calcite, and magnesian calcite, i.e., Mg-calcite) saturation states (Lebrato et al., 2016) often referring to fluctuations in $\Omega_{aragonite}$ or $\Omega_{calcite}$. Magnesium calcite (Mg-calcite) with a significant mol% magnesium in calcite (8-12%) is more soluble than both aragonite and calcite (Morse et al., 2006). New evidence suggests $\Omega_{aragonite}$ or $\Omega_{calcite}$ do not account for the Mg content of calcite (increased solubility) therefore are not appropriate estimates of seawater saturation state with respect to Mg-calcite (Lebrato et al., 2016). The same study determined that 24% of benthic calcite producing calcifiers are currently experiencing under saturated conditions (i.e., dissolution; $\Omega_{Mgcalcite\text{-}x}$). Of those, the majority (95%) were found in the tropics.

A lack of long-term measurements currently restricts our ability to interpret natural and seasonal variability of mesophotic biogeochemistry. Ultimately, this hinders our capacity to predict biogeochemical responses of these environments to future ocean

acidification and climate change scenarios. Predications of the effects of OA on calcifying benthic communities are often based on the relationship between average $\Omega_{aragonite}$ and NEC (gross calcification – gross CaCO3 dissolution) which typically changes at a rate of 102% NEC per unit change of seawater $\Omega_{aragonite}$ (Eyre et al., 2018). Predicting OA driven changes to mesophotic coral ecosystems is beyond the scope of this study. However, the estimates of NEC and NEP derived by this investigation represent the first known biogeochemical measurements for mesophotic reefs and therefore provided the critical first step towards enabling our predictive capabilities. The unique location of the study allows these measurements to be considered in the context of contemporaneous offshore changes observed at the Bermuda Atlantic Time-series Study (BATS) site. The BATS program was established in 1988 and represents the longest-running time-series for biogeochemical oceanographic data.

It should be recognized that these measurements are of the balance between calcification and $CaCO_3$ dissolution (NEC) and organic carbon cycling (NEP). As such, they might not be directly coupled to benthic calcification (i.e., estimates of framework / sediment transport) or represent specific energy pathways (e.g., $CaCO_3$ sediment dissolution = increase in DIC). However, the NEC estimates establish that the seawater chemistry of Bermuda mesophotic reefs is chemical conducive for calcification. These reef systems are in a net state of calcification (i.e., accretion of $CaCO_3$) and exhibited changes in calcification (strongest periods in the late summer) and trophic state (switch heterotrophy to autotrophy) during the investigation. These findings represent a unique yet limited snapshot of the biogeochemical conditions for Bermuda's mesophotic reefs. Decoupling the environmental controls exerted on these and mesophotic reefs in general, will require considerably longer observational time scales coupled with experimental approaches.

During the 18-month time frame of this study, mesophotic biogeochemical observations displayed a similar response to the seasonal trends established for adjacent shallow reefs (Yeakel et al., 2015; Bates, 2017). All three mesophotic reef zones were net accretive (i.e., gross calcification > gross CaCO3 dissolution) and in a net state of autotrophy. Despite this, these systems exhibited periods of variability through a trophic switch between autotrophy and heterotrophy. It remains to be determined if these signals

are indicative of the seasonal variability established Bermuda's shallow water reef system.

Whilst these data are invaluable and have begun to fill much needed knowledge gaps, the study has generated additional questions that require further examination. For example, why are the mesophotic reefs in opposing trophic states to those of the shallow reef counter parts (MCE = net autotrophic, shallow reefs = net heterotrophic; Bates, 2017)? The values established by this study demonstrate just how close these understudied ecosystems are in terms of the known boundary thresholds for low saturation states of reefs (Figure 2.2m-o). Making predictions on how these ecosystems will respond to future climate changes will be extremely difficult when it is not currently known if the biogeochemical signals are a true representation of the status of these reefs, or alternatively signals of seasonal reduction in $CaCO_3$ dissolution/bioerosion. Although these processes are yet to be fully understood, the apparent increase in NEC and NEP rates (~30%) on Bermudan shallow reefs over the last 20 years (Bates, 2017) are an indication that there is a level of resilience to the changing environment that may extend to MCEs. At what level and for how long are critical questions that will need to be urgently addressed in the near future. Finally, it should be noted that whilst these data represent the first of their kind, this study has only scratched the surface in understanding the physico-chemical parameters dictated by the water masses and benthic composition of MCEs and their extent from a biogeochemical perspective.

2.6 References

Allgeier, J. E., Burkepile, D. E., and Layman, C. A. (2017). Animal pee in the sea: consumer-mediated nutrient dynamics in the world's changing oceans. *Glob Chang Biol* 23, 2166–2178. doi: 10.1111/gcb.13625.

Andersson, A. J., and Gledhill, D. (2013). Ocean Acidification and Coral Reefs: Effects on Breakdown, Dissolution, and Net Ecosystem Calcification. *Ann Rev Mar Sci* 5, 321–348. doi: 10.1146/annurev-marine-121211-172241.

Andersson, A. J., Kuffner, I. B., MacKenzie, F. T., Jokiel, P. L., Rodgers, K. S., and Tan, A. (2009). Net Loss of CaCO3 from a subtropical calcifying community due to seawater acidification: Mesocosm-scale experimental evidence. *Biogeosciences* 6, 1811–1823. doi: 10.5194/bg-6-1811-2009.

Andersson, A. J., Yeakel, K. L., Bates, N. R., and De Putron, S. J. (2014). Partial offsets in ocean acidification from changing coral reef biogeochemistry. *Nat Clim Chang* 4, 56–61. doi: 10.1038/nclimate2050.

Atkinson, M. J. (2011). "Biogeochemistry of nutrients," in *Coral reefs: An ecosystem in transition*, eds. Z. Dubinsky and S. Stambler (Springer Netherlands), 199–206. doi: doi.org/10.1007/978-94-007-0114-4_13.

Baker, E., Puglise, K., and Harris, P. (2016). Mesophotic Coral Ecosystems - A Lifeboat for Coral Reefs? The United Nations Environment Programme and GRID-Arendal, Nairobi and Arendal.

Bates, N. R. (2002). Seasonal variability of the effect of coral reefs on seawater CO 2 and air-sea CO 2 exchange.

Bates, N. R. (2017). Twenty years of marine carbon cycle observations at Devils Hole Bermuda provide insights into seasonal hypoxia, coral reef calcification, and ocean acidification. *Front Mar Sci* 4, 1–23. doi: 10.3389/fmars.2017.00036.

Bates, N. R., Amat, A., and Andersson, A. J. (2010). Feedbacks and responses of coral calcification on the Bermuda reef system to seasonal changes in biological processes and ocean acidification. *Biogeosciences* 7, 2509–2530. doi: 10.5194/bg-7-2509-2010.

Bates, N. R., Best, M. H. P., Neely, K., Garley, R., Dickson, A. G., and Johnson, R. J. (2012). Detecting anthropogenic carbon dioxide uptake and ocean acidification in the North Atlantic Ocean. *Biogeosciences* 9, 2509–2522. doi: 10.5194/bg-9-2509-2012.

Bates, N. R., Michaels, A. F., and Knap, A. H. (1996). Alkalinity changes in the Sargasso Sea: of calcification? geochemical evidence.

Bongaerts, P., Muir, P., Englebert, N., Bridge, T. C. L., and Hoegh-Guldberg, O. (2013). Cyclone damage at mesophotic depths on Myrmidon Reef (GBR). *Coral Reefs* 32, 935. doi: 10.1007/s00338-013-1052-y.

Bongaerts, P., Ridgway, T., Sampayo, E. M., and Hoegh-Guldberg, O. (2010). Assessing the "deep reef refugia" hypothesis: Focus on Caribbean reefs. *Coral Reefs* 29, 1–19. doi: 10.1007/s00338-009-0581-x.

Bongaerts, P., Riginos, C., Brunner, R., Englebert, N., Smith, S. R., and Hoegh-Guldberg, O. (2017). Deep reefs are not universal refuges: Reseeding potential varies among coral species. *Sci Adv* 3. doi: 10.1126/sciadv.1602373.

Bridge, T. C. L., Hughes, T. P., Guinotte, J. M., and Bongaerts, P. (2013). Call to protect all coral reefs. *Nat Clim Chang* 3, 528–530. doi: 10.1038/nclimate1879.

Chassot, E., Bonhommeau, S., Dulvy, N. K., Mélin, F., Watson, R., Gascuel, D., et al. (2010). Global marine primary production constrains fisheries catches. *Ecol Lett* 13, 495–505. doi: 10.1111/j.1461-0248.2010.01443.x.

Cinner, J. E., Huchery, C., MacNeil, M. A., Graham, N. A. J., McClanahan, T. R., Maina, J., et al. (2016). Bright spots among the world's coral reefs. *Nature* 535, 416–419. doi: 10.1038/nature18607.

Coates, K. A., Fourqurean, J. W., Kenworthy, W. J., Logan, A., Manuel, S. A., and Smith, S. R. (2013). "Introduction to Bermuda: Geology, Oceanography and Climate," in, 115–133. doi: 10.1007/978-94-007-5965-7_10.

Cohen, A. (2003). Geochemical Perspectives on Coral Mineralization. *Rev Mineral Geochem* 54, 151–187. doi: 10.2113/0540151.

Colin, P. L. (2009). *Marine environments of Palau*. San Diego: Indo-Pacific Press.

Colin, P. L., and Lindfield, S. J. (2019). "Palau," in *Mesophotic Coral Ecosystems Coral Reefs of the World 12*, eds. Y. Loya, K. Puglise, and T. C. L. Bridge (Springer International Publishing), 285–320. doi: 10.1007/978-3-319-9275-0_16.

Courtney, T. A., Andersson, A. J., Bates, N. R., Collins, A., Cyronak, T., de Putron, S. J., et al. (2016). Comparing chemistry and census-based estimates of net ecosystem calcification on a rim reef in Bermuda. *Front Mar Sci* 3. doi: 10.3389/fmars.2016.00181.

Courtney, T. A., Cyronak, T., Griffin, A. J., and Andersson, A. J. (2021). Implications of salinity normalization of seawater total alkalinity in coral reef metabolism studies. *PLoS One* 16, 1–13. doi: 10.1371/journal.pone.0261210.

Cyronak, T., Andersson, A. J., Langdon, C., Albright, R., Bates, N. R., Caldeira, K., et al. (2018). Taking the metabolic pulse of the world's coral reefs. *PLoS One* 13. doi: 10.1371/journal.pone.0190872.

Dickson, A. G., and Millero, F. J. (1987). A comparison of the equilibrium constants for the dissociation of carbonic acid in seawater media. *Deep Sea Research Part A, Oceanographic Research Papers* 34, 1733–1743. doi: 10.1016/0198-0149(87)90021-5.

Dickson, A. G., Sabine, C. L., and Christian, J. R. (2007). *Guide to Best Practices for Ocean CO2 measurements.* North Pacific Marine Science Organization.

Dove, S. G., Kline, D. I., Pantos, O., Angly, F. E., Tyson, G. W., and Hoegh-Guldberg, O. (2013). Future reef decalcification under a business-as-usual CO2 emission scenario. *Proc Natl Acad Sci U S A* 110, 15342–15347. doi: 10.1073/pnas.1302701110.

Drenkard, E. J., Cohen, A. L., McCorkle, D. C., de Putron, S. J., Starczak, V. R., and Zicht, A. E. (2013). Calcification by juvenile corals under heterotrophy and elevated CO2. *Coral Reefs* 32, 727–735. doi: 10.1007/s00338-013-1021-5.

Dubinsky, Z., and Stambler, N. (2011). Coral reefs: An ecosystem in transition. *Coral Reefs: An Ecosystem in Transition*, 1–552. doi: 10.1007/978-94-007-0114-4.

Eyre, B. D., Cyronak, T., Drupp, P., De Carlo, E. H., Sachs, J. P., and Andersson, A. J. (2018). Coral reefs will transition to net dissolving before end of century. *Science (1979)* 359, 908–911. doi: 10.1126/science.aao1118.

Fox, M. D., Williams, G. J., Johnson, M. D., Radice, V. Z., Zgliczynski, B. J., Kelly, E. L. A., et al. (2018). Gradients in Primary Production Predict Trophic Strategies of Mixotrophic Corals across Spatial Scales. *Current Biology* 28, 3355-3363.e4. doi: 10.1016/j.cub.2018.08.057.

Fricke, H., and Meischner, D. (1985). Depth limits of Bermudan scleractinian corals: a submersible survey.

Glynn, P. W. (1996). Coral reef bleaching: Facts, hypotheses and implications. *Glob Chang Biol* 2, 495–509. doi: 10.1111/j.1365-2486.1996.tb00063.x.

Goodbody-Gringley, G., Marchini, C., Chequer, A. D., and Goffredo, S. (2015). Population structure of Montastraea cavernosa on shallow versus mesophotic reefs in Bermuda. *PLoS One* 10. doi: 10.1371/journal.pone.0142427.

Goodbody-Gringley, G., Noyes, T., and Smith, S. R. (2019). "Bermuda," in *Mesophotic Coral Ecosystems, Coral Reefs of the World 12*, eds. L. Yossi, K. A. Puglise, and T. Bridge (Springer International Publishing), 31–45. doi: 10.1007/978-3-319-92735-0_2.

Hinderstein, L. M., Marr, J. C. A., Martinez, F. A., Dowgiallo, M. J., Puglise, K. A., Pyle, R. L., et al. (2010). Theme section on "Mesophotic Coral Ecosystems: Characterization, Ecology, and Management." *Coral Reefs* 29, 247–251. doi: 10.1007/s00338-010-0614-5.

Hoegh-Guldberg, O. (2011). Coral reef ecosystems and anthropogenic climate change. *Reg Environ Change* 11, 215–227. doi: 10.1007/s10113-010-0189-2.

Hoegh-Guldberg, O., Mumby, P. J., Hooten, A. J., Steneck, R. S., Greenfield, P., Gomez, E., et al. (2007). Coral reefs under rapid climate change and ocean acidification. *Science (1979)* 318, 1737–1742. doi: 10.1126/science.1152509.

Hoegh-Guldberg, O., Poloczanska, E. S., Skirving, W., and Dove, S. (2017). Coral reef ecosystems under climate change and ocean acidification. *Front Mar Sci* 4. doi: 10.3389/fmars.2017.00158.

Houlbrèque, F., and Ferrier-Pagès, C. (2009). Heterotrophy in Tropical Scleractinian Corals. *Biological Reviews* 84, 1–17. doi: 10.1111/j.1469-185X.2008.00058.x.

Hughes, T. P., Rodrigues, M. J., Bellwood, D. R., Ceccarelli, D., Hoegh-Guldberg, O., McCook, L., et al. (2007). Phase Shifts, Herbivory, and the Resilience of Coral Reefs to Climate Change. *Current Biology* 17, 360–365. doi: 10.1016/j.cub.2006.12.049.

Jackson, J. B. C., Kirby, M. X., Berger, W. H., Bjorndal, K. A., Botsford, L. W., Bourque, B. J., et al. (2001). Historical overfishing and the recent collapse of coastal ecosystems. *Science (1979)* 293, 629–637. doi: 10.1126/science.1059199.

Jackson, J., Donovan, M., Cramer, K., and Lam, V. eds. (2014). Status and Trends of Caribbean Coral Reefs : 1970-2012. Gland, Switzerland: Global Coral Reef Monitoring Network, IUCN doi: 10.1016/0377-8401(86)90099-4.

Jones, R., Johnson, R., Noyes, T., and Parsons, R. (2012). Spatial and temporal patterns of coral black band disease in relation to a major sewage outfall. *Mar Ecol Prog Ser* 462, 79–92. doi: 10.3354/meps09815.

Kavanagh, L., and Galbraith, E. (2018). Links between fish abundance and ocean biogeochemistry as recorded in marine sediments. *PLoS One* 13. doi: 10.1371/journal.pone.0199420.

Kleypas, J. A., Buddemeier, R. W., Archer, D., Gattuso, J. P., Langdon, C., and Opdyke, B. N. (1999). Geochemical consequences of increased atmospheric carbon dioxide on coral reefs. *Science (1979)* 284, 118–120. doi: 10.1126/science.284.5411.118.

Kleypas, J. A., Buddemeier, R. W., and Gattuso, J. P. (2001). The future of Coral reefs in an age of global change. *International Journal of Earth Sciences* 90, 426–437. doi: 10.1007/s005310000125.

Knap, A., Michaels, A. F., Steinberg, D. K. D., Bahr, F., Bates, N., Bell, S., et al. (1997). *BATS Methods Manual*. Version 4. U.S. JGOFS Planning Office, Woods Hole.

Langdon, C., Gattuso, J.-P., and Andersson, A. (2010). "Measurements of calcification and dissolution of benthic organisms and communities," in *Guide to beast practices for ocean acidification research and data reporting*, eds. U. Riebesell, V. Fabry, L. Hansson, and J.-P. Gattuso (Luxembourg: Publications of the European Union), 213–232.

Langdon, C., Takahashi, T., Sweeney, C., Chipman, D., and Atkinson, J. (2000). rate of an experimental coral reef responds to manipulations in the concentrations of both Ca CO •. *Global Biogeochem Cycles* 14, 639–654.

Lantz, C. A., Atkinson, M. J., Winn, C. W., and Kahng, S. E. (2014). Dissolved inorganic carbon and total alkalinity of a Hawaiian fringing reef: Chemical techniques for monitoring the effects of ocean acidification on coral reefs. *Coral Reefs* 33, 105–115. doi: 10.1007/s00338-013-1082-5.

Lebrato, M., Andersson, A., Ries, J., Aronson, R., Lamare, M., Koeve, W., et al. (2016). Benthic marine calcifiers coexist with CaCO3-undersaturated seawater worldwide. *Global Biogeochem Cycles* 30, 1–16. doi: 10.1002/2015GB005260.Received.

Lewis, E., and Wallace, D. (1998). Program developed for CO2 system calculations. *Ornl/Cdiac-105*, 1–21. doi: 4735.

Logan, A. (1988). The Holocene Reefs of Bermuda. *Sedimenta* XI, 63.

Logan, A., and Murdoch, T. (2011). "Bermuda," in *Encyclopedia of modern coral reefs: structure, form and process, Earth Science Series.*, ed. D. Hopley (Dordrecht: Springer-Verlag), 469–486. doi: 10.1007/978-90-481-2639-2_46.

Loya, Y., Eyal, G., Treibitz, T., Lesser, M. P., and Appeldoorn, R. (2016). Theme section on mesophotic coral ecosystems: advances in knowledge and future perspectives. *Coral Reefs* 35, 1–9. doi: 10.1007/s00338-016-1410-7.

Loya, Y., Pulglise, K. A., and Bridge, T. C. L. eds. (2019). *Mesophotic Coral Ecosystems Coral Reefs of the World 12*. doi: 10.1007/978-3-319-92735-0.

Mehrbach, C., Culberson, C. H., Hawley, J. E., and Pytkowicx, R. M. (1973). Measurement Of The Apparent Dissociation Constants Of Carbonic Acid In Seawater At Atmospheric Pressure. *Limnol Oceanogr* 18, 897–907. doi: 10.4319/lo.1973.18.6.0897.

Moberg, F., and Folke, C. (1999). Ecological goods and services of coral reef ecosystems. *Ecological Economics* 29, 215–233. doi: 10.1016/S0921-8009(99)00009-9.

Morais, R. A., and Bellwood, D. R. (2019). Pelagic Subsidies Underpin Fish Productivity on a Degraded Coral Reef. *Current Biology* 29, 1521-1527.e6. doi: 10.1016/j.cub.2019.03.044.

Morse, J. W., Andersson, A. J., and Mackenzie, F. T. (2006). Initial responses of carbonate-rich shelf sediments to rising atmospheric pCO2 and "ocean

acidification": Role of high Mg-calcites. *Geochim Cosmochim Acta* 70, 5814–5830. doi: 10.1016/j.gca.2006.08.017.

Muehllehner, N., Langdon, C., Venti, A., and Kadko, D. (2016). Dynamics of carbonate chemistry, production, and calcification of the Florida Reef Tract (2009–2010): Evidence for seasonal dissolution. *AGU Publications* 30, 661–688. doi: 10.1002/2015GB005327.Received.

Nash, M. C., Diaz-Pulido, G., Harvey, A. S., and Adey, W. (2019). *Coralline algal calcification: A morphological and process-based understanding*. doi: 10.1371/journal.pone.0221396.

Nash, M. C., Troitzsch, U., Opdyke, B. N., Trafford, J. M., Russell, B. D., and Kline, D. I. (2011). First discovery of dolomite and magnesite in living coralline algae and its geobiological implications. *Biogeosciences* 8, 3331–3340. doi: 10.5194/bg-8-3331-2011.

Orr, J. C., Fabry, V. J., Aumont, O., Bopp, L., Doney, S. C., Feely, R. A., et al. (2005). Anthropogenic ocean acidification over the twenty-first century and its impact on calcifying organisms. *Nature* 437, 681–686. doi: 10.1038/nature04095.

Pandolfi, J. M., Bradbury, R. H., Sala, E., Hughes, T. P., Bjorndal, K. A., Cooke, R. G., et al. (2003). Global trajectories of the long-term decline of coral reef ecosystems. *Science (1979)* 301, 955–958. doi: 10.1126/science.1085706.

Pandolfi, J. M., Connolly, S. R., Marshall, D. J., and Cohen, A. L. (2011). Projecting coral reef futures under global warming and ocean acidification. *Science (1979)* 333, 418–422. doi: 10.1126/science.1204794.

Puglise, K., Hinderstein, L., Marr, J., Dowgiallo, M., and Martinez, F. (2008). Mesophotic Coral Ecosystems Research Strategy. Silver Spring.

Pyle, R. L., Copus, J. M., Pyles, R. L., and Copus, J. M. (2019). "Mesophotic Coral Ecosystems: Introduction and Overview," in *Mesophotic Coral Ecosystems, Coral Reefs of the World 12*, eds. Y. Loya, K. A. Puglise, and T. Bridge (Springer International Publishing), 3–27. doi: 10.1007/978-3-319-92735-0.

Romanó de Orte, M., Koweek, D. A., Cyronak, T., Takeshita, Y., Griffin, A., Wolfe, K., et al. (2021). Unexpected role of communities colonizing dead coral substrate in the calcification of coral reefs. *Limnol Oceanogr* 66, 1793–1803. doi: 10.1002/lno.11722.

Sarkis, S., van Beukering, P. J. H., McKenzie, E., Brander, L., Hess, S., Bervoets, T., et al. (2013). "Total Economic Value of Bermuda's Coral Reefs: A Summary," in *Coral Reefs of the United Kingdom Overseas Territories*, ed. C.R.C. Sheppard (Dordrecht: Springer Science and Business Media LLC), 201–211. doi: 10.1007/978-94-007-5965-7_15.

Semmler, R. F., Hoot, W. C., and Reaka, M. L. (2017). Are mesophotic coral ecosystems distinct communities and can they serve as refugia for shallow reefs? *Coral Reefs* 36, 433–444. doi: 10.1007/s00338-016-1530-0.

Smith, S. v., and Key, G. S. (1975). Carbon dioxide and metabolism in marine environments. *Limnol Oceanogr* 20, 493–495. doi: 10.4319/lo.1975.20.3.0493.

Spalding, M., Ravilious, C., and Green, E. (2001). *World atlas of coral reefs*. doi: 10.5860/choice.39-2540.

Stefanoudis, P. V., Rivers, M., Smith, S. R., Schneider, C. W., Wagner, D., Ford, H., et al. (2019). Low connectivity between shallow, mesophotic and rariphotic zone benthos. *R Soc Open Sci* 6, 190958. doi: 10.1098/rsos.190958.

Stefanoudis, P. v, Smith, S. R., Schneider, C., Wagner, D., Goodbody-Gringley, G., Xavier, J., et al. (2018). Bermuda Benthic Marine Life Field Identification Guide Bermuda Benthic Marine Life Field Identification Guide Deep Reef Benthos of Bermuda: Field Identification Guide. 1–168. doi: https://doi.org/10.6084/m9.figshare.7333838.v1.

Steinberg, D. K., Carlson, C. A., Bates, N. R., Johnson, R. J., Michaels, A. F., and Knap, A. H. (2001). Overview of the US JGOFS Bermuda Atlantic Time-series Study (BATS): A decade-scale look at ocean biology and biogeochemistry. *Deep Sea Res 2 Top Stud Oceanogr* 48, 1405–1447. doi: 10.1016/S0967-0645(00)00148-X.

Steinberg, D. K., Lomas, M. W., and Cope, J. S. (2012). Long-term increase in mesozooplankton biomass in the Sargasso Sea: Linkage to climate and implications for food web dynamics and biogeochemical cycling. *Global Biogeochem Cycles* 26. doi: 10.1029/2010GB004026.

Stuhldreier, I., Sánchez-Noguera, C., Roth, F., Cortés, J., Rixen, T., and Wild, C. (2015). Upwelling increases net primary production of corals and reef-wide gross primary production along the pacific coast of costa rica. *Front Mar Sci* 2. doi: 10.3389/fmars.2015.00113.

Sutherland, M. G., McLean, S. J., Love, M. R., Carignan, K. S., and Eakins, B. W. (2014). Digital Elevation Models of Bermuda : Data Sources , Processing and Analysis. Boulder.

Suzuki, A., and Kawahata, H. (2003). Carbon budget of coral reef systems: An overview of observations in fringing reefs, barrier reefs and atolls in the Indo-Pacific regions. *Tellus B Chem Phys Meteorol* 55, 428–444. doi: 10.1034/j.1600-0889.2003.01442.x.

Tanzil, J. T. I., Brown, B. E., Dunne, R. P., Lee, J. N., Kaandorp, J. A., and Todd, P. A. (2013). Regional decline in growth rates of massive Porites corals in Southeast Asia. *Glob Chang Biol* 19, 3011–3023. doi: 10.1111/gcb.12279.

Towle, E. K., Enochs, I. C., and Langdon, C. (2015). Threatened Caribbean coral is able to mitigate the adverse effects of ocean acidification on calcification by increasing feeding rate. *PLoS One* 10, 139398. doi: 10.1371/journal.pone.0123394.

Tribollet, A., Godinot, C., Atkinson, M., and Langdon, C. (2009). Effects of elevated pCO2 on dissolution of coral carbonates by microbial euendoliths. *Global Biogeochem Cycles* 23, 2006–2009. doi: 10.1029/2008GB003286.

Turner, J. A., Babcock, R. C., Hovey, R., and Kendrick, G. A. (2017). Deep thinking: A systematic review of mesophotic coral ecosystems. *ICES Journal of Marine Science* 74, 2309–2320. doi: 10.1093/icesjms/fsx085.

Wilkinson, C. (2008). Status of coral reefs of the world: 2008. Townsville.

Wilkinson, C. R. (1999). Global and local threats to coral reef functioning and existence: Review and predictions. *Mar Freshw Res* 50, 867–878. doi: 10.1071/MF99121.

Williams, G. J., Sandin, S. A., Zgliczynski, B. J., Fox, M. D., Gove, J. M., Rogers, J. S., et al. (2018). Biophysical drivers of coral trophic depth zonation. *Mar Biol* 165. doi: 10.1007/s00227-018-3314-2.

Wilson, R. W., Millero, F. J., Taylor, J. R., Walsh, P. J., Christensen, V., Jennings, S., et al. (2009). Contribution of fish to the marine inorganic carbon cycle. *Science (1979)* 323, 359–362. doi: DOI: 10.1126/science.1157972.

Wolanski, E., Colin, P., Naithani, J., Deleersnijder, E., and Golbuu, Y. (2004). Large amplitude, leaky, island-generated, internal waves around Palau, Micronesia. *Estuar Coast Shelf Sci* 60, 705–716. doi: 10.1016/j.ecss.2004.03.009.

Yeakel, K. L., Andersson, A. J., Bates, N. R., Noyes, T. J., Collins, A., and Garley, R. (2015). Shifts in coral reef biogeochemistry and resulting acidification linked to offshore productivity. *Proc Natl Acad Sci U S A* 112, 14512–14517. doi: 10.1073/pnas.1507021112.

Chapter 3. Metabarcoding inference of ichthyofauna biodiversity across a subtropical Mesophotic coral reef depth gradient

3.1 Abstract

Mesophotic coral ecosystems (MCEs) are often extensions of shallow reef communities, harbour high geographic endemism and are important refugia for vital taxonomic groups. The composition of mesophotic reef fish communities is less well understood than shallow water counterparts due to the depth related logistical challenges associated with conducting mesophotic research. The rapid development of eDNA analysis has transformed biomonitoring-based studies that target biomes that are inherently difficult to access. The application of eDNA metabarcoding could address significant knowledge gaps in understanding the level of species overlap between MCEs and shallow reefs ecosystems. This study demonstrates that 12S fish-targeted markers can detect spatial and temporal fish biodiversity variability across a depth gradient (1 – 130 m). Both species richness and beta diversity were influenced by study location and seasonality with the latter driven by species turnover. Despite previously documented faunal breaks, this study found little evidence of depth compartmentalisation of fish communities with evidence suggesting a high degree of trophic level connectivity down the depth gradient. The detected taxa included species from shallow reef, mesophotic and deep-sea origins. Of the 170 fish species detected, the most abundant detection was the invasive lionfish (*Pterois volitans*, Linnaeus 1758). To determine the influence of environmental forcings on fish biodiversity, the study utilised redundancy analysis with ~ 7% of biodiversity variability accounted for. The status of the North Atlantic Oscillation and seasonality had the greatest influence on site level species detections. This study utilised eDNA metabarcoding to reduce the logistical complexity of gaining access to the biodiversity “treasures” contained within mesophotic ecosystems.

3.2 Introduction

Mesophotic Coral Ecosystems (MCEs) occur in the middle to lower photic zone (~30–150 m) of tropical and subtropical regions (Puglise et al., 2008; Hinderstein et al., 2010). Mesophotic reefs are often extensions of shallow reef communities, harbour high geographic endemism and are important refugia for vital taxonomic groups including corals, fish, and sponges (Baker et al., 2016a; Loya et al., 2016; Kosaki et al., 2017). MCEs have been traditionally understudied and undervalued when compared to shallow reef communities. To address the data disparity in the study of MCEs, it will require the establishment of standardised and practical methodologies for comprehensive monitoring regimes to ensure effective management practices and maintenance of ecosystem health (Hoegh-Guldberg et al., 2017; Turner et al., 2017). There are significant knowledge gaps in understanding ecosystem functions within MCEs such as biogeochemical cycling, biogeographic patterns of taxa (Slattery et al., 2011; Turner et al., 2019; Eyal and Pinheiro, 2020) and the level of connectivity there is between shallow reefs ecosystems. Distinct faunal breaks between ~60 and 90 m have been documented (García-Sais et al., 2010; Bryan et al., 2013; Bejarano et al., 2014; Andradi-Brown et al., 2016b; Pinheiro et al., 2016; Rosa et al., 2016; Baldwin et al., 2018; Rocha et al., 2018; Goodbody-Gringley et al., 2019b) that are used to define the “upper” and “lower” mesophotic zones for certain fish species. Literature suggests these breaks occur at ~ 60 m in Atlantic MCEs (Pinheiro et al., 2016; Semmler et al., 2017) (Pinheiro et al., 2016; Semmler et al., 2017) and ~ 90 m for Pacific MCEs (Pyle et al., 2016). However, Baldwin et al. (2018) determined a distinct faunal break at ~ 80 m for Curaçao during an investigation of what is being termed the “rariphotic” zone: the demersal zone between the mesophotic and aphotic regions. Modelling studies by Laverick et al. (2020) lend support to faunal breaks for mesophotic benthic communities based on light availability. The same study predicted likely breaks for Bermudan mesophotic reefs to occur at ~35 m (shallow reefs/upper mesophotic) and 65 m (upper mesophotic / lower mesophotic). The relative proximity of mesophotic reefs to Bermuda reduce the logistic challenges of studying these traditionally understudied ecosystems to better understand these models.

Previous studies on Bermudan mesophotic fishes (Pinheiro et al., 2016; Goodbody-Gringley et al., 2019b) have highlighted differences in fish community composition across depth gradients. Pinheiro et al. (2016) detected increases in species richness, abundance, and biomass with increased depth in 45 – 80 m depth range. Goodbody-Gringley et al. (2019) determined a decrease in species richness with increased depth. There were differences in the community composition detected between the two studies, likely due to differing biomonitoring methodologies (underwater visual surveys vs. baited cameras). For example, a greater diversity of Muraenidae and Scaridae species were observed by BRUVs. As with all methodologies, there are associated caveats which often lead to variations in community detections. For example, baited camera assessments are a cost-effective method for generating standardised ichthyofauna data as demonstrated by the Global FinPrint initiative (www.globalfinprint.com); however, it is known that the more cryptic species are often missing (Harvey et al., 2007) from these datasets.

The development of eDNA metabarcoding has allowed non-invasive biomonitoring of inherently difficult biomes to be assessed. Despite these advancements in biomonitoring methods, there are associated limitations (Thomsen and Willerslev, 2015; Yao et al., 2022). Environmental DNA samples inherently contain both degraded target DNA and non-target DNA that can still amplify despite the use of universal primers. Universal primers can suffer from a lack of interspecific variation limiting taxa identification to species level (Thomsen et al., 2016; Collins et al., 2019; Miya et al., 2020). Incorrect interpretation of metabarcoding data can occur due to the introduction of artificial errors through contamination, PCR inhibition, sequencing errors, and insufficiently populated reference databases (Yao et al., 2022). Finally, whilst improvements on the topic are continuing to be made, at present, eDNA metabarcoding is currently considered a qualitative methodology (but see Section 1.6.1 for further details).

This chapter describes the application of this non-invasive approach to characterise spatial and temporal trends of mesophotic fish biodiversity across a depth gradient from 30 - 130 meters. Specifically, this study seeks to address the inconsistency of the community characterization determined by the two aforementioned studies (Pinheiro et al., 2016; Goodbody-Gringley et al., 2019b) and evaluate α- and β-diversity

across a depth range at three locations. Finally, the study aims to determine whether seasonality influences the levels and patterns of diversity detected at the study locations.

Since this study is the first to utilise eDNA for mesophotic fish community assessments in Bermuda, the findings aim to demonstrate the value of this methodology and promote its rapid integration into existing biomonitoring programs (e.g., using indicator species as measures of ecosystem status and measures of environmental change, invasive species management, marine spatial planning).

3.3 Methodology

3.3.1 Study Locations

The study locations used by this investigation are situated at the interface between the lower edge of shallow reefs and the upper mesophotic, and further, between the upper mesophotic and lower mesophotic boundary. The choice of study locations were defined a posteriori following the findings of a Darwin Plus (DPLUS001) Lionfish Control Initiative Project completed in 2015. The key finding of this study concluded Bermuda's mesophotic reef system (45 – 60 m depth range) contained significantly higher abundances of lionfish (Pterois sp. Oken 1817) than adjacent shallow water reefs. Average lionfish abundances on 60 m reefs were ~ 300 / hectare whereas ≤ 20m reefs were on average less than 10 individuals per hectare.

Within the context of this study, the term location refers to the general area of interest whilst site refer to discrete sampling points within each location. Three locations (Figure 3.1; BT1, BT2, BT3) ~10 km apart were established to investigate both spatial and temporal variability of mesophotic ichthyofauna. Within each location there are six core discrete sites ~ 350 m apart (Dorman et al. 2012), three "deep" outer sites at ~ 60 m depth and three inner "shallow" sites (30 - 40 m depth). An exception to this site alignment pattern had to be made at location BT3 due to the orientation of the depth contours resulting in one "shallow" site being established at 20 m depth. The repositioning of the site to a 30 m depth would have violated the minimum distance threshold between sites established to avoid the overlap of bait plumes during baited

camera assessments utilised in Chapter 4 and to allow for a more comprehensive representation of the fish community present within the study area (Yao et al., 2022) due to the implementation of a gridded sampling design.

In addition to the core 6 sites per location, surface samples (1 m) were taken at the central 60 m site with. In the latter half of the study, logistical capacity increased to allow ad hoc samples to be collected from the lower mesophotic environment (~ 70 – 140+ m; Laverick et al., 2020) at 130 m. These deeper sites were orientated seaward of the central 60 m (Figure 3.1b).

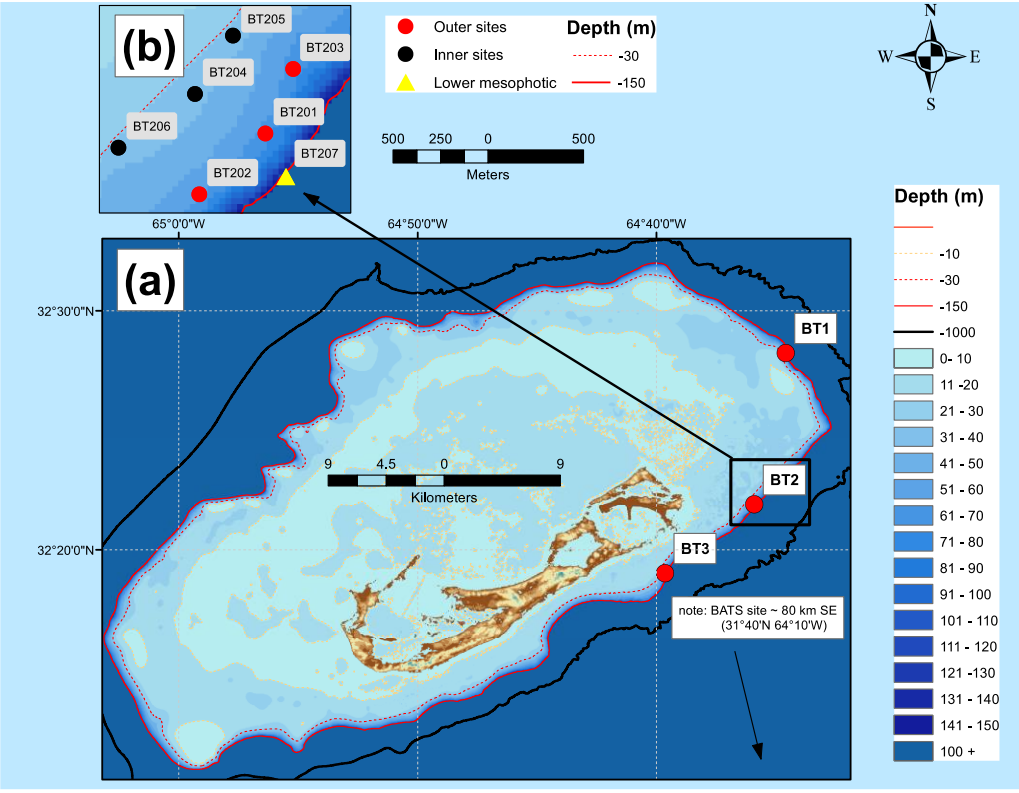

Figure 3.1. Map of Bermuda and study site locations (**a**) Bathymetric map of Bermuda illustrating the main study locations (red circles) and proximity to land and open ocean, 10 m contour line in orange, 30 m contour dashed red lines, 150 m contour solid red line, 1000 m contour solid black line. (**b**) location BT2 showing typical spatial orientation of 30 m (black circles), 60 m (red circles) and 130 m sites (yellow triangle) per location (sites ~ 350 m apart). Note, the location for reference biogeochemical measurements taken at the site of the Bermuda Atlantic Time- series Study site ~ 80 km SE of Bermuda.

3.3.2 Sample Collection

Sampling coincided with fieldwork performed for EU BEST 2.0 Projects 1634 and 2274 and as a result, were divided into separate periods, August – December 2017, April – November 2018 and finally September – October 2020. During these periods, samples were collected monthly with no more than a week separating collections from all three locations. Any slight deviation from the regime was due to inclement weather.

Environmental DNA collection approaches were optimized during a preliminary study of eDNA metabarcoding as a biodiversity monitoring tool for marine fishes of Bermuda (Noyes and Blanco-Bercial unpublished). Sample seawater was collected using a 12 L niskin lowered to a target depth (e.g., ~ 2 m above the benthos) with site depth verified via boat-mounted depth sounder. All sampling and filtering equipment were rinsed three times with 10% bleach solution and then three times with milliQ (Miya et al., 2015) prior to the collection of samples. A minimum volume of 8 L was collected to reduce false negative detection probabilities (Yao et al., 2022)**.** Sample seawater was drawn into 2 x 4L pre-rinsed Nalgene carboys that were flushed three times with sample seawater prior to filling. All sample carboys were stored on ice inside black bin bags within coolers until back at the laboratory, which ranged from 5 – 6 hours depending on the distance of the sampling location from the laboratory facilities. Cooling the samples and limiting exposure to UVB radiation served to reduce DNA degradation (Strickler et al., 2015). However, a recent study by Mächler et al. (2018) found no discernible effect of sunlight or UV on the detectability of eDNA. In the interest of maintaining a standardised procedure, the practice of keeping samples in bags on ice out of direct heat and light was the standard operating procedure.

At the first available opportunity upon return to the Bermuda Institute of Ocean Sciences (BIOS), samples were filtered through inline filter holders loaded with 47 mm 0.8 µm hydrophilic membrane polycarbonate (Takahara et al., 2012b) filters (NucleporeTM Track-Etched Membrane, Whatman®) using a vacuum filtration set up. Sample carboys remained housed within the coolers (i.e., in the dark on ice) until the filtration process for a specific carboy had begun. On average, filtration times would take 3 hours per 4 L of sample. Ideally, the full sample volume (8 L) was passed through a

single filter, however during the productive months (May – August) an additional filter would be required to achieve the desired filtered sample volume (8 L) due the retention of additional suspended matter (e.g., phytoplankton) blocking filter pores (Goldberg et al., 2016). All filters were then stored at -23ºC in a dedicated eDNA freezer until extraction.

All filtration activities were conducted in laboratory space designated for seawater filtration that had been presterilized (10% bleach wash) to minimise contamination. Whilst these areas were multiuse spaces, no fish focused activities had historically been conducted therein prior to the eDNA metabarcoding investigation.

3.3.3 Extraction and library preparation

To minimise contamination, separate laboratories were used for eDNA extractions, pre-PCR and post-PCR procedures with all laboratory spaces being cleaned prior to and post sample processing. DNA extractions from the frozen filters were performed using the E.Z.N.A. Mollusc DNA Kit (Omega Bio-Tek: Norcross, Georgia, USA) commercial kit. Modifications to the protocol included the use of 500µl ml buffer at step 2 and centrifugation for 14 minutes at 10,000 x g at step 5. Samples that required two filters to obtain the desired sample volume of 8 L were pooled during step 12 of the extraction protocol by passing the total sample through the same HiBind® DNA Mini Column. The elution step (27) was repeated twice using the same 50 µl 70°C DNA free water, in an attempt to increase DNA yield. To confirm successful DNA extraction, total DNA concentration (i.e., fish plus non-target DNA) and purity of each sample were quantified using a NanoDrop One Microvolume UV-Vis Spectrophotometer (Thermo Scientific: Waltham, Massachusetts, USA).

Library preparation was performed as a two-step Polymerase chain reaction (PCR) using AccuPower ProFi Taq PCR PreMix (Bioneer: California, USA) and the MiFish-U universal primers (12S ribosomal RNA gene 163-185 bp; Miya et al., 2015). The first step PCR was performed using 1 µl of 10 µM of both the forward and reverse primers combined with sample volume that equated to 500 ng of DNA. DNA free water was subsequently added to give a total reaction volume of 20 µl. Both positive and negative controls were run with all PCR steps to control for contamination. Positive control samples

were sourced from DNA extracts of local reef fishes incorporated into a local reference database (Noyes and Blanco-Bercial unpublished). A SimpliAmp Thermal Cycler (Applied biosystems: Foster City, California, USA) was used for the PCR, with the following thermal profile an initial denaturation at 94°C for 3 minutes followed by 30 cycles of: 30 seconds at 94°C; annealing at 60°C for 30 seconds; extension at 69°C for 30 seconds and a final extension period at 69°C for 7 minutes. For confirmation of successful PCR, the product was run on 2 % agarose gel with a Quick-Load Purple Low Molecular Weight DNA Ladder (New England Biolabs: Massachusetts, USA). PCR product was diluted (1:10) with DNA free water and 10µl used as the template for the second PCR step, combined with 1µL of 10 µM forward and reverse dual Illumina index primers in a total reaction volume of 20 µl. The reaction thermal profile followed step one. Each second step PCR was completed in triplicate with reactions pooled to give a final volume ~55 µl (after 5 µl were used for gel electrophoresis). To allow for sample identification following demultiplexing, samples were amplified with a combination of unique forward and reverse eight base-pair indexes allowing for 64 unique dual-indexed combinations. In total, 242 biological and 31 control (Field, Extraction and PCR blanks, and positive controls) were sequenced in 5 separate plate submissions. Of these, 237 were sent to the UR Genomics Research Center, University of Rochester, USA. A subset of 36 samples were sent to the Microbial Analysis, Resources, and Services (MARS), University of Connecticut Biotechnology Bioservices Center, as part of the Biodiversity and Ecosystem Services in Territories of European overseas (BEST) 2.0 Project 2274.

Sequencing protocols for both sequencing facilities were as follows, library concentration was determined using Qubit Fluorometer (Thermo Fisher Scientific) and quality assessed with an Agilent Fragment Analyser (Agilent, Santa Clara, CA). Libraries were normalized to equimolar concentrations, pooled for size selection (200 – 400 bp) using a Pippin HT (Sage Science). To normalise pooled libraries, concentrations were confirmed, and quality assessed using a Qubit Fluorometer (Thermo Fisher Scientific) and an Agilent Fragment analyser (Agilent, Santa Clara, CA). Sequencing was performed using a V2 Reagent Kit and standard flow cell with paired end reads of 250 bp with custom sequencing primers on an Illumina MiSeq platform (Illumina, San Diego, CA, USA).

3.3.4 Bioinformatics

Demultiplexed samples were analysed in MOTHUR ver 1.44.3 (Schloss et al., 2009) following an updated pipeline of Blanco-Bercial (2020). Contigs were aligned with a Phred quality score threshold of 30 and any resulting reads that were shorter than 115 bp or had ambiguities were removed. Retained unique sequences were aligned against the 12S region from the MitoFish Reference Database (Sato et al., 2018) and trimmed to the length of the region. All incomplete reads, those that did not reach both ends of the alignment were discarded. Chimeric sequences were removed using VSEARCH (Rognes et al., 2016) implemented within MOTHUR. Single variants (= 100% Molecular Operational Taxonomic Units; Porter and Hajibabaei., 2018) were obtained using DEBLUR implemented within MOTHUR (differences = 1). The resulting variants were taxonomically identified by BLASTing again the GenBank nucleotide database. Taxa similarity thresholds were set at 99% for species level assignments (Stat et al., 2019; Juhel et al., 2020). Retained MOTU assignments were passed through a second step of taxonomic confirmation through comparison to a custom-made database of fishes' native to Bermuda's marine environment (Noyes and Blanco-Bercial unpublished; see appendices for details on FASTA sequences). BLAST results were manually checked, and taxonomic nomenclature was based on the World Register of Marine Species (WoRMS; http://www.marinespecies.org/)

3.3.5 Data Analysis

All downstream analyses were performed in R version 3.5.3 (Team and R Core Team, 2019) using the following packages: betapart v1.5.4 (Baselga and Orme, 2012), FSA_0.9.1 (Ogle et al., 2021), iNEXT_2.0.20 (Hsieh et al., 2016) and vegan v2.5-6. An initial read depth of ≥5 was applied to the raw dataset to remove singletons and the likelihood of false detections. This was followed by the removal of all nonmarine taxa (e.g., *Bos taurus, Homo sapiens*). Next, all control samples were investigated for any suspected contamination reads from target taxa with a resultant application of a threshold approach-based on negative controls for those taxa detected (Deiner et al., 2017). Detected target taxa (i.e., teleost and elasmobranchs) reads were averaged across the

control samples pooled by sequence run (5 plate submissions in total). This process was applied independently to each taxon identified in the control samples (Table 3.1). The average number of contamination reads per taxa detected were then used as a correction factor specifically for that species (Bokulich et al., 2013; Port et al., 2016a; Deiner et al., 2017). The correction factor was then applied to all biological samples within the corresponding sequencing run. The remaining data were checked for taxonomic misassignments with corrections made to the genera of *Abudefduf* (Forsskål 1775), *Clepticus* (Bloch & Schneider 1801), *Mulloidichthys* (Whitley 1929), *Thalassoma* (Swainson 1839). A species similarity threshold for these genera was set at 98% since only a single species from each genus has been verified and documented in Bermuda to date.

Table 3.1. Summary of fish species detected in eDNA metabarcoding negative controls.

Species	**Common Name**	**Species**	**Common Name**
Acanthurus tractus	Ocean surgenfish	*Pterois volitans*	Red firefish
Canthigaster rostrata	Snarpnose-pufferfish	*Scarus taeniopterus*	Princess parrotfish
Decapterus macarellus	Mackerel scad	*Schedophilus ovalis*	Imperial blackfish
Halichoeres maculipinna	Clown wrasse	*Synodus intermedius*	Sand diver
Lutjanus griseus	Grey snapper	*Thalassoma bifasciatum*	Bluehead wrasse
Paranthias furcifer	Creole-fish		

Bubble plots of proportional read counts were generated to summarise the spatial and temporal community detections of taxa. Sequence data were pooled in two ways, first, sequence data were pooled to visualize interannual variability (Figure 3.4). Data were categorized as “Spring” (March – May), “Summer” (June – August), “Autumn” (September – November) and “Winter” (December – February). Secondly by depth to show species detections across a (Figure 3.5) depth gradient. The categorisation of seasons was based on a posteriori knowledge of shallow reef temperature climatology for Bermuda (Jones, 2007; Hochberg, 2014) since there are no long-term temperature climatology records for the Bermudan mesophotic reefs. For reference, in situ temperatures at the time of sample collection have been graphically displayed (Figure 3.2). Species of interest to marine resource managers were highlighted in both bubble plots categorised by trophic guild (Goodbody-Gringley et al., 2019b) and in accordance

with local regulations (Fisheries Protected Species Order 1978; Protected Species Amendment Order 2016) in addition to those managed by the International Commission for the Conservation of Atlantic Tunas (ICCAT). Spatial and temporal variation in α- and β-diversity were evaluated using a modified approach of Mariani et al. (2021b). Taxon richness of individual sampling sites was defined as α-diversity. Beta diversity metrics were defined as per Baselga and Orme (2012) with total β-diversity deemed as the variation in species composition amongst sites. Turnover was determined as the replacement of species between sites whilst nestedness was defined as species loss between sites (i.e., 'taxon subsets'). To test for between factor influence on β-diversity (season and location), a cross factor design was tested using PERMANOVA. Sequence data were converted to presence/absence for downstream β-diversity. Matrices were built based on Jaccard Dissimilarity measures, tested using permutational multivariate analysis of variance (PERMANOVA), and graphically represented using non-metric MultiDimensional Scaling (nMDS).

To discern potential environmental drivers of fish communities, redundancy analysis was used to model multivariate responses through a combination of regression and principal component analysis (PCA). Environmental data (Table 3.4) were standardised to zero mean and unit variance to account for the expression in different units and scales using the decostand function implemented through VEGAN v2.5-6. A Hellinger transformation was applied to the species data (reads) whereby abundance values are divided by the sample total abundance and then square-root transformed (Legendre and Gallagher, 2001). It was not possible to pair the full suite of eDNA samples with abiotic variables therefore analyses have been performed on a subset of data (n = 205).

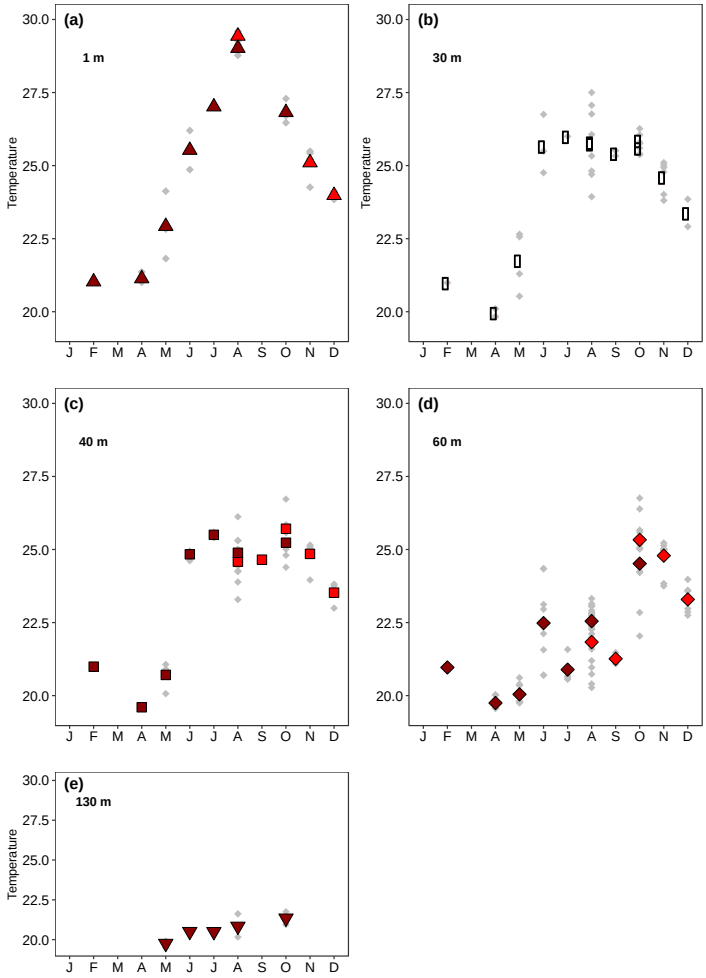

Figure 3.2 Mean temperature (°C) of surface water (1 m) and mesophotic reefs data at 30 m, 40 m, 60 m and 130 m depths. (**a – e**; 2017 mean red symbols, 2018 mean dark red symbols, *in situ* measurements light grey circles). Note, no 130 m samples were collected 2017.

3.4 Results

All biological samples produced detectable target DNA resulting in a raw detection of 107,164 amplicon sequence variants (ASVs) totalling 6,360,726 reads. After the removal of sequences assigned to non-marine taxa, application of the read depth and species assignment thresholds, these values were reduced to 4067 MOTUs and 2,063,581 reads respectively. Overall, 170 fish taxa and 1 elasmobranch were detected over the course of the study. The most abundant taxa identified was *Pterois volitans*

(327,714 reads; Linnaeus 1758), an invasive species which was recorded at all depths (Figure 3.6) across all seasons (Figure 3.7).

The greatest number of samples were taken from BT2 as indicated by sample size-based rarefication and extrapolation curves (Figure 3.3b). The same curves imply taxon diversity had reached a plateau for all locations which would infer a suitable level of sampling had been reached to assess the community structure of these three mesophotic locations.

Alpha diversity differed across locations (Table 3.2; Figure 3.2a), where the lowest taxon richness was observed from BT2 and significantly lower than BT1 and BT3 respectively. There was no significant difference in taxon richness between BT1 and BT3 (Figure 3.3a).

Beta diversity at all three locations (Table 3.3, Figure 3.3ci) was driven by taxon replacement (turnover, 99.33%) versus taxon subgroups (nestedness; 0.67%). However, location did have an influence on nestedness – resultant (R^2 = 0.0.36, p = 0.024) meaning there was a level of retention of similar taxa between locations. Total β diversity followed the same trend as α diversity (Table 3.3) where measures differed between location. However, as indicated by the stress values in the non-metric multidimensional scaling plots for total β-diversity (Figure 3.3ci; stress = 0.245) and turnover (Figure 3.3ci; stress = 0.334), caution is advised in the interpretation of these results as stress values >0.2 – 0.35 are likely to yield plots that are close to arbitrary. The visual representation of these data (nMDS) illustrates that there is no apparent separation of these data by location (i.e., when locations are not clustering together).

Table 3.2 Summary of analyses statistically comparing rank-based α-diversity variation between sampling locations, sampling depth (m) and time of year (Kruskal-Wallis H test). Variation in community α-diversity between each sampling location, sampling depth (m) and time of year (Dunn's test)

a-Diversity	**Kruskal-Wallis H**			**Dunn's test (Kruskal-Wallis multiple comparison)**	
	df	***H***	***P***	***Z***	***P.adj***
Location	2	22.445	**0.001**		
Comparison					
BT1-BT2				3.756	**0.001**
BT1-BT3				-0.790	0.430
BT2-BT3				-4.246	**0.001**
Depth (m)	5	12.846	**0.023**		
Comparison					
1 - 20				-1.671	0.203
1 - 30				-2.407	0.080
1 - 40				-2.807	0.075
1 - 60				-2.226	0.098
1 - 130				-0.018	0.986
20 - 30				0.041	1.000
20 - 40				-0.270	0.908
20 - 60				0.332	0.925
30 - 40				-0.546	0.798
30 - 60				0.575	0.847
40 - 60				1.214	0.375
130 - 20				-1.581	0.213
130 - 30				-2.171	0.090
130 - 40				-2.536	0.084
130 - 60				-1.973	0.121
Season	6	59.5	**0.001**		
Comparison					
Autumn 2017 - Autumn 2018				-1.845	0.114
Autumn 2017 - Autumn 2020				0.971	0.435
Autumn 2018 - Autumn 2020				2.507	**0.028**
Autumn 2017 - Spring 2018				-1.385	0.233
Autumn 2018 - Spring 2018				0.716	0.586
Autumn 2020 - Spring 2018				-2.180	0.061
Autumn 2017 - Summer 2017				-5.482	**0.001**
Autumn 2018 - Summer 2017				-2.977	**0.009**
Autumn 2020 - Summer 2017				-5.779	**0.001**
Spring 2018 - Summer 2017				-4.289	**0.001**
Autumn 2017 - Summer 2018				1.496	0.202
Autumn 2018 - Summer 2018				3.106	**0.007**
Autumn 2020 - Summer 2018				0.304	0.799
Spring 2018 - Summer 2018				2.934	**0.009**
Summer 2017 - Summer 2018				6.930	**0.001**
Autumn 2017 - Winter 2017				0.570	0.663
Autumn 2018 - Winter 2017				1.899	0.110
Autumn 2020 - Winter 2017				-0.179	0.858
Spring 2018 - Winter 2017				1.514	0.210
Summer 2017 - Winter 2017				4.497	**0.001**
Summer 2018 - Winter 2017				-0.431	0.736

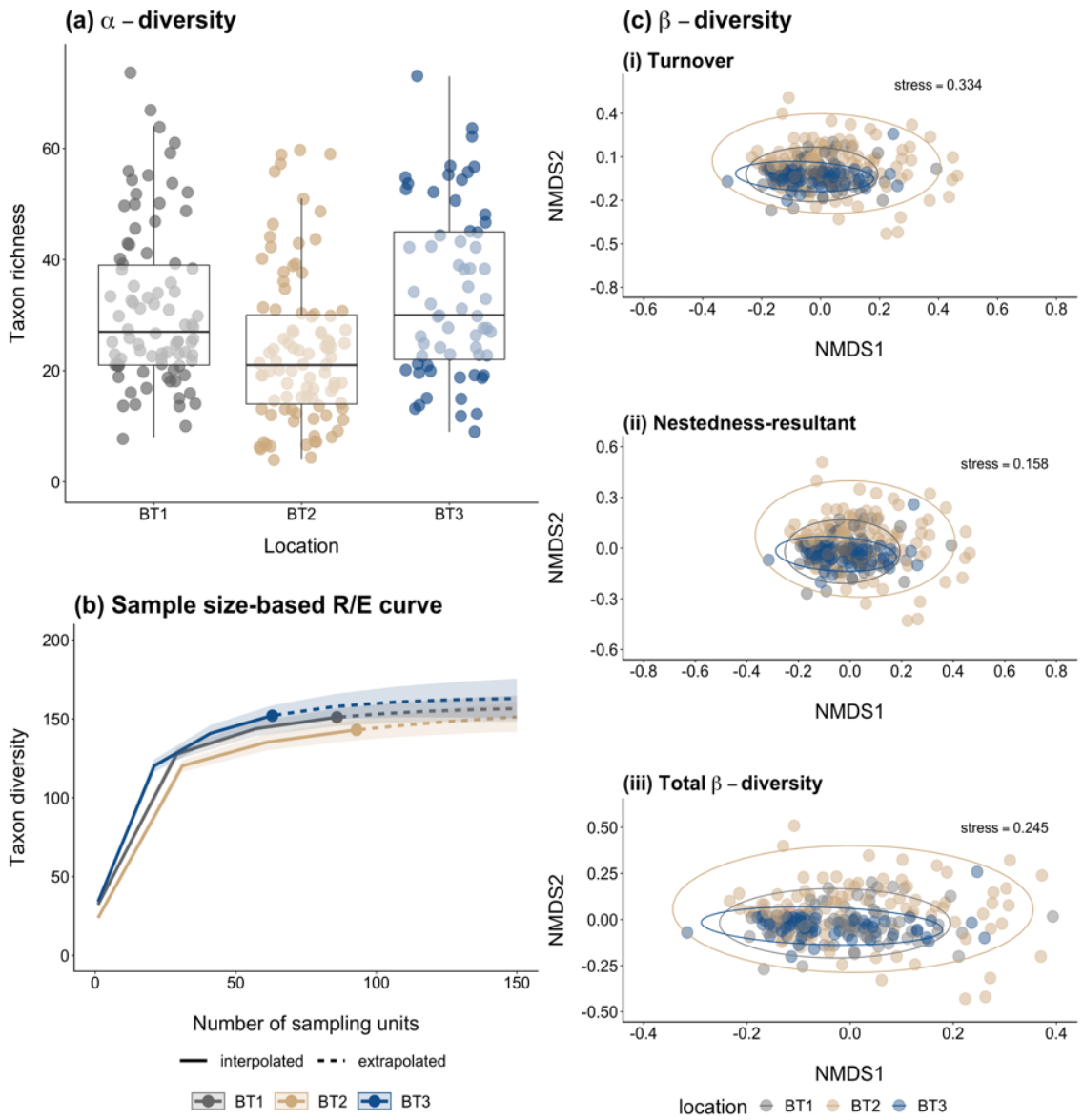

Figure 3.3. Summaries of α- and β-diversity between locations BT1 (dark gray symbols and lines), BT2 (peril symbols and lines), BT3 (blue symbols and lines): (**a**) boxplot of taxon richness, boxes indicating 25th, 50th and 75th percentiles and whiskers sow 5th and 95th percentiles. (**b**) sample size-based rarefication and extrapolation curves, (**ci-iii**) non-metric multidimensional scaling plots of β-diversity components.

Species richness differed across the mesophotic reef depth gradient (Table 3.2) however, none of the pairwise depth comparisons were statically different. It is likely that the 130 m sites (Figure 3.4) are driving the overall α-diversity difference with the caveat that there is an indication of under sampling present in the R/E curves for depth (Figure

3.4b), caution would be advised in the interpretation of this finding. Whilst there were differences between communities present across the depth gradient (total β diversity; R^2 0.02, p = 0.004), there were no significant differences when β diversity was partitioned into taxon replacement (Figure 3.4ci) or nestedness-resultant (Figure 3.4cii). This is illustrated by the non-metric multidimensional scaling (nMDS) plots for both metrics which slow little to no separation of the reef zones. However, the stress value for the turnover nMDS (0.333) indicates a close to arbitrary placement of these data and therefore caution is advised when with respect to interpretation.

Table 3.3. Summary of analyses statistically comparing variation in site community composition (β-diversity, Jaccard dissimilarity) accessed with a cross factor analysis between, location, depth, and season (PERMANOVA).

b diversity (Jaccard dissimilarity)	**Community similarity (PERMANOVA)**				
		df	*F*	R^2	*P*
Turnover					
(99.33%)	**location**	2	4.192	0.033	**0.001**
	depth	5	1.151	0.023	0.228
	season_year	6	2.403	0.056	**0.001**
	location:depth	8	1.177	0.037	0.166
	location:season_year	10	0.884	0.035	0.769
	depth:season_year	25	0.966	0.095	0.642
	location:depth:season_year	30	0.982	0.115	0.562
Nestedness - resultant					
(0.67%)	**location**	2	4.841	0.036	**0.024**
	depth	5	1.923	0.036	0.160
	season_year	6	6.816	0.152	**0.001**
	location:depth	8	0.945	0.028	0.516
	location:season_year	10	2.295	0.085	**0.036**
	depth:season_year	25	0.978	0.091	0.493
	location:depth:season_year	30	-0.022	-0.002	1.000
Total ß-diversity					
(100%)	**location**	2	4.801	0.036	**0.001**
	depth	5	1.380	0.026	**0.004**
	season_year	6	3.660	0.083	**0.001**
	location:depth	8	1.120	0.034	0.093
	location:season_year	10	1.244	0.047	**0.005**
	depth:season_year	25	0.923	0.087	0.919
	location:depth:season_year	30	0.908	0.103	0.971

The apparent lack of between depth influence was also evident when the community taxa was categorising by trophic guild with there being little change in the trophic community structure across all depth ranges (1 m to 130m) as indicated by the

proportional read counts (PRC, Figure 3.8). The trophic PRC plot shows there to be limited vertical advection of eDNA material from shallow too deep since PRC values do not all accumulatively increase in size from left to right (i.e., 1 m to 130 m).

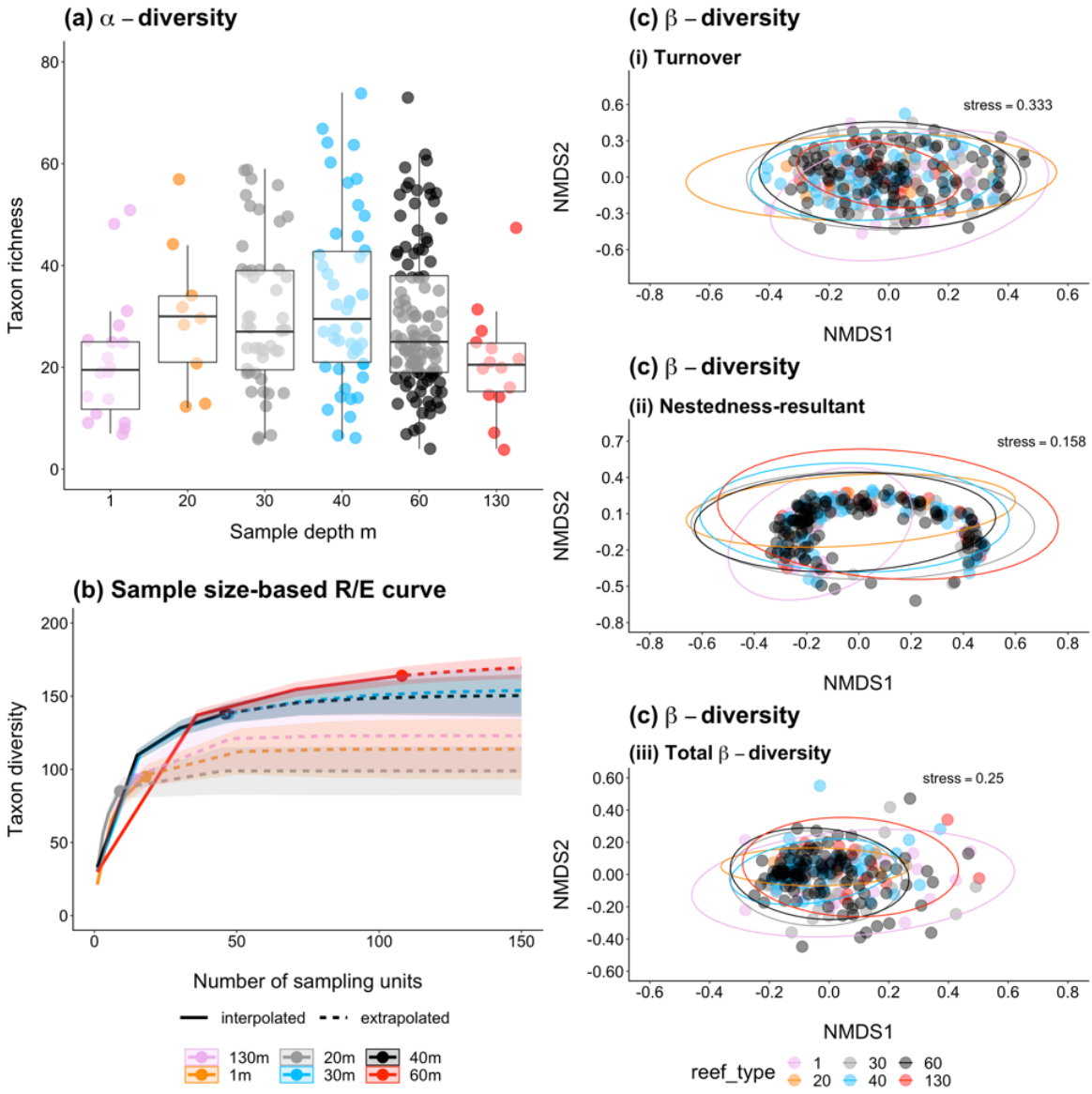

Figure 3.4. Summaries of α- and β-diversity pooled across sample depths. 1 m (purple circles/lines/ellipses), 20 m (orange circles/lines/ellipses), 30 m (grey circles/lines/ellipses), 40 m (blue circles/lines/ellipses), 60m (black circles/lines/ellipses), 130 m (red circles/lines/ellipses): (**a**) boxplot of taxon richness, boxes indicating 25th, 50th and 75th percentiles and whiskers sow 5th and 95th percentiles.

(**b**) sample size-based rarefication and extrapolation curves, (**ci-iii**) non-metric multidimensional scaling plots of β-diversity components.

Alpha diversity across locations (Table 3.2; Figure 3.5) significantly differed by season and year (H = 59.5, *p* = 0.001). Taxon richness was highest during the Summer 2017 period for all locations whilst the lowest taxon richness for all locations corresponded to the following summer period (2018). Pairwise comparisons between the different seasons indication the differences are predominantly between summer and autumn periods (Table 3.2). However, there appears to be interannual variability across all locations (Figure 3.5).

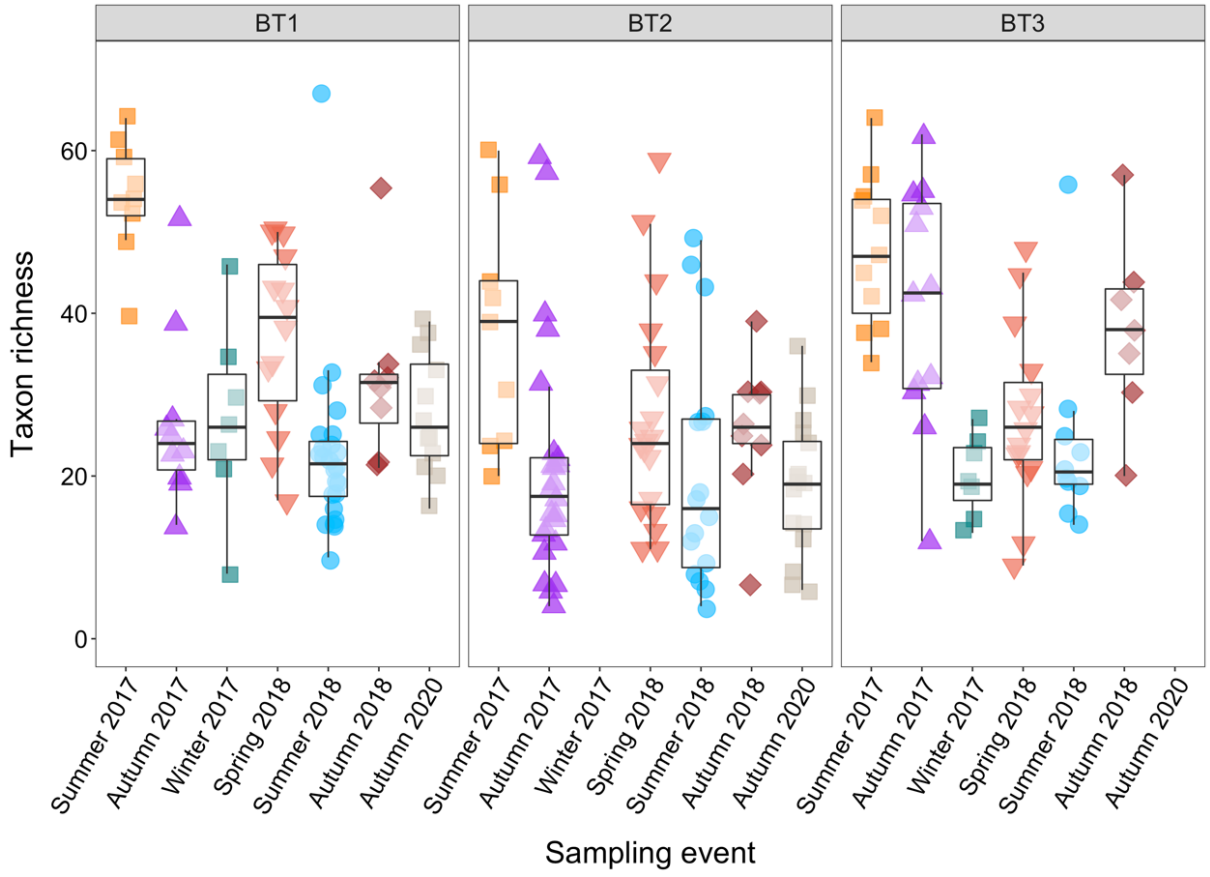

Figure 3.5. Summaries of α-diversity seasonal comparison across the three study locations, Summer 2017 (orange squares), Autumn 2017 (purple squares), Winter 2017 (green squares), Spring 2018 (red inverted triangles). Summer 2018 (blue circles). Autumn 2018 (dark red diamonds), Autumn 2020 (grey square). Note, sampling was not possible in Winter 2017 at BT2 and Autumn 2020 at BT3 due to inclement weather.

Figure 3.6 Bubble plot showing proportional read counts for taxa classified by trophic position (Deep seas species are categorised by origin) pooled by sampling depth across the three locations for the duration of the study. Taxa are identified in accordance with local management status (yellow = Protected, Orange dots = Regulated) and International Commission for the Conservation of Atlantic Tunas status (ICCAT, Blue dots), Additionally, endemic (Black dots) and invasive species (Red dots) have been highlighted. The trophic classifications are represented as Sharks (SH), Macro Carnivores (MC), Mobile Invertebrate Feeders (MIF), Omnivores (OM), Planktivore (PL), Roving Herbivores (RH), Sessile Invertebrate Feeders (SIF), Territorial Herbivores (TH) and Deep-sea species (DS).

Figure 3.7. Bubble plot showing proportional read counts for taxa classified by trophic position (Deep seas species are categorised by origin) pooled by season across the three locations for the duration of the study. Taxa are identified in accordance with local management status (yellow = Protected, Orange dots = Regulated) and International Commission for the Conservation of Atlantic Tunas status (ICCAT, Blue dots), Additionally, endemic (Black dots) and invasive species (Red dots) have been highlighted. The trophic classifications are represented as Sharks (SH), Macro Carnivores (MC), Mobile Invertebrate Feeders (MIF), Omnivores (OM), Planktivore (PL), Roving Herbivores (RH), Sessile Invertebrate Feeders (SIF), Territorial Herbivores (TH) and Deep-sea species (DS).

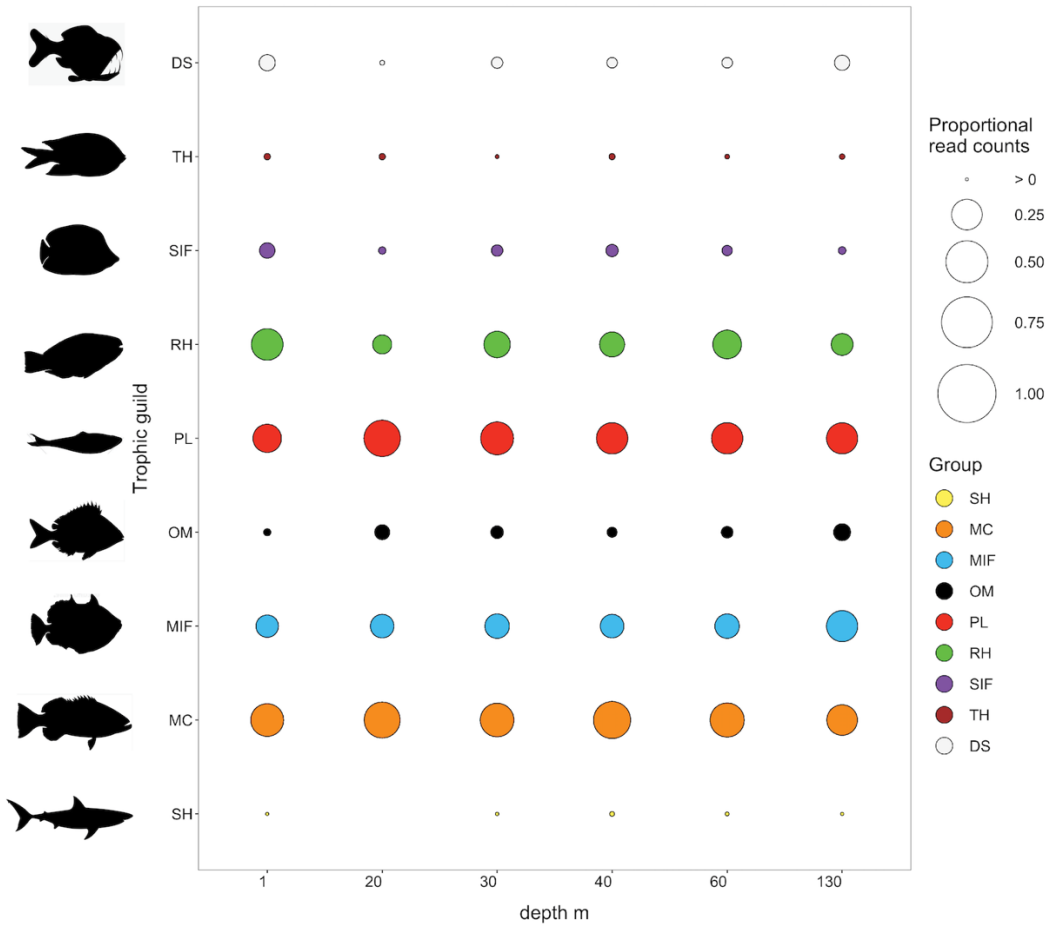

Figure 3.8. Bubble plot showing proportional read counts for taxa pooled across depth ranges classified by trophic position. The trophic classifications are represented as Sharks (SH), Macro Carnivores (MC), Mobile Invertebrate Feeders (MIF), Omnivores (OM), Planktivore (PL), Roving Herbivores (RH), Sessile Invertebrate Feeders (SIF), Territorial Herbivores (TH) and Deep-sea species (DS).

Beta diversity of mesophotic reefs across the seasons was primarily driven by species turnover (99.33%; Table 3.3). Yet, nestedness-resultant did play a larger role for some seasons meaning at certain times of the year, there was a retention of taxa between season, and not just replacement. To a lesser degree, location had an influence on the level of retention between seasons (R^2 = 0.085, p = 0.036). Seasons explained the greatest level of total β diversity variability for MCEs (R^2 = 0.083, p = 0.001) however, seasonal variation did vary between locations (R^2 = 0.047, p = 0.005).

Redundancy analysis accounted for 7.10% (R^2_{adj} = 0.071) of the total variance within the species matrix with the adjusted values of the first two axes accounting for <

1.00% of the total variance. A global test of the full RDA output (F = 2.0435, p = 0.001; permutations = 999) confirms a linear relationship exists between the species matrix and abiotic variables (i.e., the relationship between the assemblage of fish species detected at a site and abiotic conditions; Table 3.4). As indicated by the length of the blue arrows (Figure 3.9), the status of the North Atlantic Oscillation index (NAO) and seasonality had the greatest influence on the site level species diversity. The NAO index is based on differences of the surface sea-level pressure between the Subtropical (Azores) High and the Subpolar Low.

Table 3.4. Summary of abiotic variables used for Redundancy Analysis (RDA)

Abbrevation	Decription	Abbrevation	Decription
NAO	North Atlantic Oscillation index	pH	pH
T	measured temperature (˚C) at time of eDNA collection	Revelle	Revelle Factor
PSU	Practical Salinity Units	Ca	Ω Calcite
NEC	Net Ecosystem Calcification	Ar	Ω Aragonite
NEP	Net Ecosystem Productivity		

Negative winter NAO events cause deeper mixed layer depths resulting in greater productivity blooms (increases in phytoplankton and zooplankton abundances) through an increased advection of nutrients into the surface waters. These events have been linked to short-term increases in shallow reef calcification rates and switches to net heterotrophy (Yeakel et al., 2015). Calcification refers to net ecosystem calcification (NEC) as derived by the alkalinity anomaly-water residence time technique (Andersson and Gledhill, 2013), heterotrophic rates are a measure of net ecosystem production (NEP; Romanó de Orte et al., 2021). See Chapter 2 section 2.2 “Seawater Carbonate Chemistry Determination” for a more in-depth description.

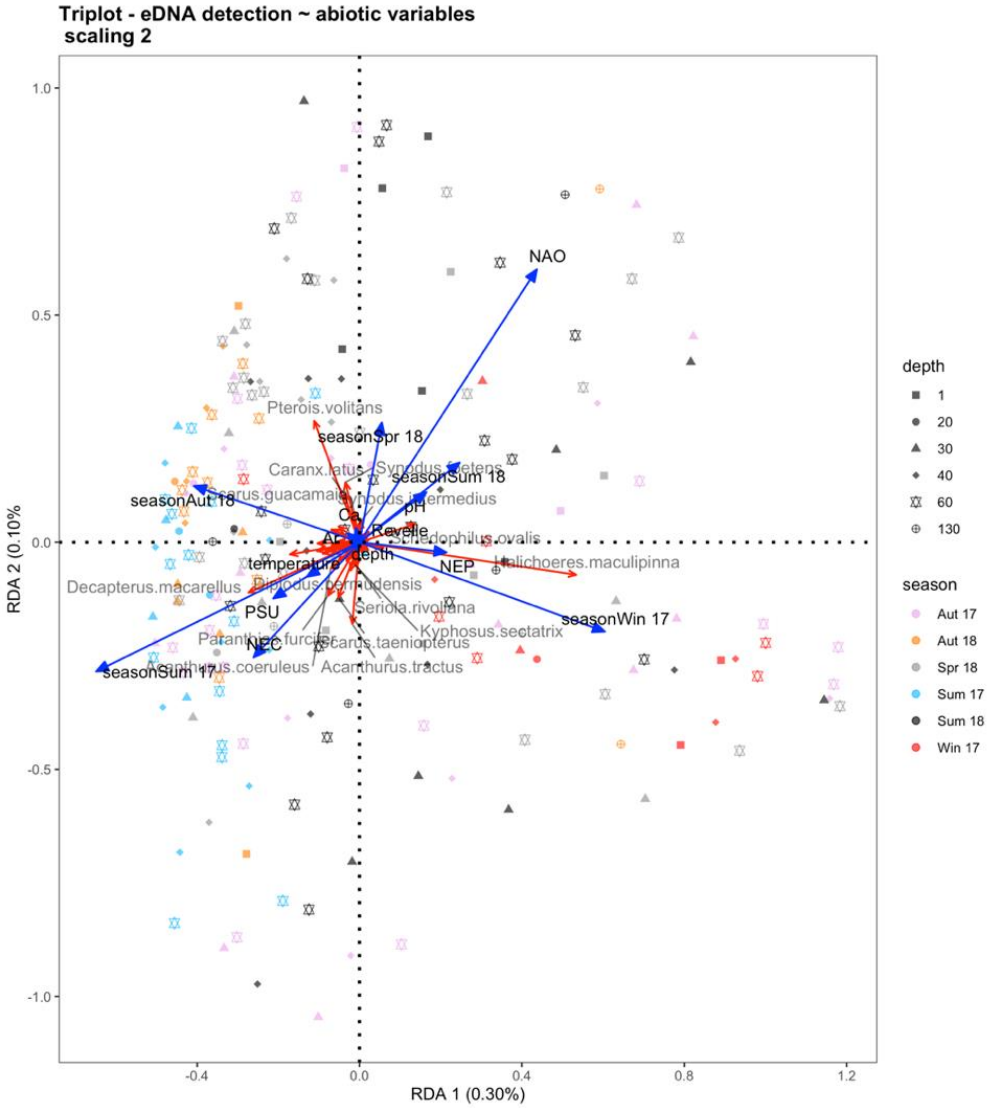

Figure 3.9. RDA Triplot of Hellinger-transformed species data constrained by abiotic factors (Table 3.3), scaling 2 correlation plot with site fitted scores. Red arrows indicate species, the blue arrows represent explanatory variables. Shapes represent physical site depth (m), colours represent seasons. Note, the full suite of species has not been visualized to limit the plotting space from becoming overwhelmed with data points.

3.5 Discussion

This study represents the first application of eDNA metabarcoding on Bermudan mesophotic reefs and provides a comprehensive view of fish biodiversity found within these ecosystems. The investigation was conducted across a depth gradient over multiple seasons and at three discrete locations. Representative fish taxa from shallow reef, mesophotic and oceanic environments were detected across depth gradient (Figures 3.6 & 3.7) of the three study locations in all seasons. To give context to the local study region, mesophotic reefs form a narrow band around the shallow reef platform (Figure 3.1) and act as the physical link between these and the open ocean, a concept recently proposed for all mesophotic systems (Eyal and Pinheiro, 2020). Determining the level of species biodiversity within mesophotic reefs and the linkage between adjacent ecosystems, are key components for 1) assessing the vulnerability of MCEs to natural and anthropogenic impacts, 2) establishing the role MCEs play in mitigating the same stressors for shallow reef counterparts.

An early assumption for mesophotic communities was one of a holistic system projected to act as refugia for both fish and benthic species (Glynn, 1996; Bongaerts et al., 2010). The determination of distinct faunal breaks (Rocha et al., 2018; Lesser et al., 2019; Pinheiro et al., 2019; Tamir et al., 2019) has led to an alternative view, one that now considers mesophotic communities as taxonomically distinct.

This study determined temporal and seasonal nuances had a greater influence than depth over the fish communities associated with these reef systems. Although depth related influences were detected in both α-diversity (Table 3.2) and β diversity (Table 3.3), post hoc analyses determined they were not detected in either pairwise depth comparisons or turnover and nestedness-resultant metrics of β diversity. It is postulated that an under sampling of the 130 m reef system (Figure 3.4b) has driven the detected differences in overall biodiversity.

As further evidence against taxonomic compartmentalisation across the depth ranges, this study showed there to be comparable trophic structures across the region when partitioned by depth (Figure 3.8). These results are not consistent with previous Caribbean studies (Bejarano et al., 2014; Andradi-Brown et al., 2016a) which generally demonstrated a decrease in herbivores fishes with depth. More interestingly, this study is

not consistent with a recent study of Bermudan reef fish composition across the shallow reef to rariphotic ecosystems (Stefanoudis et al., 2019a) which determined a stark decrease in herbivores below 30 m. The reason for the decline was undetermined but was postulated to be a result of natural variability, methodology differences between previous mesophotic studies and declines in living coral cover. The latter association with herbivories fishes was not a trend noted in the Caribbean based studies (Bejarano et al., 2014; Andradi-Brown et al., 2016a). Without further investigation this study is unable to determine why there is a disparity in depth related influence on fish biodiversity. However, caution would be advised with interpreting these depth related influences and as such, have not been deemed as a major driver of fish biodiversity within this study.

The findings of this this study support species overlap between mesophotic and shallow reef fish communities and does not detect a distinct faunal break (i.e., a holistic system). This is an important finding as it supports the concept of the "Deep Reef Refuge Hypothesis" (Bongaerts et al., 2010, 2017). In brief, it is the concept that these deeper reef ecosystems could act as a refuge for shallow water species and potentially provide source larvae (re-seeding potential) to their shallow water counterparts. Work by Cinner et al. (2016) concluded that proximity to deep-water refuges correlated with areas of increased reef health based on environmental and socioeconomic metrics. Genetic connectivity between shallow-mesophotic coral communities has exhibited ambiguous patterns to date (Serrano et al., 2014), thus inhibiting a general consensus on the function of mesophotic reefs in shallow reef recovery processes (Baker et al., 2016a; Bongaerts et al., 2017). One potential explanation for these results could be Bermuda's unique biogeographical characteristics (Stefanoudis et al., 2019a) i.e., high latitude tropical coral reefs isolated from the wider Caribbean which could lead to plasticity within species depth ranges leading to a greater level of species overlap between the upper mesophotic and shallow reef counterparts (Pinheiro et al., 2016).

The species overlap across depth determined by this study are supported by previous work in Bermuda's upper mesophotic reefs (Pinheiro et al., 2016), by providing evidence to support possible refuge like services through shallow water species overlap e.g., *Scarus* (Forsskål 1775) and *Sparisoma* species (Swainson 1839). Scaridae (Rafinesque 1810) were detected throughout the study region across all depths (Figure

3.6) and all seasons (Figure 3.7). Partially due to the rapid decline in parrotfish abundance, the Government of Bermuda proactively banned the use of fish pots (Butler et al., 1993) and subsequently classified all parrotfishes as full protected (Figure 3.8, Roaming Herbivores classification (RH)), in an effort to protect reef fish species. An evaluation of the of the recovery success of Scaridae post fish pot ban, determined post recruitment abundance (> 5 cm FL) to have increased by a factor of 2.46 over the course of a nine-year study period (Luckhurst and Farrell, 2013). The study was conducted solely in the shallow reef environment and noted there to be no increase in Scaridae recruits (< 5 cm FL). This finding implies an increase in post fish pot recruitment abundance was likely due to the relocation of individuals versus an increase in overall population. The five study species of parrotfish, *Scarus taeniopterus* (Lesson 1829), *Scarus vetula* (Bloch & Schneider 1801), *Sparisoma viride* (Bonnaterre 1788), *Sparisoma aurofrenatum* (Valenciennes 1840) and *Scarus iseri* (Bloch 1789) were all detected in the current study across all depth ranges (1 – 130 m). The researcher postulates the likely origin of the post recruitment individuals detected by Luckhurst and Farrell (2013), to be of mesophotic reef origin.

The findings of this study have demonstrated that geographical location influences both α- and β diversity of fish communities across the three mesophotic locations. The central location (BT2) had the lowest species richness of the three (n = 143; Figure 3.3a) whilst there was no discernible different in richness between BT1 (n = 152) and BT3 (n = 153). For context, there have been 133 species observed and or collection from the Bermuda mesophotic to rariphotic ecosystems (Stefanoudis et al., 2019a). A notable difference across the locations were the detection levels of carangids which were generally 20 – 50% lower at BT2. Surprisingly, this trend included the second most abundant species detected during the study; *Decapterus macarellus* (296,342 total reads; Cuvier 1833). *Decapterus* are a highly mobile carangid that are believed to be ubiquitous across Bermuda's mesophotic reef system if anecdotal observations from local fishers targeting the species are to be believed. In general, this family of fishes are highly mobile with no documented site fidelity behaviour exhibited locally. This is not true for the black grouper (*Mycteroperca bonaci* Poey 1860), a commercially important species that forms spawning aggregations in the upper mesophotic. There are two seasonally protected

areas (April – November), one to the southwest of the island, the second situated to the northeast. The extent of the protection zone for the latter aggregation incorporates the BT1 study location. This proximity to a confirmed aggregation was reflected in greater detection rates for this species at BT1 (17,398). Surprisingly, this was not the case for the red hind (*Epinephelus guttatus* Linnaeus 1758) which are known to utilise the same spawning aggregations albeit at different periods of the year. The highest detection of *E. guttatus* (4,583 reads) occurred at BT3, a location that is not known to be utilized for spawning by this commercially important species.

The only elasmobranch detected during the study was the Tiger shark (*Galeocerdo cuvier* Péron & Lesueur, 1822) with the greatest read counts occurring at location BT2 (508 reads). Given the known limitations of MiFish-U primers for amplifying elasmobranchs (Miya et al., 2015), it was not surprising that only one species of shark was detected during the study. Despite these limitations, these low detection rates are comparable to findings of Goodbody-Gringley et al. (2019) which observed low abundance of *G. cuvier* and Galapagos shark (*Carcharhinus galapagensis* Snodgrass and Heller 1905) at 50 m depths within their BRUVs dataset. The study by (Pinheiro et al., 2016) sighted Carcharhinus sp. during survey dives, however they were not included in the dataset. Developing a greater understanding of local shark biodiversity and distribution patterns has become a priority for marine resources managers with a nascent "Shark Management Action Plan" in development with elasmobranch biodiversity assessments being provided by the DARWIN PLUS (145) "Assessing the mobile fish biodiversity of Bermuda's deep seas". It should be noted that during the preliminary optimization of the method used for this study (data not presented in this study), paired MiFish-U/MiFish-E trials were conducted at the local aquarium by sampling tanks that housed known communities including sharks. The MiFish-U primers successfully detected the elasmobranch housed in the tanks, whilst the MiFish-E primers did not hence the use of the single assay in the full investigation.

It was anticipated that *Pterois sp*. would be detected during the study due to locations being determined based on the 2015 findings of a lionfish control initiative. What was not known was the extent to which they would be detected. There are two known species of lionfish in Bermuda, *Pterois volitans* (Linnaeus, 1758) and *P. miles* (Bennett,

1828), the former is the dominant species as reflected by the detection level in this study. It was also the species with the highest total read count (327,714 reads) and detected at all depth ranges and throughout all seasons. Goodbody-Gringley et al. (2019a) documented dense aggregations of lionfish at two of the 60 m sites investigated during this study. The findings of this study support the notion of increased lionfish abundance at depth with the highest detection rates being exhibited at the 60 m sites (Figure 3.6). Seawater temperature (Figure 3.2) was determined to have the greatest influence on lionfish distribution in the study by Goodbody-Gringley et al. (2019), with the highest abundances associated with cooler seawater. The opposite trend was found by this study, the greatest number of reads were associated with the warmer seasons for these two species (Figure 3.9). This warm water association would support the higher proportional read counts found in the 1 m samples. It is hypothesised that lionfish spawning behaviour could lead to increases in shallow water reads (i.e., 1 m samples) due to the positive buoyancy of lionfish egg masses. Whilst spawning behaviour is yet to be documented in Bermuda, it would not be impossible to inadvertently sample reproductive material during the sample collection process.

The reason for opposing associations of lionfish with seawater temperature between the two studies are not currently apparent, however warrant further investigation to optimise the efficacy of biodiversity protection and invasive management plans. For reference purposes, sites BT1 and BT2 are referred to as North Northeast (120 lionfish /hectare) and XL (760 lionfish / hectare) in the Goodbody-Gringley et al. (2019) study.

Adopting a robust suite of methodologies for understanding biodiversity and the underlying environmental drivers of species biogeographical patterns are valuable tools for setting and adapting effective management procedures. There are two key factors to focus on when looking at the mesophotic community (1) understanding the “if” and “where” faunal breaks occur and (2) to understand the linkages of communities, studies must vary both spatially and temporally to truly garner an accurate assessment of representative fauna that utilise the ecosystem of focus. From a management perspective, this is of particular relevance for resource managers and very apt for the current marine spatial planning initiative being undertaken by the Government of Bermuda (hereon known as the “Government”). The Government has committed to the

protection of 20% of its Economic Exclusive Zone through the Bermuda Ocean Prosperity Programme by the end of 2022. However, the effectiveness of such initiatives can be undermined by a lack of data on the habitats and species they seek to protect. Using the findings of the current study as a basis, management of Bermudan mesophotic fish species should consider the inclusion of multiple locations to account for the spatial variability of fish biodiversity. Secondly, the detected interannual variability of fish communities would suggest management measures be implemented on an annual duration verse seasonally (i.e., existing grouper spawning aggregation closures). Finally, depth would play less of a role in determining management decisions. However, notwithstanding the aforementioned caveats for depth driven biodiversity, considerations should be given to the management of the full mesophotic depth strata after further investigation of the lower portion of the system.

Utilising eDNA metabarcoding to assess mesophotic fish communities has reduced the logistical complexity of gaining access to the biodiversity “treasures” contained within these ecosystems. The increase in such knowledge can only allow for more informed management and conservation decisions. On the one hand, increased scientific knowledge on the role these systems may play in terms of linkage between shallow water reefs and the open ocean (Eyal and Pinheiro, 2020) could give us greater insight into the responses of shallow reef systems to continued climate related shifts. However, this should not be the source reasoning behind future mesophotic scientific research. As demonstrated by this and other studies (Pinheiro et al., 2016; Semmler et al., 2017; Rocha et al., 2018), there is variation in mesophotic communities, so until biodiversity and ecosystem services of these systems are fully understood, they should be considered as separate communities. As such, these communities warrant greater scientific focus (Eyal and Pinheiro, 2020). Environmental DNA metabarcoding is a powerful tool of which new applications are continuing to be developed (Djurhuus et al., 2020; Mariani et al., 2021b). In this sense, the future of mesophotic research is bright.

3.6 References

Andersson, A. J., and Gledhill, D. (2013). Ocean Acidification and Coral Reefs: Effects on Breakdown, Dissolution, and Net Ecosystem Calcification. *Ann Rev Mar Sci* 5, 321–348. doi: 10.1146/annurev-marine-121211-172241.

Andradi-Brown, D. A., Gress, E., Wright, G., Exton, D. A., and Rogers, A. D. (2016a). Reef fish community biomass and trophic structure changes across shallow to upper- Mesophotic reefs in the mesoamerican barrier reef, Caribbean. *PLoS One* 11. doi: 10.1371/journal.pone.0156641.

Andradi-Brown, D., Macaya-Solis, C., Exton, D., Gress, E., Wright, G., and Rogers, A. (2016b). Assessing caribbean shallow and mesophotic reef fish communities using Baited-Remote Underwater Video (BRUV) and diver-operated video (DOV) survey techniques. *PLoS One* 11. doi: 10.1371/journal.pone.0168235.

Baker, E. K., Puglise, K. A., and Harris, P. T. (2016). Mesophotic coral ecosystems - a lifeboat for coral reefs?

Baldwin, C. C., Tornabene, L., and Robertson, D. R. (2018). Below the Mesophotic. *Sci Rep* 8. doi: 10.1038/s41598-018-23067-1.

Baselga, A., and Orme, C. D. L. (2012). Betapart: An R package for the study of beta diversity. *Methods Ecol Evol* 3, 808–812. doi: 10.1111/j.2041-210X.2012.00224.x.

Bejarano, I., Appeldoorn, R. S., and Nemeth, M. (2014). Fishes associated with mesophotic coral ecosystems in La Parguera, Puerto Rico. *Coral Reefs* 33, 313–328. doi: 10.1007/s00338-014-1125-6.

Blanco-Bercial, L. (2020). Metabarcoding Analyses and Seasonality of the Zooplankton Community at BATS. *Front Mar Sci* 7, 1–16. doi: 10.3389/fmars.2020.00173.

Bokulich, N. A., Subramanian, S., Faith, J. J., Gevers, D., Gordon, J. I., Knight, R., et al. (2013). Quality-filtering vastly improves diversity estimates from Illumina amplicon sequencing. *Nat Methods* 10, 57–59. doi: 10.1038/nmeth.2276.

Bongaerts, P., Ridgway, T., Sampayo, E. M., and Hoegh-Guldberg, O. (2010). Assessing the “deep reef refugia” hypothesis: Focus on Caribbean reefs. *Coral Reefs* 29, 1–19. doi: 10.1007/s00338-009-0581-x.

Bongaerts, P., Riginos, C., Brunner, R., Englebert, N., Smith, S. R., and Hoegh-Guldberg, O. (2017). Deep reefs are not universal refuges: Reseeding potential varies among coral species. *Sci Adv* 3. doi: 10.1126/sciadv.1602373.

Bryan, D. R., Kilfoyle, K., Gilmore, R. G., and Spieler, R. E. (2013). Characterization of the mesophotic reef fish community in south Florida, USA. *Journal of Applied Ichthyology* 29, 108–117. doi: 10.1111/j.1439-0426.2012.02055.x.

Butler, J. N., Bumett-Herkes, J., Barnes, J. A., and Ward, J. (1993). The bermuda fisheries a tragedy of the commons averted? *Environment* 35, 7–33. doi: 10.1080/00139157.1993.9929067.

Cinner, J. E., Huchery, C., MacNeil, M. A., Graham, N. A. J., McClanahan, T. R., Maina, J., et al. (2016). Bright spots among the world’s coral reefs. *Nature* 535, 416–419. doi: 10.1038/nature18607.

Collins, R. A., Bakker, J., Wangensteen, O. S., Soto, A. Z., Corrigan, L., Sims, D. W., et al. (2019). Non-specific amplification compromises environmental DNA metabarcoding with COI. *Methods Ecol Evol* 10, 1985–2001. doi: 10.1111/2041-210X.13276.

Deiner, K., Bik, H. M., Mächler, E., Seymour, M., Lacoursière-Roussel, A., Altermatt, F., et al. (2017). Environmental DNA metabarcoding: Transforming how we survey animal and plant communities. *Mol Ecol* 26, 5872–5895. doi: 10.1111/mec.14350.

Djurhuus, A., Closek, C. J., Kelly, R. P., Pitz, K. J., Michisaki, R. P., Starks, H. A., et al. (2020). Environmental DNA reveals seasonal shifts and potential interactions in a marine community. *Nat Commun* 11, 1–9. doi: 10.1038/s41467-019-14105-1.

Eyal, G., and Pinheiro, H. T. (2020). Mesophotic ecosystems: The link between shallow and deep-sea habitats. *Diversity (Basel)* 12, 1–4. doi: 10.3390/d12110411.

García-Sais, J. R., Castro-Gomez, R. L., Sabater-Clavell, J., Esteves, R., Williams, S., and Carlo, M. (2010). Mesophotic benthic habitats and associated marine communities at Abrir La Sierra, Puerto Rico. *Differences*, 122.

Glynn, P. W. (1996). Coral reef bleaching: Facts, hypotheses and implications. *Glob Chang Biol* 2, 495–509. doi: 10.1111/j.1365-2486.1996.tb00063.x.

Goldberg, C. S., Turner, C. R., Deiner, K., Klymus, K. E., Thomsen, P. F., Murphy, M. A., et al. (2016). Critical considerations for the application of environmental DNA methods to detect aquatic species. *Methods Ecol Evol* 7, 1299–1307. doi: 10.1111/2041-210X.12595.

Goodbody-Gringley, G., Eddy, C., Pitt, J. M., Chequer, A. D., and Smith, S. R. (2019a). Ecological Drivers of Invasive Lionfish (Pterois volitans and Pterois miles) Distribution Across Mesophotic Reefs in Bermuda. *Front Mar Sci* 6, 1–12. doi: 10.3389/fmars.2019.00258.

Goodbody-Gringley, G., Noyes, T., and Smith, S. R. (2019b). “Bermuda,” in *Mesophotic Coral Ecosystems, Coral Reefs of the World 12*, eds. L. Yossi, K. A. Puglise, and T. Bridge (Springer International Publishing), 31–45. doi: 10.1007/978-3-319-92735-0_2.

Harvey, E. S., Cappo, M., Butler, J. J., Hall, N., and Kendrick, G. A. (2007). Bait attraction affects the performance of remote underwater video stations in assessment of demersal fish community structure. *Mar Ecol Prog Ser* 350, 245–254. doi: 10.3354/meps07192.

Hinderstein, L. M., Marr, J. C. A., Martinez, F. A., Dowgiallo, M. J., Puglise, K. A., Pyle, R. L., et al. (2010). Theme section on “Mesophotic Coral Ecosystems: Characterization, Ecology, and Management.” *Coral Reefs* 29, 247–251. doi: 10.1007/s00338-010-0614-5.

Hochberg, E. J. (2014). Marine Environmental Program, 2004-2011 Synthesis Report. Submitted by the Bermuda Institute of Ocean Sciences to the Bermuda Department of Environmental Protection, Ministry of Health and Environment.

Hoegh-Guldberg, O., Poloczanska, E. S., Skirving, W., and Dove, S. (2017). Coral reef ecosystems under climate change and ocean acidification. *Front Mar Sci* 4. doi: 10.3389/fmars.2017.00158.

Hsieh, T. C., Ma, K. H., and Chao, A. (2016). iNEXT: an R package for rarefaction and extrapolation of species diversity (Hill numbers). *Methods Ecol Evol* 7, 1451–1456. doi: 10.1111/2041-210X.12613.

Jones, R. (2007). Marine Environmental Program Annual Report: 2006-2007. Annual report submitted by the Bermuda Institute of Ocean Sciences to the Bermuda Department of Environmental Protection, Ministry of Environment and Sport.

Juhel, J. B., Utama, R. S., Marques, V., Vimono, I. B., Sugeha, H. Y., Kadarusman, et al. (2020). Accumulation curves of environmental DNA sequences predict coastal fish diversity in the coral triangle: EDNA predict fish diversity. *Proceedings of the Royal Society B: Biological Sciences* 287. doi: 10.1098/rspb.2020.0248rspb20200248.

Kosaki, R. K., Pyle, R. L., Leonard, J. C., Hauk, B. B., Whitton, R. K., and Wagner, D. (2017). 100% endemism in mesophotic reef fish assemblages at Kure Atoll, Hawaiian Islands. *Marine Biodiversity* 47, 783–784. doi: 10.1007/s12526-016-0510-5.

Laverick, J. H., Tamir, R., Eyal, G., and Loya, Y. (2020). A generalized light-driven model of community transitions along coral reef depth gradients. *Global Ecology and Biogeography*, 1–11. doi: 10.1111/geb.13140.

Legendre, P., and Gallagher, E. D. (2001). Ecologically meaningful transformations for ordination of species data. *Oecologia* 129, 271–280. doi: 10.1007/s004420100716.

Lesser, M. P., Slattery, M., Laverick, J. H., Macartney, K. J., and Bridge, T. C. (2019). Global community breaks at 60 m on mesophotic coral reefs. *Global Ecology and Biogeography* 28, 1403–1416. doi: 10.1111/geb.12940.

Loya, Y., Eyal, G., Treibitz, T., Lesser, M. P., and Appeldoorn, R. (2016). Theme section on mesophotic coral ecosystems: advances in knowledge and future perspectives. *Coral Reefs* 35, 1–9. doi: 10.1007/s00338-016-1410-7.

Luckhurst, B. E., and Farrell, S. O. (2013). Rapid Recovery of Parrotfish (Scaridae) and Surgeonfish (Acanthuridae) Populations Following the Fish Pot Ban in Bermuda Recuperación Rapida de las Poblaciones de Loros (Scaridae) y Navajones (Acanthuridae) Luego de la Prohibición del Uso de Nasas. *66th Gulf and Caribbean Fisheries Institute*, 301–306.

Mächler, E., Osathanunkul, M., and Altermatt, F. (2018). Shedding light on eDNA: neither natural levels of UV radiation nor the presence of a filter feeder affect eDNA-based detection of aquatic organisms. *PLoS One* 13. doi: 10.1371/journal.pone.0195529.

Mariani, S., Harper, L. R., Collins, R. A., Baillie, C., Wangensteen, O. S., McDevitt, A. D., et al. (2021). Estuarine molecular bycatch as a landscape-wide biomonitoring tool. *Biol Conserv* 261, 109287. doi: 10.1016/j.biocon.2021.109287.

Miya, M., Gotoh, R. O., and Sado, T. (2020). *MiFish metabarcoding: a high-throughput approach for simultaneous detection of multiple fish species from environmental DNA and other samples*. Springer Japan doi: 10.1007/s12562-020-01461-x.

Miya, M., Sato, Y., Fukunaga, T., Sado, T., Poulsen, J. Y., Sato, K., et al. (2015). MiFish, a set of universal PCR primers for metabarcoding environmental DNA from fishes: detection of more than 230 subtropical marine species. *R Soc Open Sci* 2, 150088. doi: 10.1098/rsos.150088.

Ogle, D. H., Doll, J. C., Wheeler, P., and A, D. (2021). FSA: Fisheries Stock Analysis. R package version 0.9.1.

Pinheiro, H. T., Goodbody-Gringley, G., Jessup, M. E., Shepherd, B., Chequer, A. D., and Rocha, L. A. (2016). Upper and lower mesophotic coral reef fish communities evaluated by underwater visual censuses in two Caribbean locations. *Coral Reefs* 35, 139–151. doi: 10.1007/s00338-015-1381-0.

Pinheiro, H. T., Shepherd, B., Castillo, C., Abesamis, R. A., Copus, J. M., Pyle, R. L., et al. (2019). Deep reef fishes in the world's epicenter of marine biodiversity. *Coral Reefs* 38, 985–995. doi: 10.1007/s00338-019-01825-5.

Port, J. A., O'Donnell, J. L., Romero-Maraccini, O. C., Leary, P. R., Litvin, S. Y., Nickols, K. J., et al. (2016). Assessing vertebrate biodiversity in a kelp forest ecosystem using environmental DNA. *Mol Ecol* 25, 527–541. doi: 10.1111/mec.13481.

Porter, T. M., and Hajibabaei, M. (2018). Over 2.5 million COI sequences in GenBank and growing. *PLoS One* 13, 1–16. doi: 10.1371/journal.pone.0200177.

Puglise, K., Hinderstein, L., Marr, J., Dowgiallo, M., and Martinez, F. (2008). Mesophotic Coral Ecosystems Research Strategy. Silver Spring.

Pyle, R. L., Boland, R., Bolick, H., Bowen, B. W., Bradley, C. J., Kane, C., et al. (2016). A comprehensive investigation of mesophotic coral ecosystems in the Hawaiian Archipelago. *PeerJ* 4, e2475. doi: 10.7717/peerj.2475.

Rocha, L. A., Pinheiro, H. T., Shepherd, B., Papastamatiou, Y. P., Luiz, O. J., Pyle, R. L., et al. (2018). Mesophotic coral ecosystems are threatened and ecologically distinct from shallow water reefs. *Science (1979)* 361, 281–284. doi: 10.1126/science.aaq1614.

Rognes, T., Flouri, T., Nichols, B., Quince, C., and Mahé, F. (2016). VSEARCH: A versatile open source tool for metagenomics. *PeerJ* 2016, 1–22. doi: 10.7717/peerj.2584.

Romanó de Orte, M., Koweek, D. A., Cyronak, T., Takeshita, Y., Griffin, A., Wolfe, K., et al. (2021). Unexpected role of communities colonizing dead coral substrate in the calcification of coral reefs. *Limnol Oceanogr* 66, 1793–1803. doi: 10.1002/lno.11722.

Rosa, M. R., Alves, A. C., Medeiros, D. V., Coni, E. O. C., Ferreira, C. M., Ferreira, B. P., et al. (2016). Mesophotic reef fish assemblages of the remote St. Peter and St. Paul's Archipelago, Mid-Atlantic Ridge, Brazil. *Coral Reefs* 35, 113–123. doi: 10.1007/s00338-015-1368-x.

Sato, Y., Miya, M., Fukunaga, T., Sado, T., and Iwasaki, W. (2018). MitoFish and mifish pipeline: A mitochondrial genome database of fish with an analysis pipeline for environmental DNA metabarcoding. *Mol Biol Evol* 35, 1553–1555. doi: 10.1093/molbev/msy074.

Schloss, P. D., Westcott, S. L., Ryabin, T., Hall, J. R., Hartmann, M., Hollister, E. B., et al. (2009). Introducing mothur: Open-source, platform-independent, community-supported software for describing and comparing microbial communities. *Appl Environ Microbiol* 75, 7537–7541. doi: 10.1128/AEM.01541-09.

Semmler, R. F., Hoot, W. C., and Reaka, M. L. (2017). Are mesophotic coral ecosystems distinct communities and can they serve as refugia for shallow reefs? *Coral Reefs* 36, 433–444. doi: 10.1007/s00338-016-1530-0.

Serrano, X. M., Baums, I. B., O'Reilly, K., Smith, T. B., Jones, R. J., Shearer, T. L., et al. (2014). Geographic differences in vertical connectivity in the Caribbean coral Montastraea cavernosa despite high levels of horizontal connectivity at shallow depths. *Mol Ecol* 23, 4226–4240. doi: 10.1111/mec.12861.

Slattery, M., Lesser, M. P., Brazeau, D., Stokes, M. D., and Leichter, J. J. (2011). Connectivity and stability of mesophotic coral reefs. *J Exp Mar Biol Ecol* 408, 32–41. doi: 10.1016/j.jembe.2011.07.024.

Stat, M., John, J., DiBattista, J. D., Newman, S. J., Bunce, M., and Harvey, E. S. (2019). Combined use of eDNA metabarcoding and video surveillance for the assessment of fish biodiversity. *Conservation Biology* 33, 196–205. doi: 10.1111/cobi.13183.

Stefanoudis, P. V., Gress, E., Pitt, J. M., Smith, S. R., Kincaid, T., Rivers, M., et al. (2019). Depth-dependent structuring of reef fish assemblages from the shallows to the rariphotic zone. *Front Mar Sci* 6, 1–16. doi: 10.3389/fmars.2019.00307.

Strickler, K. M., Fremier, A. K., and Goldberg, C. S. (2015). Quantifying effects of UV-B, temperature, and pH on eDNA degradation in aquatic microcosms. *Biol Conserv* 183, 85–92. doi: 10.1016/j.biocon.2014.11.038.

Takahara, T., Minamoto, T., Yamanaka, H., Doi, H., and Kawabata, Z. (2012). Estimation of fish biomass using environmental DNA. *PLoS One* 7, 3–10. doi: 10.1371/journal.pone.0035868.

Tamir, R., Eyal, G., Kramer, N., Laverick, J. H., and Loya, Y. (2019). Light environment drives the shallow-to-mesophotic coral community transition. *Ecosphere* 10. doi: 10.1002/ecs2.2839.

Team, R. C., and R Core Team (2019). R: A language and environment for statistical computing.

Thomsen, P. F., Møller, P. R., Sigsgaard, E. E., Knudsen, S. W., Jørgensen, O. A., and Willerslev, E. (2016). Environmental DNA from seawater samples correlate with trawl catches of subarctic, deepwater fishes. *PLoS One* 11, 1–22. doi: 10.1371/journal.pone.0165252.

Thomsen, P. F., and Willerslev, E. (2015). Environmental DNA - An emerging tool in conservation for monitoring past and present biodiversity. *Biol Conserv* 183, 4–18. doi: 10.1016/j.biocon.2014.11.019.

Turner, J. A., Babcock, R. C., Hovey, R., and Kendrick, G. A. (2017). Deep thinking: A systematic review of mesophotic coral ecosystems. *ICES Journal of Marine Science* 74, 2309–2320. doi: 10.1093/icesjms/fsx085.

Turner, J., Andradi-Brown, D., Gori, A., Bongaerts, P., Burdett, H., Ferrier-Pagès, C., et al. (2019). “Key Questions for Research and Conservation of Mesophotic Coral Ecosystems and Temperate Mesophotic Ecosystems,” in *Mesophotic Coral Ecosystems Coral Reefs of the World 12* (Loya, Yossi Puglise, Kimberly A Bridge, Tom C L), 989–1003. doi: 10.1007/978-3-319-92735-0.

Yao, M., Zhang, S., Lu, Q., Chen, X., Zhang, S. Y., Kong, Y., et al. (2022). Fishing for fish environmental DNA: Ecological applications, methodological considerations, surveying designs, and ways forward. *Mol Ecol*, 5132–5164. doi: 10.1111/mec.16659.

Yeakel, K. L., Andersson, A. J., Bates, N. R., Noyes, T. J., Collins, A., and Garley, R. (2015). Shifts in coral reef biogeochemistry and resulting acidification linked to offshore productivity. *Proc Natl Acad Sci U S A* 112, 14512–14517. doi: 10.1073/pnas.1507021112.

Chapter 4. Complementary assessments of the upper / lower across mesophotic interface via eDNA metabarcoding and baited remote underwater video systems (BRUVs)

4.1 Abstract

The complimentary nature of eDNA metabarcoding and BRUVs allows for a greater accuracy of biodiversity assessments and were chosen to characterise fish biodiversity at the upper mesophotic / lower mesophotic interface (~ 60 - 65 m), a depth zone previously quantified as a faunal break in other mesophotic regions. Locally, this depth zone has and remains an important area for local commercial fisheries. In total, 155 species from 137 genera were detected by eDNA metabarcoding whilst total of 85 species from 53 genera were detected by BRUVs. The combined species detection totalled 182 species of which 90 where unique detections by this mesophotic study when compared to previous studies of Bermuda's mesophotic reefs. Of these detections, 38 species were commercially important and a further 15 species were of mesopelagic and bathypelagic origin. Both methodologies determined differences in α-diversity between study locations with each method independently detecting the highest species richness at location BT3. The species richness at each location was dominated by species (~ 80%) known to occur throughout the upper mesophotic and shallow reef system whilst species only known to inhabit the mesophotic accounted for ~6% at each location. These findings infer a lack of a faunal break at the ~ 60 m sites and suggest a high level of species continuity with the adjacent shallower reef systems. Despite the high degree of species overlap, there was evidence of depth specialist species e.g., the Bermuda chromis (*Chromis bermudae* Nichols 1920*)*, an endemic species, that was identified using both methodologies. This study successfully generated data for a multi-seasonal and multi locational snapshot of biodiversity utilising complimentary methodologies. Overall, the two collaborative methods employed in this study have recorded 38% of the total fish biodiversity currently published for Bermuda. The complementary use of eDNA and baited cameras are the future for biomonitoring of these fish communities.

4.2 Introduction

Providing managers and policy makers with high quality scientific data is key in to allowing them to implement an effective marine spatial planning policy through an ecosystem-based approach. Environmental DNA (eDNA) is proving to be a valuable tool for ecosystem monitoring in a wide range of environments (Bohmann et al., 2014; Kelly et al., 2014; Port et al., 2016b; Deiner et al., 2017) including marine systems (Miya et al., 2020). The collection of eDNA sequences have proven successful for determining species diversity and community structure over different spatial and temporary timescales (Thomsen and Willerslev, 2015), environmental gradients (Kelly et al., 2016) and detecting cryptic and elusive species (Baker et al., 2016a; Gargan et al., 2017; Boussarie et al., 2018). The decreasing cost and increasing reliability of utilising eDNA for community assessments is rapidly making eDNA-based studies a tool of choice for ecologists and natural resource managers. However, government agencies are often not willing to change monitoring methodologies before proof of concept has been established. The species richness metrics generated by eDNA metabarcoding are not that dissimilar to traditional assessment methods (e.g., BRUVs); however, eDNA has the potential to provide a more “complete” biodiversity assessment due to the method’s efficiency in detecting cryptic, low-abundance, transient and rare taxa (Port et al., 2016b; Weltz et al., 2017; Yamamoto et al., 2017; Boussarie et al., 2018; Aglieri et al., 2020; Gold et al., 2020). In addition, the economic efficiency of eDNA metabarcoding allows biomonitoring to be conducted at high spatial and temporal resolutions which when paired with biotic measurements, would greatly benefit ecosystem-based management approaches (Yao et al., 2022). Existing metabarcoding sequence data sets can be datamined for alternative taxa, i.e., ‘molecular by-catch’ (Mariani et al., 2021b). There has been an increased call for eDNA sequence repositories termed “biobanks” (Jarman et al., 2018; Berry et al., 2021) that would operate in a similar way to current DNA reference database repositories (e.g., NCBI GenBank). Sequencing could be datamined as and when improvements to existing and/or future databases were made. To increase or optimise taxonomic detections, existing DNA extracts could be amplified with optimised assays (e.g., Tele02) or alternative assays that target different taxa and/or regions.

Despite the benefits of the metabarcoding approach, there are uncertainties and artefacts inherent to the methodology. The samples often contain a combination of degraded target taxa DNA (Collins et al., 2018) and non-target DNA that may co-amplify (Stat et al., 2017). Inhibition of DNA amplification or the introduction of false positives throughout multiple stages (e.g., sampling, DNA extraction, amplification, and sequencing) can lead to the misinterpretation of sequencing data sets. Assays can and do exhibit primer affinity bias, whilst bioinformatic processing can lead to the creation of technical artifacts. All of these reasons combined with a lack of knowledge about target taxa shedding rates mean that the quantitative ability of eDNA metabarcoding is the topic of much debate.

Baited Remote Underwater Video systems (BRUVs) are non-destructive, cost-effective fishery-independent sampling units (Langlois et al., 2010) that produce spatially explicit quantitative data on reef ichthyofauna abundance and diversity. Baited camera techniques can survey a broad range of species (increased through the presence of bait; Harvey et al., 2007; Dorman et al., 2012) and as such have been utilized in various marine environments (Whitmarsh et al., 2017), including for the assessment of pelagic species (Santana-Garcon et al., 2014). In addition, the video footage creates a permanent record that is especially useful for life stage and behavioural observations (Barley et al., 2016), allowing third-party verification of species identification and for use in education and outreach initiatives. Whilst the presence of bait can increase species richness, it can also be bias towards certain trophic guilds (i.e., carnivores; Stobart et al. 2007) leading to underrepresentation of smaller cryptic species (Lowry et al., 2012). Screen saturation (Schobernd et al., 2014) due to abundant taxa can lead to an underestimation of the population due a physical limit of the number of individuals able to fit in the field of view. It is not always possible to distinguish be congers (e.g., lionfish)

With the exception of an invasive species focused project (Goodbody-Gringley et al., 2019a), Bermudan mesophotic fish community investigations have been conducted across a depth gradient and not on a specific depth strata (Pinheiro et al., 2016; Goodbody-Gringley et al., 2019b; Stefanoudis et al., 2019a). This chapter aims to provide an interdisciplinary assessment of fish biodiversity from the upper mesophotic / lower mesophotic interface (~ 60 - 65 m) by utilising a combination of eDNA metabarcoding and

BRUVs (Stat et al., 2019; Aglieri et al., 2020). Specifically, the assessment will investigate the existence of a faunal break (Lesser et al., 2019) through the identification of depth specialist species. To determine if trends can be applied to the wider Bermudan mesophotic / lower mesophotic interface, variations in α- and β-diversity will be assessed both spatially and temporally.

4.3 Methodology

Surveys were conducted monthly between August – December 2017 and every two months between May and October 2018. Site locations followed the 60 m depth contour and were situated ~350 m (Figure 4.1) apart to maintain site fidelity during BRUVs deployments by minimising the influence of bait plumes between sites (Harvey et al., 2007). Active steps to minimise cross contamination between eDNA sampling and BRUVs bait were taken at all times through the following procedures;

1. Seawater samples were collected prior to BRUVs deployments.
2. Assisting personnel were each assigned to only one methodology.
3. External surfaces of eDNA storage coolers and BRUVs equipment were sprayed with 10% bleach solution and rinsed prior to loading on sampling vessel and post deployments.
4. Sampling equipment were kept in separate locations on the sampling vessel.
5. BRUVs bait was kept frozen in a sealed container until use.

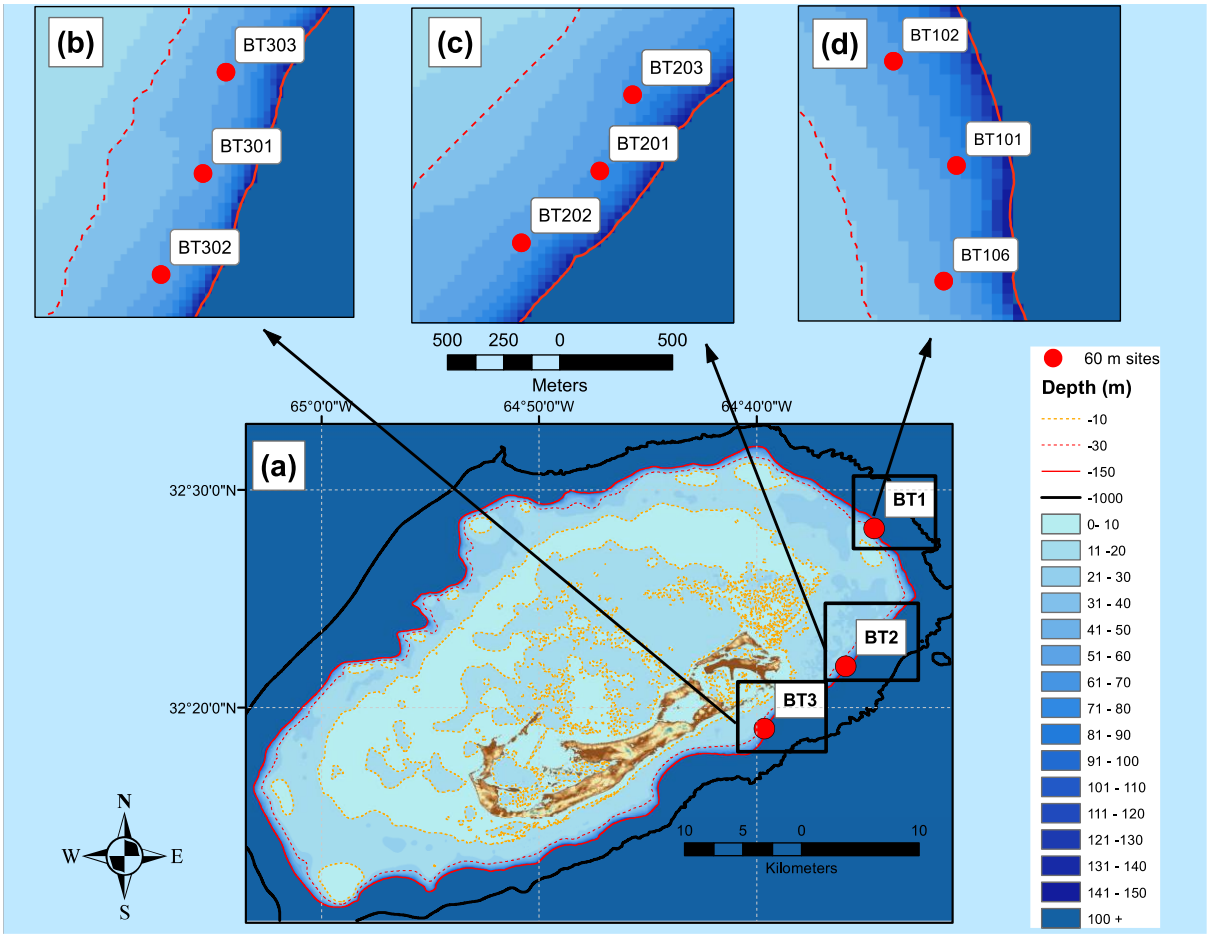

Figure 4.1. (**a – d**), 30 m depth contour dashed red line, 150 m depth solid red line, (**a**). Map of Bermuda and study locations (red circles), 10 m contour orange dotted line, 1000 m contour solid black line. (**b**) Bathymetric map of Location BT3, red circles = 60 m sites, (**c**) Bathymetric map of Location BT2, red circles = 60 m sites, (**d**) Bathymetric map of Location BT1, red circles = 60 m sites

4.3.1 Environmental DNA

For a detailed description of the sample collection, processing, and bioinformatics, see Chapter 3, sections 3.2.2 – 3.2.4. A synopsis of the methods are as follows, 8 L of seawater per sample were collected ~ 2 m above the benthos and filtered through 0.8 µm hydrophilic membrane polycarbonate filters and frozen prior to extraction using an E.Z.N.A. Mollusc DNA Kit (Omega Bio-Tek: Norcross, Georgia, USA) commercial kit. Library preparation was performed as a two-step Polymerase chain reaction (PCR) using AccuPower ProFi Taq PCR PreMix (Bioneer: California, USA) and the 12S MiFish-U universal primers (Miya et al., 2015) with sample identification facilitated through the use

of unique eight base-pair indexes. All sequencing was performed on an Illumina MiSeq platform. Resulting Molecular Operation Taxonomic Units (MOTUs) were taxonomically identified by BLASTing against the GenBank nucleotide database and assigned to the species level at a 99% similarity threshold whilst genus level was assigned at a 95% threshold (Stat et al., 2019). To mitigated for contamination, control samples were investigated for any suspected contamination reads from target taxa with a resultant application of a threshold approach-based on negative controls for those taxa detected (see previous Chapter; Deiner et al., 2017). The threshold correction factor was then applied to all biological samples within the corresponding sequence run (n = 5).

4.3.2 Baited Remote Underwater Video systems (BRUVs)

Single GoPro™ Hero 3+ cameras in Golem Gear underwater housings (1000 m depth rated) were mounted inside purpose built galvanized steel frames. The frames provided multiple functions by allowing cameras to be mounted at a set distance (45 cm) from the benthos, acted as ballast during deployments and provided protection for the camera housings during deployment and recovery. All cameras were set to record at 1080 definition on medium field of view with each system baited with ~ 700 g of chopped Redear herring, (*Harengula humeralis* Cuvier, 1829) placed in plastic mesh and suspended ~ 1.5 m in front of the cameras. The bait bag was suspending on flexible conduit to allow the bait to maintain contact with the benthos. Having the bait in contact with the benthos has been known to increase sightings of crypto-benthic species (M. Cappo pers. Commun.). Systems were left to record on the seafloor for a minimum of 1 hour between the hours of 11:00 – 16:00. All recordings were made using ambient light. Video footage was annotated using EventMeasure software (www.seagis.com.au) which is specifically designed for logging and reporting events that occur in digital imagery. The measurement matrix generated during the annotations was relative abundance and defined as the maximum number of individuals per species seen at once during a 60-minute video or “MaxN”. The 60-minute observation period began once the system had become stable after contacting the benthos with fish species identified to the lowest taxonomic level possible. The exception to this level of identification was for lionfish

(*Pterois* sp. Oken 1817). Whilst the dominant species in Bermuda is *P. volitans* (Linnaeus 1758), it is not possible to visually distinguish between its congener *P. miles* (Bennett, 1828) with 100 % certainty. Therefore, they have both been pooled to genus level.

It should be noted that any bait-related biases such as the area of attraction or species attracted are deemed constant throughout the dataset. Whilst every attempt was made to survey the same sites through deployment at the same latitude and longitude (Garmin GPS +/- 5 m accuracy), the orientation of BRUVs cannot be controlled for during deployment therefore is of a stochastic nature (see Figure 4.2).

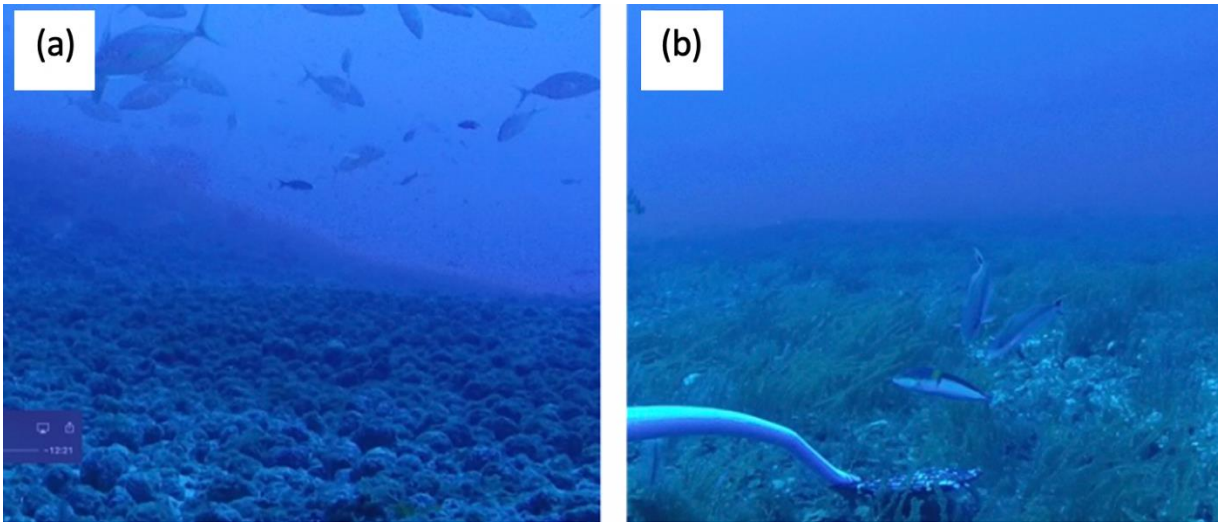

Figure 4.2. Seabed complexity observed at site BT1 on survey 1 (**a**) and survey 4 (**b**) differences are caused by changes in BRUVs orientation upon contact with the seabed (depth ~ 60 m). Image (**a**) depicts rhodolith beds foreground with ~ 5 m reef structure in the background and a shoal of Gwelly jacks (*Pseudocaranx dentex*, Bloch & Schneider 1801) in the field of view. Image (**b**) depicts rhodolith beds and brown algae (*Sporochnus bolleanus*, Montagne 1856), two Sand tilefish (*Malacanthus plumieri*, Bloch 1786) and one terminal phase Yellowhead wrasse (*Halichoeres garnoti*, Valenciennes 1839).

Habitat metrics were visually estimated from BRUVs imagery for each deployment and composed of slope, relief (structural complexity) and nine benthic categories (rubble and sand, hard bottom, live coral, gorgonians, crustose coraline algae (CCA), rhodoliths, macroalgae, turf algae, sponges). Benthic categories were estimated as percentage cover, relief was categorised as per the six-point scale of Wilson et al. (2007) and slope was grading on a 6-point scale from flat to vertical.

It was deemed not appropriate to pool habitat metrics due to a lack of knowledge on Bermudan mesophotic benthic community seasonality and the stochastic nature of deploying BRUVs to 60 m.

Abiotic variables generated in Chapter 2 were matched to sampling sites used for this assessment of the upper / lower mesophotic interface (Table 4.1). See Chapter 2 for explicit details on how abiotic data were derived.

4.3.3 Data analysis

All downstream analyses were performed in R version 3.5.3 (R Core Team, 2019) using the packages adespatial v 0.3-7 (Dray et al., 2021), betapart v1.5.4 (Baselga and Orme, 2012), iNEXT_2.0.20 (Hsieh et al., 2016) and vegan v2.5-6 (Oksanen et al., 2019). To be consistent with BRUVs derived taxonomic assignments, eDNA detections of *Pterois volitans* and *P. miles* were pooled to genus level. Variation in α- (taxon richness of individual samples) and β-diversity were investigated between assessment methodologies whilst β-diversity was also considered at the genus level.

Dissimilarity matrices for both α- and β-diversity separated by methodology were built based on Jaccard Dissimilarity measures, and graphically represented using non-metric MultiDimensional Scaling (nMDS). The effect of season and location (BT1, BT2, BT3) were tested on α-diversity using permutational multivariate analysis of variance (PERMANOVA). Beta diversity was partitioned into taxon replacement (turnover) or taxon subgroups (nestedness-resultant) and tested for the effects of location and season using PERMANOVA.

To determine if species detections for both methodologies were influenced by environmental forcings (explanatory variables of benthic community composition, abiotic conditions, and seasonality), a canonical form of principal component analysis (redundancy analysis; RDA) was applied to each dataset independently and visualized with a tripod (RDA biplots with explanatory variables plotted as arrows). Both a global test and test of the canonical axes with 999 permutations were performed on the resultant RDA outputs. Prior to the implementation of the RDA, a Hellinger transformation was applied to both the BRUVs and eDNA species datasets whereby abundance values are

divided by the sample total abundance and then square-root transformed (Legendre and Gallagher, 2001). The environmental variables were standardised to zero mean and unit variance (Table 4.1).

Table 4.1. Summary of abiotic and biotic explanatory variables used for Redundancy Analysis (RDA)

Abbrevation	Decription	Abbrevation	Decription
Ar	Ω Aragonite	CCA	Crustose coralline algae
Ca	Ω Calcite	coral	Living coral
DIC	Dissolved Inorganic Carbon	gorgonians	Gorgonian
NAO	North Atlantic Oscillation index	hard bottom	Hard bottom
NEC	Net Ecosystem Calcification	macroalgae	Macroalgae
NEP	Net Ecosystem Productivity	rhodoliths	Rhodolith
pH	pH	sediment	Unconcolidated benthos
PSU	Practical Salinity Units	turf	Turf algae
Revelle	Revelle Factor	Sum 17	Summer 2017
T	measured temperature (˚C) at time of eDNA collection	Win 17	Winter 2017
TA	total Alkalinity	Spr 18	Spring 2018
slope	Reef slope	Sum 18	Summer 2018
relief	relief	Aut 18	Autumn 2018

4.4 Results

In total 67 paired collections of seawater for eDNA analysis and BRUVs deployments met the sampling criteria and were included in the downstream analyses. The 12S amplicon libraries produced 6,360,726 raw reads. After the removal of singletons, the application of the minimum read count threshold (5 reads) and assignment to genus level, the number of reads was reduced to 2,097,857. When taxa assignments were further refined to species level, reads where reduced to 769,623 in total. Overall, there were a total of 155 species from 137 genera detected by eDNA metabarcoding (Figure 4.3). Importantly, the bait (*Harengula humeralis* Cuvier,1829) utilised for the BRUVs was not detected. Baited cameras detected a total of 85 species from 53 genera which equated to ~45% less species and ~60% less genera than eDNA. The greater detection rates of fish taxa by eDNA were consistent at both the species and genus level across all three survey locations (Figure 4.3).

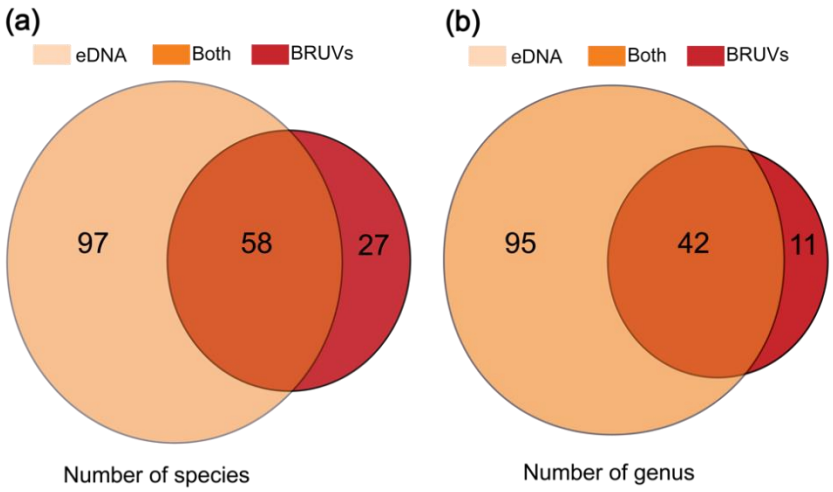

Figure 4.3. Venn diagrams of the number of corresponding and unique (**a**) species (**b**) genera detected by the two assessment methodologies, Baited Under Water Video systems (BRUVs; red semi circles) and environmental DNA (eDNA; peach semi circles). The orange intersect indicates the number of species (a) and genera (b) detected by both methodologies.

Sample size-based rarefaction/extrapolation (R/E) curves (Figure 4.4) imply taxon diversity had reached a plateau at all locations which would infer a suitable level of sampling had been reached to assess the community structure of these three mesophotic locations for both methodologies.

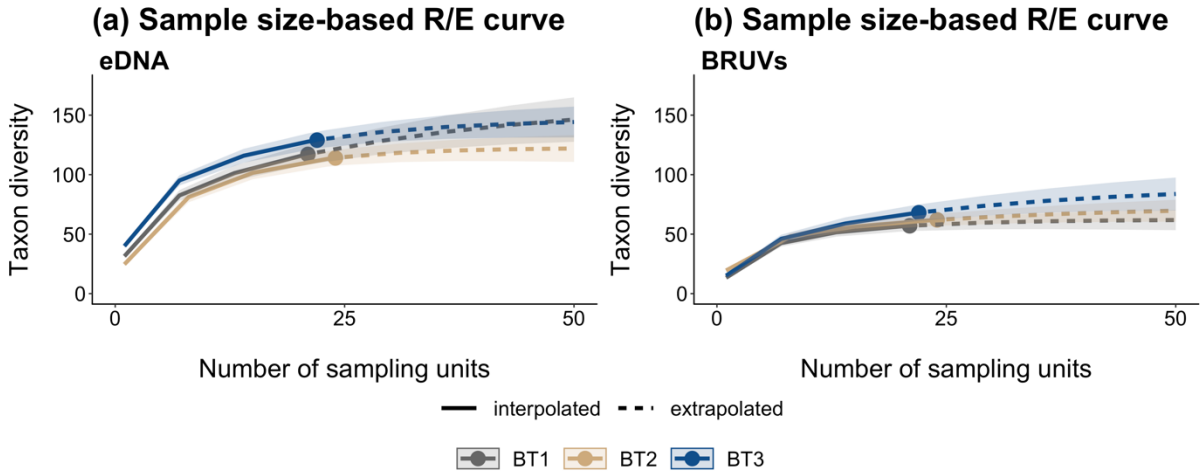

Figure 4.4. Sample size-based rarefaction/extrapolation (R/E) curves for each location BT1 (dark gray symbols and lines), BT2 (peril symbols and lines), BT3 (blue symbols and lines): (**a**) environmental DNA (eDNA) metabarcoding methodology, (**b**) Baited Remote Underwater Video systems (BRUVs) methodology.

Differences in α-diversity between locations were detected by both methodologies (Table 4.2) with each method independently detecting the highest taxon richness detected at location BT3 (eDNA, n = 129, BRUVs, n = 68).

Table 4.2. Summary statistics of 60 m mesophotic community similarity and interactions detected by eDNA metabarcoding and BRUVS: quantative (Bray-Curtis dissimilarity) data, sampling season, location, species trophic guild as well as interactions (PERMANOVA). Binary (Jaccard's coefficient) data, community variances (ANOVA); community similarity, sampling season, location as well as interactions (PERMANOVA). Statistically significant tests are in bold. Note, variables are treated sequentially in the PERMANOVA analysis.

eDNA	**Jaccard: Community similarity (PERMANOVA)**				**BRUVs**	**Jaccard: Community similarity (PERMANOVA)**			
Interaction		***df***	***F***	***P***	**Interaction**		***df***	***F***	***P***
season year		5	3.570	0.024	**0.002**	season year	5	0.653	0.007	0.732
location		2	4.781	0.013	**0.001**	**location**	2	5.625	0.025	**0.003**
season year:location		9	1.259	0.015	0.207	season year:location	9	0.543	0.011	0.936

eDNA	**Jaccard: Homogeneity of multivariate dispersons (ANOVA)**				**Jaccard: Community similarity (PERMANOVA)**				
	Mean distance to centroid ± SE	***df***	***F***	***P***	**Interaction**	***df***	***F***	***R²***	***P***
Turnover		2	2.495	0.090	**season year**	5	1.609	0.118	**0.008**
BT1 (94.14%)	0.345 ± 0.035				**location**	2	1.899	0.056	**0.005**
BT2 (94.83%)	0.405 ± 0.016				season year:location	9	0.709	0.094	0.964
BT3 (93.01%)	0.314 ± 0.010								
Nestedness-resultant		2	0.175	0.840	**season year**	5	8.256	0.285	**0.001**
BT1 (5.86%)	0.109 ± 0.011				**location**	2	6.603	0.091	**0.004**
BT2 (5.17%)	0.114 ± 0.010				**season year:location**	9	4.455	0.277	**0.001**
BT3 (6.99%)	0.126 ± 0.008								
Total ß-diversity		2	12.887	**<0.001**	**season year**	5	2.725	0.169	**0.001**
BT1 (100%)	0.476 ± 0.002				**location**	2	2.850	0.071	**0.001**
BT2 (100%)	0.524 ± 0.003				**season year:location**	9	1.234	0.138	**0.011**
BT3 (100%)	0.438 ± 0.004								

BRUVs	**Jaccard: Homogeneity of multivariate dispersons (ANOVA)**				**Jaccard: Community similarity (PERMANOVA)**				
	Mean distance to centroid ± SE	***df***	***F***	***P***	**Interaction**	***df***	***F***	***R²***	***P***
Turnover		2	3.235	**0.046**	season year	5	1.101	0.070	0.326
BT1 (95.17%)	0.437 ± 0.028				**location**	2	6.225	0.159	**0.001**
BT2 (92.73%)	0.320 ± 0.026				season year:location	9	1.156	0.133	0.223
BT3 (94.68%)	0.427 ± 0.037								
Nestedness-resultant		2	0.084	0.919	season year	5	2.183	0.215	0.214
BT1 (4.83%)	0.110 ± 0.014				location	2	-3.724	-0.147	0.993
BT2 (7.27%)	0.124 ± 0.005				season year:location	9	-0.293	-0.052	0.943
BT3 (5.32%)	0.116 ± 0.026								
Total ß-diversity		2	6.257	**0.003**	season year	5	1.030	0.071	0.386
BT1 (100%)	0.550 ± 0.003				**location**	2	4.038	0.112	**0.001**
BT2 (100%)	0.450 ± 0.017				season year:location	9	1.004	0.125	0.448
BT3 (100%)	0.541 ± 0.013								

The lowest taxon richness detected by BRUVs was at BT1 (n = 57; Z = -3.557, *p* = 0.001; Figure 4.5) while there was no significant difference between BT1 (n =116) and BT2 (n = 114; Z = 1.114, *p* = 0.265) for eDNA detections.

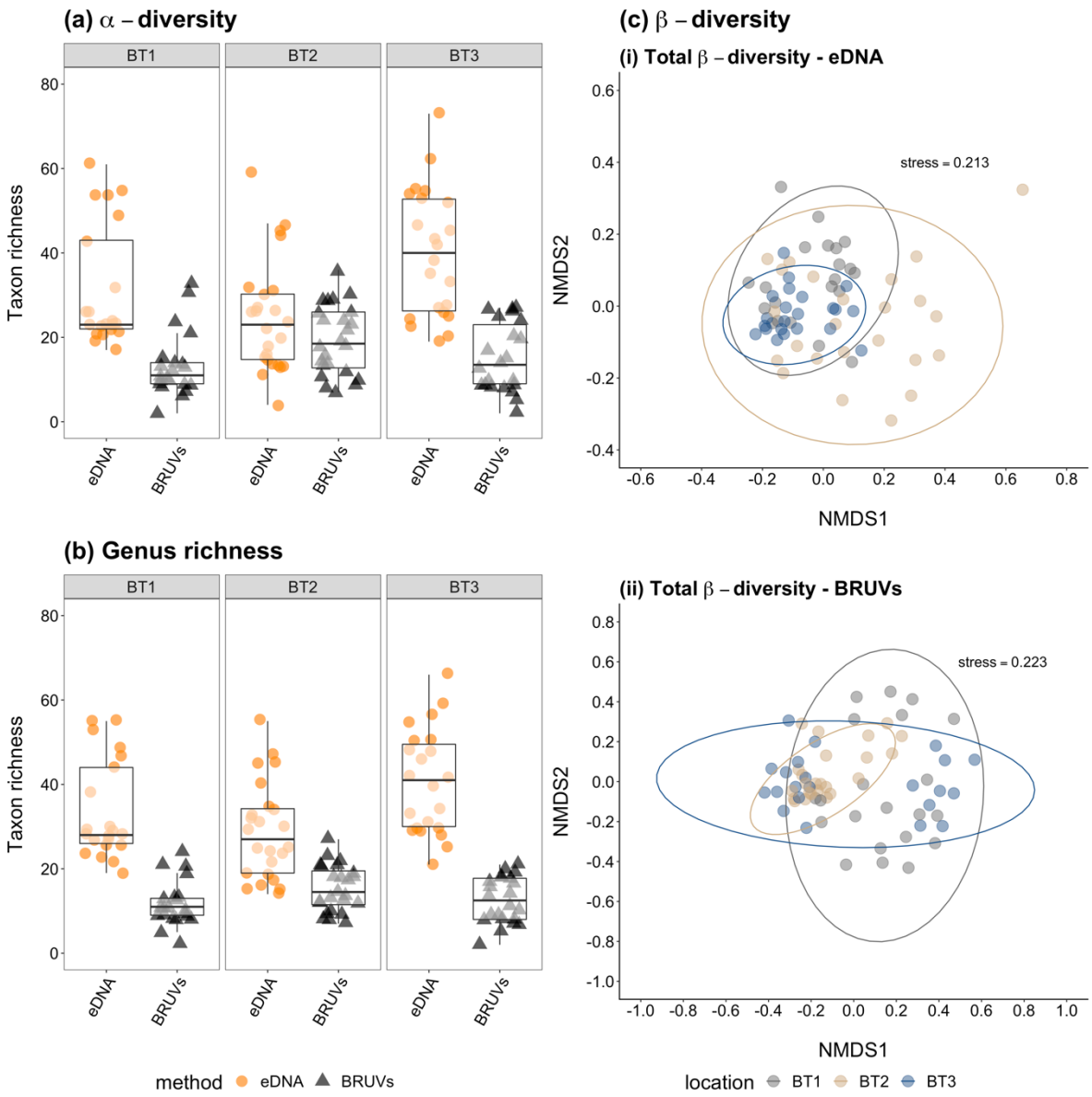

Figure 4.5. Summaries of α- and β-diversity between locations partitioned by sampling methodology: (**a**) boxplot of species richness, boxes indicating 25th, 50th and 75th percentiles and whiskers show 5th and 95th percentiles, eDNA (orange triangles) and BRUVs (dark grey circles). (**b**) boxplot of genus richness, boxes indicating 25th, 50th and 75th percentiles and whiskers show 5th and 95th percentiles, eDNA (orange triangles) and BRUVs (dark grey circles) (**c**) non-metric multidimensional scaling plots of β-diversity components, eDNA (triangles) and BRUVs (circles), locations: BT1 (dark grey symbols and ellipses), BT2 (peril symbols and ellipses), BT3 (blue symbols and ellipses).

Additionally, seasonal differences in α-diversity were detected by eDNA metabarcoding with differences occurring between summer 2017 and autumn 2017 (Z =

-3.223, p = 0.006), summer 2018 and autumn 2018 (Z = 2.557, p = 0.040), summer 2017 – summer 2018 (Z = 3.904, p = 0.001), autumn 2018 - winter 2017 (Z = 2.514, p = 0.036) and summer 2017 - winter 2017 (Z = 3.568, p = 0.003; Figure 4.5). Notably, there were no effects of location and seasonality combined on α-diversity detected by either method.

Beta diversity of each of the three locations was primarily driven by turnover (Table 4.2). Although turnover is not significant for eDNA, it is almost significant (p = 0.090) and exerts a stronger influence on β diversity than nestedness-resultant (p = 0.840). The location did influence the degree of which the proportion of taxa at a given location were replaced by differing taxa from an alternative location. Differences in the level of turnover detected by eDNA at BT1 and BT2 were negligible at 94.13% and 94.83% respectively. When the two methodologies were considered collectively, species turnover has the greatest influence on β diversity at location BT1. The influence of seasonality was only significant on eDNA derived community data; however, the influence was measured across the components of beta diversity. There was greater variability in nested-resultant detected within the eDNA samples across location, season, and the interaction between the two. Location influenced total β-diversity determined by both methods, however it had a stronger influence on the BRUVs dataset versus the eDNA metabarcoding (R^2 = 0.112, R^2 = 0.071; Figure 4.5)

Redundancy analysis accounted for approximately half of the variance within each fish community matrix (eDNA; R^2 0.502, BRUVs; R^2 = 0.494). Overall, both assessments showed there to be a degree of separation between the three locations, however this was most evident in the BRUVs derived dataset (Figure 4.6b). The associations between the environmental metrics and the communities were not consistent between the two methods. Environmental DNA detected community data exhibiting stronger associations with abiotic variables, whereas the BRUVs detected community associated more with the biotic variables. The different associations would be anticipated since eDNA samples are from a fluid environment that contains a “soup” of eDNA material from the surrounding area whereas visual methodologies (i.e., BRUVs) are strictly linked to observations that in this case, would be biased towards benthic associated species.

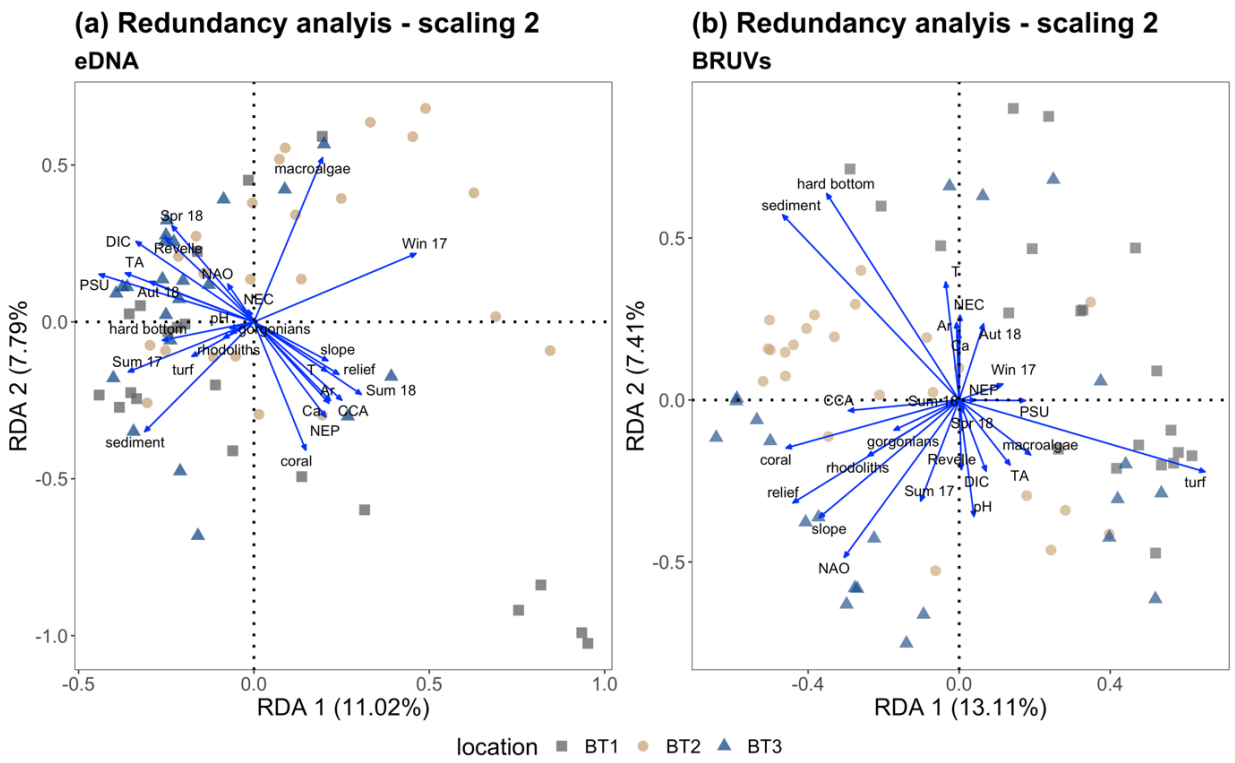

Figure 4.6. Redundancy analysis ordination diagram (triplots): location BT1 (dark grey square), BT2 (peril circles), BT3 (blue triangles). (a) environmental DNA (eDNA) metabarcoding community detection, (b) Baited Remote Underwater Video systems (BRUVs) community detection, explanatory variables (benthic composition and standardised physicochemical variables) blue arrows. First axis is horizontal, second axis is vertical. The angles among arrows denote the degree of correlation between the individual variables, and the smaller the angle, the greater the positive correlation. Negatively correlated variables are pointing in opposite directions.

All of the mesopelagic and bathypelagic fishes detected (n = 15) were only detected by the eDNA metabarcoding approach. Of these species, half are representatives of the highly migratory lanternfish family *Myctophidae* (Gill 1893).

Table 4.3. Summary of deep-sea species detected by eDNA metabarcoding. Depth ranges as published on fishbase.org (Froese and Pauly, 2022). Note, (*) denotes the usual depth range preference of a species.

Species	Common Name	Depth range (m)
Alepisaurus ferox	Long snouted lancetfish	0 - 1830
Anoplogaster cornuta	Common fangtooth	500 - 200 (*)
Bolinichthys nikolayi	Lanternfish	25 - 1760
Ceratoscopelus maderensis	Madeira lantern fish	51 - 1480
Cyclothone pallida	Tan bristlemouth	600 - 1800 (*)
Diaphus effulgens	Headlight fish	0 - 6000
Diaphus mollis	Soft lanternfish	50 - 600
Diplospinus multistriatus	Striped escolar	50 - 1000
Eustomias obscurus	Barbed dragonfish	20 - 1900
Gempylus serpens	Snake mackerel	0 - 600
Gonichthys cocco	Cocco's lanternfish	425 - 650 (*)
Hygophum hygomii	Bermuda lanternfish	0 - 1485
Lampadena atlantica	Lanternfish	60 - 1000
Nannobrachium lineatum	Lanternfish	60 - 1150
Nemichthys curvirostris	Pale threadtail snipe eel	0 - 2000

This study recorded 38 commercially important species between the two methodologies (Table 4.4). The species were broadly categorised as reef dwellers (n=25), pelagic dwellers (n=7) and baitfish (n=6). Environmental DNA detected various species of interest including *Makaira nigricans* (Lacepède 1802) a species listed as Threatened by the IUCN Red list and included in the International Commission for the Conservation of Atlantic Tunas (ICCAT). The endemic *Anchoa choerostoma* (Goode 1874) was additionally detected which is listed as Endangered. BRUVs and eDNA methodologies recorded the Near Threatened *Lutjanus synagris* (Linnaeus 1758) and *Mycteroperca bonaci* (Poey 1860) alongside globally Vulnerable species such as *Balistes capriscus* (Gmelin 1789), *Lachnolaimus maximus* (Walbaum 1792), *Lutjanus campechanus* (Poey 1860) and *Mycteroperca interstitialis* (Poey 1860). Although not a fishery target species, eDNA also detected *Galeocerdo cuvier* (Péron & Lesueur 1822) a Near Threatened highly migratory shark species and the Critically Endangered *Anguilla anguilla* (Linnaeus 1758).

Table 4.4. Summary of species of interest listed by IUCN status and the method of detection used to record presence.

Species	Common name	Origin	BRUVs only	eDNA only	BRUVs and eDNA	IUCN Status
Anchoa choerostoma	Bermuda anchovy	Baitfish		X		Endangered
Auxis rochei	Bullet tuna	Pelagic		X		Least Concern
Auxis thazard	Skipjack tuna	Pelagic		X		Least Concern
Balistes capriscus	Grey triggerfish	Reef		X		Vulnerable
Calamus bajonado	Jolthead porgy	Reef	X			Least Concern
Caranx latus	Horse-eye jack	Reef			X	Least Concern
Caranx lugubris	Black jack	Reef			X	Least Concern
Caranx ruber	Bar jack	Reef			X	Least Concern
Carcharhinus galapagensis	Galpagos shark	Reef	X			Least Concern
Cephalopholis fulva	Coney	Reef			X	Least Concern
Clupea harengus	Atlantic Herring	Baitfish		X		Least Concern
Decapterus macarellus	Mackerel scad	Baitfish		X		Least Concern
Diplodus bermudensis	Bermuda bream	Reef		X		Least Concern
Elagatis bipinnulata	Rainbow runner	Pelagic	X			Least Concern
Epinephelus guttatus	Red hind	Reef			X	Least Concern
Euthynnus alletteratus	Little tunny	Pelagic		X		Least Concern
Haemulon flavolineatum	French grunt	Reef			X	Least Concern
Haemulon sciurus	Bluesstriped grunt	Reef			X	Least Concern
Hemiramphus bermudensis	Bermuda halfbeak	Reef		X		Least Concern
Hypoatherina harringtonens	Reef silverside	Baitfish		X		Least Concern
Jenkinsia lamprotaenia	Dwarf round herring	Baitfish		X		Least Concern
Katsuwonus pelamis	Skipjack tuna	Pelagic		X		Least Concern
Lachnolaimus maximus	Hogfish	Reef			X	Vulnerable
Lutjanus campechanus	Northern red snapper	Reef		X		Vulnerable
Lutjanus griseus	Grey snapper	Reef			X	Least Concern
Lutjanus synagris	Lane snapper	Reef			X	Near Threatened
Makaira nigricans	Blue Marlin	Pelagic		X		Vulnerable
Mugil curema	White mullet	Reef		X		Least Concern
Mycteroperca bonaci	Black grouper	Reef			X	Near Threatened
Mycteroperca interstitialis	Yellowmouth grouper	Reef	X			Vulnerable
Ocyurus chrysurus	Yellowtail snapper	Reef			X	Data Deficient
Opisthonema oglinum	Atlantic thread herring	Baitfish		X		Least Concern
Paranthias furcifer	Creolefish/barber	Reef			X	Least Concern
Pseudocaranx dentex	White trevally	Reef			X	Least Concern
Sardinella aurita	Round sardinella	Baitfish		X		Least Concern
Seriola dumerili	Greater amberjack	Reef			X	Least Concern
Seriola rivoliana	Almaco jack/bonita	Reef			X	Least Concern
Sphyraena barracuda	Barracuda	Reef			X	Least Concern

4.5 Discussion

The suite of observational methodologies utilised in this study demonstrates their suitability for capturing the diversity of ichthyofaunal assemblages in Bermuda's mesophotic coral ecosystems. A failure to establish complementary ecosystem-based approaches for the protection of fish and invertebrate species as stated by Strategic Goal B; Target 6 of the Aichi Biodiversity Targets serves as a reminder of the 1) incomplete knowledge on global biodiversity, 2) the enormity at hand in which to rapidly obtain these data. The increasing popularity of eDNA-based assessments and the steady change from comparative method-based studies to those of a complementary nature have greatly boosted the capacity to cast a much larger net as to the biodiversity present in any given ecosystem (Djurhuus et al., 2020).

Chapter 3 established there to be faunal continuity down the mesophotic depth gradient notwithstanding the caveat linked to under sampling of 130 m habitats. This study combined eDNA metabarcoding and BRUVs to focus on a depth zone (~ 60 - 65 m) previously quantified as a faunal break in other mesophotic regions (Bejarano et al., 2014; Fukunaga et al., 2016; Page et al., 2016; Pinheiro et al., 2016; Pyle et al., 2016; Rosa et al., 2016; Baldwin et al., 2018; Lesser et al., 2019) to explicitly investigate if this phenomenon was true for Bermuda.

Locally, this depth zone has and remains an important area for local commercial fisheries (Faiella, 2003) for spiny lobsters (*Panulirus argus* Latreille 1804) and both demersal and pelagic fin fishes. To date, the most comprehensive fish centric Bermudan mesophotic studies have been conducted across a depth gradient and not on a specific depth strata (Pinheiro et al., 2016; Goodbody-Gringley et al., 2019b; Stefanoudis et al., 2019a). The one exception to this was the study on the ecological drivers of an invasive species (Goodbody-Gringley et al., 2019a). Accumulatively, these studies documented 173 species ranging from 30 m into the rariphotic zone (> 150 m) with no previous use of eDNA metabarcoding. The combined species detections from this study totalled 182 species of which 90 where unique to this study for mesophotic focused investigations.

Previous studies have demonstrated differences between methodologies through a greater affinity for certain taxa (Kelly et al., 2017; Boussarie et al., 2018; Stat et al.,

2019; Aglieri et al., 2020) with a tendency for eDNA biodiversity assessments to have a higher taxa detection rate over other methods likely due to the persistence of target DNA within the study region (Thomsen et al., 2012; Collins et al., 2018). Whilst there was commonality of taxa cross the two methods, both contributed unique detections to the overall dataset (Figure 4.3). This highlights the complimentary nature of the two methodologies thus allowing for a greater accuracy of the biodiversity assessment. Whilst it may seem counterintuitive to combine two methods whereby one can be a source of contamination for the second (Stat et al., 2019), with appropriate protocols in place, the risks of contamination can be mitigated against. In the case of this study, the bait species was not detected in any of the field samples.

This study revealed that geographical location in combination with species turnover between locations were major drivers of the fish community present at the upper mesophotic, lower mesophotic interface. At each location, the species richness of these communities was dominated by species (~ 80%) known to occur throughout the upper mesophotic and shallow reef system. Species richness for mesophotic species accounted for ~6% at each location. These findings infer a lack of a faunal break at the 60 m sites and suggest a high level of species continuity with the adjacent shallower reef systems. These results agree with previous findings on Bermuda mesophotic fish communities (Pinheiro et al., 2016), that determined a high degree of turnover was documented between 70 – 90, i.e., below the 60 m sites. A study on the vertical connectivity of the scleractinian coral *Montastraea cavernosa* (Linnaeus 1767), determined Bermudan shallow reefs were likely to be dependent on deep reef counterparts between the 4 – 60 m range. This suggests that the continuity of species between the shallow reef and upper mesophotic within Bermuda, occurs for multiple taxa.

Whilst there was a high degree of species overlap between shallow reefs and the upper mesophotic, there is increasing evidence that particular species in the Bermudan ichthyofauna are depth specialists. *Chromis bermudae* (Nichols 1920*)*, an endemic species, was identified using both methodologies in this study and found at the upper mesophotic and lower mesophotic interface and is in accordance with Stefanoudis *et al.* (2019) and Goodbody-Gringley et al*.* (2019). The observations of *Chromis insolata* (Cuvier 1830), *Centropyge argi* (Woods and Kanazawa 1951), and *Serranus phoebe*

(Poey 1882) were comparable to the findings of Stefanoudis et al. (2019a). This study proposes two additional specialist species *Prognathodes aculeatus* (Poey 1860) and *Serranus annularis* (Poey 1860) to the mesophotic, more specifically the upper and lower mesophotic interface, with the caveat that further exploration of deeper depth ranges into the rariphotic needs to be conducted. It should be noted that both these species where only detected using BRUVs observations (Table 4.5).

4.5.1 Taxa Detections

Pterois sp.[4] (Oken 1817) was the only species that was detected in all eDNA samples suggesting a ubiquitous distribution across the 60 m depth range. However, it was only observed on 37 of the 67 BRUVs deployments. Based on behavioural observations of *Pterois* sp. made during the annotation of video footage, it is plausible that individuals are present but out of the field of view. The wrasse *Thalassoma bifasciatum* (Bloch 1791) and carangid, *Decapterus macarellus* (Cuvier 1883) were detected in ~ 90 % of the eDNA samples (100% at genus level). *Thalassoma bifasciatum* is a facultative cleaner species and provides valuable ecosystem services and was determined to be the top teleost prey species of *Pterois* sp. in a study by Eddy et al. (2016). *D. macarellus* is targeted by fishers as preferred bait for demersal fishing in mesophotic ecosystems albeit not on an industrial scale. The flyingfish genus *Cheilopogon* (Lowe 1841) accounted for ~ 50% of the eDNA detections at genus level. Flyingfish were not observed by BRUVs and a literature search of known depth ranges suggest this species is generally close to the sea surface (< 20 m). A likely explanation for the higher read count is the predator prey avoidance behaviour employed by this genus. As the common name suggests, flyingfish use modified pectoral fins to “fly” away from predators before collapsing their wings and splashing back into the water. This action is very likely to sluff off eDNA material and in time, fall as “marine snow” into the 60 m depth strata being surveyed by this study. Literature reports of eDNA persistence within marine environments vary but can persist for up to 48 hrs (Collins et al., 2018).

[4] For the purposes of this study, *Pterois volitans* and *Pterois miles* are deemed *Pterois* sp. for all observations and reads and are pooled by method due to the uncertainty of correct visual determination of the species.

Recent assessments to determine *in situ* eDNA residence times have reduced detectability to between 2 – 7.5 hrs (Murakami et al., 2019; Ely et al., 2021). An estimate of 0.5 days residence time (N. Bates pers. Comms.) was used for the calcification and productivity assessments of these same locations (Chapter 2). The mesophotic reefs surrounding Bermuda are highly dynamic environments with water currents recorded at 0.8 – 1.0 m/s at BT2 (R. Johnson pers. Comms). However, hydrological regimes have not been quantified for these environments. The *Cheilopogon* genus is ubiquitous within the surface waters above the mesophotic reefs and surrounding pelagic environment therefore advection of eDNA from this genus from surface to deep would be likely within the currently known eDNA residence times.

Elasmobranchs have a noticeably low detection rate with in the two datasets with each method detecting one species, *Carcharhinus galapagensis* (Snodgrass & Heller 1905; BRUVs) and *Galeocerdo cuvier* (Péron & Lesueur, 1822; eDNA). The known lack of affinity of the chosen MiFish-U primers for amplifying elasmobranchs (Miya et al., 2015), meant low detections were not a surprise. Since the commencement of this study, the less-than-ideal affinity for elasmobranchs has been addressed through the development of the Elas02 primers (Taberlet et al., 2018) which are modified MiFish primers. The Elas02 primer higher affinity for elasmobranchs were demonstrated in a recent assessment of shark and ray biodiversity of Reunion Island (Mariani et al., 2021a).

The single visual observation of *C. galapagensis* was unexpected. Baited camera (BRUVs) methodology has been adopted by Global Finprint, a global initiative led by Florida International University (FIU, U.S.A) due to the affinity for sharks to be attracted to the bait. One explanation for the lack of observations could be due to behaviour patterns of reef sharks. Papastamatiou et al. (2015b) observed a reverse diel pattern in *C. galapagensis* behaviour with individuals migrating to the shallow reefs systems during the day and returning to mesophotic reefs during dark periods. All BRUVs deployments were exclusively during the day to utilise ambient light at depth. Therefore, the combination of animal movement away from the target depth strata and low specificity of eDNA would make detections for either method less than optimal.

The 60 – 70 m depth range has historically been an important area for the local commercial fishing industry and a target area for the deployment of fish pots. In 1990, the

Government of Bermuda proactively banned the use of fish pots (Butler et al., 1993) in an effort to protect reef fish species that had either demonstrated sharp declines in abundances e.g., groupers or increased fishing pressure e.g., parrotfishes. As a result of this change in legislation, all scarids where fully protected in 1993. This study detected 10 of the 14 parrotfishes accepted as part of the Bermuda ichthyofauna (Smith-Vaniz et al., 1999; Smith-Vaniz and Collette, 2013), eight of which were common to both methods and one species that was unique to each method.

In addition to the detection of protected species, the complementarity of these methodologies allowed for data to be gathered on the presence of commercially important species of concern. Although the island has been designated as having advanced capacity for targeting specific species, Bermuda's fishery is primarily for local consumption and classified as artisanal (FAO, 2022 https://www.fao.org/fishery/en/facp/bmu). However, should the island's fishing capacity increase, these data will enhance future fisheries best management practices.

The detection of mesopelagic species (Table 4.3) provides a notable example of the differences in detection abilities between the two methodologies. As to be expected, these deep-sea species were only detected by the molecular based approach (eDNA) and not observed by BRUVs. It should be recognised that the inclusion of mesopelagic species in the eDNA dataset is not an admission by the author that these species utilise mesophotic ecosystems, rather that the DNA signatures were present at the time of sampling. This is likely a direct result of the increased detection ability of eDNA over other methods and site proximity to the open ocean (~ 1 km). However, they were retained for two reasons, 1) mesopelagic species are known to exhibit diel migration patterns into the upper 200 m (Dypvik and Kaartvedt, 2013), a phenomenon that has been captured by eDNA metabarcoding (Canals et al., 2021), 2) these detections serve as additional biodiversity information and therefore fit with the recent analogy of Mariani et al., (2021b) on the concept of 'molecular by-catch'.

Table 4.5. Summary of select species and associated primary habitat[5] and the method of detection used to record presence.

Habitat	Species	Common name	Detection method
Pelagic	*Auxis rochei*	Bullet tuna	eDNA
Pelagic	*Auxis thazard*	Little tunny	eDNA
Pelagic	*Elagatis bipinnulata*	Frigate tuna	BRUVs
Pelagic	*Euthynnus alletteratus*	Little tunny	eDNA
Pelagic	*Katsuwonus pelamis*	Skipjack tuna	eDNA
Pelagic	*Makaira nigricans*	Blue marlin	eDNA
Pelagic	*Anguilla anguilla*	European eel	eDNA
Mesophotic	*Enchelycore carychroa*	Chestnut moray	eDNA
Mesophotic	*Gymnothorax polygonius*	Polygon moray	eDNA
Mesophotic	*Decodon puellaris*	Red hogfish	BRUVs
Mesophotic	*Halichoeres bathyphilus*	Greenband wrasse	BRUVs
Mesophotic	*Chromis cf. enchrysura*	Colbalt chromis	BRUVs
Mesophotic	*Chromis insolata*	Sunshinefish	BRUVs
Mesophotic	*Prognathodes aculeatus*	Longsnout butterflyfish	BRUVs
Reef	*Gymnothorax miliaris*	Goldentail moray	eDNA
Reef	*Gymnothorax moringa*	Spotted moray	BRUVs
Reef	*Gymnothorax vicinus*	Purplemouth moray	eDNA
Shallow reef	*Bathygobius curacao*	Notch-tongue goby	eDNA
Shallow reef	*Gerres cinereus*	Yellowfin mojarra	eDNA
Shallow reef	*Ulaema lefroyi*	Mottled mojarra	eDNA
Shallow reef	*Diplodus bermudensis*	Bermuda porgy	eDNA
Shallow reef	*Hemiramphus bermudensis*	Bermuda halfbeak	eDNA
Shallow reef	*Anchoa choerostoma*	Bermuda anchovy	eDNA
Shallow reef	*Hypoatherina harringtonensis*	Reef silverside	eDNA
Shallow reef	*Jenkinsia lamprotaenia*	Dwarf round herring	eDNA
Shallow reef	*Mugil curema*	White mullet	eDNA
Shallow reef	*Stegastes leucostictus*	Beaugregory	eDNA
Shallow reef	*Stegastes planifrons*	Threespot damselfish	eDNA

Understanding and accepting the benefits and limitations of eDNA metabarcoding and BRUVs was the primary reason for the combined use of the two methodologies and therefore increase capacity for characterising the mesophotic fish community at the 60 - 65 m depth zone. Whilst differences in taxa detections (Stat et al., 2019; Aglieri et al., 2020) were anticipated, which taxa responsible for these likely differences were unknown.

[5] Primary habitat has been deem determined based on species details on fishbase.org (Froese and Pauly, 2022) and Noyes' knowledge of Bermudan reef fish communities.

As previously discussed, all detected deep-sea species where unique to eDNA. Similarly, those species primarily associated with a pelagic habitat were almost exclusively detected by eDNA (Table 4.5). This result is supported by the differing associations the two methods have with respect to abiotic (eDNA) and biotic (BRUVs) variables (Figure 4.6). Interestingly and unexpectedly, most moray eel species were detected by eDNA and not BRUVs. A previous assessment of Bermudan mesophotic reefs utilising BRUVs and underwater visual census (UVC), morays were only detected by BRUVs (Goodbody-Gringley et al., 2019b). It could be anticipated that the presence of bait would act as an attractant for these species since bait presence has been determined to be biased towards carnivorous fishes (Stobart et al., 2007; Lowry et al., 2012). One possible explanation could be the presence of larger predators (i.e., sharks) within the vicinity of the site deterring morays from approaching the bait (Clementi et al., 2021). The use of alternative eDNA assays (e.g., Elas02 Taberlet et al., 2018) may increase elasmobranch detection and allow this theory to be tested. A final noteworthy distinction between the unique species detected by each method, of the 34 shallow water reef species detected, eDNA detected all but one (*Chaetodon ocellatus* Bloch 1787). Baited cameras observed four unique species highlighting the complementary benefits of utilising both methodologies.

4.5.2 Benefits of combined eDNA and BRUVs assessments

The combined use of eDNA and BRUVs assessments allows for an increased detection of target taxa (Kelly et al., 2017; Boussarie et al., 2018; Stat et al., 2019; Aglieri et al., 2020). In addition, the imagery generated by the BRUVs provided a secondary data stream that cannot be provided by eDNA, namely a way to quantify benthic habitat and provide a visual record of the status of that habitat. The importance of which has been demonstrated by the redundancy analysis of both the eDNA and BRUVs derived fish community data. In both cases, the explanatory variables accounted for ~ 50% of the variability within the respective fish community datasets. This study notes there were differing community associations between the fish community datasets and benthic predictors that were likely a facet of how the fish community datasets were obtained,

visual versus metabarcoding approach. Conceptually, eDNA has been subsampled on a 3D scale, i.e., water sampler (niskin) is open top and bottom allowing water entrance from all sides. BRUVs on the other hand, is 2D since the field of view is a fixed orientation for the duration of the survey. Therefore, taxa are observed within the context of the benthic habitat and will be mostly biased by species that swim into the field of view. Environmental DNA associations are likely to reflect a broader habitat association due to either the active and / or passive transport of extracellular DNA. Irrespective of the resolution of these associations, the combination of these datasets can enhance spatial ecology and conservation modelling capacity. A point that was highlighted by Aglieri et al. (2020) through the use of eDNA to simultaneously derive functional diversity on multiple habitats and suggest their application to observational data that has greater spatial resolution. Ultimately, this would increase the effectiveness of marine spatial planning initiatives.

A facet that has not been included in recent publications that utilised both methodologies (Boussarie et al., 2018; Stat et al., 2019; Aglieri et al., 2020) are the additional applications of these data that are not directly related to science. Whilst broader impacts are a ubiquitous requirement for research grants, they are often secondary to the science that is being conducted. BRUVs allow for multimedia friendly outreach material without additional costs or activities to the project and can result in novel behavioural observations that at of interest to multiple groups (Barley et al., 2016). As part of this study, short video clips with briefs on species were posted to various mainstream social media. A play on words with the title, “25 days of fishmas” enabled the broader communication of the visual findings of the project to the non-scientific community.

4.6 Conclusion

The biomonitoring assessment of the upper mesophotic, lower mesophotic interface with complementary methodologies has enabled a high-resolution evaluation of a depth zone established as a faunal break for mesophotic communities. The application of eDNA metabarcoding and BRUVs has enabled the detection of additional species to be considered as part of the community within this understudied ecosystem. Utilised in

conjunction, these methodologies improve detection performance for biomonitoring and allowed relationships between abiotic and biotic variables and the two methodologies to be explored to determine controls on mesophotic fish biodiversity. The relationships established by this study indicate BRUVs (benthic deployments) derived data will correlate with benthic metrics and eDNA datasets will align more with abiotic measurements associated physico-chemistry.

Baited cameras provided a 2-D permanent, cross-verifiable record for benthos and behavioural records. Similarly, eDNA sequences and remaining DNA extracts provide the opportunity for datamining for further biological information (Mariani et al., 2021b) and/or archiving ("biobanks") for comparison to future reference databases. Environmental DNA increased species and genus detection rate by 55% and 39% respectively by capturing a fluid and interactive 3-D water column. This study has demonstrated increased capacity of sampling effort through unique species detections by both methods and as a result, an additional 90 species are proposed to utilise mesophotic coral ecosystems increasing previous research findings of Bermuda's mesophotic ichthyofauna by 34% (Pinheiro et al., 2016; Goodbody-Gringley et al., 2019b; Stefanoudis et al., 2019a). Data additionally reconfirmed the presence of 93 species recorded in previous publications on Bermuda's MCEs (Goodbody-Gringley et al., 2019b; Stefanoudis et al., 2019; Appendix 1).

This study successfully generated data for a multi-seasonal and multi locational snapshot of biodiversity utilising complimentary methodologies, recording 182 species in total with ~ 80 % of these species known to occur throughout the upper mesophotic and shallow reef systems. Overall, the two collaborative methods employed in this study have recorded 38% of the total fish biodiversity for Bermuda published by (Smith-Vaniz et al., 1999; Smith-Vaniz and Collette, 2013) of which 38 species (Table 4.4) have either local or international commercial importance.

Geographical location in combination with species turnover between locations were major drivers of the fish community present at the upper mesophotic, lower mesophotic interface. However, species richness at each of the study locations was dominated by species (~ 80%) known to occur throughout the upper mesophotic and shallow reef system. Mesophotic fish species accounted for ~6% at each location. This infers a lack of a faunal break at the 60 m sites and suggest a high level of species

continuity with the adjacent shallower reef systems. These finding is important for effective marine spatial planning. For example, should the theoretical goal of Bermuda's marine managers be to protect the endemic *Chromis bermudae*, protection measures including the 60 – 65 m habitats would incidentally provide benefit to a large portion of the shallow reef fish species. Additionally, these measures would need to factor in geographical location and explicitly include the management of the invasive lionfish since the eDNA detections for this species was ubiquitous through this interface zone.

Future assessments that combine both eDNA metabarcoding and BRUVs will benefit from hydrological quantification (i.e., Acoustic Doppler Current Profilers; ADCPs) to allow for a greater interpretation of the advection of genetic material into the study region. In addition, the quantification of water velocity and direction will allow for greater determination of the variability of abiotic variables these communities experience. For example, temperature fluctuations of 1 – 3 degrees C over the course of 30 mins have been recorded on Caribbean mesophotic reefs (Bongaerts et al., 2015), whilst greater extremes have been documented in the Pacific (Wolanski et al., 2004; Colin, 2009; Colin and Lindfield, 2019).

The incorporation of an elasmobranch-specific metabarcoding assay (e.g., Elas02) would improve detection rates and aid the characterisation of shark and ray diversity (Mariani et al., 2021a) and potential migration patterns in and out of mesophotic reef system (Papastamatiou et al., 2015c; Shipley et al., 2017).

Further sampling of extended depth ranges (> 60 m) will determine the extend shallow water species depth ranges extend into mesophotic biomes. Finally, this study highlights the need for a more complete local ichthyofaunal genetic database to allow further refinement of spatial and temporal biodiversity patterns which will enable more effective marine spatial planning policy through an ecosystem-based approach.

4.7 References

Aglieri, G., Baillie, C., Mariani, S., Cattano, C., Calò, A., Turco, G., et al. (2020). Environmental DNA effectively captures functional diversity of coastal fish communities. *Mol Ecol*, 1–13. doi: 10.1111/mec.15661.

Baker, E. K., Puglise, K. A., and Harris, P. T. (2016). Mesophotic coral ecosystems - a lifeboat for coral reefs?

Baldwin, C. C., Tornabene, L., and Robertson, D. R. (2018). Below the Mesophotic. *Sci Rep* 8. doi: 10.1038/s41598-018-23067-1.

Barley, S. C., Mehta, R. S., Meeuwig, J. J., and Meekan, M. G. (2016). To knot or not? Novel feeding behaviours in moray eels. *Marine Biodiversity* 46, 703–705. doi: 10.1007/s12526-015-0404-y.

Baselga, A., and Orme, C. D. L. (2012). Betapart: An R package for the study of beta diversity. *Methods Ecol Evol* 3, 808–812. doi: 10.1111/j.2041-210X.2012.00224.x.

Bejarano, I., Appeldoorn, R. S., and Nemeth, M. (2014). Fishes associated with mesophotic coral ecosystems in La Parguera, Puerto Rico. *Coral Reefs* 33, 313–328. doi: 10.1007/s00338-014-1125-6.

Berry, O., Jarman, S., Bissett, A., Hope, M., Paeper, C., Bessey, C., et al. (2021). Making environmental DNA (eDNA) biodiversity records globally accessible. *Environmental DNA* 3, 699–705. doi: 10.1002/edn3.173.

Bohmann, K., Evans, A., Gilbert, M. T. P., Carvalho, G. R., Creer, S., Knapp, M., et al. (2014). Environmental DNA for wildlife biology and biodiversity monitoring. *Trends Ecol Evol* 29, 358–367. doi: 10.1016/j.tree.2014.04.003.

Bongaerts, P., Frade, P. R., Hay, K. B., Englebert, N., Latijnhouwers, K. R. W., Bak, R. P. M., et al. (2015). Deep down on a Caribbean reef: Lower mesophotic depths harbor a specialized coral-endosymbiont community. *Sci Rep* 5. doi: 10.1038/srep07652.

Boussarie, G., Bakker, J., Wangensteen, O. S., Mariani, S., Bonnin, L., Juhel, J. B., et al. (2018). Environmental DNA illuminates the dark diversity of sharks. *Sci Adv* 4. doi: 10.1126/sciadv.aap9661.

Butler, J. N., Bumett-Herkes, J., Barnes, J. A., and Ward, J. (1993). The bermuda fisheries a tragedy of the commons averted? *Environment* 35, 7–33. doi: 10.1080/00139157.1993.9929067.

Canals, O., Mendibil, I. I., Santos, M. M., Irigoien, X., Rodríguez-Ezpeleta, N., and Rodríguez-Ezpeleta, N. (2021). Vertical stratification of environmental DNA in the open ocean captures ecological patterns and behavior of deep-sea fishes. 6. doi: doi.org/10.1101/2021.02.10.430594.

Clementi, G. M., Bakker, J., Flowers, K. I., Postaire, B. D., Babcock, E. A., Bond, M. E., et al. (2021). Moray eels are more common on coral reefs subject to higher human pressure in the greater Caribbean. *iScience* 24. doi: 10.1016/j.isci.2021.102097.

Colin, P. L. (2009). *Marine environments of Palau*. San Diego: Indo-Pacific Press.

Colin, P. L., and Lindfield, S. J. (2019). “Palau,” in *Mesophotic Coral Ecosystems Coral Reefs of the World 12*, eds. Y. Loya, K. Puglise, and T. C. L. Bridge (Springer International Publishing), 285–320. doi: 10.1007/978-3-319-9275-0_16.

Collins, R. A., Wangensteen, O. S., O'Gorman, E. J., Mariani, S., Sims, D. W., and Genner, M. J. (2018). Persistence of environmental DNA in marine systems. *Commun Biol* 1, 185. doi: 10.1038/s42003-018-0192-6.

Deiner, K., Bik, H. M., Mächler, E., Seymour, M., Lacoursière-Roussel, A., Altermatt, F., et al. (2017). Environmental DNA metabarcoding: Transforming how we survey animal and plant communities. *Mol Ecol* 26, 5872–5895. doi: 10.1111/mec.14350.

Djurhuus, A., Closek, C. J., Kelly, R. P., Pitz, K. J., Michisaki, R. P., Starks, H. A., et al. (2020). Environmental DNA reveals seasonal shifts and potential interactions in a marine community. *Nat Commun* 11, 1–9. doi: 10.1038/s41467-019-14105-1.

Dorman, S. R., Harvey, E. S., and Newman, S. J. (2012). Bait effects in sampling coral reef fish assemblages with stereo-BRUVs. *PLoS One* 7, 1–12. doi: 10.1371/journal.pone.0041538.

Dray, A. S., Bauman, D., Blanchet, G., Borcard, D., Clappe, S., Guenard, G., et al. (2021). Package ' adespatial .' doi: 10.1890/11-1183.1>.Maintainer.

Dypvik, E., and Kaartvedt, S. (2013). Vertical migration and diel feeding periodicity of the skinnycheek lanternfish (Benthosema pterotum) in the Red Sea. *Deep Sea Res 1 Oceanogr Res Pap* 72, 9–16. doi: 10.1016/j.dsr.2012.10.012.

Eddy, C., Pitt, J., Morris, J. A., Smith, S., Goodbody-Gringley, G., and Bernal, D. (2016). Diet of invasive lionfish (Pterois volitans and P. miles) in Bermuda. *Mar Ecol Prog Ser* 558, 193–206. doi: 10.3354/meps11838.

Ely, T., Barber, P. H., Man, L., and Gold, Z. (2021). Short-lived detection of an introduced vertebrate eDNA signal in a nearshore rocky reef environment. *PLoS One* 16. doi: 10.1371/journal.pone.0245314.

Faiella, G. (2003). *Fishing in Bermuda*. Oxford: Macmillian Education.

Froese, R., and Pauly, D. (2022). FishBase. *World Wide Web electronic publication*. Available at: www.fishbase.org [Accessed March 20, 2004].

Fukunaga, A., Kosaki, R. K., Wagner, D., and Kane, C. (2016). Structure of mesophotic reef fish assemblages in the Northwestern Hawaiian Islands. *PLoS One* 11. doi: 10.1371/journal.pone.0157861.

Gargan, L. M., Morato, T., Pham, C. K., Finarelli, J. A., Carlsson, J. E. L., and Carlsson, J. (2017). Development of a sensitive detection method to survey pelagic biodiversity using eDNA and quantitative PCR: a case study of devil ray at seamounts. *Mar Biol* 164. doi: 10.1007/s00227-017-3141-x.

Gold, Z., Sprague, J., Kushner, D. J., Zerecero, E., and Barber, P. H. (2020). eDNA metabarcoding as a biomonitoring tool for marine protected areas. *bioRxiv preprint* 258889, 1–34. doi: 10.1101/2020.08.20.258889.

Goodbody-Gringley, G., Eddy, C., Pitt, J. M., Chequer, A. D., and Smith, S. R. (2019a). Ecological Drivers of Invasive Lionfish (Pterois volitans and Pterois miles) Distribution Across Mesophotic Reefs in Bermuda. *Front Mar Sci* 6, 1–12. doi: 10.3389/fmars.2019.00258.

Goodbody-Gringley, G., Noyes, T., and Smith, S. R. (2019b). "Bermuda," in *Mesophotic Coral Ecosystems, Coral Reefs of the World 12*, eds. L. Yossi, K. A. Puglise, and T. Bridge (Springer International Publishing), 31–45. doi: 10.1007/978-3-319-92735-0_2.

Harvey, E. S., Cappo, M., Butler, J. J., Hall, N., and Kendrick, G. A. (2007). Bait attraction affects the performance of remote underwater video stations in assessment of

demersal fish community structure. *Mar Ecol Prog Ser* 350, 245–254. doi: 10.3354/meps07192.

Hsieh, T. C., Ma, K. H., and Chao, A. (2016). iNEXT: an R package for rarefaction and extrapolation of species diversity (Hill numbers). *Methods Ecol Evol* 7, 1451–1456. doi: 10.1111/2041-210X.12613.

Jarman, S. N., Berry, O., and Bunce, M. (2018). The value of environmental DNA biobanking for long-term biomonitoring. *Nat Ecol Evol* 2, 1192–1193. doi: 10.1038/s41559-018-0614-3.

Kelly, R. P., Closek, C. J., O'Donnell, J. L., Kralj, J. E., Shelton, A. O., and Samhouri, J. F. (2017). Genetic and manual survey methods yield different and complementary views of an ecosystem. *Front Mar Sci* 3, 1–11. doi: 10.3389/FMARS.2016.00283.

Kelly, R. P., O'Donnell, J. L., Lowell, N. C., Shelton, A. O., Samhouri, J. F., Hennessey, S. M., et al. (2016). Genetic signatures of ecological diversity along an urbanization gradient. *PeerJ* 2016. doi: 10.7717/peerj.2444.

Kelly, R. P., Port, J. A., Yamahara, K. M., and Crowder, L. B. (2014). Using environmental DNA to census marine fishes in a large mesocosm. *PLoS One* 9. doi: 10.1371/journal.pone.0086175.

Legendre, P., and Gallagher, E. D. (2001). Ecologically meaningful transformations for ordination of species data. *Oecologia* 129, 271–280. doi: 10.1007/s004420100716.

Lesser, M. P., Slattery, M., Laverick, J. H., Macartney, K. J., and Bridge, T. C. (2019). Global community breaks at 60 m on mesophotic coral reefs. *Global Ecology and Biogeography* 28, 1403–1416. doi: 10.1111/geb.12940.

Lowry, M., Folpp, H., Gregson, M., and Suthers, I. (2012). Comparison of baited remote underwater video (BRUV) and underwater visual census (UVC) for assessment of artificial reefs in estuaries. *J Exp Mar Biol Ecol* 416–417, 243–253. doi: 10.1016/j.jembe.2012.01.013.

Mariani, S., Fernandez, C., Baillie, C., Magalon, H., and Jaquemet, S. (2021a). Shark and ray diversity, abundance and temporal variation around an Indian Ocean Island, inferred by eDNA metabarcoding. *Conserv Sci Pract* 3, 1–10. doi: 10.1111/csp2.407.

Mariani, S., Harper, L. R., Collins, R. A., Baillie, C., Wangensteen, O. S., McDevitt, A. D., et al. (2021b). Estuarine molecular bycatch as a landscape-wide biomonitoring tool. *Biol Conserv* 261, 109287. doi: 10.1016/j.biocon.2021.109287.

Miya, M., Gotoh, R. O., and Sado, T. (2020). *MiFish metabarcoding: a high-throughput approach for simultaneous detection of multiple fish species from environmental DNA and other samples*. Springer Japan doi: 10.1007/s12562-020-01461-x.

Miya, M., Sato, Y., Fukunaga, T., Sado, T., Poulsen, J. Y., Sato, K., et al. (2015). MiFish, a set of universal PCR primers for metabarcoding environmental DNA from fishes: detection of more than 230 subtropical marine species. *R Soc Open Sci* 2, 150088. doi: 10.1098/rsos.150088.

Murakami, H., Yoon, S., Kasai, A., Minamoto, T., Yamamoto, S., Sakata, M. K., et al. (2019). Dispersion and degradation of environmental DNA from caged fish in a marine environment. *Fisheries Science* 85, 327–337. doi: 10.1007/s12562-018-1282-6.

Oksanen, A. J., Blanchet, F. G., Friendly, M., Kindt, R., Legendre, P., Mcglinn, D., et al. (2019). Vegan. *Encyclopedia of Food and Agricultural Ethics*, 2395–2396. doi: 10.1007/978-94-024-1179-9_301576.

Page, H. N., Andersson, A. J., Jokiel, P. L., Rodgers, K. S., Lebrato, M., Yeakel, K., et al. (2016). Differential modification of seawater carbonate chemistry by major coral reef benthic communities. *Coral Reefs* 35, 1311–1325. doi: 10.1007/s00338-016-1490-4.

Papastamatiou, Y. P., Meyer, C. G., Kosaki, R. K., Wallsgrove, N. J., and Popp, B. N. (2015a). Movements and foraging of predators associated with mesophotic coral reefs and their potential for linking ecological habitats. *Mar Ecol Prog Ser* 521, 155–170. doi: 10.3354/meps11110.

Papastamatiou, Y. P., Meyer, C. G., Kosaki, R. K., Wallsgrove, N. J., and Popp, B. N. (2015b). Movements and foraging of predators associated with mesophotic coral reefs and their potential for linking ecological habitats. *Mar Ecol Prog Ser* 521, 155–170. doi: 10.3354/meps11110.

Pinheiro, H. T., Goodbody-Gringley, G., Jessup, M. E., Shepherd, B., Chequer, A. D., and Rocha, L. A. (2016). Upper and lower mesophotic coral reef fish communities evaluated by underwater visual censuses in two Caribbean locations. *Coral Reefs* 35, 139–151. doi: 10.1007/s00338-015-1381-0.

Port, J. A., O'Donnell, J. L., Romero-Maraccini, O. C., Leary, P. R., Litvin, S. Y., Nickols, K. J., et al. (2016). Assessing vertebrate biodiversity in a kelp forest ecosystem using environmental DNA. *Mol Ecol* 25, 527–541. doi: 10.1111/mec.13481.

Pyle, R. L., Boland, R., Bolick, H., Bowen, B. W., Bradley, C. J., Kane, C., et al. (2016). A comprehensive investigation of mesophotic coral ecosystems in the Hawaiian Archipelago. *PeerJ* 4, e2475. doi: 10.7717/peerj.2475.

R Core Team (2019). R: A language and environment for statistical computing.

Rosa, M. R., Alves, A. C., Medeiros, D. V., Coni, E. O. C., Ferreira, C. M., Ferreira, B. P., et al. (2016). Mesophotic reef fish assemblages of the remote St. Peter and St. Paul's Archipelago, Mid-Atlantic Ridge, Brazil. *Coral Reefs* 35, 113–123. doi: 10.1007/s00338-015-1368-x.

Santana-Garcon, J., Newman, S. J., and Harvey, E. S. (2014). Development and validation of a mid-water baited stereo-video technique for investigating pelagic fish assemblages. *J Exp Mar Biol Ecol* 452, 82–90. doi: 10.1016/j.jembe.2013.12.009.

Schobernd, Z. H., Bacheler, N. M., and Conn, P. B. (2014). Examining the utility of alternative video monitoring metrics for indexing reef fish abundance. *Canadian Journal of Fisheries and Aquatic Sciences* 71, 464–471. doi: 10.1139/cjfas-2013-0086.

Shipley, O. N., Howey, L. A., Tolentino, E. R., Jordan, L. K. B., Ruppert, J. L. W., and Brooks, E. J. (2017). Horizontal and vertical movements of Caribbean reef sharks (Carcharhinus perezi): Conservation implications of limited migration in a marine sanctuary. *R Soc Open Sci* 4. doi: 10.1098/rsos.160611.

Smith-Vaniz, W., and Collette, B. (2013). Fishes of Bermuda. *Smith-Vaniz, William and Collette, Bruce B.* 19, 165.

Smith-Vaniz, W. F., Collette, B. B., and Luckhurst, B. E. (1999). *Fishes of Bermuda: history, zoogeography,annotated checklist, and identification keys*. American Society of Ichthyologists and Herpetologists.

Stat, M., Huggett, M. J., Bernasconi, R., Dibattista, J. D., Berry, T. E., Newman, S. J., et al. (2017). Ecosystem biomonitoring with eDNA: Metabarcoding across the tree of life in a tropical marine environment. *Sci Rep* 7, 1–11. doi: 10.1038/s41598-017-12501-5.

Stat, M., John, J., DiBattista, J. D., Newman, S. J., Bunce, M., and Harvey, E. S. (2019). Combined use of eDNA metabarcoding and video surveillance for the assessment of fish biodiversity. *Conservation Biology* 33, 196–205. doi: 10.1111/cobi.13183.

Stefanoudis, P. V., Gress, E., Pitt, J. M., Smith, S. R., Kincaid, T., Rivers, M., et al. (2019). Depth-dependent structuring of reef fish assemblages from the shallows to the rariphotic zone. *Front Mar Sci* 6, 1–16. doi: 10.3389/fmars.2019.00307.

Stobart, B., García-Charton, J. A., Espejo, C., Rochel, E., Goñi, R., Reñones, O., et al. (2007). A baited underwater video technique to assess shallow-water Mediterranean fish assemblages: Methodological evaluation. *J Exp Mar Biol Ecol* 345, 158–174. doi: 10.1016/j.jembe.2007.02.009.

Taberlet, P., Bonin, A., Zinger, L., and Coissac, E. (2018). *Environmental DNA: For Biodiversity Research and Monitoring*. Oxford University Press doi: 10.1093/oso/9780198767220.001.0001.

Thomsen, P. F., and Willerslev, E. (2015). Environmental DNA - An emerging tool in conservation for monitoring past and present biodiversity. *Biol Conserv* 183, 4–18. doi: 10.1016/j.biocon.2014.11.019.

Thomsen, P., Kielgast, J., Iversen, L., Møller, P., Rasmussen, M., and Willerslev, E. (2012). Detection of a Diverse Marine Fish Fauna Using Environmental DNA from Seawater Samples. *PLoS One* 7, 1–9. doi: 10.1371/journal.pone.0041732.

Weltz, K., Lyle, J. M., Ovenden, J., Morgan, J. A. T., Moreno, D. A., and Semmens, J. M. (2017). Application of environmental DNA to detect an endangered marine skate species in the wild. *PLoS One* 12, 1–16. doi: 10.1371/journal.pone.0178124.

Whitmarsh, S. K., Fairweather, P. G., and Huveneers, C. (2017). What is Big BRUVver up to? Methods and uses of baited underwater video. *Rev Fish Biol Fish* 27, 53–73. doi: 10.1007/s11160-016-9450-1.

Wilson, S. K., Graham, N. A. J., and Polunin, N. V. C. (2007). Appraisal of visual assessments of habitat complexity and benthic composition on coral reefs. *Mar Biol* 151, 1069–1076. doi: 10.1007/s00227-006-0538-3.

Wolanski, E., Colin, P., Naithani, J., Deleersnijder, E., and Golbuu, Y. (2004). Large amplitude, leaky, island-generated, internal waves around Palau, Micronesia. *Estuar Coast Shelf Sci* 60, 705–716. doi: 10.1016/j.ecss.2004.03.009.

Yamamoto, S., Masuda, R., Sato, Y., Sado, T., Araki, H., Kondoh, M., et al. (2017). Environmental DNA metabarcoding reveals local fish communities in a species-rich coastal sea. *Sci Rep* 7. doi: 10.1038/srep40368.

Yao, M., Zhang, S., Lu, Q., Chen, X., Zhang, S. Y., Kong, Y., et al. (2022). Fishing for fish environmental DNA: Ecological applications, methodological considerations, surveying designs, and ways forward. *Mol Ecol*, 5132–5164. doi: 10.1111/mec.16659.

Chapter 5. General Discussion

The novel findings of the research outlined in this thesis represent the first of their kind for Mesophotic Coral Ecosystems (MCEs). The mesophotic zone surrounding Bermuda covers 76 km^2 which equates to 8% of habitats > 30 m (908 km^2). The study sought to address the data disparity on MCEs and establish practical methodologies for comprehensive monitoring regimes to ensure effective management practices and maintenance of ecosystem health (Hoegh-Guldberg et al., 2017; Turner et al., 2017). Three mesophotic reef locations were monitored between August 2017 - October 2018 and September – October 2020 to contribute invaluable data to knowledge gaps in the understanding of the ecosystem functions of biogeochemical cycling, biogeographic patterns of taxa (Slattery et al., 2011; Turner et al., 2019; Eyal and Pinheiro, 2020) and the level of connectivity between mesophotic and shallow reefs fish communities for Bermuda.

The major goals of this this study were to (1) establish the biogeochemical status (accretion or dissolution and autotrophic or heterotrophic) of mesophotic reefs at these locations (2) assess ichthyofauna biodiversity across a mesophotic depth gradient utilising eDNA metabarcoding (3) explicitly characterise fish biodiversity at a depth determined to be the upper / lower mesophotic interface (faunal break) in other mesophotic regions, using complementary assessment methodologies of eDNA metabarcoding and Baited Remote Underwater Video systems (BRUVs).

This study has established the overall status of the mesophotic ecosystem through the first known measurements of net ecosystem calcification (accretion vs. dissolution) and net ecosystem production (autotrophy vs. heterotrophy) using the widely accepted alkalinity anomaly-water residence time technique. This was achieved over an 18-month time frame through biogeochemical monitoring across a depth gradient (30 – 60 m).

Measurements determined that MCEs exhibit seasonal changes in biogeochemical processes (i.e., the balance of photosynthesis, respiration, calcification, and $CaCO_3$ dissolution). Overall, seawater chemistry was chemically conducive for calcification (mean $\Omega_{aragonite}$ = 3.58, mean $\Omega_{calcite}$ = 5.44), however, these systems are near the threshold for a transition from coral reef to non-coral reef community ($\Omega_{aragonite}$ =

3.4) and at the global limit for reef development ($\Omega_{aragonite}$ = 3.0 - 3.5; Figure 2.2). Mesophotic reefs demonstrated biogeochemical interannual variability through strong periods of calcification in the late summer with a clear switch from heterotrophy to autotrophy (Figure 2.3, Table 2.3). The peak calcification period for all three depth ranges (30 m, 40 m, and 60 m) occurred in September and October followed by a period of equilibrium and or dissolution in the winter months. This switch between net accretion and net dissolution has been documented on a seasonal basis for Bermuda's shallow reefs (Yeakel et al., 2015; Muehllehner et al., 2016; Bates, 2017; Cyronak et al., 2018), but since these are the first known measurements for MCEs, direct comparisons with other mesophotic systems are not possible.

Seasonal feedback between components of shallow reef ecosystems and $CaCO_3$ and calcification rate suppression has been demonstrated by Bates et al. (2010) and hypothesised as the Carbonate Chemistry Coral Reef Ecosystem Feedback hypothesis (CREF). Moving in a seaward direction, shallow mesophotic sites (~30 m depth) are dominated by hermatypic scleractinian corals whilst deeper sites exhibit greater benthic heterogeneity as macroalgae (Stefanoudis et al., 2019b) and rhodolith beds become more dominant. Due to the relative lack of scleractinian corals on MCEs, a significant contribution to Net Ecosystem Calcification may be derived from encrusting crustose coralline algae (CCA) and rhodoliths. Rhodoliths and CCA perform valuable ecosystem services of substrate provision through calcification and their contribution to NEC may have been previously underestimated in other studies.

Given that biological carbonates are the largest carbon reservoirs in the biosphere (i.e., aragonite, calcite, and magnesian calcite; (Cohen, 2003), to truly comprehend the level of resilience mesophotic coral reef systems have to anthropogenic and natural stressors, understanding the interactions and feedbacks that drive these biogeochemical processes (e.g., calcification rates, thermal regimes, flow dynamics) are fundamental. This study supports the concept that mesophotic reefs, at least for Bermuda, are a "connective boundary layer" between the open ocean and shallow reefs with episodic advection of biomass, that occurs during negative winter North Atlantic Oscillation (NAO) events. This study has generated critical biogeochemical measurements for MCEs by establishing that mesophotic seawater chemistry is chemically conducive for calcification

(Figure 2.2m-o) and these systems are in a state of net calcification Figure 2.3a,c,e). This trend mirrors the seasonal documented biogeochemical shifts observed on the shallow water reef systems of Bermuda (Bates, 2017) with one significant difference, this study estimated the overall status of the mesophotic system to be net autotrophic which is the opposite of the trophic evaluation for Bermuda shallow reefs (net heterotrophic). These findings present an interesting conundrum since shallow water reefs would be predicted to derive carbon by way of the inorganic carbon cycle (i.e., photosynthesis) due to greater levels of surface irradiance. However, as discussed in Chapter 2, there are energetic benefits when zooxanthellate corals utilise both inorganic and organic carbon sources (photosynthesis + respiration). It does raise the question about the exact composition of the primary calcifiers at mesophotic depths and if we truly are "taking the metabolic pulse" of these communities (Cyronak et al., 2018). Reef fishes are intrinsically linked to the biogeochemical status of reef systems not least through the production and excretion of $CaCO_3$ as an osmoregulatory product due to the constant swallowing of seawater (Wilson et al., 2009) in addition to the provision of 3D complexity, carbon derived energy pathways and oxygen availability (Kavanagh and Galbraith, 2018).

This study represents the first application of eDNA metabarcoding on Bermudan mesophotic reefs and only the second known application globally (Muff et al., 2022). Through the application of a 12S fish-targeted assay (MiFish), this study has been able to detect both spatial and temporal fish biodiversity variability across a mesophotic depth gradient (1 – 130 m) and provide a comprehensive view of the fish assemblages found within these ecosystems. Representative taxa from shallow reef, mesophotic and oceanic environments were detected at all three study locations (Figure 3.6 & 3.7). An early assumption for mesophotic communities was one of a holistic system that provided refuge to fish and benthic species (Glynn, 1996; Bongaerts et al., 2010). The determination of distinct faunal breaks (Rocha et al., 2018; Lesser et al., 2019; Pinheiro et al., 2019; Tamir et al., 2019) has led to an alternative view, one that now considers mesophotic communities as taxonomically distinct. The findings of this study, supports earlier assumptions of MCEs as unified systems. The detection of species overlaps between mesophotic and shallow reef fish communities does not conform to the notion of a faunal

break with taxonomically distinct zones as previously described (Rocha et al., 2018; Lesser et al., 2019; Pinheiro et al., 2019; Tamir et al., 2019).

Despite the seasonal influence and species turnover between locations, there were limited changes in community structure when trophic guilds were partitioned by depth (1 m to 130m). Results indicate that these findings were unlikely due to the vertical advection of genetic material from shallow reefs into mesophotic reefs (Figure. 3.8) and act as further evidence against taxonomic compartmentalisation across the depth ranges. These results are not consistent with previous Caribbean studies (Bejarano et al., 2014; Andradi-Brown et al., 2016a) which generally demonstrated a decrease in species richness with depth, specifically herbivorous fishes. Previous studies on Bermudan mesophotic fishes (Pinheiro et al., 2016; Goodbody-Gringley et al., 2019b) have highlighted differences in fish community composition across depth gradients. This was not the conclusion for this study, results from eDNA metabarcoding aligned with the concept of the "Deep Reef Refuge Hypothesis" proposed by Bongaerts et al. (2010, 2017) in that detected mesophotic species have the potential to act as a refuge for shallow water species. In addition, this study determined that the study region shared a communality of species both spatially and temporally supporting the notion that the Bermudan upper mesophotic should be considered as an extension of shallow water coral reef ecosystems based on their representative fish fauna.

The application of eDNA metabarcoding to Bermuda's mesophotic fish community, has demonstrated the intrinsic value of this approach (e.g., greater taxa detection, similar communities across depth gradient) a therefore promote its rapid integration into existing biomonitoring programs (e.g., using indicator species as measures of ecosystem status and measures of environmental change, invasive species management, marine spatial planning). Not only are these ecosystems linked through a similarity of species composition but they are also connected biogeochemically.

The final component of this thesis explicitly investigated the 60 m depth zone of Bermuda's mesophotic reefs through the application of eDNA metabarcoding and baited remote underwater video systems (BRUVs). The ~ 60 – 65 m depth zone represents a potential interface between the upper mesophotic and lower mesophotic zones and is a known faunal break for fish communities in other mesophotic regions (Bejarano et al.,

2014; Fukunaga et al., 2016; Page et al., 2016; Pinheiro et al., 2016; Pyle et al., 2016; Rosa et al., 2016; Baldwin et al., 2018; Lesser et al., 2019). The study is the first known application of eDNA metabarcoding and BRUVs to investigate mesophotic fish biodiversity in addition to the depth specific investigation of the upper/lower mesophotic interface.

The study has increased the capacity of sampling effort and successfully generated data for a multi-seasonal and multi-locational snapshot of fish biodiversity utilising complimentary methodologies. The study recorded a total of 182 species of which 90 where unique detections by this investigation when compared to previous studies of Bermuda's mesophotic fish communities (Pinheiro et al., 2016; Goodbody-Gringley et al., 2019b, 2019a; Stefanoudis et al., 2019b, 2019a). Of these detections, 38 species were commercially important (Table 4.4) and a further 15 species were of mesopelagic and bathypelagic origin (Table 4.3). Overall, the two collaborative methods recorded 38% of the total fish biodiversity for Bermuda (Smith-Vaniz et al., 1999; Smith-Vaniz and Collette, 2013). Additionally, this study proposed two additional specialist species *Prognathodes aculeatus* (Poey 1860) and *Serranus annularis* (Poey 1860) to the mesophotic specific taxa. It should be noted that both these species where only detected using BRUVs observations.

Whilst there was a high degree of species overlap between shallow reefs and the upper mesophotic, there were community differences observed between locations by BRUVs which were driven by observations of roving herbivores e.g., scarids. Trends identified by this study can be applied to the wider Bermudan mesophotic / lower mesophotic interface whilst measurements of α- and β-diversity serve as a critical measure for future biodiversity surveys of this transitional interface.

Utilised in conjunction, these methodologies improve detection performance and allow the opportunity for data exploration of how abiotic and biotic parameters may be driving biodiversity within locations. The study determined that environmental DNA detected community data exhibiting stronger associations with abiotic variables, whereas the BRUVs detected community associated more with the biotic variables. The different associations would be anticipated since eDNA samples are from a fluid environment that contain a "soup" of eDNA material from the surrounding area whereas visual

methodologies (i.e., BRUVs) are strictly linked to observations that in this case, would be bias towards benthic associated species (Figure 4.6).

Baited camera observations provide a 2-D permanent, cross-verifiable record for benthos diversity and species behavioural records, while eDNA increased species and genus detection rate by 55% and 39% respectively by capturing a fluid and interactive 3-D water column. Environmental DNA additionally provide a permanent record of sequences. In a similar fashion to genetic database repositories, these sequences could be deposited into a “biobank” (Jarman et al., 2018; Berry et al., 2021). Existing sequences could then be datamined, whilst DNA extracts could be amplified with either optimised assays (e.g., Tele02) or alternative assays that target different taxa and/or markers.

This study concluded that geographical location in combination with species turnover between locations were major drivers of the fish community present at the upper mesophotic, lower mesophotic interface. At each location, the species richness of these communities was dominated by species (~ 80%) known to occur throughout the upper mesophotic and shallow reef system. Species richness for mesophotic species accounted for ~6% at each location. These findings conclude there is a lack of a faunal break at Bermudan 60 m mesophotic sites and suggest a high level of species continuity with the adjacent shallower reef systems.

The findings of this 60 m depth investigation, agree with previous findings of Bermuda mesophotic fish communities (Pinheiro et al., 2016), that determined a high degree of turnover was documented below the 60 m upper / lower mesophotic interface between 70 – 90 m (i.e., below the interface investigated by this thesis). The presence of shallow-water species adds weight to the hypothesis of “matching habitat choice” (Edelaar et al., 2008; Pinheiro et al., 2016), whereby species adaptions allow them to recruit to alternative habitats often due to limited primary habitat space (i.e., shallow reef systems).

Whilst there was commonality of taxa detections between eDNA and BRUVs, both contributed unique detections to the overall dataset. The study highlights the complimentary nature of the two methodologies thus allowing for a greater accuracy of biodiversity assessments. Environmental DNA detections are likely to reflect a broader habitat association due to either the active and / or passive transport of extracellular DNA.

The successful collection of eDNA sequences enabled the determination of species diversity and community structure over different spatial and temporary timescales (Thomsen and Willerslev, 2015), environmental gradients (Kelly et al., 2016) and detected cryptic and elusive species (Baker et al., 2016a; Gargan et al., 2017; Boussarie et al., 2018) such as depth specialist *Chromis* sp. Whereas, BRUVs provided relative abundance, benthic community metrics and a permanent visual record. The combination of these eDNA and BRUVs datasets will enable the enhancement of spatial ecology and conservation modelling efforts for MCEs in Bermuda (e.g., Bermuda Ocean Prosperity Programme).

5.1 Overall Conclusion

The overarching goal of this thesis was to establish the biogeochemical status of Bermudan mesophotic coral ecosystems (MCEs) and provide a comprehensive understanding of the ichthyofaunal biodiversity that utilise these ecosystems. The complementary use of eDNA metabarcoding and BRUVs produced a more “complete” biodiversity assessment of ichthyofauna as demonstrated by the detections of species unique to each methodology.

This study determined that mesophotic biogeochemical processes display annual variability that follow similar patterns to interannual trends documented for the adjacent shallow reef system (Yeakel et al., 2015; Bates, 2017). The mean Net Ecosystem Calcification (NEC) for the collective mesophotic reef system and individual reef depths investigated were positive and therefore indicative of net calcification (Figure 2.3a,c,e). All three depth ranges (30 m, 40 m, and 60 m) exhibited a seasonal trophic switch between autotrophy and heterotrophy. However, in contrast to the established net heterotrophic trend for the adjacent shallow reefs (Bates, 2017), the overall status of the mesophotic system was net autotrophic.

With respect to fish communities, the findings of the study suggest Bermuda’s MCEs could serve as a potential refuge for shallow water species as demonstrated by the shared commonality of species measured across the depth gradient. However, communities exhibit geographical variability and are driven by species turnover.

Bermuda's unique biogeographical characteristics (Stefanoudis et al., 2019a) i.e., high latitude tropical coral reefs isolated from the wider Caribbean, could enable species to exhibit plasticity within depth ranges leading to a greater level of species overlap between the upper mesophotic and shallow reef counterparts (Pinheiro et al., 2016). Environmental DNA produced valid detections of mesopelagic fish species however, it was beyond the scope of the study to be able to determine if these species utilise mesophotic ecosystems or detection was a result of eDNA advection and the detection ability of the metabarcoding approach.

Future assessments will greatly benefit from the inclusion of hydrological quantification (i.e., Acoustic Doppler Current Profilers; ADCPs) coupled with eDNA metabarcoding and BRUVs which will allow for a greater interpretation of the advection of genetic material into the study region. Additionally, biogeochemistry measurements with be further enhanced by the incorporation of hydrological data. The status of the North Atlantic Oscillation (NAO) was determined to have the greatest influence on site level species diversity and warrants further study. Negative NAO winter events have been linked to short-term increases in shallow water reef calcification and zooplankton abundance, moving the system into a net heterotrophic status and as such influence fish biodiversity. The quantification of water movement by ADCP measurements will assist in determining the level of advection of biological material and open ocean water (i.e., different biogeochemical properties) onto mesophotic reefs. Finally, the incorporation of elasmobranch-specific assays (e.g., Elas02) would greatly improve detection rates and aid the characterise of shark and ray biogeographical patterns of a class of taxa that was potentially underrepresented by both methodologies.

The findings presented in this study represent the first of their kind for determining the biogeochemical status of mesophotic reefs. In addition, the detection of the spatial and temporal variability of mesophotic ichthyofaunal biodiversity, demonstrate the power of utilising a multiple detection approach. Overall, this study derived fish biodiversity patterns that will enable more effective marine resource management.

5.2 References

Andradi-Brown, D. A., Gress, E., Wright, G., Exton, D. A., and Rogers, A. D. (2016). Reef fish community biomass and trophic structure changes across shallow to upper-Mesophotic reefs in the mesoamerican barrier reef, Caribbean. *PLoS One* 11. doi: 10.1371/journal.pone.0156641.

Baker, E. K., Puglise, K. A., and Harris, P. T. (2016). Mesophotic coral ecosystems - a lifeboat for coral reefs?

Baldwin, C. C., Tornabene, L., and Robertson, D. R. (2018). Below the Mesophotic. *Sci Rep* 8. doi: 10.1038/s41598-018-23067-1.

Bates, N. R. (2017). Twenty years of marine carbon cycle observations at Devils Hole Bermuda provide insights into seasonal hypoxia, coral reef calcification, and ocean acidification. *Front Mar Sci* 4, 1–23. doi: 10.3389/fmars.2017.00036.

Bejarano, I., Appeldoorn, R. S., and Nemeth, M. (2014). Fishes associated with mesophotic coral ecosystems in La Parguera, Puerto Rico. *Coral Reefs* 33, 313–328. doi: 10.1007/s00338-014-1125-6.

Berry, O., Jarman, S., Bissett, A., Hope, M., Paeper, C., Bessey, C., et al. (2021). Making environmental DNA (eDNA) biodiversity records globally accessible. *Environmental DNA* 3, 699–705. doi: 10.1002/edn3.173.

Bongaerts, P., Ridgway, T., Sampayo, E. M., and Hoegh-Guldberg, O. (2010). Assessing the “deep reef refugia” hypothesis: Focus on Caribbean reefs. *Coral Reefs* 29, 1–19. doi: 10.1007/s00338-009-0581-x.

Boussarie, G., Bakker, J., Wangensteen, O. S., Mariani, S., Bonnin, L., Juhel, J. B., et al. (2018). Environmental DNA illuminates the dark diversity of sharks. *Sci Adv* 4. doi: 10.1126/sciadv.aap9661.

Cohen, A. (2003). Geochemical Perspectives on Coral Mineralization. *Rev Mineral Geochem* 54, 151–187. doi: 10.2113/0540151.

Cyronak, T., Andersson, A. J., Langdon, C., Albright, R., Bates, N. R., Caldeira, K., et al. (2018). Taking the metabolic pulse of the world’s coral reefs. *PLoS One* 13. doi: 10.1371/journal.pone.0190872.

Edelaar, P., Siepielski, A. M., and Clobert, J. (2008). Matching habitat choice causes directed gene flow: A neglected dimension in evolution and ecology. *Evolution (N Y)* 62, 2462–2472. doi: 10.1111/j.1558-5646.2008.00459.x.

Eyal, G., and Pinheiro, H. T. (2020). Mesophotic ecosystems: The link between shallow and deep-sea habitats. *Diversity (Basel)* 12, 1–4. doi: 10.3390/d12110411.

Fukunaga, A., Kosaki, R. K., Wagner, D., and Kane, C. (2016). Structure of mesophotic reef fish assemblages in the Northwestern Hawaiian Islands. *PLoS One* 11. doi: 10.1371/journal.pone.0157861.

Gargan, L. M., Morato, T., Pham, C. K., Finarelli, J. A., Carlsson, J. E. L., and Carlsson, J. (2017). Development of a sensitive detection method to survey pelagic biodiversity using eDNA and quantitative PCR: a case study of devil ray at seamounts. *Mar Biol* 164. doi: 10.1007/s00227-017-3141-x.

Glynn, P. W. (1996). Coral reef bleaching: Facts, hypotheses and implications. *Glob Chang Biol* 2, 495–509. doi: 10.1111/j.1365-2486.1996.tb00063.x.

Goodbody-Gringley, G., Eddy, C., Pitt, J. M., Chequer, A. D., and Smith, S. R. (2019a). Ecological Drivers of Invasive Lionfish (Pterois volitans and Pterois miles) Distribution Across Mesophotic Reefs in Bermuda. *Front Mar Sci* 6, 1–12. doi: 10.3389/fmars.2019.00258.

Goodbody-Gringley, G., Noyes, T., and Smith, S. R. (2019b). "Bermuda," in *Mesophotic Coral Ecosystems, Coral Reefs of the World 12*, eds. L. Yossi, K. A. Puglise, and T. Bridge (Springer International Publishing), 31–45. doi: 10.1007/978-3-319-92735-0_2.

Hoegh-Guldberg, O., Poloczanska, E. S., Skirving, W., and Dove, S. (2017). Coral reef ecosystems under climate change and ocean acidification. *Front Mar Sci* 4. doi: 10.3389/fmars.2017.00158.

Jarman, S. N., Berry, O., and Bunce, M. (2018). The value of environmental DNA biobanking for long-term biomonitoring. *Nat Ecol Evol* 2, 1192–1193. doi: 10.1038/s41559-018-0614-3.

Kavanagh, L., and Galbraith, E. (2018). Links between fish abundance and ocean biogeochemistry as recorded in marine sediments. *PLoS One* 13, 1–22. doi: 10.1371/journal.pone.0199420.

Kelly, R. P., O'Donnell, J. L., Lowell, N. C., Shelton, A. O., Samhouri, J. F., Hennessey, S. M., et al. (2016). Genetic signatures of ecological diversity along an urbanization gradient. *PeerJ* 2016. doi: 10.7717/peerj.2444.

Lesser, M. P., Slattery, M., Laverick, J. H., Macartney, K. J., and Bridge, T. C. (2019). Global community breaks at 60 m on mesophotic coral reefs. *Global Ecology and Biogeography* 28, 1403–1416. doi: 10.1111/geb.12940.

Muehllehner, N., Langdon, C., Venti, A., and Kadko, D. (2016). Dynamics of carbonate chemistry, production, and calcification of the Florida Reef Tract (2009–2010): Evidence for seasonal dissolution. *AGU Publications* 30, 661–688. doi: 10.1002/2015GB005327.Received.

Muff, M., Jaquier, M., Marques, V., Ballesta, L., Deter, J., Bockel, T., et al. (2022). Environmental DNA highlights fish biodiversity in mesophotic ecosystems. *Environmental DNA*, 1–17. doi: 10.1002/edn3.358.

Page, H. N., Andersson, A. J., Jokiel, P. L., Rodgers, K. S., Lebrato, M., Yeakel, K., et al. (2016). Differential modification of seawater carbonate chemistry by major coral reef benthic communities. *Coral Reefs* 35, 1311–1325. doi: 10.1007/s00338-016-1490-4.

Pinheiro, H. T., Goodbody-Gringley, G., Jessup, M. E., Shepherd, B., Chequer, A. D., and Rocha, L. A. (2016). Upper and lower mesophotic coral reef fish communities evaluated by underwater visual censuses in two Caribbean locations. *Coral Reefs* 35, 139–151. doi: 10.1007/s00338-015-1381-0.

Pinheiro, H. T., Shepherd, B., Castillo, C., Abesamis, R. A., Copus, J. M., Pyle, R. L., et al. (2019). Deep reef fishes in the world's epicenter of marine biodiversity. *Coral Reefs* 38, 985–995. doi: 10.1007/s00338-019-01825-5.

Pyle, R. L., Boland, R., Bolick, H., Bowen, B. W., Bradley, C. J., Kane, C., et al. (2016). A comprehensive investigation of mesophotic coral ecosystems in the Hawaiian Archipelago. *PeerJ* 4, e2475. doi: 10.7717/peerj.2475.

Rocha, L. A., Pinheiro, H. T., Shepherd, B., Papastamatiou, Y. P., Luiz, O. J., Pyle, R. L., et al. (2018). Mesophotic coral ecosystems are threatened and ecologically distinct

from shallow water reefs. *Science (1979)* 361, 281–284. doi: 10.1126/science.aaq1614.

Rosa, M. R., Alves, A. C., Medeiros, D. V., Coni, E. O. C., Ferreira, C. M., Ferreira, B. P., et al. (2016). Mesophotic reef fish assemblages of the remote St. Peter and St. Paul's Archipelago, Mid-Atlantic Ridge, Brazil. *Coral Reefs* 35, 113–123. doi: 10.1007/s00338-015-1368-x.

Slattery, M., Lesser, M. P., Brazeau, D., Stokes, M. D., and Leichter, J. J. (2011). Connectivity and stability of mesophotic coral reefs. *J Exp Mar Biol Ecol* 408, 32–41. doi: 10.1016/j.jembe.2011.07.024.

Smith-Vaniz, W., and Collette, B. (2013). Fishes of Bermuda. *Smith-Vaniz, William and Collette, Bruce B.* 19, 165.

Smith-Vaniz, W. F., Collette, B. B., and Luckhurst, B. E. (1999). *Fishes of Bermuda: history, zoogeography,annotated checklist, and identification keys*. American Society of Ichthyologists and Herpetologists.

Stefanoudis, P. V., Gress, E., Pitt, J. M., Smith, S. R., Kincaid, T., Rivers, M., et al. (2019a). Depth-dependent structuring of reef fish assemblages from the shallows to the rariphotic zone. *Front Mar Sci* 6, 1–16. doi: 10.3389/fmars.2019.00307.

Stefanoudis, P. V., Rivers, M., Smith, S. R., Schneider, C. W., Wagner, D., Ford, H., et al. (2019b). Low connectivity between shallow, mesophotic and rariphotic zone benthos. *R Soc Open Sci* 6, 190958. doi: 10.1098/rsos.190958.

Tamir, R., Eyal, G., Kramer, N., Laverick, J. H., and Loya, Y. (2019). Light environment drives the shallow-to-mesophotic coral community transition. *Ecosphere* 10. doi: 10.1002/ecs2.2839.

Thomsen, P. F., and Willerslev, E. (2015). Environmental DNA - An emerging tool in conservation for monitoring past and present biodiversity. *Biol Conserv* 183, 4–18. doi: 10.1016/j.biocon.2014.11.019.

Turner, J. A., Babcock, R. C., Hovey, R., and Kendrick, G. A. (2017). Deep thinking: A systematic review of mesophotic coral ecosystems. *ICES Journal of Marine Science* 74, 2309–2320. doi: 10.1093/icesjms/fsx085.

Turner, J., Andradi-Brown, D., Gori, A., Bongaerts, P., Burdett, H., Ferrier-Pagès, C., et al. (2019). "Key Questions for Research and Conservation of Mesophotic Coral Ecosystems and Temperate Mesophotic Ecosystems," in *Mesophotic Coral Ecosystems Coral Reefs of the World 12* (Loya, Yossi Puglise, Kimberly A Bridge, Tom C L), 989–1003. doi: 10.1007/978-3-319-92735-0.

Yeakel, K. L., Andersson, A. J., Bates, N. R., Noyes, T. J., Collins, A., and Garley, R. (2015). Shifts in coral reef biogeochemistry and resulting acidification linked to offshore productivity. *Proc Natl Acad Sci U S A* 112, 14512–14517. doi: 10.1073/pnas.1507021112.

Appendices

6.1 Chapter 3 - Appendices

Table S3.1. Bermuda genetic sequence reference database – 12S eDNA marker gene

FDBcode_specimen	FAMILY	GENUS	SPECIES	species	Sequence
FDB001.02	Balistidae	*Canthidermis*	*sufflamen*	*Canthidermis sufflamen*	AAATTAGGGCCGAACGCTTTCAAGGCTGTTATACGCACCCGAAAGTAAGAAGTACAACAACGAAAGTGGCCCTATAAACCCTGAACCCACGAAAGCTAAGGCA
FDB002.03	Carangidae	*Caranx*	*crysos*	*Caranx crysos*	ACTAAAGCCGAACACCCTCAAAGCTGTTATACGCTCCCGAGGGTATGAAGCCCTACTACGAAAGTGGCTTTAACTCTCCTGACCCCACGAAAGCTGTGAAA
FDB003.02	Serranidae	*Cephalopholis*	*fulva*	*Cephalopholis fulva*	ACTAAAGCGGAAACCCCTCAAAGCTGTCATACGCTCCCGAGGATATGAAGTCCAACTACGAAAGTGGCTTTATCTCTCCTGACCCCACGAAAGCTGTGACA
FDB005.05	Carangidae	*Decapterus*	*macarellus*	*Decapterus macarellus*	ACTAAAGCCGAATGCTCCCTAAGCTGTTATACGCTCTCGAGAGTTAGAAGACCTTTTTCGAAAGTAGCTTTATTATGTTGAATCCACGAAAGCTAAGACA
FDB007.04	Scombridae	*Euthynnus*	*alletteratus*	*Euthynnus alletteratus*	CTAAAGCCGAACACCTTCAGGGCAGTTATACGCATCCGAAGGCACGAAGCCCCACCACGAAAGTGGCTTTATGACCCCTGACCCCACGAAAGCTATGACA
FDB008.02	Kyphosidae	*Kyphosus*	*sectatrix*	*Kyphosus sectatrix*	AACTAAAGCCGAACGCCCTCAGGGCTGTTATACGCTCCCGAAGGTAAGAAGTTCAATCACGAAAGTGGCTTTATATCAGCTGAATCCACGAAAGCTATGACA
FDB009.13	Lutjanidae	*Ocyurus*	*chrysurus*	*Ocyurus chrysurus*	ACTAAAGCCGAATGCTCCCTAAGCTGTTATACGCTCTCGAGAGTTAGAAGACCTTTTTCGAAAGTAGCTTTATTATGTTGAATCCACGAAAGCTAAGACA
FDB017.01	Triakidae	*Mustelus*	*canis insularis*	*Mustelus canis insularis*	ACTAAAGCCGAATGCTCCCTAAGCTGTTATACGCTCTCGAGAGTTAGAAGACCTTTTTCGAAAGTAGCTTTATTATGTTGAATCCACGAAAGCTAAGACA
FDB022.01	Carcharhinidae	*Galeocerdo*	*cuvier*	*Galeocerdo cuvier*	CTAAAGCCGAATGCTCCCTAAGCTGTTATACGCTCTCGAGAGTTAGAAGACCTTTTTCGAAAGTGGCTTTATTATGTTGAATCCCCGAAAGCTTAGACA
FDB024.01	Carcharhinidae	*Prionace*	*glauca*	*Prionace glauca*	ACTAAAGCCGAATGCTCCCTAAGCTGTTATACGCTCTCGAGAGTTAGAAGACCTTTTTCGAAAGTAGCTTTATTATGTTGAATCCACGAAAGCTAAGACA
FDB033.01	Dasyatidae	*Dasyatis*	*violacea*	*Dasyatis violacea*	ACTAAAGCCGAATGCTCCCTAAGCTGTTATACGCTCTCGAGAGTTAGAAGACCTTTTTCGAAAGTGGCTTTATTATGTTGAATCCACGAAAGCTAAGACA
FDB034.01	Myliobatidae	*Aetobatus*	*narinari*	*Aetobatus narinari*	ACTAAAGCCGAATGCTCCCTAAGCTGTTATACGCTCTCGAGAGTTAGAAGACCTTTTTCGAAAGTAGCTTTATTATGTTGAATCCACGAAAGCTAAGACA
FDB039.01	Albulidae	*Albula*	*vulpes*	*Albula vulpes*	ACTAAAGCCGAATGCTCCCTAAGCTGTTATACGCTCTCGAGAGTTAGAAGACCTTTTTCGAAAGTAGCTTTATTATGTTGAATCCACGAAAGCTAAGACA
FDB040.01	Anguillidae	*Anguilla*	*rostrata*	*Anguilla rostrata*	ACTAAAGCCGAACATCCTCAAGACTGTCGTACGTTTCCGAGGATATGAAGTCCCCCTACGAAAGTGGCTTTAACTCTCCTGACCCCACGAAAGCTGTGACA
FDB052.01	Muraenidae	*Gymnothorax*	*maderensis*	*Gymnothorax maderensis*	ACTAAAGCCGAATGCTCCCTAAGCTGTTATACGCTCTCGAGAGTTAGAAGACCTTTTTCGAAAGTAGCTTTATTATGTTGAATCCACGAAAGCTAAGACA
FDB053.01	Muraenidae	*Gymnothorax*	*miliaris*	*Gymnothorax miliaris*	ACTAAAGCCGAACATCCTCAAGACTGTCGTACGTTTCCGAGGATATGAAGTCCCCCTACGAAAGTGGCTTTAACTCTCCTGACCCCACGAAAGCTGTGACA
FDB053.01	Muraenidae	*Gymnothorax*	*miliaris*	*Gymnothorax miliaris*	ACTAAAGCCGAACATCCTCAAGACTGTCGTACGTTTCCGAGGATATGAAGTCCCCCTACGAAAGTGGCTTTAACTCTCCTGACCCCACGAAAGCTGTGACA
FDB054.02	Muraenidae	*Gymnothorax*	*moringa*	*Gymnothorax moringa*	ACTAAAGCCGAATGCTCCCTAAGCTGTTATACGCTCTCGAGAGTTAGAAGACCTTTTTCGAAAGTAGCTTTATTATGTTGAATCCACGAAAGCTAAGACA
FDB063.01	Ophichthidae	*Myrichthys*	*ocellatus*	*Myrichthys ocellatus*	ACTAAAGCCGAATGCTCCCTAAGCTGTTATACGCTCTCGAGAGTTAGAAGACCTTTTTCGAAAGTAGCTTTATTATGTTGAATCCACGAAAGCTAAGACA
FDB065.01	Ophichthidae	*Myrophis*	*punctatus*	*Myrophis punctatus*	ACTAAAGCCGAACATCCTCAAGACTGTCGTACGTTTCCGAGGATATGAAGTCCCCCTACGAAAGTGGCTTTAACTCTCCTGACCCCACGAAAGCTGTGACA
FDB070.01	Congridae	*Conger*	*esculentus*	*Conger esculentus*	ACTAAAGCCGAATGCTCCCTAAGCTGTTATACGCTCTCGAGAGTTAGAAGACCTTTTTCGAAAGTAGCTTTATTATGTTGAATCCACGAAAGCTAAGACA
FDB072.01	Congridae	*Heteroconger*	*longissimus*	*Heteroconger longissimus*	ACTAAAGCCGAATGCTCCCTAAGCTGTTATACGCTCTCGAGAGTTAGAAGACCTTTTTCGAAAGTAGCTTTATTATGTTGAATCCACGAAAGCTAAGACA
FDB074.01	Engraulidae	*Anchoa*	*choerostoma*	*Anchoa choerostoma*	ACTAAAGCCGAATGCTCCCTAAGCTGTTATACGCTCTCGAGAGTTAGAAGACCTTTTTCGAAAGTAGCTTTATTATGTTGAATCCACGAAAGCTAAGACA
FDB075.01	Clupeidae	*Harengula*	*humeralis*	*Harengula humeralis*	ACTAAAGCCGAATGCTCCCTAAGCTGTTATACGCTCTCGAGAGTTAGAAGACCTTTTTCGAAAGTGGCTTTATTATGTTGAATCCACGAAAGCTAAGACA
FDB076.01	Clupeidae	*Jenkinsia*	*lamprotaenia*	*Jenkinsia lamprotaenia*	AACTAAAGCCGAATGCTCCCTAAGCTGTTATACGCTCTCGAGAGTGAGAAGACCTTTTTCGAAAGTAGCTTTATTATGTTGAATCCACGAAAGCTAAGACA
FDB078.01	Aulopidae	*Aulopus*	*filamentosus*	*Aulopus filamentosus*	ACTAAAGCCGAACATCCTCAAGACTGTCGTACGTTTCCGAGGATATGAAGTCCCCCTACGAAAGTGGCTTTAACTCTCCTGACCCCACGAAAGCTGTGACA
FDB080.02	Synodontidae	*Synodus*	*foetens*	*Synodus foetens*	GCTAGAGGAAAATGCCTTCCAAGCTGTTATACGCACCCGGAGGTAAGAAAAACCCGCACGAAAGACCCTCTAATTAATATGAACCCACGACAGCTTTGGCA
FDB080.03	Synodontidae	*Synodus*	*foetens*	*Synodus foetens*	GCTAGAGGAAAATGCCTTCCAAGCTGTTATACGCACCCGGAGGTAAGAAAAACCCGCACGAAAGACCCTCTAATTAATATGAAGCCACGGCAGCTTTGGCA
FDB081.03	Synodontidae	*Synodus*	*intermedius*	*Synodus intermedius*	TCTAGAGGAAAACACCTTTCAAACTGTTATACGCACCCAAAGGTAAGAAAAACTTGCACGAAAGTCCCTCTAATAAATCCGAATCCACGACAGCTCTGGTA
FDB081.04	Synodontidae	*Synodus*	*intermedius*	*Synodus intermedius*	TCTAGAGGAAAACACCTTTCAAACTGTTATACGCACCCAAAGGTAAGAAAAACTTGCACGAAAGTCCCTCTAATAAATCCGAATCCACGACAGCTCTGGTA
FDB084.01	Alepisauridae	*Alepisaurus*	*ferox*	*Alepisaurus ferox*	AACTAAAGCCGAATGCTCCCTAAGCTGTTATACGCTCTCGAGAGTTAGAAGACCTTTTTCGAAAGTAGCTTTATTATGTTGAATCCACGAAAGCTAAGACA
FDB093.01	Bythidae	*Ogilbia*	*cayorum*	*Ogilbia cayorum*	ACCAAACTAAAGTCGAACGCCCCCAAAGCCGTTATACGCACCCGGCGGCATGAAGCACAATTACAAAAGTAACTTTAACATATTCCTGAACCCACGAAATCTAAGACA
FDB095.01	Moridae	*Antimora*	*rostrata*	*Antimora rostrata*	ACTAAAGCCGAATGCTCCCTAAGCTGTTATACGCTCTCGAGAGTTAGAAGACCTTTTTCGAAAGTAGCTTTATTATGTTGAATCCACGAAAGCTAAGACA
FDB096.01	Moridae	*Laemonema*	*yarrellii*	*Laemonema yarrellii*	TATAGAGTTGAATGGCCTCAATTCAGTTAAATGCACTCGAAGTCATGAAGCACAATAACGAAAGTAGCTCTACCAAATCCCTGACTCCACGAAAACCATAACA

FDBcode_specimen	FAMILY	GENUS	SPECIES	species	Sequence
FDB097.01	Moridae	*Physiculus*	*karrerae*	*Physiculus karrerae*	AACTAAAGCCGAACGCCCTCAGGGCTGTTATACGCTCCCGAAGGTAAGAAGTTCAATCACGAAAGTGGC TTTATATCAGCTGAATCCACGAAAGCTATGACA
FDB099.01	Antennariidae	*Antennarius*	*multiocellatus*	*Antennarius multiocellatus*	AACTAAAGCCGAATGCTCCCTAAGCTGTTATACGCTCTCGAGAGTTAGAAGACCTTTTTCGAAAGTAGCT TTATTATGTTGAATCCACGAAAGCTAAGACA
FDB103.01	Antennariidae	*Histrio*	*histrio*	*Histrio histrio*	ACTAAAGCCGAACACCCTCATGACTGTCGTACGCTCCCCAGGAGATGAAGCCCAACTACGAAAGTGGCT TTAACTCTCCTGAACCCACGAAAGCTTAGACA
FDB107.01	Mugilidae	*Mugil*	*curema*	*Mugil curema*	ACTAAAGCCGAACATCCTCAAGACTGTCATACGCTTCCGAGGATATGAAGTCCCCCTACGAAAGTGGCTT TATCTCTCCTGACCCCACGAAAGCTGTGACA
FDB109.01	Mugilidae	*Mugil*	*trichodon*	*Mugil trichodon*	AACTAAAGCGGAAAATCCTCAAAGCGGTCATACGCTCCCGAGGGTATGAAATCCATCTACGAAAGTGGC TTTATTTCTCCTGAACCCACGAAAGCTGTGAAA
FDB111.01	Atherinidae	*Hypoatherina*	*harringtonensis*	*Hypoatherina harringtonensis*	ACCAAACTAAAGTCGAACGCCCCCAAAGCCGTTATACGCACCCGGCGGCATGAAGCACAATTACAAAAG TAACTTTAACATATTCCTGAACCCACGAAATCTAAGACA
FDB113.01	Belonidae	*Platybelone*	*argalus argalus*	*Platybelone argalus argalus*	ACTAAAGCCGAATGCTCCCTAAGCTGTTATACGCTCTCGAGAGTTAGAAGACCTTTTTCGAAAGTAGCTT TATTATGTTGAATCCACGAAAGCTAAGACA
FDB125.01H99054K1B	Exocoetidae	*Hirundichthys*	*rondeletii*	*Hirundichthys rondeletii*	ACTAAAGCCGAACATCCTCAAGACTGTCGTACGTTTCCGAGGATATGAAGTCCCCCTACGAAAGTGGCTT TAACTCTCCTGACCCCACGAAAGCTGTGACA
FDB128.01	Exocoetidae	*Prognichthys*	*glaphyrae*	*Prognichthys glaphyrae*	ACTAAAGCCGAACATCCTCAAGACTGTCGTACGTTTCCGAGGATATGAAGTCCCCCTACGAAAGTGGCTT TAACTCTCCTGACCCCACGAAAGCTGTGGCA
FDB129.01	Exocoetidae	*Prognichthys*	*occidentalis*	*Prognichthys occidentalis*	ACTAAAGCCGAATGCTCCCTAAGCTGTTATACGCTCTCGAGAGTTAGAAGACCTTTTTCGAAAGTAGCTT TATTATGTTGAATCCACGAAAGCTAAGACA
FDB133.01	Hemiramphidae	*Hyporhamphus*	*unifasciatus*	*Hyporhamphus unifasciatus*	ACTAAAGCCGAATGCTCCCTAAGCTGTTATACGCTCTCGAGAGTTAGAAGACCTTTTTCGAAAGTAGCTT TATTATGTTGAATCCACGAAAGCTAAGACA
FDB136.01	Trachichthyidae	*Hoplostethus*	*mediterraneus*	*Hoplostethus mediterraneus*	ACTAAAGCCGAACATTCTCAGAGCTGTTATACGCACCCGAGGACATGAAGCACCACTACGAAAGTGGCT TTACCTTTCCTGAACCCACGAAAGCTATGACA
FDB138.01	Holocentridae	*Holocentrus*	*adscensionis*	*Holocentrus adscensionis*	ACTAAAGCCGAATGCTCCCTAAGCTGTTATACGCTCTCGAGAGTTAGAAGACCTTTTTCGAAAGTGGCTT TATTATGTTGAATCCACGAAAGCTAAGACA
FDB142.01	Holocentridae	*Sargocentron*	*coruscum*	*Sargocentron coruscum*	AAACTAAAGCCAAACACCTTCAGAACTGTTATACGTACCCGAAGGCATGAAGAACTACCACGAAAGTGG CTTTACCCGCCCTGAGCCCACGAAAGCTATGTCA
FDB152.02	Syngnathidae	*Hippocampus*	*reidi*	*Hippocampus reidi*	ACTAAAGCCGAACTCCCTCATTGCTGTCATACGCTCCCGAGGGTAAGAAGCCCAACTACGAAAGTGGCTT TTTCCCACCTGAACCCACGAAAGCTGTGACA
FDB152.01	Syngnathidae	*Hippocampus*	*reidi*	*Hippocampus reidi*	TAAAGTTAAACATCTTCCAGGCTGTTATACGCACCCGAAGGTATGAAATTCATTTACGAAAGTGACTTTA CCAAAACTGAACCCACGAAAGCTATGAAA
FDB159.01	Aulostomidae	*Aulostomus*	*maculatus*	*Aulostomus maculatus*	AGTAAAACTAAAAGAACACGGAGCAGTGTAACGCCAACACCGTGTGTCGGAGAACCAGAAACGAAAGT AGTTTTATGCATCTTGACTCCACGAAAGCTTAGAAA
FDB160.01	Fistulariidae	*Fistularia*	*tabacaria*	*Fistularia tabacaria*	ACTAAAGCCGAATGCTCCCTAAGCTGTTATACGCTCTCGAGAGTTAGAAGACCTTTTTCGAAAGTAGCTT TATTATGTTGAATCCACGAAAGCTAAGACA
FDB163.01	Scorpaenidae	*Pontinus*	*castor*	*Pontinus castor*	ACTAAAGCCGAACATCCTCAAGACTGTCGTACGTTTCCGAGGATATGAAGTCCCCCTACGAAAGTGGCTT TAACTCTCCTGACCCCACGAAAGCTGTGACA
FDB168.01	Scorpaenidae	*Scorpaena*	*plumieri*	*Scorpaena plumieri*	ACTAAAGCCGAATGCTCCCTAAGCTGTTATACGCTCTCGAGAGTTAGAAGACCTTTTTCGAAAGTAGCTT TATTATGTTGAATCCACGAAAGCTAAGACA
FDB175.01	Serranidae	*Alphestes*	*afer*	*Alphestes afer*	ACTAAAGCCGAATGCTCCCTAAGCTGTTATACGCTCTCGAGAGTTAGAAGACCTTTTTCGAAAGTGGCTT TATTATGTTGAATCCACGAAAGCTAAGACA
FDB179.01	Serranidae	*Diplectrum*	*formosum*	*Diplectrum formosum*	ACTAAAGCCGAACATCCTCAAGACTGTCGTACGTTTCCGAGGATATGAAGTCCCCCTACGAAAGTGGCTT TAACTCTCCTGACCCCACGAAAGCTGTGACA
FDB180.01	Serranidae	*Epinephelus*	*adscensionis*	*Epinephelus adscensionis*	ACTAAAGCCGAATGCTCCCTAAGCTGTTATACGCTCTCGAGAGTTAGAAGACCTTTTTCGAAAGTAGCTT TATTATGTTGAATCCACGAAAGCTAAGACA
FDB182.01	Serranidae	*Epinephelus*	*guttatus*	*Epinephelus guttatus*	ACTAAAGCCGAATGCTCCCTAAGCTGTTATACGCTCTCGAGAGTGAGAAGACCTTTTTCGAAAGTGGCT TTATTATGTTGAATCCACGAAAGCTTAGACA
FDB186.01	Serranidae	*Epinephelus*	*niveatus*	*Epinephelus niveatus*	ACTAAAGCCGAATGCTCCCTAAGCTGTTATACGCTCTCGAGAGTTAGAAGACCTTTTTCGAAAGTAGCTT TATTATGTTGAATCCACGAAAGCTAAGACA
FDB194.01	Serranidae	*Hypoplectrus*	*puella*	*Hypoplectrus puella*	ACTAAAGCCGAACATCCTCAAGACTGTCGTACGTTTCCGAGGATATGAAGTCCCCCTACGAAAGTGGCTT TAACTCTCCTGACCCCACGAAAGCTGTGACA
FDB198.01	Serranidae	*Mycteroperca*	*interstitalis*	*Mycteroperca interstitalis*	ACTAAAGCCGAATGCTCCCTAAGCTGTTATACGCTCTCGAGAGTTAGAAGACCTTTTTCGAAAGTAGCTT TATTATGTTGAATCCACGAAAGCTAAGACA
FDB199.01	Serranidae	*Mycteroperca*	*microlepis*	*Mycteroperca microlepis*	ACTAAAGCGGAACTCCCTCATAGCTGTTATACGCTCCCGAGGGTAAGAAGCCCAACCACGAAAGTGGCT TTTTCCATCCTGAACCCACGAAAGCTCTGACA
FDB201.01	Serranidae	*Mycteroperca*	*venenosa*	*Mycteroperca venenosa*	AACTAAAGCCGAATGCTCCCTAAGCTGTTATACGCTCTCGAGAGTTAGAAGACCTTTTTCGAAAGTAGCT TTATTATGTTGAATCCACGAAAGCTAAGACA
FDB208.01	Serranidae	*Rypticus*	*saponaceus*	*Rypticus saponaceus*	AAACTAAAGCCGAATGCTCCCTAAGCTGTTATACGCTCTCGAGAGTATGAAGTCCCTTTTCGAAAGTGGC TTTATTATGCTGAATCCACGAAAGCTTATACA
FDB217.01	Priacanthidae	*Pristigenys*	*alta*	*Pristigenys alta*	ACTAAAGCCGAATGCTCCCTAAGCTGTTATACGCTCTCGAGAGTTAGAAGACCTTTTTCGAAAGTAGCTT TATTATGTTGAATCCACGAAAGCTAAGACA
FDB221.01	Apogonidae	*Apogon*	*planifrons*	*Apogon planifrons*	ACTAAAGCCGAACCTCCTCAAAGCTGTCATACGCTCCCGAGGGTATGAAGTCCAACTACGAAAGTGGCT TTAACTCACCTGAACCCACGAAAGCTGTGACA
FDB228.01	Apogonidae	*Phaeoptxy*	*pigmentaria*	*Phaeoptxy pigmentaria*	TAAAGCCAAACATCTCCAAGGTTGTATAACGCATTCGGAGACACGAAGCCCATCTACGAAAGTGGCTTT ATACTCTTTGAACCCACGAAAGCTAGGGAA
FDB229.01	Malacanthidae	*Caulolatilus*	*bermudensis*	*Caulolatilus bermudensis*	ACTAAAGCCGAACCCCCTCAAAGCTGTCATACGCTCCCGAGGGTAAGAAGCCCAACTACGAAAGTGGCT TTAATTAACCTGAACCCACGAAAGCTGTGACA

FDBcode_specimen	FAMILY	GENUS	SPECIES	species	Sequence
FDB231.01	Malacanthidae	*Malacanthus*	*plumieri*	*Malacanthus plumieri*	ACTAAAGCCGAATGCTCCCTAAGCTGTTATACGCTCTCGAGAGTTAGAAGACCTTTTTCGAAAGTAGCTTTATTATGTTGAATCCACGAAAGCTAAGACA
FDB233.01	Pomatomidae	*Pomatomus*	*saltatrix*	*Pomatomus saltatrix*	ACTAAAGCCGAATGCTCCCTAAGCTGTTATACGCTCTCGAGAGTTAGAAGACCTTTTTCGAAAGTAGCTTTATTATGTTGAATCCACGAAAGCTAAGACA
FDB243.01	Carangidae	*Alectis*	*ciliaris*	*Alectis ciliaris*	ACTAAAGCCGAATGCTCCCTAAGCTGTTATACGCTCTCGAGAGTTAGAAGACCTTTTTCGAAAGTGGCTTTATTATGTTGAATCCACGAAAGCTAAGACA
FDB249.01	Carangidae	*Chloroscombrus*	*chrysurus*	*Chloroscombrus chrysurus*	ACTAAAGCCGAATGCTCCCTAAGCTGTTATACGCTCTCGAGAGTTAGAAGACCTTTTTCGAAAGTAGCTTTATTATGTTGAATCCACGAAAGCTAAGACA
FDB249.01	Carangidae	*Chloroscombrus*	*chrysurus*	*Chloroscombrus chrysurus*	ACTAAAGCCGAATGCTCCCTAAGCTGTTATACGCTCTCGAGAGTTAGAAGACCTTTTTCGAAAGTAGCTTTATTATGTTGAATCCACGAAAGCTAAGACA
FDB257.01	Carangidae	*Seriola*	*fasciata*	*Seriola fasciata*	ACTAAAGCCGAATGCTCCCTAAGCTGTTATACGCTCTCGAGAGTTAGAAGACCTTTTTCGAAAGTAGCTTTATTATGTTGAATCCACGAAAGCTAAGACA
FDB265.01	Bramidae	*Taractichthys*	*longipinnis*	*Taractichthys longipinnis*	AACTAAAGCCGAATGCTCCCTAAGCTGTTATACGCTCTCGAGAGTTAGAAGACCTTTTTCGAAAGTAGCTTTATTATGTTGAATCCACGAAAGCTAAGACA
FDB267.01	Lutjanidae	*Etelis*	*oculatus*	*Etelis oculatus*	ACTAAAGCCGAACATCCTCAAGACTGTCGTACGTTTCCGAGGATATGAAGTCCCCCTACGAAAGTGGCTTTAACTCTCCTGACCCCACGAAAGCTGTGACA
FDB273.01	Lutjanidae	*Lutjanus*	*synagris*	*Lutjanus synagris*	AAATTAGAGTCGAACGCTTTCAAGGCTGTTATACGCACCCGAAAGTAAGAAGCACAACAACGAAAGTGGCTCTACTAATTCTGAACCCACGAAAGCTAAGGTA
FDB274.01	Lutjanidae	*Lutjanus*	*vivanus*	*Lutjanus vivanus*	ACTAAAGCCGAACATCCTCAAGACTGTCGTACGTTTCCGAGGATATGAAGTCCCCCTACGAAAGTGGCTTTAACTCTCCTGACCCCACGAAAGCTGTGACA
FDB275.01	Lutjanidae	*Pristipomoides*	*macrophthalmus*	*Pristipomoides macrophthalmus*	ACTAAAGCCGAACATCCTCAAGACTGTCGTACGTTTCCGAGGATATGAAGTCCCCCTACGAAAGTGGCTTTAACTCTCCTGACCCCACGAAAGCTGTGACA
FDB277.01	Lobotidae	*Lobotes*	*surinamensis*	*Lobotes surinamensis*	ACTAAAGCCGAACATCCTCAAGACTGTCGTACGTTTCCGAGGATATGAAGTCCCCCTACGAAAGTGGCTTTAACTCTCCTGACCCCACGAAAGCTGTGACA
FDB287.01	Haemulidae	*Haemulon*	*carbonarium*	*Haemulon carbonarium*	AAATTAGAGTCAAACGCTTTCAAGGCTGTTATACGCACCCGAAAGTAAGAAGCACAACAACGAAAGTGGCTCTACTAATTCTGAACCCACGAAAGCTAAGGTA
FDB288.03	Haemulidae	*Haemulon*	*flavolineatum*	*Haemulon flavolineatum*	ACTAAAGCCGAATGCTCCCTAAGCTGTTATACGCTCCCGAGAGTTAGAAGACCTTTTTCGAAAGTGGCTTTATTATGTTGAATCCACGAAAGCTAAGACA
FDB292.01	Haemulidae	*Orthopristis*	*chrysoptera*	*Orthopristis chrysoptera*	ACTAAAGCCGAATGCTCCCTAAGCTGTTATACGCTCTCGAGAGTTAGAAGACCTTTTTCGAAAGTAGCTTTATTATGTTGAATCCACGAAAGCTAAGACA
FDB294.01	Sparidae	*Calamus*	*bajonado*	*Calamus bajonado*	ACTAAAGCCGAACATCCTCAAGACTGTCGTACGTTTCCGAGGATATGAAGTCCCCCTACGAAAGTGGCTTTAACTCTCCTGACCCCACGAAAGCTGTGACA
FDB297.03	Sparidae	*Lagodon*	*rhomboides*	*Lagodon rhomboides*	AAATTAGAGTCGAACGCTTTCAAGGGTGTTATACGCACCCGAAAGTAAGAAGCACAACAACGAAAGTGGCTCTACTAATTCTGAACCCACGAAAGCTAAGGTA
FDB302.01	Mullidae	*Pseudupeneus*	*maculatus*	*Pseudupeneus maculatus*	ACTAAAGCCGAATGCTCCCTAAGCTGTTATACGCTCTCGAGAGTTAGAAGACCTTTTTCGAAAGTAGCTTTATTATGTTGAATCCACGAAAGCTAAGACA
FDB304.01	Pempheridae	*Pempheris*	*schomburgkii*	*Pempheris schomburgkii*	ACTAAAGCCGAACATCCTCAAGACTGTCGTACGTTTCCGAGGATATGAAGTCCCCCTACGAAAGTGGCTTTAACTCTCCTGACCCCACGAAAGCTGTGACA
FDB305.01	Chaetodontidae	*Chaetodon*	*aculeatus*	*Chaetodon aculeatus*	ACTAAAGCCGAACATCCTCAAGACTGTCGTACGTTTCCGAGGATATGAAGTCCCCCTACGAAAGTGGCTTTAACTCTCCTGACCCCACGAAAGCTGTGACA
FDB308.01	Chaetodontidae	*Chaetodon*	*sedentarius*	*Chaetodon sedentarius*	ACTAAAGCCGAACATCCTCAAGACTGTCGTACGTTTCCGAGGATATGAAGTCCCCCTACGAAAGTGGCTTTAACTCTCCTGACCCCACGAAAGCTGTGACA
FDB325.01	Pomacentridae	*Microspathodon*	*chrysurus*	*Microspathodon chrysurus*	ACTAAAGCCGAACATCCTCAAGACTGTCGTACGTTTCCGAGGATATGAAGTCCCCCTACGAAAGTGGCTTTAACTCTCCTGACCCCACGAAAGCTGTGACA
FDB327.01	Pomacentridae	*Stegastes*	*partitus*	*Stegastes partitus*	ACTAAAGCCGAATGCTCCCTAAGCTGTTATACGCTCTCGAGAGTTAGAAGACCTTTTTCGAAAGTGGCTTTATTATGTTGAATCCACGAAAGCTAAGACA
FDB328.01	Pomacentridae	*Stegastes*	*planifrons*	*Stegastes planifrons*	ACTAAAGCCGAATGCTCCCTAAGCTGTTATACGCTCTCGAGAGTTAGAAGACCTTTTTCGAAAGTAGCTTTATTATGTTGAATCCACGAAAGCTAAGACA
FDB330.01	Labridae	*Bodianus*	*pulchellus*	*Bodianus pulchellus*	ACTAAAGCGGAACCCCCTCAAAGCTGTTATACGCTCCCGAAGGTATGAACCCCAACTACGAAAGTGGCTTTATAAAACCTGAACCCACGAAAGCTATGAAA
FDB336.01	Labridae	*Halichoeres*	*bathyphilus*	*Halichoeres bathyphilus*	ACTAAAGCCGAACTCCCTCATAGCTGTCATACGCTCCCGAGGATATGAAGCCCAACTACGAAAGTGGCTTTACCCTACCTGAACCCACGAAAGCTGTGACA
FDB344.01	Labridae	*Lachnolaimus*	*maximus*	*Lachnolaimus maximus*	ACTAAAGCCGAACATCCTCAAGACTGTCGTACGTTTCCGAGGATATGAAGTCCCCCTACGAAAGTGGCTTTAACTCTCCTGACCCCACGAAAGCTGTGACA
FDB345.01H99054K1B	Labridae	*Thalassoma*	*bifasciatum*	*Thalassoma bifasciatum*	ACTAAAGCCGAACATCCTCAAGACTGTCGTACGTTTCCGAGGATATGAAGTCCCCCTACGAAAGTGGCTTTAACTCTCCTGACCCCACGAAAGCTGTGACA
FDB348.01	Labridae	*Xyrichtys*	*splendens*	*Xyrichtys splendens*	ACTAAAGCCGAACATCCTCAAGACTGTCGTACGTTTCCGAGGATATGAAGTCCCCCTACGAAAGTGGCTTTAACTCTCCTGACCCCACGAAAGCTGTGACA
FDB352.01	Scaridae	*Scarus*	*coelestinus*	*Scarus coelestinus*	ACTAAAGCCGAATGCTCCCTAAGCTGTTATACGCTCTCGAGAGTTAGAAGACCTTTTTCGAAAGTAGCTTTATTATGTTGAATCCACGAAAGCTAAGACA
FDB355.01	Scaridae	*Scarus*	*iseri*	*Scarus iseri*	AAACTAGAGCTGAATTTCTTCAAAGCTGTTATACGCTCATGAAAACTAGAAAATCAACCACGAAGGTGGCTCTAATCACCCCTGACACCACGAAAGCTATGACA
FDB370.01	Blenniidae	*Entomacrodus*	*nigricans*	*Entomacrodus nigricans*	ACTAAAGCCGAACATCCTCAAGACTGTCGTACGTTTCCGAGGATATGAAGTCCCCCTACGAAAGTGGCTTTAACTCTCCTGACCCCACGAAAGCTGTGACA
FDB371.01	Blenniidae	*Hypleurochilus*	*bermudensis*	*Hypleurochilus bermudensis*	CTAAAGCCGAATGCTCCCTAAGCTGTTATACGCTCTCGAGAGTTAGAAGACCTTTTTCGAAAGTAGCTTTATTATGTTGAATCCACGAAAGCTAAGACA
FDB373.01	Blenniidae	*Parablennius*	*marmoreus*	*Parablennius marmoreus*	ACTAAAGCCGAACATCCTCAAGACTGTCGTACGTTTCCGAGGATATGAAGTCCCCCTACGAAAGTGGCTTTAACTCTCCTGACCCCACGAAAGCTGTGACA

FDBcode_specimen	FAMILY	GENUS	SPECIES	species	Sequence
FDB374.01	Blenniidae	*Scartella*	*cristata*	*Scartella cristata*	ACTAAAGCCGAACATCCTCAAGACTGTCGTACGTTTCCGAGGATATGAAGTCCCCCTACGAAAGTGGCTT TAACTCTCCTGACCCCACGAAAGCTGTGACA
FDB375.01	Callionymidae	*Diplogrammus*	*pauciradiatus*	*Diplogrammus pauciradiatus*	AATAAGGCCGAACTCACTCCTGACTGTTATACGTTACGAAATGAAGAAGTACTAATACGAAAGTAGCCT TAATTTATTGAAGCCACGAAAGCCACGACA
FDB376.01	Callionymidae	*Paradiplogrammus*	*bairdi*	*Paradiplogrammus bairdi*	ACTAAAGCCGAACATCCTCAAGACTGTCGTACGTTTCCGAGGATATGAAGTCCCCCTACGAAAGTGGCTT TAACTCTCCTGACCCCACGAAAGCTGTGACA
FDB380.01	Gobiidae	*Bathygobius*	*curacao*	*Bathygobius curacao*	ACTAAAGCCGAACGCCCTCAAAGCAGTTATACGCATTCGAAGGTATGAAGTTCTACCACGAAAGTGGCT TTAAACACTATTGAACCCACGAAAGCTAGGGAA
FDB385.01	Gobiidae	*Coryphopterus*	*personatus*	*Coryphopterus personatus*	ACTAAAGCCGAACATCCTCAAGACTGTCGTACGTTTCCGAGGATATGAAGTCCCCCTACGAAAGTGGCTT TAACTCTCCTGACCCCACGAAAGCTGTGACA
FDB394.01	Gobiidae	*Lythrypnus*	*mowbrayi*	*Lythrypnus mowbrayi*	ACTAAAGCCGAACATCCTCAAGACTGTCGTACGTTTCCGAGGATATGAAGTCCCCCTACGAAAGTGGCTT TAACTCTCCTGACCCCACGAAAGCTGTGACA
FDB403.01	Acanthuridae	*Acanthurus*	*chirurgus*	*Acanthurus chirurgus*	ACTAAAGCCGAATGCTCCCTAAGCTGTTATACGCTCTCGAGAGTTAGAAGACCTTTTTCGAAAGTAGCTT TATTATGTTGAATCCACGAAAGCTAAGACA
FDB406.01	Sphyraenidae	*Sphyraena*	*barracuda*	*Sphyraena barracuda*	ACTAAAGCCGAATGCTCCCTAAGCTGTTATACGCTCTCGAGAGTTAGAAGACCTTTTTCGAAAGTAGCTT TATTATGTTGAATCCACGAAAGCTAAGACA
FDB408.01	Gempylidae	*Epinnula*	*magistralis*	*Epinnula magistralis*	ACTAAAGCCGAATGCTCCCTAAGCTGTTATACGCTCTCGAGAGTTAGAAGACCTTTTTCGAAAGTGGCTT TATTATGTTGAATCCACGAAAGCTAAGACA
FDB409.01	Gempylidae	*Gempylus*	*serpens*	*Gempylus serpens*	ACTAAAGCCGAACGCCTTCAGAGCAGTTATACGCACCCGAAGGTATGAAGCCCCACTACGAAAGTGGCT TTACACCCCCTGACCCCACGAAAGCTATGGCA
FDB409.01	Gempylidae	*Gempylus*	*serpens*	*Gempylus serpens*	ACTAAAGCCGAACGCCTTCAGAGCAGTTATACGCACCCGAAGGTATGAAGCCCCACTACGAAAGTGGCT TTACACCCCCTGACCCCACGAAAGCTATGGCA
FDB410.01	Gempylidae	*Lepidocybium*	*flavobrunneum*	*Lepidocybium flavobrunneum*	ACTAAAGCCGAATGCTCCCTAAGCTGTTATACGCTCTCGAGAGTTAGAAGACCTTTTTCGAAAGTAGCTT TATTATGTTGAATCCACGAAAGCTAAGACA
FDB411.01	Gempylidae	*Lepidocybium*	*americana*	*Lepidocybium americana*	ACTAAAGCCGAATGCTCCCTAAGCTGTTATACGCTCTCGAGAGTTAGAAGACCTTTTTCGAAAGTGGCTT TATTATGTTGAATCCACGAAAGCTAAGACA
FDB431.01	Centrolophidae	*Hyperoglyphe*	*perciformis*	*Hyperoglyphe perciformis*	ACTAAAGCCGAACATCCTCAAGACTGTCGTACGTTTCCGAGGATATGAAGTCCCCCTACGAAAGTGGCTT TAACTCTCCTGACCCCACGAAAGCTGTGACA
FDB431.01	Centrolophidae	*Hyperoglyphe*	*perciformis*	*Hyperoglyphe perciformis*	ACTAAAGCGGAACCCCTTCAAGACTGTTATACGCTCCCGAGGGTATGAAGCCCATCTACGAAAGTGGCT TTAACTCTCCTGAACCCACGAAAGCTCTGACA
FDB440.01	Bothidae	*Bothus*	*lunatus*	*Bothus lunatus*	ACTAAAGCCGAATGCTCCCTAAGCTGTTATACGCTCTCGAGAGTTAGAAGACCTTTTTCGAAAGTAGCTT TATTATGTTGAATCCACGAAAGCTAAGACA
FDB446.01	Balistidae	*Canthidermis*	*maculata*	*Canthidermis maculata*	ACTAAAGCCGAATGCTCCCTAAGCTGTTATACGCTCTCGAGAGTTAGAAGACCTTTTTCGAAAGTAGCTT TATTATGTTGAATCCACGAAAGCTAAGACA
FDB449.01	Monacanthidae	*Aluterus*	*monoceros*	*Aluterus monoceros*	AATTAAAGTCGAATGTTTTCAAAGCTGTTATACGCATACGAGAACTAGAAGCCCAACAACGAAGGTGAC TTTACAGTTTCTGAACCCACGAAAGCTAAGGCA
FDB449.03	Monacanthidae	*Aluterus*	*monoceros*	*Aluterus monoceros*	AATTAAAGTCGAATGTTTTCAAAGCTGTTATACGCATACGAGAACTAGAAGCCCAACAACGAAGGTGAC TTTACAGTTTCTGAACCCACGAAAGCTAAGGCA
FDB449.04	Monacanthidae	*Aluterus*	*monoceros*	*Aluterus monoceros*	ACTAAAGCCGAATGCTCCCTAAGCTGTTATACGCTCTCGAGAGTTAGAAGACCTTTTTCGAAAGTAGCTT TATTATGTTGAATCCACGAAAGCTAAGACA
FDB452.01	Monacanthidae	*Cantherhines*	*macrocerus*	*Cantherhines macrocerus*	ACTAAAGCCGAATGCTCCCTAAGCTGTTATACGCTCTCGAGAGTTAGAAGACCTTTTTCGAAAGTAGCTT TATTATGTTGAATCCACGAAAGCTAAGACA
FDB453.01	Monacanthidae	*Cantherhines*	*pullus*	*Cantherhines pullus*	ACTAAAGCCGAATGCTCCCTAAGCTGTTATACGCTCTCGAGAGTTAGAAGACCTTTTTCGAAAGTAGCTT TATTATGTTGAATCCACGAAAGCTAAGACA
FDB466.01	Tetraodontidae	*Lagocephalus*	*lagocephalus*	*Lagocephalus lagocephalus*	ACTAAAGCCGAATGCTCCCTAAGCTGTTATACGCTCTCGAGAGTTAGAAGACCTTTTTCGAAAGTAGCTT TATTATGTTGAATCCACGAAAGCTAAGACA
FDB474.01	Molidae	*Ranzania*	*laevis*	*Ranzania laevis*	ACTAAAGCCGAACCCCTTCAAAGCTGTTATACGCTCCCGAGGGTATGAAGCCCATCTACGAAAGTGGCTT TAACTCTCCTGACCCCACGAAAGCTCTGACA
FDB653	NA	*Cheilopogon*	*sp*	*Cheilopogon sp*	ACTAAAGCGGAACCCCCTCATTGCTGTCATACGCTCCCGAGAGGATGAACCCCAACTACGAAGGTGGCT TTATAAAACCTGAACCCACGAAAGCTAAGAAA
FDB354	NA	*Scarus*	*guacamaia*	*Scarus guacamaia*	TTAAAGCCGCACACCTTCAAAGCTGTTATACGCACCCGAAGTCTAGAAGCCCAATTACAAAAGTAGCTTT ATCCTCCCAGACCCCACGAAAGCTCTGGCA
FDB005	NA	*Decapterus*	*macarellus*	*Decapterus macarellus*	ACTAAAGCCGAACATCCTCAAGACTGTCGTACGTTTCCGAGGATATGAAGTCCCCCTACGAAAGTGGCTT TAACTCTCCTGACCCCACGAAAGCTGTGACA
FDB010	NA	*Pterois*	*sp*	*Pterois sp*	AACTAGAGCTGAATTTCTTCAAAGCTGTTATACGCTCATGAAAACTAGAAAATCGACCACGAAAGTGGC TCTAATCATCCCTGACACCACGAAAGCTATGACA
FDB490	NA	*Parablennius*	*sp*	*Parablennius sp*	ACTAAAGCCGAATGCTCCCTAAGCTGTTATACGCTCTCGAGAGTTAGAAGACCTTTTTCGAAAGTAGCTT TATTATGTTGAATCCACGAAAGCTAAGACA

6.2 Chapter 4 - Appendices

Table S4.1. Summary of this study in comparison to previous mesophotic fish biodiversity studies. B=Baited Remote Underwater Video Systems (BRUVs) E= environmental DNA (eDNA), X = pooled visual assessment methods (diver based. underwater visual surveys and underwater visual surverys from a submersible)

*Recorded as *Acanthurus bahianus/chirurgus* in Stefanoudis et al 2019, **Casual observation in Stefanoudis et al 2019, ***Recorded as *Kyphosus incisor/sectatrix* in Stefanoudis et al 2019

Species	Noyes 2022	GGG et al., 2019	Stefanoudis et al., 2019
Abudefduf saxatilis	E		
Acanthocybium solandri		X	
Acanthostracion polygonius	B,E	X	
Acanthostracion quadricornis	B		
*Acanthurus chirurgus**	B	X	X
Acanthurus coeruleus	B,E	X	
Acanthurus tractus	B,E	X	X
Ahlia egmontis	E		
Alectic ciliaris			X
Alepisaurus ferox	E		X
Aluterus monoceros	E		X
Aluterus scriptus	E		
Amblycirrhitus pinos			X
Anchoa choerostoma	E		
Anguilla anguilla	E		
Anoplogaster cornuta	E		
Antennarius ocellatus			X
Anthias tenuis			X
Antigonia capros			X
Apogon evermanni		X	
Apogon gouldi			X
Apogon imberbis	E		
Ariosoma balearicum	E		
Aulopus filamentosus			X
Aulostomus maculatus	B,E	X	
Aulostomus strigosus			X
Auxis rochei	E		
Auxis thazard	E		
Balistes capriscus	E	X	
Bathygobius curacao	E		

Species	Noyes 2022	GGG et al., 2019	Stefanoudis et al., 2019
Bodianus pulchellus	B,E	X	
Bodianus rufus	B,E	X	
Bolinichthys nikolayi	E		
Bothus lunatus	E	X	
Bothus robinsi	E		
Brotula barbata			X
Calamus bajonado	B	X	
Calamus calamus	B	X	
Cantherhines macrocerus	B	X	
Cantherhines pullus	E	X	
Canthidermis sufflamen	E	X	
Canthigaster rostrata	B,E	X	X
Carangoides bartholomaei	B,E	X	
Caranx crysos	E		
Caranx latus	B,E	X	
Caranx lugubris	B,E	X	X
Caranx ruber	B,E	X	
Carcharhinus falciformis		X	
Carcharhinus galapagensis	B	X	X
Caulolatilus bermudensis			X
Centropyge argi	B,E	X	
Cephalopholis cruentata	B	X	
Cephalopholis fulva	B,E	X	
Ceratoscopelus maderensis	E		
Chaetodon capistratus	B,E	X	
Chaetodon ocellatus	B	X	
Chaetodon sedentarius	B,E	X	
Chaetodon striatus	B,E		
Channomuraena vittata			X
Cheilopogon cyanopterus	E		
Cheilopogon exsiliens	E		
Chlopsis dentatus			X
Chloroscombrus chrysurus			X
Chromis bermudae	B,E	X	
Chromis cf. enchrysura	B		
Chromis cyanea	B,E		
Chromis enchrysura		X	
Chromis insolata	B		X
Clepticus parrae	B,E	X	
Clupea harengus	E		
Conger esculentus			X
Conger triporiceps		X	X
Cookeolus japonicus			X
Coryphopterus sp.		X	X
Cryptotomus roseus	B,E		
Cyclothone pallida	E		
Dactylopterus volitans	B		X
Decapterus macarellus	E		
Decapterus tabl			X
Decodon puellaris	B	X	
Diaphus dumerilii	E		
Diaphus effulgens	E		

Species	Noyes 2022	GGG et al., 2019	Stefanoudis et al., 2019
Diaphus mollis	E		
Diodon holocanthus	B,E	X	
Diodon hystrix	E	X	
Diplodus bermudensis	E	X	
Diplospinus multistriatus	E		
Echeneis naucrates	E		
Elagatis bipinnulata	B		
Emblemaria atlantica	E		
Enchelycore carychroa	E		
Epinephelus adscensionis		X	
Epinephelus drummondhayi		X	
Epinephelus guttatus	B,E	X	
Epinephelus morio		X	
Epinephelus mystacinus			X
Epinephelus niveatus			X
Epinephelus striatus			X
Etelis oculatus			X
Eucinostomus jonesii	E		
Eustomias obscurus	E		
Euthynnus alletteratus	E		
Fistularia tabacaria	B	X	
Galeocerdo cuvier	E	X	
Gempylus serpens	E		
Gephyroberyx darwinii			X
Gerres cinereus	E		
Gnatholepis cauerensis	E	X	
Gnatholepis thompsoni		X	
Gobiosoma macrodon	B		
Gonichthys cocco	E		
Gymnothorax funebris		X	
*Gymnothorax maderensis***			X
Gymnothorax miliaris	E		
Gymnothorax moringa	B	X	
Gymnothorax polygonius	E	X	X
Gymnothorax vicinus	E		
Haemulon aurolineatum	B,E	X	
Haemulon flavolineatum	B,E	X	X
Haemulon macrostomum	B	X	
Haemulon melanurum	B,E		
Haemulon sciurus	B,E	X	
Halichoeres bathyphilus	B	X	
Halichoeres bivittatus	E		
Halichoeres garnoti	B	X	
Halichoeres maculipinna	E	X	
Halichoeres radiatus	B,E	X	
Hemiramphus bermudensis	E		
Heteroconger longissimus		X	
Histrio histrio	E		
Holacanthus bermudensis	B,E	X	
Holacanthus ciliaris	E		
Holacanthus tricolor	B,E	X	
Holocanthus tricolor			X

Species	Noyes 2022	GGG et al., 2019	Stefanoudis et al., 2019
Holocentrus adscensionis	B	X	
Holocentrus rufus		X	
Hoplostethus occidentalis			X
Hygophum hygomii	E		
Hypoatherina harringtonensis	E		
Isurus oxyrinchus			X
Jenkinsia lamprotaenia	E		
Katsuwonus pelamis	E		
Kyphosus bigibbus	E		
Kyphosus cinerascens	E		
*Kyphosus sectatrix****	B,E	X	X
Kyphosus vaigiensis	E		
Lachnolaimus maximus	B,E	X	
Lactophrys trigonus	B	X	
Lactophrys triqueter	B,E	X	
Laemonema yarrellii	E		X
Lagocephalus lagocephalus	E		
Lagodon rhomboides	E		
Lampadena atlantica	E		
Lobotes surinamensis	E		
Lutjanus analis		X	
Lutjanus buccanella			X
Lutjanus campechanus	E		
Lutjanus griseus	B,E	X	
Lutjanus synagris	B,E	X	
Lutjanus vivanus			X
Lythrypnus mowbrayi			X
Lythrypnus spilus			X
Makaira nigricans	E		
Malacanthus plumieri	B,E	X	
Megalops atlanticus	E		
Melichthys niger	E	X	
Microspathodon chrysurus	E		
Mobula birostris			X
Monacanthus tuckeri	B,E		
Moringua edwardsi	E		
Mugil curema	E		
Mulloidichthys martinicus	B,E	X	
Mustelus canis insularis			X
Mycteroperca bonaci	B,E	X	X
Mycteroperca interstitalis	B	X	X
Mycteroperca venenosa			X
Myripristis jacobus			X
Nannobrachium lineatum	E		
Nemaclinus atelestos			X
Nemichthys curvirostris	E		
Nomeus gronovii	E		
Ocyurus chrysurus	B,E	X	
Ogilbia cayorum	E		
Opisthonema oglinum	E		
Ostichthys trachypoma			X
Paranthias furcifer	B,E	X	X

Species	Noyes 2022	GGG et al., 2019	Stefanoudis et al., 2019
Parasphyraenops atrimanus			X
Pempheris schomburgkii	E		
Phaeoptyx conklini			X
Platybelone argalus	E		
Plectrypops retrospinis	B,E		X
Polymixia lowei			X
Polymixia nobilis			X
Polyprion americanus			X
Pontinus castor			X
Priacanthus arenatus			X
Priolepis hipoliti	E		
Prionace glauca			X
Pristigenys alta			X
Pristipomoides macrophthalmus			X
Prognathodes aculeatus	B	X	
Prognathodes cf. guyanensis			X
Pronotogrammus martinicensis			X
Pseudocaranx dentex	B,E	X	X
Pseudupeneus maculatus	B,E	X	X
Pterois sp.	B,E	X	X
Pteroplatytrygon violacea			X
Regalecus glesne			X
Rypticus saponaceus	B	X	
Sardinella aurita	E		
Sargocentron bullisi		X	
Sargocentron coruscum	E		
Scarus coelestinus	B,E	X	
Scarus coeruleus		X	
Scarus guacamaia	B,E	X	X
Scarus iseri	B,E		
Scarus taeniopterus	B,E	X	X
Scarus vetula	B,E	X	
Schedophilus ovalis	E		
Schedophilus velaini	E		
Scomberomorus cavalla		X	
Scorpaena albifimbria			X
Scorpaena isthmensis			X
Seriola dumerili	B,E	X	
Seriola fasciata			X
Seriola rivoliana	B,E	X	
Serranus annularis	B		X
Serranus phoebe	B,E	X	
Serranus tigrinus		X	
Serrivomer beanii	E		
Sparisoma atomarium	B		X
Sparisoma aurofrenatum	B,E	X	
Sparisoma chrysopterum	B,E	X	
Sparisoma rubripinne	E	X	
Sparisoma viride	B,E	X	
Sphoeroides spengleri	B	X	
Sphyraena barracuda	B,E	X	
Squalus cubensis			X

Species	Noyes 2022	GGG et al., 2019	Stefanoudis et al., 2019
Stegastes leucostictus	E		
Stegastes partitus	E	X	
Stegastes planifrons	E		
Stephanolepis hispida	E		
Syacium papillosum			X
Synodus foetens	E	X	
Synodus intermedius	B,E		
Synodus synodus	E		
Thalassoma bifasciatum	B,E	X	
Trachinotus goodei	E		
Tylosurus crocodilus	E		
Ulaema lefroyi	E		
Uraspis secunda			X
Uroconger syringinus	E		
Uropterygius macularius			X
Xanthichthys ringens	B,E	X	
Xyrichtys martinicensis	E		
Xyrichtys splendens	E		